Palaeoconductivity, lake level fluctuations and trace element history of the Aral Sea since 400 AD: assessing the impact of natural climatic variability and anthropogenic activity.

Submitted in the fulfilment of the degree of Doctor of Philisophy
in the University of London

By

Patrick John Eliot Austin

Department of Geography
University College London

ProQuest LLC
789 East Eisenhower Parkway
P.O. Box 1346
Ann Arbor, MI 48106-1346

ABSTRACT

As part of the INTAS funded CLIMAN project into Holocene climatic variability and the evolution of human settlement in the Aral Sea basin, fossil diatoms obtained from Chernyshov Bay in the Aral Sea have been examined in order to reconstruct conductivity and lake level change since ca. 400 AD. In an effort to establish whether fluctuations in lake level are a result of natural climatic variation or human activity across the region, the values of $\delta^{13}C$ of organic material ($\delta^{13}C_{org}$) have also been determined. The extent of anthropogenic impact on the lake has also been assessed by ascertaining the history of trace metal (Cd, Pb and Hg) contamination.

Palaeoconductivity has been derived using the EDDI diatom-conductivity transfer function. Results indicate a waterbody that fluctuates between fresh and oligosaline conditions which is punctuated by three phases of elevated conductivity, all within the mesosaline range and corresponding low lake levels at ca. 400 AD, ca. 1195 – 1355 AD and ca. 1780 AD to the present day. These regressions are confirmed by diatom habitat requirements, where, due to the morphology of the lake, planktonic species are indicative of regressive phases.

The C/N ratio of organic material ($\leq$ 10) throughout the core indicates that $\delta^{13}C_{org}$ provides a record of within lake productivity rather than switches of vegetation in the lake's catchment. The highest values are seen to correspond with high diatom inferred conductivity and low lake levels, due to increased salinity, residence time and algal productivity. This suggests that the severity of the observed lake level changes were a result of the natural diversion of the principal source of the lake's hydrological inputs, the Amu Darya river and anthropogenic activity in the form of irrigation, social upheaval and military conflict.

Since 400 AD, the trace metal record from Chernyshov Bay indicates no local or long range anthropogenic contamination of Pb and Hg. Increases of Cd over the last ca. 100 years may be related to increased fertilizer application in tandem with increased cultivation in the region.

ACKNOWLEDGEMENTS

First and foremost I would like to thank Dr. Anson Mackay who supervised this project. This thesis has benefited enormously from his excellent advice, enthusiasm and guidance.

I would also like to thank Professor Melanie Leng at the NERC Isotope and Geosciences Laboratory (NIGL) at the British Geological Survey where the organic carbon isotope analysis was undertaken and Dr. John Boyle Liverpool University where heavy metal analysis was performed. They provided invaluable help not only when visiting their respective institutions but were also helpful when trying to make sense of the excellent data obtained.

This project was part of a larger investigation into Holocene climatic variability and the evolution of human settlement in the Aral Sea basin and I would like to express my thanks to Hedi Oberhaensli at GFZ in Potsdam, Germany who was in charge of the overall project. She was always ready to discuss the project and made me feel welcome during the many visits I made to GFZ. Other members of the CLIMAN team, in particular: Nick Aladin (Zoological Institute, Russian Academy of Sciences), Nik Boroffka (GFZ, Potsdam) and Danis Nourgaliev (Kazan State University) were again ready to discuss aspects of this project which were at times confusing to say the least. A special note of thanks must go to Philippe Sorrel a fellow postgraduate student. We both started work on the same material at the end of 2002 and over the last 36 months or so we have spent much time discussing results and ideas via email, phone and more satisfyingly over the odd beer or two in some of Potsdam's finer watering holes.

Others I would like to thank are Dr. Jane Reed at Hull University with whom I spent a few days examining the Aral Sea diatom flora and Janet Hope, Tula Cloke and Ian Patmore for assistance in the laboratory at UCL and similarly Irene Cooper at Liverpool University. Discussions regarding diatoms in salt lakes with Dr. Roger Flower were both enlightening and amusing. Professor Rene Letolle at the Université Pierre et Marie Curie, Paris has always been ready to share with me his extensive knowledge of the Aral Sea and kindly sent me one of his last copies of *Aral* which he

co-wrote with Monique Mainguet. This was an extremely valuable reference source and helped improve my French no end.

I also owe a great deal of thanks to friends at the ECRC. In particular David Morley, Patrick Rioual, Tom Davidson, George Swann, Jon Tyler, Adam Young, Jo Thorpe and Carl Sayer, all of whom provided assistance of one kind or another, at one time or another while also perhaps more importantly providing many moments of light relief. On that note thanks also goes to: Chris Coombes, Pete Charlton, Jamie Forester, Tim Mawdesley, Rob Miller, Paul Reilly, Pete Tiley, Ian Walker and Richard Williams for their articulate and enlightened analysis of major sporting events and just about everything else over the past 36 months. The emails never failed to make me laugh, long may it last. I would also like to thank Doug Taylor who was a near constant companion on the 0607 train from deepest Sussex to London Bridge and is no doubt relieved that he can now get on with work in peace.

Finally I owe a great deal of thanks to my parents and brothers who have never failed to provide encouragement during an education bonanza that started with an HND in Wine Studies almost ten years ago and ends here (I promise!) and of course to Deborah, who been a constant source of support for the past eight years, has always allowed me the time and freedom to concentrate on this project and at least *appeared* to look interested when I start discussing unicellular alge and the world's endorheic regions for the umpteenth time and last but by no means least, Freya who has heard more about those subjects than must be healthy for a seven year old.

Contents

List of figures

Chapter 1

Chapter 2

Chapter 3

Chapter 4

Chapter 5

Chapter 6

List of Tables

Chapter 2

Chapter 3

Chapter 4

Chapter 6

"Even for the matter-of-fact minds of our day, there is, apart from the remoteness of its situation, a veil of mystery enveloping Lake Aral, which is sufficiently provocative of the interest of the most phlegmatic observer. That the most ancient classic historians should have spoken of countries which are situated farther to the north and to the east, yet should have omitted all mention of an inland sea which is one hundred times larger than the Lake of Geneva is an enigma stimulating enough to demand a solution."

Major Herbert Wood, Royal Engineers. *The shores of Lake Aral.* Smith Elder, London, 1876.

Chapter one

Introduction

In recent years, the climatic and environmental changes that have occurred over the past two millennia have been the subject of much debate, both in the scientific and political arenas. The last 2000 years is an important time frame in which human activity has radically altered the environment, and which includes 3 distinct episodes of climatic fluctuations, i) the Medieval Warm Period (MWP, ca. 800 – 1200 AD), ii) the Little Ice Age (LIA, ca. 1200-1800 AD) and iii) the current warming episode commencing ca. 1850 AD, during which time global surface temperatures are seen to have increased by 0.6°C (Houghten et al., 2001). Two other, less well documented, shifts are also seen to occur, i) the Roman Warm Period (RWP, ca. 100 BC – 400 AD) and ii) the Dark Ages Cold Period (DACP ca. 400 – 800 AD).

Human activity (e.g. deforestation and irrigation) has been a major factor in environmental change over the past two millennia and is often, although not always, a response to natural climatic variability, and in particular that of moisture availability. Climate variability over the last ~ 2000 years, while not as severe as other episodes seen in the geological record has nevertheless been invoked as having severe societal consequences, particularly on ancient civilizations such as the Maya in modern day Mexico (Hodell et al., 1995; 2001; Curtis et al., 1996; Haug et al., 2003), the Tiwanaku culture in the Bolivian Altiplano (Abbot et al., 1997; Bindford et al., 1997), the Anasazi in the southern United States (deMenocal, 2001), early Norse cultures in Greenland (Broecker et al., 1975; Jenssen et al., 2004) and the early English settlements of Roanoke and Jamestown in Virginia (Stahle et al., 1998).

Of vital importance are the timing and intensity of these climatic shifts. For example, the MWP is seen to be independent of any *large scale* anthropogenic activity that is generally held to be the cause of the warming of the late 20th century (Mann and Jones 2003; Luterbacher et al., 2004, Moberg et al., 2005; Osborn and Briffa, 2006), giving succour to those who feel that the present warming trend is nothing but a result of the dynamic nature of the earth's climate (e.g. Soon and Baliunas, 2003). Hence the

importance of placing the current climatic situation in a longer-term context and the continuing need for high resolution records of late Holocene climate change from around the globe and in particular those regions from where such records are scarce, such as Central Asia

This first chapter will focus upon observed climatic changes over the last 2000 years which may be responsible for global and regional environmental change and the mechanisms that drive them. In the second chapter, which deals exclusively with the Aral Sea, the history of habitation in the region is discussed along with the potential impacts of human activity upon the lake level over this period.

1.1 Late Holocene climatic variation

On the evidence of Holocene glacial advances in the southern Yukon Territory and Alaska, Denton and Karlén (1973) proposed a pattern of climatic variations, in particular periods of deterioration, throughout the present interglacial. Over the last decade, information derived from marine cores obtained from the sub-polar north Atlantic (Bond et al., 1997; 1999; Bianci and McCave, 1999) has combined with that retrieved from the Greenland GRIP and GISP2 ice core records (O'Brien et al., 1995; Alley et al., 1997) confirming that the Holocene, a period previously thought to have been climatically stable, when compared with the later stages of the Pleistocene (Figure 1.1) has nevertheless been subjected to episodes of climatic fluctuation.

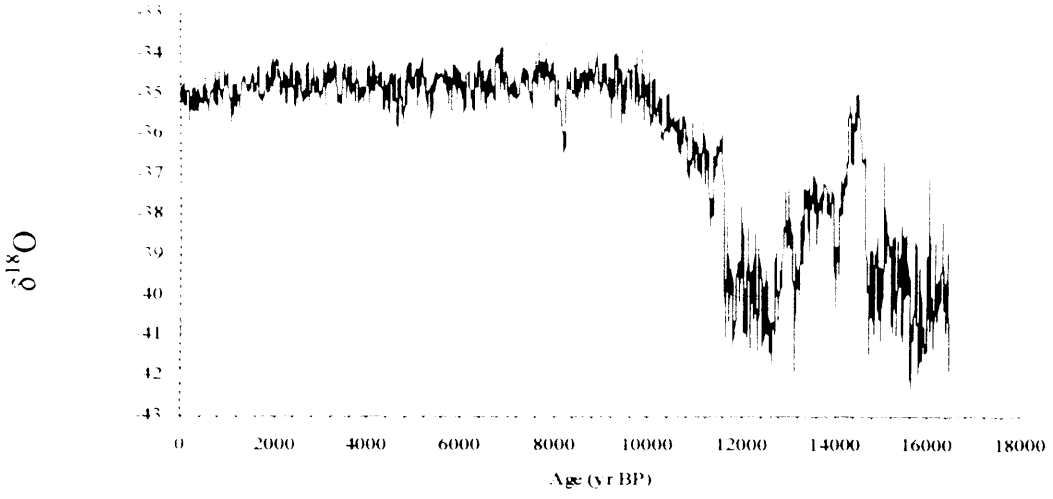

Figure 1.1. GRIP Bi-decadal record of $\delta^{18}O$ fluctuations from the Late Glacial to the present day. Stuiver et. al (1995).

With a frequency of 1500 ± 500 years, the sub-Milankovitch millennial-scale climate cycle found to be in operation during the last glaciation (Daansgard et al., 1993) has been seen to continue into the present interglacial, the cyclicity of these events being statistically the same (Bond et al., 1997).

Recent efforts to analyse climatic change over the past two millennia have focused on high resolution studies of ice cores (e.g. Thompson et al., 1985, 1986, 1988, 2002), tree rings (e.g. Cook et al., 1999, 2002, 2004; Briffa et al., 2001; Esper et al., 2002a, 2002b), speleothems (Procter, 2000; McDermott et al., 2001; Paulsen et al., 2003), borehole temperature measurements (Huang et al., 1997a, 1997b, 2000; Steig et al., 1998), lake sediments (e.g. Overpeck et al., 1997; Joynt and Wolfe, 2001; Le Blanc et al., 2004; Jensen et al., 2004) and coral (eg. Quinn et al., 1998; Cole et al., 2000; Cobb et al., 2003). To these have been added temperature reconstructions on a hemispheric or even global scale, based on modelling experiments using estimated climatic forcings (e.g. Crowley, 2000; Shindell et al., 2001; Gerber et al., 2003) and empirical reconstructions (Figure 1.2) which combine proxy indicators with records obtained through early instrumental observations and documentary evidence (e.g. Mann et al., 1998, 1999; Briffa et al., 2001; Jones et al., 2001; Mann and Jones, 2003; Luterbacher et al., 2004; Osborn and Briffa, 2006). These are primarily restricted to the Northern Hemisphere (NH) and even then generally to regions north of 30°N. The lack of data sets from the Southern Hemisphere (SH) renders it particularly difficult to establish reliable global temperature reconstructions in this fashion.

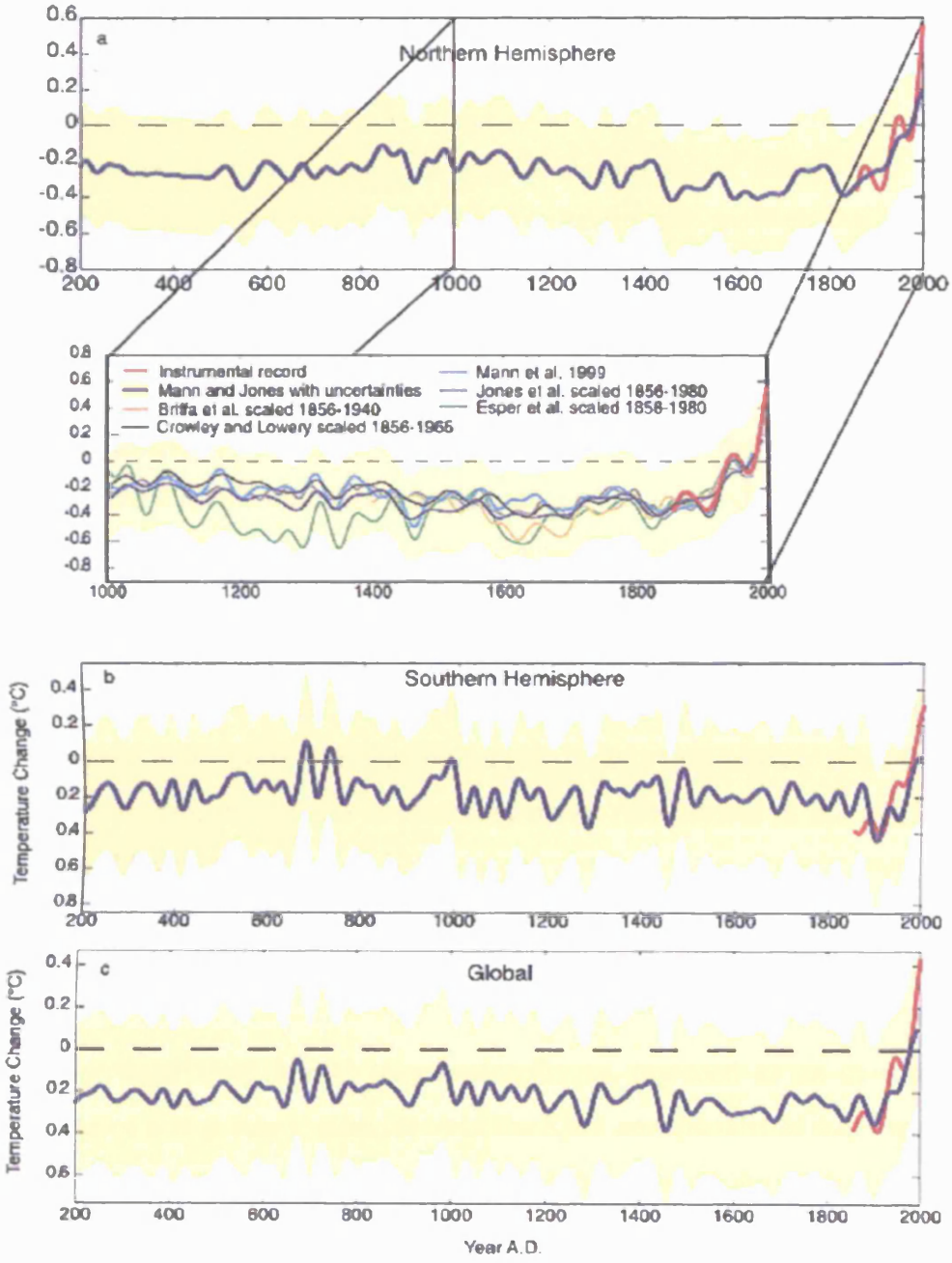

Figure 1.2. Northern Hemisphere (a), Southern Hemisphere (b) and global surface (c) annual temperature (°C) reconstruction from 200 AD to the present day referenced to the 1961 – 1990 mean (dashed line). A comparison of NH temperatures for the past 1000 years are seen in the expansion of Figure 1.2a highlighting low frequency variations for this period. All series have been smoothed with a 40-year Gaussian weighted filter. Refs; Mann and Jones (2003), Briffa et al., (1998), Crowley and Lowrey (2000), Mann et al., (1999), Jones et al., (1999), Esper et al., (2002). Image available on line at: (http://www.ncdc.noaa.gov/paleo/pubs/jones2004/fig5.jpg) Downloaded 05/05/05.

1.2 The Roman Warm Period (RWP) and the Dark Ages Cold Period (DACP)

Several key points emerge from the reconstructions above, chiefly that the present warming is unparalleled within the last two millennia, and secondly that the climate of this period has been anything but stable. What follows are some examples of the RWP and the ensuing DACP. The later MWP and LIA are then discussed in more detail.

The term Roman Warm Period (RWP) is used to describe the approximate timing of a late Holocene climatic optimum that was concordant with the dominance of the Roman Empire. High resolution speleothem derived $\delta^{18}O$ records from southwest Ireland (McDermott et al., 2001) provide evidence of warmer temperatures at 2000 cal. yr BP. In Northwest Spain the timing of this period of increased temperatures is seen to vary, occurring from 0 – 500 AD (Martinez-Cortizas et al., 1999), to 250 cal. BC – 450 cal. AD (Despart et al., 2003). To the north, in the Swiss Alps, glacier retreat from 200 BC – 50 AD is indicative a shorter warming phase (Holzhauser et al., 2005). In North America, Meyer and Pierce (2003) suggest that increased drought and fires in the Yellowstone region from 2350 – 2050 cal. yr BP are also indicative of warmer temperatures that are concordant with the RWP.

The Dark Ages Cold Period may essentially be regarded as an episode of lower temperatures that is sandwiched between the RWP and the later MWP. Some examples of this are: reduced temperatures at ca. 600 cal. yr BP following the warm phase in southwest Ireland identified by McDermott et al., (2001), this is also seen in Irish peat bog records reconstructed by Blackford and Chambers (1991). These correspond with a decline in agriculture and the development of forests in Scandinavia at around 500 AD (Berglund, 2001) and reduced temperatures in the Norwegian Sea (Jansen and Koç, 2000) and ice-rafted debris (IRD) event 1 at ca. 1400 cal. yr BP (Bond et al., 1997). Further to the south on the Iberian penninsula, colder conditions are considered to have lasted from 450 – 950 cal. yr AD.

1.3 The Little Ice Age and the Medieval Warm Period

The LIA is the best documented of all late Holocene episodes of climatic fluctuation and is widely considered to be a global event (Grove, 1988; Bradley and Jones, 1992). NH temperature reconstructions for the LIA (Fig 1.2) would appear to suggest a cooling of < 1° C relative to the late 20th century in common with more recent reconstructions (Luterbacher et al., 2004; Moberg et al., 2005). Cooling though, varies, being more pronounced in some areas than others, possibly reflecting changes in atmospheric circulation with cold, dry winters in central Europe during the late 1600s being consistent with the negative phase of the North Atlantic Oscillation (NAO – Folland et al., 2001 [see section 1.6.5.]). It is important to note however that the term LIA (and indeed MWP, DACP, and RWP) are now thought to have *'limited utility'* in describing trends in hemispheric or global temperatures over the last millennia (Folland et al., 2001) where regional, intra and inter-hemispheric onset, extent and intensity may be particularly variable.

1.3.1 Temporal and spatial evidence for climate change during the LIA and MWP

In Norway, glaciers reached their maximum extension in the mid 18th century. This occurred in the mid 19th century in the European Alps (Nesje and Dahl, 2003) contrasting with tree ring temperature reconstructions from Spain suggesting coldest conditions between 1400 – 1600 AD (Manrique and Fernandez-Cancio, 2000). In the Middle East however, isotopic evidence from the Eastern Mediterranean indicate a period of cold, arid conditions at around 1770 AD (Schilman et al., 2001). In Alaska, glacial expansion is considered to have commenced ca. 1250 AD with maximum advances from 1600 – 1800 AD (Wiles and Calkin, 1994; Calkin et al., 2001). Further south on the Yucatan peninsula cold and dry conditions have been recorded during the mid 15th century AD (Hodell et al., 2005). In the Southern Hemisphere, speleothems from New Zealand's North Island indicate coldest conditions from 1440 – 1680 AD (Williams et al., 1999). Tree ring data put this cold episode from 1600 – 1700 AD and indicate that it occurred on New Zealand's South Island between 1500 – 1550 (D' Arrigo et al., 1998). Conversely no cold episode is detected in tree rings from Tasmania (Cook et al., 2000). This contrasts with other data from the Southern

Hemisphere; tree rings from Patagonia indicating a long cool interval from 1270 – 1660 AD while glacial expansion occurred between 1300 – 1400 AD and 1600 – 1700 AD (Luckman and Villalba, 2001) this latter example of two separate glacial advances indicating the complex nature of the LIA. This suggests not a single prolonged cold episode but a two or even three phase LIA with distinctive cold periods interspersed with warm episodes. This is also seen in glacial expansion in North America, Scandinavia and the European Alps (Wiles and Calkin, 1994; Grove, 2001; Calkin et al., 2001) and also recorded in speleothem records from southwest Ireland (McDermott et al., 2001).

The MWP is rather less well documented and was initially described by Lamb (1965) who after an extensive examination of documentary records concluded that an episode of increased warmth during the 11th and 12th centuries AD occurred over much of the North Atlantic, southern Greenland and Iceland. Almost 40 years later this is seen as a somewhat simplistic definition, as the MWP would appear to manifest itself at anytime between 800 – 1200 AD (Broecker, 2001) and even as late as 1500 AD (Jensen et al., 2004) while also appearing to vary in intensity (Esper, et al., 2002a; Mann and Jones, 2003). Reconstructed temperatures for the Northern Hemisphere (Figure 1.2) appear to suggest that temperatures from 1000 – 1300 AD were ~ 0.2°C higher than those from 1400 – 1800 AD, and also lower than mid 20th century temperatures. As with the LIA, regional evidence is variable. Southern Greenland is seen to have undergone a warm phase from 800 – 1250 AD (Jensen et al., 2004) while in Scandinavia this was seen to have been initiated later, lasting from from 1100 – 1200 AD. In Arctic Canada glacio-lacustrine varves indicate warm summer temperatures from 1200 – 1350 AD (Moore et al., 2001) while Le Blanc et. al (2004) detected a longer period of warming from 850 – 1400 AD. In the eastern Mediterranean this is seen to have occurred around 1200 AD and been accompanied by increased moisture (e.g. Issar, 1998; Schilman et al., 2001).

Of perhaps greater significance is the manifestation of the MWP as an arid event from ca. 1000 – 1200 AD in the Northern Great Plains and the western States of the United States (Laird et al., 1998; Cook et. al; 2004; Stahle et al., 2000). This supports Stine's (1994) findings which indicate coincident extreme drought in locations as far apart as California and Patagonia for two centuries prior to 1112 AD. Cook et al., (2004) have

suggested that increased temperatures during this period over the tropical Pacific Ocean promote upwelling in the eastern Pacific and subsequent cool La Nina like conditions which are associated with drought in the western United States.

1.4 The last two millennia in Central Asia

Definitions of the Central Asian region (Figure 1.3) abound and may vary according to both human and physical geography (e.g. Adshead, 1993). It can however be seen to comprise the former Soviet Central Asian Republics (Kazakhstan, Kirghizstan, Turkmenestan, Tadjikhastan and Uzbekistan), central and western China and the Tibetan Plateau and Mongolia. This may be broadened to include neighbouring regions such as Afghanistan and southern central Russia.

Figure 1.3.Map of Asia and Central Asia. Courtesy Philippe Sorrel

In accordance with records form the rest of the globe, the Central Asian climate has, over the past two millennia, been subjected to complex climatic fluctuations. Ice core records from the Guliya ice cap on the Tibetan-Qinghai Plateau (Thompson et al., 1995) indicate two extended dry episodes from 1075 – 1375 AD and 1775 – 1900 AD. Conversely the LIA from Guliya is recorded as increased moisture from ~1500 – 1700

AD. The $\delta^{18}O$ record from Dunde ice cap, further to the east, illustrates cold climatic conditions centred around 800 AD and 1500 AD with a warmer phase ~ 1300 AD (Yao and Thompson, 1992) and is supported by pollen analysis suggesting that warm dry summers and windy conditions prevailed during the MWP while the LIA resulted in cool moist conditions (Liu, et al., 1998). Records of Asian monsoon variations detected in the redness of sediments from Qinghai Lake suggest a 1000 year long humid MWP (200 – 1220 AD) followed by an arid LIA (1220 – 1600 AD). A DACP from 100 BC – 200 AD is also indicated (Ji et. al 2005), a time frame that corresponds with a wide range of evidence indicating the RWP in many regions (section 1.2).

In a review of the climatic fluctuations of the Tibetan Plateau, Bao et al., (2003) highlight the asynchronous nature of changes in this region, the north east generally warm from 800 – 1300 AD and then experiencing a cool period from ca. 1400 – 1900 AD while the southern region was warm from 600 – 800 AD and then experienced a cool climate warming up again from 1150 – 1400 AD with coolest LIA temperatures occurring in the 1600s. A 6000 year record of climate contained in peat deposits bordering Central Asia in north east China (Hong et al., 2000) highlights many changes over the last two millennia in which both the MWP and the LIA can be clearly identified, the latter appearing to be punctuated by several episodes of less severe conditions. In contrast with the moist conditions seen in the ice cap data, the LIA in northern regions of China is generally seen as an arid episode (Song, 2000) in all probability due to the weakening of the Asian monsoon (Thompson et al., 1995). Speleothems from central China also preserve records of the MWP (965 – 1475 AD) and the LIA from 1475 – 1845 AD during which time there were three prominent cold phases, the most severe coincident with the Maunder Minimum (Paulsen et al., 2003). Further to the north in Lake Baikal, Siberia the MWP is seen to occur from ca. 880 – 1180 AD and the LIA from 1180 – 1840 AD (Mackay et al., 2005). Tree ring records from Mongolia spanning the last 500 years (Jacoby et al., 1996; D'Arrigo et al., 2000) point to the coldest episode of the LIA occurring in the 1800s while those from the northwest Karakorum exhibit particularly low growth rate indicative of low temperatures at ca. 1200 AD, 1480 AD, 1650 AD and 1810 AD while optimum conditions are centred around 1350 AD (Esper, et al., 2002b).

The record of change from the west of the Central Asian region is less well documented than the others discussed above. Levels of lake Issyk-kul in the Tien Shan are seen to be lower than the present day from 800 – 1600 AD while increased levels and lower temperatures are recorded from 1600 – 1900 AD (Ricketts pers. comm). Savoskul (1997) and Savoskul and Solomina (1996, 2004) detected three phases of glacial advance in the inner Tien Shan centred around 200 AD, 1200 AD and an LIA advance characterised by three episodes of expansion centred around 1550 AD, 1750 AD and 1825 AD suggesting that the LIA was the least extensive of the advances of the last two millennia. This conflicts with the data obtained by Yafeng and Jaiwen (1990) who stated that maximium expansion was ca. 1700 AD, although their site was at the edge of the range and in all possibly in receipt of some moisture from the Asian monsoon which is unlikely to have been the case for the inner range locations. Peat formation at the end of a glacier in the Tien Shan at ca. 1000 AD is seen as indicative of a warm phase. Tree ring analysis (Esper et al., 2001; Esper et al., 2002b) illustrates favourable climatic conditions from 618 – 1139 AD followed by a prolonged cold period from 1140 – 1874 AD interspersed with episodes of both climatic improvement and severe deterioration. In the Pamir to the south east, glacial advance interspersed by a warm episode indicated by a soil horizon formed on a lateral moraine of the Abramova glacier at ca. 1000 AD is seen to have occurred at ca 500 – 800 AD and ca 1500 – 1800 AD (Zech, 2000; Narama, 2002).

1.5 Causes of observed climatic shifts

It has been suggested that the anthropogenic era of global warming (the anthropocene) was initiated by forest clearance and the emissions of Greenhouse Gases (GHG – notably CO_2 and CH_4) many thousands of years ago and that observed atmospheric CO_2 reductions during the first half of the last millennium were a consequence of the growth of new forests on land abandoned as a result of plague pandemics (Ruddimann (2003; Ruddimann et al., 2005). Many models which attempt to reconstruct present day conditions relying on natural forcing mechanisms only, fail to reproduce the present warming (Stott et al., 2001; Bertrand et al., 2002; Widmann and Tett, 2003). The current warming trend is thus almost certainly a direct consequence of human activity over approximately the last 150 years and increased GHG emissions since the industrial revolution (Etheridge et al., 1998a, 1998b; Houghton et al., 2001).

The climatic fluctuations discussed all occurred during episodes of low global human population, which during the 1300s, is estimated to have been ca. 360 million (http://www.census.gov/ipc/www/worldhis.html). Consequently the forcing of climate change prior to the increase in GHG emissions since the industrial revolution must have been a result of natural, external or internal, mechanisms, or if Ruddiman (2003) is correct, early anthropogenic activity (i.e. deforestation and the burning of wood for fuel) which was in all probability reinforced by changes in climate.

1.6 Forcing Mechanisms

1.6.1. Orbital forcing

The Milankovitch scale orbital forcing with cycles of ca. 110,000 years (the eccentricity cycle), 42,000 years (the obliquity cycle) and 22,000 years (the precessional cycle) are responsible for the distribution of solar energy across the planet and consequently drive the major climate cycles i.e. glacial – interglacial cycles (Hays et al., 1976; Imbrie et al., 1992, 1993). Whereas the eccentricity cycle influences the amount of solar energy received by the Earth, obliquity and precession influence the distribution of this energy across the Earth's surface (in terms of both latitude and season). At the beginning of the Holocene, precessional changes led to the initiation of higher summer insolation than present at all latitudes of the northern hemisphere. This has declined by ~ 10% over the last 12 ka (Bradley, 2003, Nesje et al., 2005) and probably explains the general reduction in temperatures from the early Holocene to the present day. However orbital forcing is thought to act at too long time scales to be responsible for climatic fluctuations limited to the late Holocene, thus one must look to forcing mechanisms that act on a shorter time scale and are more likely to represent the dominant forcings of climatic variability (Jones and Mann, 2004).

1.6.2 Solar forcing

Solar forcing, of which there are many known cycles, the most prominent being of 11, 22, 88, 211 and 2200 years, brings about direct changes in the amount of energy (total solar irradiance or TSI) that is intercepted by the atmosphere (Bradley, 2003). For some, the sun plays a dominant role in forcing the climate system (e.g. Eddy, 1976;

Lean et al, 1995; Mann et al, 1999; Hodell et al., 2001) and as such has been invoked to explain changes in sea level atmospheric pressure (Kelly, 1979), sea surface temperatures (Reid, 1987), equatorial wind patterns (Labitzke and Van Loon, 1988), land air temperatures (Friis-Christensen and Lassen, 1991) and monsoon variability in the tropics (Fleitmann et al., 2003; Wang et al., 2005). Others however, conclude that its role in directly influencing climate change is ambiguous at best and that anomalous solar activity might simply instigate internal earth system feedbacks which are themselves a greater catalyst for any observed changes in climate (e.g. Rind, 2002).

1.6.2.1 Sunspot numbers

The role of the sun in climate variability was being investigated as far back as the late 1800s and centred around the presence and absence of sunspots caused by large scale magnetic fields in the solar atmosphere (Lean et. al, 1992). In 1843 Heinrich Schwabe determined that sunspots and sunspot numbers vary (having a maximum and minimum) over an 11 year cycle, commonly referred to as a Schwabe or solar cycle. It has been suggested that sunspot activity is responsible for as much as 95% of the variance of TSI (Frolich and Lean, 1998), values of which (previously thought to have been fixed at 1368°W/m^2) are seen to shift in the order of 0.1% over a solar cycle (Willson and Hudson, 1991; Willson, 1997).

A 70 year period, termed the Maunder Minimum from ca. 1645 to 1715, exhibited little or no sunspot activity and corresponds with the coldest part of the LIA, leading Eddy (1976) to suggest that the concordant climatic deterioration was a direct consequence of reduced solar activity. Lean et al., (1992; 1995; 2000) determined that TSI values for this period were reduced by 0.24% when compared with the mean value recorded for 1980-1986 of 1367.54°W/m^2 equating to a cooling in the range of 0.2°C – 0.6°C.

1.6.2.2 Cosmogenic isotopes

Changes in the values of cosmogenic isotopes, in particular ^{10}Be and ^{14}C, serve as a proxy record of solar activity prior to the period for which records exist (Stuiver and

Braziunas, 1993) with both exhibiting similar fluctuations over the last ca. 400 years (Bard et al., 2000).

Fluctuations of ^{14}C values within tree rings enabled Eddy (1976) to establish three distinct periods of anomalous solar activity during the last millennium, the Maunder Minimum; an earlier episode of low solar activity from ca. 1460 AD – 1550 AD (The Spörer Minimum) and a period of high activity from ca. 1100 – 1300 that coincides with the MWP. Stuiver and Quay, (1980) established two further episodes, 1282 – 1342 AD (the Wolf Minimum) and a later episode centred around 1810 (the Dalton Minimum). The LIA cooling of between 0.2°C – 0.6°C (Lean, 2000; Lean et al., 1992, 1995) is somewhat lower than the estimates of ~1°C discussed earlier strengthening the argument for the contemporaneous role of other forcing mechanisms.

1.6.3 Volcanic forcing

Volcanic forcing is thought to have contributed to climatic cooling throughout the Holocene (Zielinski, et al., 1994), with many short term (i.e. interannual) variations being explained by volcanic activity (Lamb, 1970; Lamb, 1977; Grove, 1998, Shindell et al., 2003). Large eruptions naturally input a considerable volume of ash and dust into the atmosphere, however, it is the presence of sulphur laden aerosols that is primarily responsible for the absorbtion and reflection of incoming solar radiation (Hoffman and Solomon, 1989).

Significant eruptions may consequently lead to global average stratospheric warming and surface cooling over several years (Robock and Mao, 1992; Robock, 2000), with major events having significant consequences for temperatures across large parts of the globe. Tree ring density measurements indicate Northern Hemisphere cooling of 0.81°C in North America and Fennoscandia following the 1600 AD eruption of Huaynaputina in Peru (Briffa et al., 1998). Regional responses to such events vary (Robock and Mao, 1992; Shindell et al., 2003) Robock and Mao (1992) demonstrated that temperatures in continental interiors of the Northern Hemisphere after 12 eruptions between 1883-1992 increased during the first winter after large tropical volcanic eruptions, the first or second winter after mid-latitude eruptions and in the second winter following eruptions in the high latitudes of both the Northern and

Southern Hemispheres. These changes are linked to shifting atmospheric patterns which led to the advection of warm maritime air over the continental land masses. The concordant cooling observed in the sub-tropics was simply the effect of reduced incoming solar radiation as a consequence of the increased atmospheric aerosol loading (Robock and Mao, 1992).

Attention has recently been focused on the ability of volcanic eruptions to influence climate variability over longer timescales. Shindell et. al, (2003) argue that while volcanic forcing may be regionally important on a year to year basis its importance is seen to diminish over longer periods. However Bradley (2003) argues that climatic change might result if eruptions had been greater in magnitude and frequency and/or occurred in clusters, especially if the resultant cooling was able to initiate other internal feedbacks.

Porter (1986) found a strong correlation between the timing of Northern Hemisphere glacier readvances and peaks of SO_4^{2-} in the Greenland ice core as far back as 1600 AD leading him to conclude that these volcanic eruptions may have contributed to the cooling witnessed in the Maunder Minimum. Crowley (2002) goes on to say that a cluster of eruptions between 1666 – 1696 AD were responsible for the intense cooling at the end of the Maunder Minimum. Bauer et. al (2003) go somewhat further stating that simulations double the effect of solar induced cooling in the Maunder Minimum while tripling it in the earlier Wolf, Spörer and later Dalton Minima.

1.6.4 Ocean forcing

Due to its volume, heat storage capacity and inertia, the ocean is the only serious candidate for driving and maintaining long term (i.e. hundreds to thousands of years) climatic change. Episodes of climatic deterioration that are seen to occur on a ~1500 year cycle have been recorded in North Atlantic deep water (Pisas et al., 1973; Bond et al., 1997; Bianchi and McCave, 1999). Bond et. al, (1997) were able to distinguish 8 specific ice-rafted debris (IRD) events at, 1400, 2800, 4200, 5900, 8100, 10,300 and 11,100 years ago, during which time cool ice-bearing waters from north of Iceland migrated as far south as the United Kingdom. These events are seen to have statistically the same pacing as the larger scale Dansgaard-Oeschger (DO) events that

are particularly prominent in MIS 3 (Broecker, 1994) and are contemporaneous with Holocene changes of atmospheric circulation above Greenland (O'Brien et al., 1995). The cause of these IRD events is attributed to the cessation of North Atlantic Deep Water (NADW) formation (Bianchi and McCave, 1999) and the subsequent "switching off" of the thermohaline circulation, or global conveyor belt (Figure 1.4) which brings warm salty tropical water at a depth of ~ 800 m from the Gulf of Mexico to the North Atlantic and Nordic Seas. Here, water rises, and in so doing give up heat to the atmosphere before sinking and returning south. It has been estimated that this process results in the release of ~ 5 x 10^{21} cal of heat, equating to ca. 25% of the solar heat that reaches the surface of the Atlantic north of 35°N (Broecker and Denton, 1990).

Failure of NADW formation is attributed to an increased freshwater flux into the North Atlantic and Nordic Seas due to melting sea ice and grounded ice sheets, increased precipitation or a shift in the location of the atmospheric polar front (Maslin et al., 2003). Bianchi and McCave (1999) suggested that NADW formation was comparable to modern values during the MWP but was reduced during the LIA. This is supported by Broecker et. al (1999) who suggest that an oscillation of deep water formation in the North Atlantic and Southern Ocean led to a reduction of poleward heat transport during the LIA with opposite conditions prevailing during the MWP.

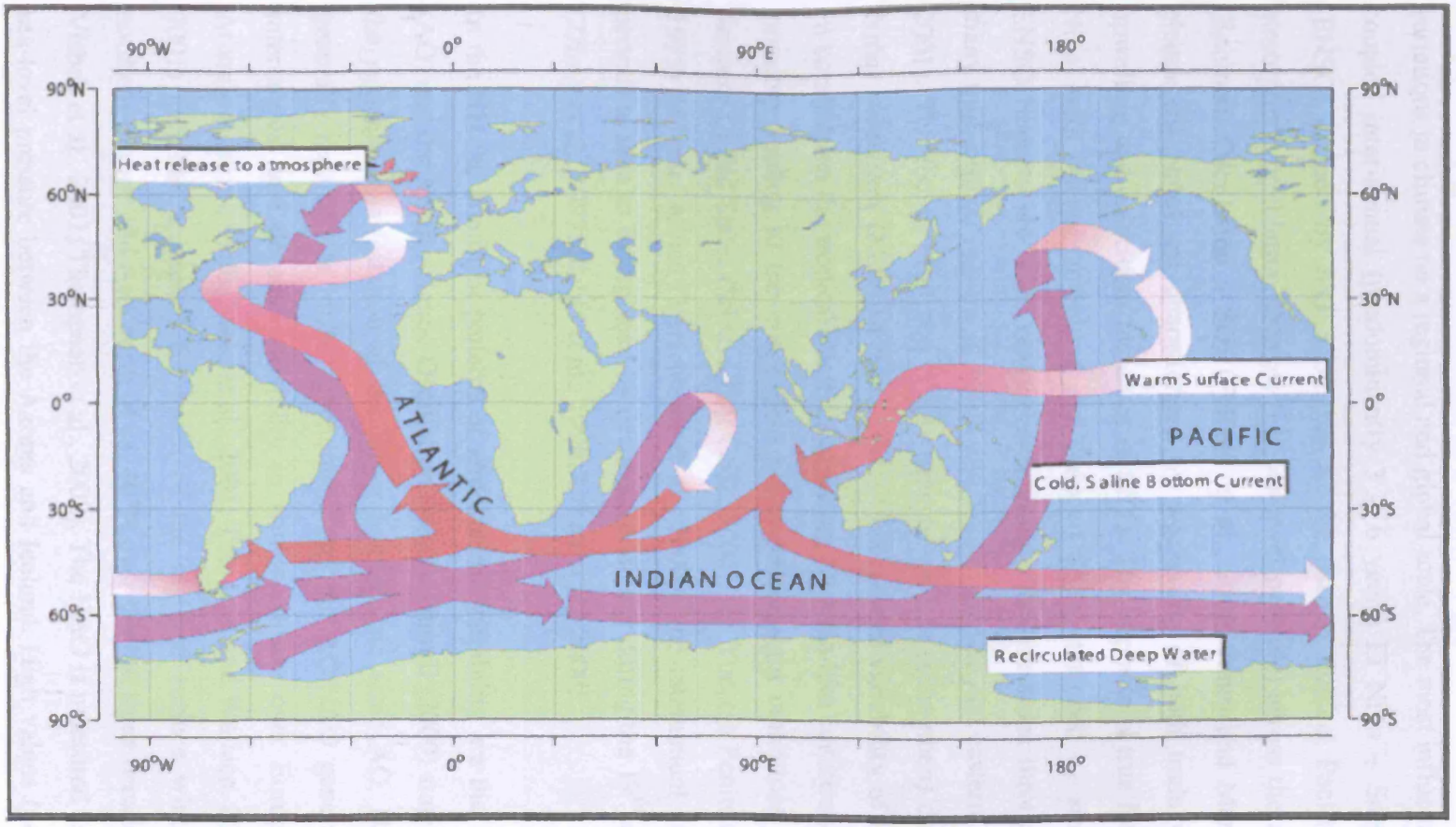

Figure 1.4. The global thermohaline circulation. Deep water cold currents are indicated by dark arrows, light arrows indicate warm water currents. The location of heat release to the atmosphere in the North Atlantic is indicated. After Broecker and Denton (1990). Image available online at http://www.clivar.ogr/publications/other_pubs/clivar_transp/d3_transp.html.

1.6.5 Atmospheric circulation and teleconnections.

Changes or fluctuations in atmospheric circulation are a major contributor to variations in climate on a regional and global scale. The most influential of these is the coupled inter-annual (predominantly 3 – 6 years) El Niño – Southern Oscillation (ENSO) defined by SST anomalies in the eastern tropical Pacific (El Niño) and atmospheric circulation changes (i.e. sea-level pressure) across the equatorial Pacific (Southern Oscillation – SO) (Folland et al., 2001; Jones and Mann, 2004). Warm phases (El Niño) are characterised by weakening of both trade winds and ocean upwelling and coincident increases in SSTs. The opposite is true for cold phases (La Niña) with intense upwelling and reduced SSTs enhanced by strong trade winds. ENSO impacts are wide ranging exhibiting teleconnections throughout the tropics, many mid-latitude regions of North and South America and eastern Asia (Jones et al., 2001). The Indian Monsoon is also seen to weaken (strengthen) during El Niño (La Niña) conditions (Ninglian et al., 2003). Interannual variability of ENSO is recorded in corals from the tropical Pacific suggesting La Niña-like conditions at ca. 1000 AD, possibly leading to the concordant prolonged drought conditions witnessed in the western United States (Stine, 1994; Cook, 2004), the Yucatan Peninsula (Hoddel et al., 1995) and east Africa (Verschuren et al., 2000). The interannual variability in these periods is seen to be replaced by decadal variability during the 19th and 20th centuries (Zhang et al., 1997; Stahle et al., 1998; Urban et al., 2000).

In the NH the dominant patterns of atmospheric variability are the Arctic Oscillation (AO) and the North Atlantic Oscillation (NAO). Hurrell (2000) states that the NAO is the regional manifestation of the larger hemispheric scale AO. However, they are generally regarded as related phenomena and the AO/NAO generates much of the inter-annual and decadal variability in winter climate over Europe and the North Atlantic (Hurrell, 1996; Jones et al., 2001; Thomson and Wallace, 2001; Visbek et al., 2001) and has accounted for much of the regional surface winter warming over northern Europe and Asia north of ca. 40°N over the last three decades (Hurrell, 1996; Visbek et al., 2001; Thompson et al., 2002). The NAO is measured as the difference in sea-level pressure between the Azores and Iceland. High values (positive phases) of the NAO as has been the overall trend since the early 1970s are associated with strong westerly winds across Europe and the transport of moisture laden air masses from the

North Atlantic. These bring warm conditions to northern Europe and further downstream to Asia and enhanced moisture to higher latitudes (Figure 1.5, 1.6). The more southerly areas, stretching as far as Turkey and the Middle East remain drier and colder (Cullen and deMenocal, 2000). Conversely during a negative phase of the NAO, the strength of the westerly flow decreases across northern Europe resulting in potentially much colder and drier conditions across these regions (Hurrell, 1995, 1996) with warmer and wetter conditions across much of southern Europe (Figure 1.6).

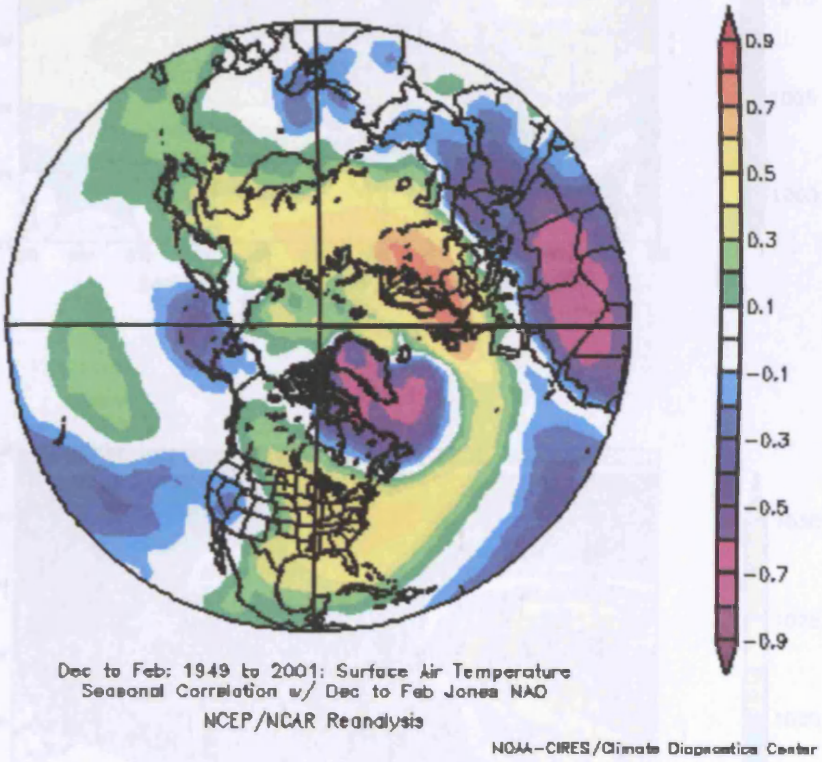

Figure 1.5. Spatial correlation of mean winter (DJFM) NH surface air temperatures and the NAO index. Image provided by the NOAA-CIRES Climate Diagnostics Center, Boulder Colorado from their Web site at http://www.cdc.noaa.gov/

Evidence from ice-cover trends on Lake Baikal in Siberia (Livingstone, 1999; Todd and Mackay, 2003) and isotope records from the Tibetan Plateau (Ninglain et al., 2003) indicate a link to the AO/NAO and teleconnections over a great distance, while in the Aral Sea region the NAO is thought to contribute to the current desiccation (Small et al., 1999) and anomalous precipitation events over the last 30 years (Nezlin et al., 2005).

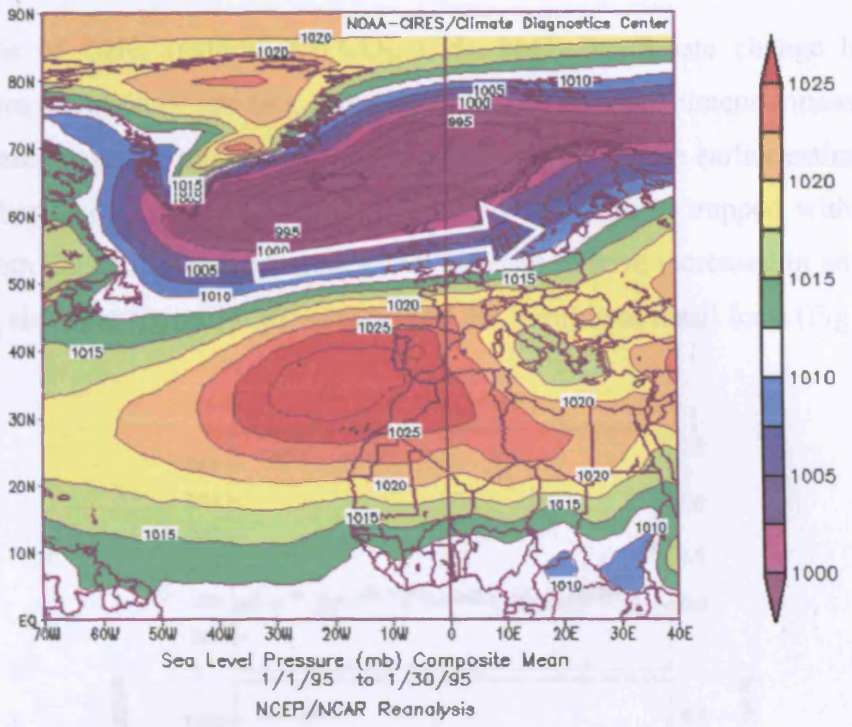

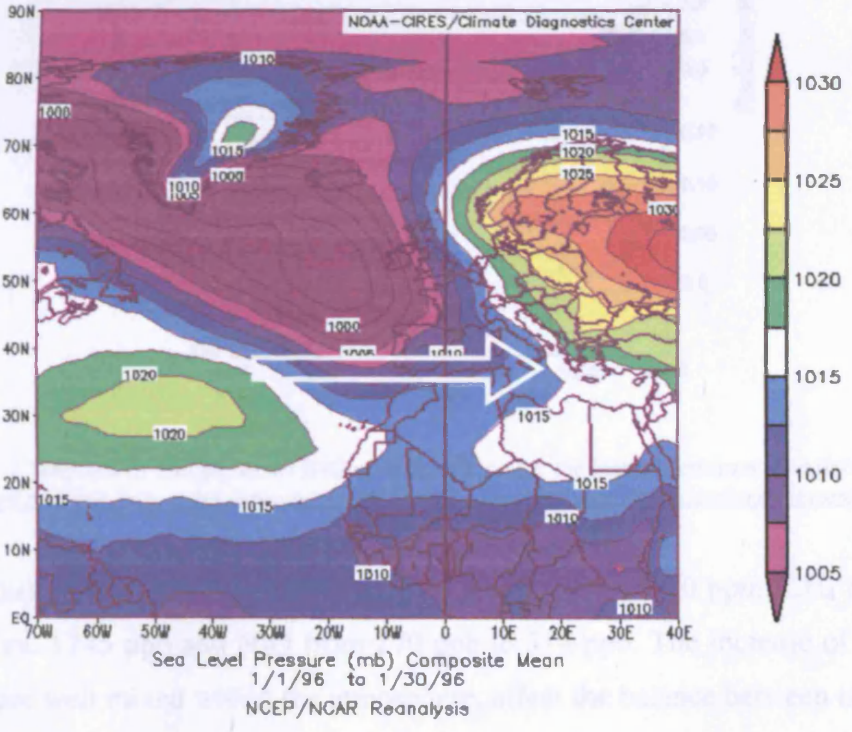

Figure 1.6. Positive (top panel) and negative phase (lower panel) of the NAO and subsequent effect upon the transport of moisture, illustrated by white arrow across Scandanavia, Europe and North Africa. See text for details. Image created 25/04/06 and provided by the NOAA-CIRES Climate Diagnostics Center, Boulder Colorado from their Web site at http://www.cdc.noaa.gov/

1.6.6 Greenhouse Gas (GHG) emissions

The role of GHG (particularly CO_2, CH_4, N_2O) in climate change has received enormous attention of late (e.g. Houghten et al., 2001). Instrumental measurements of these gases began in the latter half of the 20th century, while earlier estimates of their atmospheric concentration is determined from air bubbles trapped within ice cores from both Greenland and Antarctica. All are seen to have increased in an exponential fashion since the Industrial Revolution and the burning of fossil fuels (Fig 1.7).

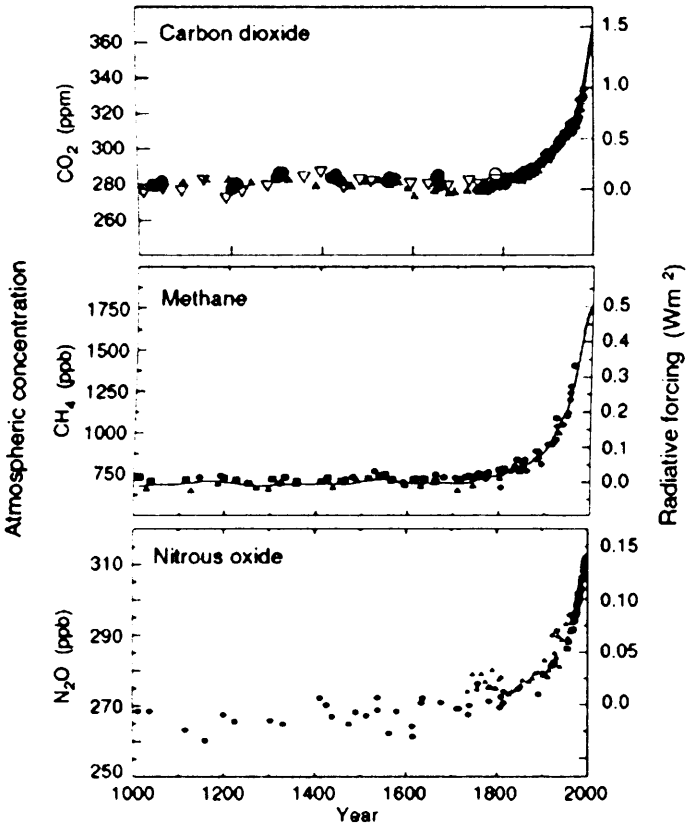

Figure 1.7. Records of atmospheric GHG concentrations for the last millennium. Available online at http://www.msc-smc.ec.gc.ca/education/scienceofclimatechange/understanding/greenhouse_gases/index_e.html

Since this period CO_2 has risen from ca. 280 ppm to ca. 370 ppm, CH_4 from ca. 700 ppb to ca. 1745 ppb and N_2O from 270 ppb to 314 ppb. The increase of these gases, which are well mixed within the atmosphere, affect the balance between incoming and outgoing radiation at the top of the troposphere by trapping part of the outgoing infrared radiation (Reynaud et al., 1997) and as such represent a global radiative forcing (Jones and Mann, 2004), estimates of the contribution of which are illustrated (Figure 1.7). In contrast to solar forcing however, GHG concentrations can represent

both the cause and an effect of climatic change. Increased levels of CH_4 is a prime example of this, CH_4 acts to warm the climate and as it does so, melting permafrost in arctic regions releases more CH_4. The small changes in CO_2 and CH_4 prior to the industrial period (Figure 1.7) are seen to represent not forcing of temperature but rather changes in terrestrial carbon intake as a consequence of temperature changes (Gerber et al., 2003).

Chapter Two

The Aral Sea

2.1 Introduction

The first part of this chapter introduces the concept of saline lakes, the processes responsible for their formation and where they are found. The second part then focuses exclusively on the Aral Sea, its location, climate and provides details of the lake in both its pre desiccation state and the changes that have occurred since 1960 and the onset of irrigation that has led to the current regression. The chapter concludes with the aims and objectives of this thesis.

2.1.1 Distribution and characteristics of saline lakes

Emmanuel de Martonne (1928) recognised two principal types of drainage regime; the first category of through-flowing or ocean drainage he termed exorheism and the second of interior basin drainage he termed endorheism. Thus in exorheic regions rivers rise and reach the sea, conversely endorheic regions (Figure 2. 1) are characterised by the failure of their rivers to reach the sea, instead; i) flowing either into a terminal lake as is the case with the Volga into the Caspian, the Amu Darya and Syr Darya into the Aral Sea or ii) simply terminating, more likely than not in the middle of a desert or iii) winding up as large inland deltaic regions, the best example of which is the Okavango in southern Africa. A third category arheism was proposed on the basis of no rivers rising in an area whatsoever due to extreme aridity, (de Martonne, 1928). As with endorheic regions arheic lakes are found in semi-arid and arid environments. Although it should be noted that some allogenic rivers (those that derive their discharge from outside the local area) can flow through arheic regions to the sea, the prime example being the lower reaches of the Nile (Hutchinson, 1957) and the southern Atacama where three perennial rivers which form in the Andes flow across the desert into the Pacific (Cooke et al., 1993).

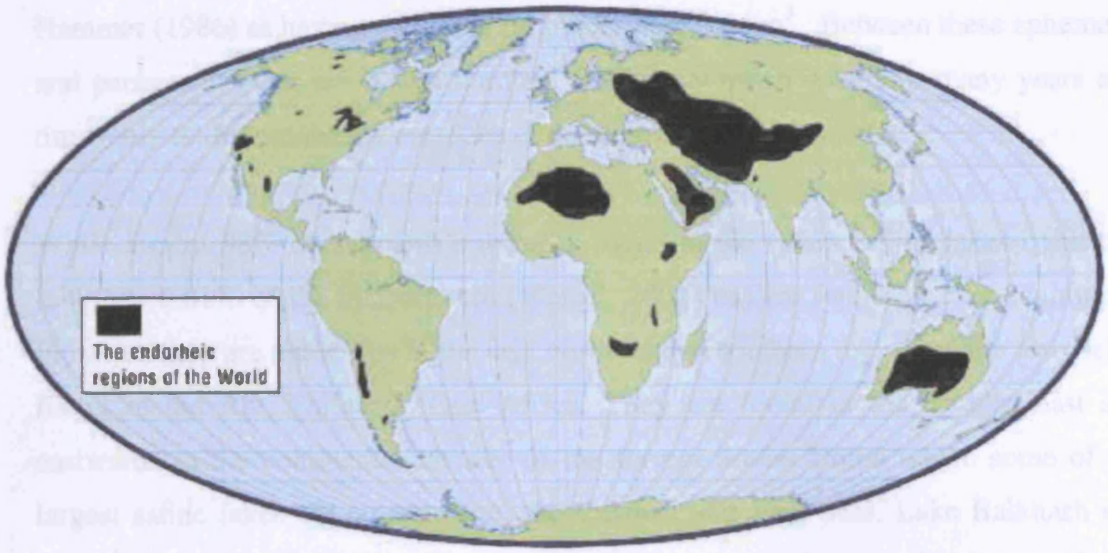

Figure 2.1. The endorheic regions of the world.

The term athalassic has also been used to describe all inland waters which have not been joined to the sea during recent geological time, regardless of salinity. This would then preclude the Caspian Sea as it was part of the both the Tethys and Samartian Seas, but not the Aral Sea which while similarly being linked to the former Neogene seas has been subjected to severe desiccation, and thus contains no relict marine waters (Hammer, 1986)

2.1.2 Lake formation

The formation of saline lakes is dependent on three basic conditions: i) the outflow of water must be restricted, ii) evaporation must exceed the inflow, and iii) the inflow must be sufficient to maintain a standing body of water (Eugster and Hardie, 1978). Importantly saline lakes may be either 'closed' with no fluvial input in which case their hydrological balance is maintained by precipitation and possibly groundwater or they may be 'terminal' lakes, receiving inputs from rivers, precipitation and groundwater as is the case with the Aral Sea. In either instance there will be no surface outflow. A wide range of saline lakes exist, from ephemeral waterbodies (playas or sebkhas) formed by deflation processes which may occupy essentially planer surfaces with no discernible depression or standing water (Yechili and Wood, 2002), to large permanent lakes formed by tectonic activity such as the Aral, Caspian and Dead Seas. However, saline lakes of this size are very much in the minority with only 24 listed by

Hammer (1986) as having a volume of greater than 0.5 km^3. Between these ephemeral and permanent lakes are a vast number which may retain water for many years at a time, only to dry out during episodes of extreme drought.

While almost 98% of the earth's water is found in the ocean, saline lakes constitute less than 0.01% of the hydrosphere (Wetzel, 2001) but are found on every continent. In Africa they are numerous in the arid northern and southern regions while also being found in the Rift Valley of East Africa. They are found in the Middle East and eastwards to the continental interior of the former Soviet Union where some of the largest saline lakes are situated (i.e. the Caspian and Aral Seas, Lake Balkhash and Issyk-kul) and on the Tibetan Plateau and northern India. In Australia they are found in every state and are especially numerous in the semi-arid regions of Victoria, while in North America they are found in the western Provinces and States of Canada and the United States. In Europe they are found in the Seewinkel region of Eastern Austria, Hungary, The Carmargue region of southern France, Spain and Yugoslavia (Williams, 1981). They also appear on the Bolivian Altiplano, and in Antarctica.

2.1.3 Salinity classification.

The classification of salinity in saline lakes, defined as *the sum total of all ion concentrations, or total ion concentration* (Hutchinson, 1957; Williams and Sherwood, 1994), has been the focus of much attention (Williams, 1981; Williams and Sherwood, 1994). All lakes will have an ionic composition of some degree thus what constitutes the boundary between freshwater lakes and salt lakes? Hammer (1986) reviews the history of the debate; a limit of 5 g/l TDS was proposed by Beadle (1974) while Williams (1981) suggested a limit of 3 g/l TDS which is higher than others, particularly that of 0.5 g/l TDS determined at the Venice Symposium on the classification of brackish waters (Societas Internationalis Limnologiae, 1959).

The measurement of salinity may be acquired directly or indirectly, the former simply through the determination of ionic content and its summation, while the determination of density or conductivity provides effective means of the indirect measurement of salinity. Conductivity is the more widely used and is the measure of electrical current flow through a solution, the ease of which will increase as ionic content increases and

thus reflect total ionic concentration. In this particular study conductivity (measured as log10 μS/cm or backtransformed to mS/cm) is used to measure salinity, the classification of which (table 2.1) is based on the modified Venice Symposium Classification for north African waters (Gasse et al, 1987).

Table 2.1. Classification of water based upon salinity content (from Reed, 1997)

Classification	Salinity (g/l TDS)	Conductivity (mS/cm)
Metasaline/hypersaline	40->300	>50
Eusaline	30-40	40-50
Polysaline	20-30	25-40
Mesosaline	5-20	7.5-25
Oligosaline	0.5-5	0.5-7.5
Freshwater	<0.5	<0.5

2.1.4 Brine composition

While marine waters are dominated by chlorides, and freshwater systems generally dominated by carbonates, the anion composition of saline lakes varies between carbonates, sulphates and chlorides in combination with major cations: Na^{+}, Mg^{2+} and Ca^{2+} (Fritz et al., 1999). The anion composition of saline lakes is diverse compared with cation composition in which Na tends to dominate the vast majority of brines with those dominated by Ca^{2+} and Mg^{2+} generally less common (Eugster and Hardie, 1979). The source of the ionic constituents is generally a result of chemical weathering reactions combined with the interaction of inflowing ground and surface waters with bedrock and surface deposits (Fritz et al., 1999). Atmospheric precipitation and the fallout of solutes may also add to the ionic composition (Wetzel, 2001). The process of weathering and brine composition means that the local and regional geology is responsible for much of the ionic composition, thus lakes in different regions will be dominated by different ions. For example those in the northern Great Plains are dominated by sulphates, East Africa by carbonates and those in Australia by chlorides (Reed, 1997). Consequently a few particular major brine types exist for saline lakes across the world (Table 2. 2)

Table 2.2. Brine types and resultant mineral formation. (From Eugster and Hardie, 1979)

Brine type	Saline mineral
Ca-Mg-Na-(K)-Cl	Antarcticite, Bischofite, Carnallite, Halite, Sylvite, Tachyhydrite
Na-(Ca)-SO_4-Cl	Gypsum, Glauberite, Halite, Mirabilite, Thenardite
Mg-Na-(Ca)-SO_4-Cl	Bischofite, Bloedite, Epsomite, Glauberite, Gypsum, Halite, Hexahydrite, Kieserite, Mirabilite, Thenardite
Na-CO_3-Cl	Halite, Nahcolite, Natron, Thermonatrite, Trona
Na-CO_3-SO_4-Cl	Burkeite, Halite
Na-CO_3-SO_4-Cl	Mirabilite, Nahcolite, Natron, Thenardite, Thermonatrite

Evaporative concentration of solutes leads to the precipitation of minerals (Table 2.2), subsequently affecting the composition of the remaining waters (Eugster and Hardie, 1979). This is controlled by the chemical divide concept (Hardie and Eugster, 1970). As the concentration of solutes increases, mineral precipitation will remove some of the reacting solutes, consequently those with the lowest original concentration will see this decline still further while that of the other solutes increases. The early precipitation products being those that are least soluble and result in the formation of carbonate and gypsum after which point brine concentration must increase many fold prior to the deposition of other salts such as Halite (NaCl), Mirabilite ($Na_2SO_4 \bullet 10H_2O$) and Thenardite (Na_2SO).

2.2. The Aral Sea: regional physical geography, geology and climate

The Aral Sea is surrounded by a range of physical environments (Figure 2.2). To the east lie the mountain ranges of Tien Shan (7439 m) and Pamir (7495 m) while those of the Kopet Dag (2246 m) border Iran in the south. The west of the region is dominated by flat, low-lying arid and semi-arid plains in which the Karakum and the Kyzylkum deserts are located.

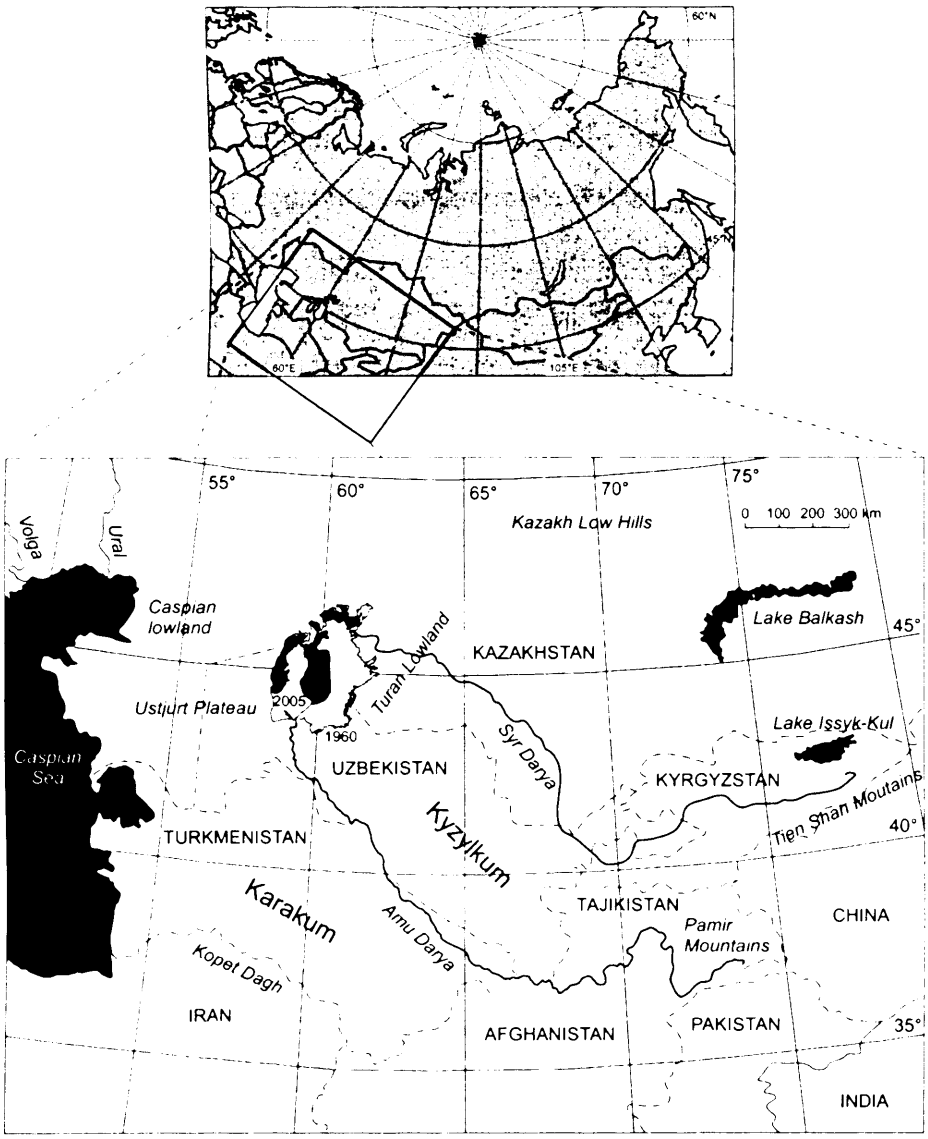

Figure 2.2. Map showing the location of the Aral Sea and the physical geography of Central Asia. Courtesy, Philippe Sorrel.

Flowing through the two deserts are Central Asia's two largest rivers, the Amu Darya (formerly The Oxus) and Syr Darya (The Jaxartes) and the large inland waterbodies of the Caspian and Aral Seas. The low lying areas in the west of the region, which (along with much of the Tien Shan and Pamir) comprise much of the former Soviet Central Asia, are formed of two broad structural basins separated by the higher Ustyurt Plateau (264 m). The westerly depression is occupied by the Caspian Sea (-28 m a.s.l.) and the eastern by a large topographic low, the active graben of the Turanian Plain. The broad topography of this region is a result of a combination of Neogene tectonic activity and marine regressions and transgressions, the largest of which resulted in the Sarmatian Sea covering an area from the Mediterranean eastwards to the Tien Shan and Pamir (Letolle and Mainguet, 1993).

After the Sarmatian Sea retreated eastwards towards the basins of the present day Black and Mediterranean Seas, regional tectonics led to the isolation of the Turanian plain from the rest of Asia (Walter and Box, 1985). The majority of the Turanian plain has an elevation of less than 200 m a.s.l., occupies an area of ca. 3.5m km^2 (Letolle and Mainguet, 1993) and runs from the base of the Kopet Dag escarpment (Figure 2.2) in a northeasterly direction into western Siberia, with which it is linked by the Tourgai depression or corridor, a large down-faulted area filled with horizontal Jurassic, Cretaceous, Palaeogene and Neogene strata (Nalivkin, 1973). In the centre of the Turanian plain are two large depressions formed by Pliocene tectonic activity: i) the Sarykamysh basin, the deepest part of which is presently occupied by Lake Sarykamysh and ii) 100 km to the north east, the larger Aral Basin in which the present day Aral Sea is located (Figs. 2.2 and 2.3).

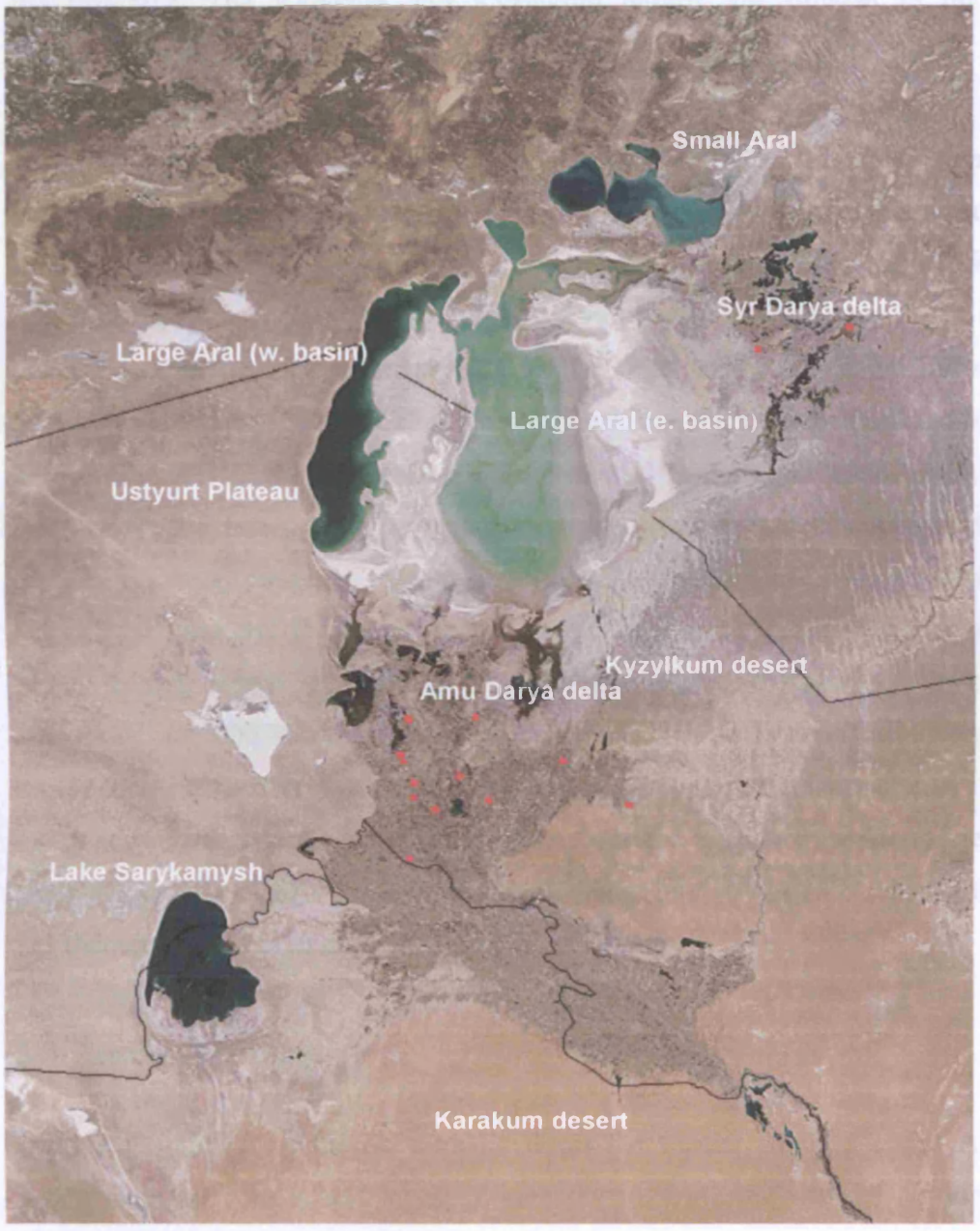

Figure 2. 3. Landsat satellite image of The Aral Sea and surrounding area. The red spots are heat anomalies (e.g. fires) detected by the satellite. The large white areas are salt crusts. Image taken 23/09/05 and available online at http://rapidfire.sci.gsfc.nasa.gov. Downloaded 30/12/05.

The Aral Sea is bordered on all sides by arid and semi arid zones, known locally as the Priaralye. The Karakum and Kyzylkum deserts are situated to the south, southwest and east and the Ustyurt Plateau to the west (Figs. 2.2 and 2.3).

The Karakum is primarily covered by elongated ridges of fixed sand topped by smaller mobile barchan dunes (Lydolph, 1977). Numerous salt pans are situated in low lying depressions. The centre of the desert is a basin filled with 400-600m of fluvial sediments deposited as a result of a former course of the Amu Darya (Walter and Box, 1985) and the presently dry Uzboi river valley is situated between the Sarykamysh and the Caspian Sea. Two smaller rivers, the Tzendhen and the Murghab with headwaters in the Kopet Dag and north east Afghanistan respectively, simply terminate in the desert. The Kyzylkum desert is located between the lower reaches of the Amu Darya, (much of which acts as a frontier between Turkmenistan and Uzbekistan) and Syr Darya rivers, and borders the eastern shore of the Aral Sea. Sands in this region tend to be stabilised and there are Palaeozoic outcrops at elevations of 700-900m. The Zerevshan river flows through the Kyzylkum terminating in the desert just short of the Amu Darya. The Ustyurt Plateau (264 m a.s.l.) lies between the Aral and the Caspian Seas and is fringed by fault zones on all sides, the resultant cliffs are termed "chinks" and lead to scarps bordering the Aral Sea that are 25m high in the north and almost 200m high in the south.

2.3 Regional climate

Lydolph (1977) states that in climatic terms the former Soviet Central Asia (the region most relevant in this investigation) extends from the Kopet Dag northwards into central Kazakhstan and from the Caspian in the west to the Tien Shan and Pamir mountains in the east. The vast surface area and dramatically differing relief allows the region to be split in to two zones; the mountainous Tien Shan and Pamir and the low lying arid Turanian Plain which may be further subdivided into a Northern (Kazakhstan) and Southern (Iran-Turanian) zone (Lioubimtseva, 2004).

During the winter months the anticyclonic Siberian High, which dominates Eastern and Central Siberia and Kazakhstan, extends its influence over the whole of Central Asia (Figure 2.4). Cold continental air is transported along the westward extension of

its southern periphery bringing northerly surface winds to the region. This results in the deposition of loess at the foot of the Kopet Dag (Mainguet et al., 2002) and the generally north-south alignment of dunes in the Karakum and Kyzylkum deserts (Figure 2.3 shows this to be particularly prominent in the latter). In the north, mean January temperatures are commonly -10°C to -15°C, with those in the south averaging 0°C (Glazovsky, 1995). The extreme conditions result in ice cover of both the Aral and Caspian Seas during the winter months.

The location and intensity of the Siberian High will control the penetration into the region of Mediterranean storms brought in with the westerly jet stream. Subsequently, low rates of winter precipitation are common over the north Tien Shan. Despite these low values, an increasing trend has been exhibited over the last 60 years possibly due to enhanced influence of the westerlies and a gradual weakening of the Siberian High, a possible consequence of rising global temperatures (Aizen et al., 2001; Mokhov, 2004). As the impact of the Siberian High is reduced further to the south and east (Figure 2.4), the result is an increased influence of southwest cyclonic circulation and subsequent influx from the Eastern Mediterannean of moisture laden air masses across Central Asia to the southern Tien Shan and Pamir with higher winter precipitation than is seen further northwards (Aizen et al., 2001). These will be more prominent when cyclones are situated in the Eastern Mediterranean resulting in increased precipitation over the Levant rather than covering the Western Mediterranean which leads to drier conditions (Enzel et al., 2003).

Teleconnections are thought to further influence the precipitation regime, negative (positive) phases of the NAO leading to increased (decreased) winter precipitation over the Tien Shan and the low lying plains, conversely positive (negative) NAO phases result in increased (decreased) aridity (Aizen et al., 1999; Small et al 1999) with the probability of above average winter precipitation in the Tien Shan and Pamir being just 0 – 7% (Aizen et al., 2001). Arpe et al., (2000) have also suggested a link between the El Nino Southern Oscillation (ENSO) and fluctuating levels of the Caspian Sea since the 1840s. Whether this can be said to hold true for the Aral Sea is uncertain.

As the Siberian High weakens in the spring and summer months (Figure 2.4), the area falls under the influence of the Azores High. Embedded cyclonic storms that have formed in the Eastern Mediterranean are transported eastwards by the westerly jet stream. Isotopic analysis from all GNIP stations in Central Asia confirm that it is this source, rather than the Indian Monsoon that provides moisture to the region (Kreutz et al, 2003).

Low levels of precipitation (155-270 mm) occur over the northern Turanian Plain with mean summer temperatures of 26°C - 28°C. The Iran Turanian Plain to the south receives the majority of its annual rainfall (ca. 100 mm) in the winter and spring largely associated with the northern migration of the Iranian branch of the polar front and the ensuing cyclonic activity. Mean July temperatures in this region are 32°C (Lioubimtseva, 2004) and precipitation is low, a result of the movement into the region of warm and dry tropical continental air from the south.

Throughout the year the dominant surface winds are from the north, north-east and north-west. Severe dust storms are also common throughout the region and in particular across the Aral Sea itself, their frequency and magnitude having increased since the mid 1970s (Zavialov, 2005), with material from the bed of the newly exposed eastern basin being transported south and south west (O'hara et al., 2000).

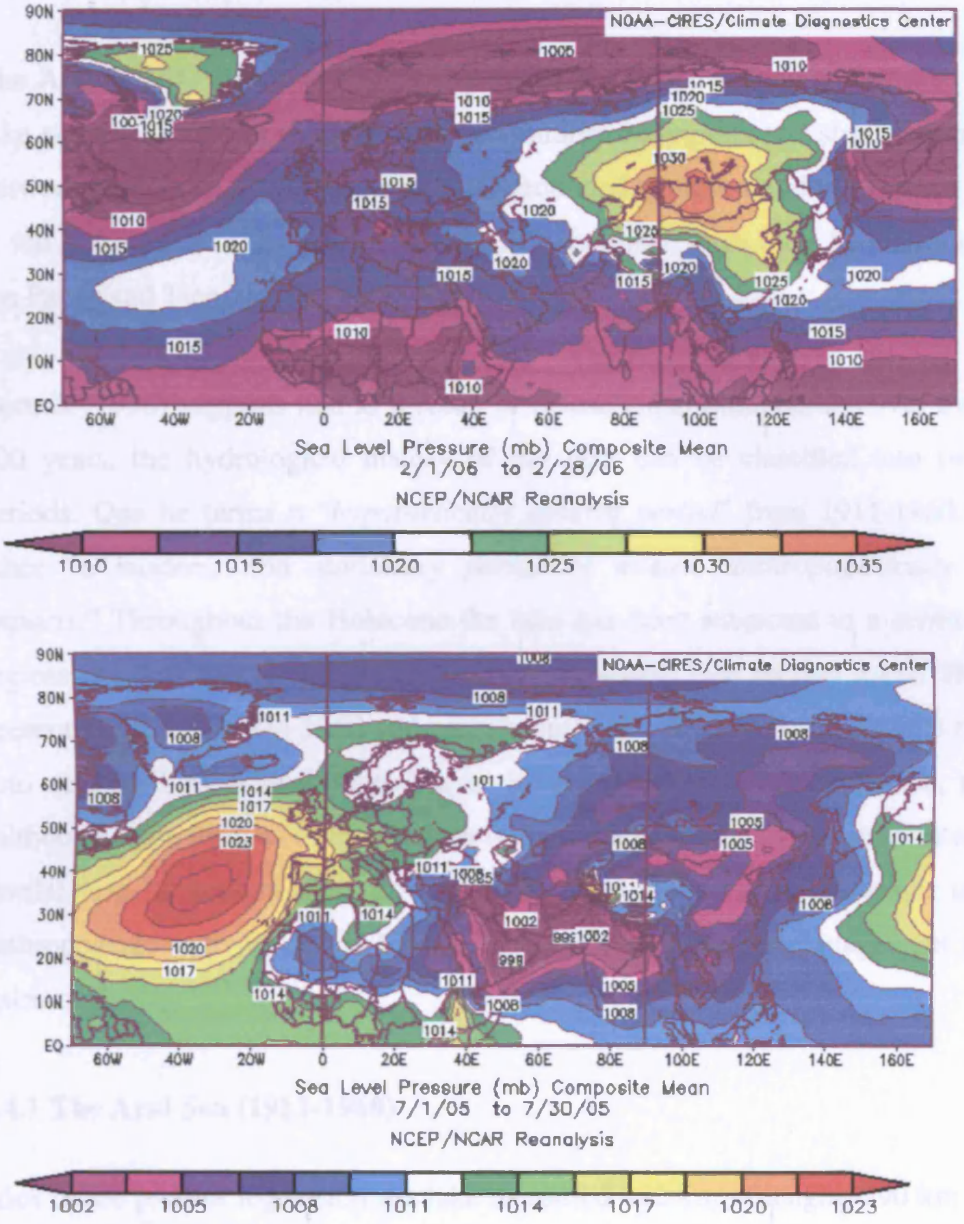

Figure 2.4. Mean global sea level pressure (hPa) for January 2006 (top panel) and b) July 2005 (lower). The extent of the Siberian High across Asia in February can be clearly seen. By July this has disappeared. Image created 25/04/06 and provided by the NOAA-CIRES Climate Diagnostics Center, Boulder Colorado from their Web site at http://www.cdc.noaa.gov/

2.4 The Aral Sea - characteristics

The Aral Sea (43°24'N - 46°56'N and 58°12'E - 61°59'E) is a large saline terminal lake situated in one of the world's major endorheic regions and straddles the border between Kazakahstan and Uzbekistan. Surrounded by desert and semi desert zones, it is fed by the Amu Darya and Syr Darya rivers which have their headwaters high in the Pamir and Tien Shan respectively.

Bortnik (1996) suggests that as a result of instrumental observations over the last ca. 100 years, the hydrological history of the lake can be classified into two major periods. One he terms a "*hypothetically natural period*" from 1911-1960, and the other "*a modern, non stationary period of intense anthropogenically induced impacts.*" Throughout the Holocene the lake has been subjected to a series of these regressions both anthropogenic and naturally induced (see section 2.11). This latter, present phase, started in 1960 and consequently any description of the lake must take into account both what is regarded as its conventionally natural period, pre 1960 (although some form of human impact due to irrigation may have contributed to lake levels) and its present state of low lake level, the severity of which is due to anthropogenic activity in the form of irrigation and the mismanagement of water resources.

2.4.1 The Aral Sea (1911-1960)

Prior to the present regression the lake measured 492 km in length, 290 km in width and had a shoreline of nearly 3000 km (Figure 2.5). Surface elevation was 53 m a.s.l., it had a surface area of 66,140 km^2 (making it the world's fourth largest lake by area) and a water volume of 1012 km^3 (Ginzburg et al., 2003). Instrumental measurements from 1911-1960 recorded an average salinity of 10g/l (Glazovsky, 1995).

Figure 2.5 shows the bathymetric profile of the lake prior to the current regression. During high lake levels, it is composed of three basins: the northern basin has a maximum depth of 35 m and is connected to the much larger southern portion of the lake by the shallow Berg Strait (13 m). The southern portion comprises an extensive shallow eastern basin, bordering the Kyzylkum desert, with a maximum depth of

29 m and a deeper western basin from which it is separated by the north-south running Arkhangelskiy horst, the highest point of which is Vozrozhdeniya Island. This western basin reaches a maximum depth of 67 m (-15 m a.s.l.) at its western edge in a trough bordering the Ustyurt Plateau. The average depth of the entire lake is 16.1 m. Three large islands Barsakelmes (133 km^2), Kokaral (273 km^2) and Vozrozhdeniya (216 km^2) combine with as many as 1100 smaller islands, particularly along the shallow eastern and south eastern coasts, to provide a land surface area of 2230 km^2 within the lake itself (Glazovsky, 1995).

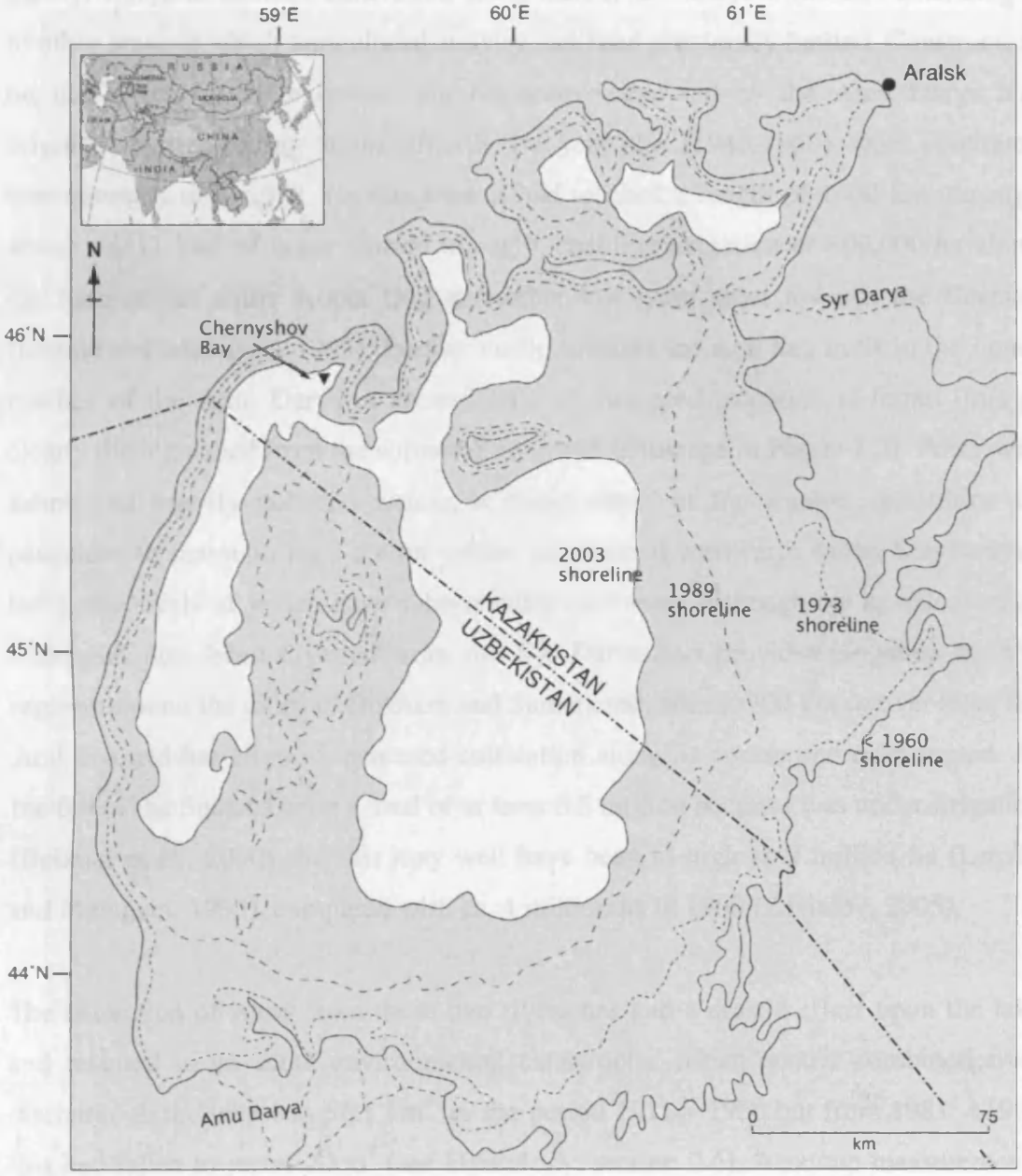

Figure 2.5. The present-day extent of the Aral Sea in relation to the pre-desiccation 1960 lake level. The coring location of Chernyshov Bay in the western basin of the Large Aral is also indicated (see chapter 3 for more details). Image courtesy of the drawing office at University College London.

2.4.2. The Aral Sea post 1960

In 1950 the Soviet government set about the implementation of a series of plans to increase agricultural output, particularly that of cotton, in the Central Asian Republics (Letolle and Mainguet, 1993). This involved the diversion, through an extensive network of reservoirs and canals, of large volumes of water from the Amu Darya and

the Syr Darya to increase cultivation along their river valleys while also extending it to other areas in which agricultural activity had been previously limited. Construction on the largest of these canals, the Karakum Canal fed by the Amu Darya had originally started during Stalin's fourth five year plan (1946-1950), work continued intermittently until 1982. By this time it had reached a length of 1600 km, through which ca. 11 km^3 of water flowed annualy, enabling irrigation of 800,000 ha along the base of the entire Kopet Dag and other low-lying areas towards the Caspian (Letolle and Mainguet, 1993). Further north, towards the Aral Sea itself in the upper reaches of the Amu Darya, a second area of increased irrigation is found (this is clearly distinguished from the surrounding desert landscape in Figure 2.2). From here, saline and heavily polluted waters, a direct result of the wanton application of pesticides to maintain high cotton yields, are drained westwards to the Sarykamysh Lake, the levels of which have subsequently increased. Although not as extensively, water has also been diverted from the Syr Darya and provides irrigation for the regions around the cities of Bukhara and Samarkand, almost 700 km upriver from the Aral Sea and has allowed increased cultivation along its course and delta region. At the fall of the Soviet Union a total of at least 6.5 million hectares was under irrigation (Boomer et al., 2000) and this may well have been as high as 9 million ha (Letolle and Mainguet, 1993), compared with ca. 4 million ha in 1960 (Zavialov, 2005).

The extraction of water from these two rivers has had a drastic effect upon the lake and resulted in an acute environmental catastrophe. Mean annual combined river discharge to the lake was 56.1 km^3 for the period 1911 – 1960 but from 1981 – 1990 this had fallen to just 4.2 km^3 (see Hydrology, section 2.6). Accurate measurements of discharge into the lake are difficult (because of the retention of water in the delta regions of the Amu Darya and Syr Darya) however it is thought that this had increased to ca. 9 km^3 during the 1990s (Zavialov, 2005). The decline in river discharge from its two feeder rivers which accounted for the vast majority of the lakes hydrological input has seen a rapid decrease in lake level area, and volume (table 2.3). This has resulted in significant changes in the bathymetry of the lake occurring in the shallow eastern basin bordering the Kyzylkum desert (Figure 2.3). There the maximum depth is now only 7m (Zavailov et al., 2003) compared with 29m in 1960 (Salokhiddinnov and Khakinov, 2004).

By 2001 the eastern coast of the sea had receded by as much as 100 km (Kravtsova, 2001). Consequently there has been a reduction in the number of small islands while the larger Barsakelmes, Korakal and Vojredzhneya Islands have all since become attached to the surrounding land. The maximum depth of the western basin still exceeds 40 m (Zavailov et al., 2003). The morphology of this basin is such that changes in the coastline of this area are thought to be negligible, with a recession of no more than 1 or 2 km, (Kravtsova, 2001). These two basins remain, for the time being, connected by the narrow (3km) shallow (1.5 m) Kundalay Strait.

The greatest change however had occurred by 1989 by which time the lake level had fallen to 39 m a.s.l. forming two separate water bodies, the northern Small Aral and the southern Large Aral (Figure 2.3). This has acted as a respite for the Small Aral fed by the Syr Darya (Figure 2.6, table 2.3) which over the last 14 years has seen its lake level rise to ca. 41 m a.s.l. and its salinity drop to 17-18 g/kg (Friedrich and Oberhaensli, 2004). GIS derived measurements indicate that the Small Aral now has a surface area of 2930 km^2 and a volume of 21.5 km^3 (Friedrich and Oberhaensli, 2004) compared with pre 1960 surface area measurements for the northern basin of ca. 6000 km^2 and a water volume of ca. 80 km^3.

Table 2.3. Changes in level, area, volume and salinity of the Aral Sea as a whole and after splitting into the Large and Small Aral in 1989. Sources 1= Ginzberg 2003; 2 = Bortnik and Chistayeva 1990; 3 = Friedrich and Oberhaensli (2004).

Year	**Level (m a.s.l.)**		**Area (km^2)**		**Volume (km^3)**		**Salinity (g/l)**	
1960 [1]	53		66000		1012		10	
1989 [2]	39		36500		328		29	
	Small	**Large**	**Small**	**Large**	**Small**	**Large**	**Small**	**Large**
2003 [3]	41	30	2930	17350 E = 12140 W = 5210	21	109 E = 32.8 W = 76.2	17-18	E = ca. 150 W = 82

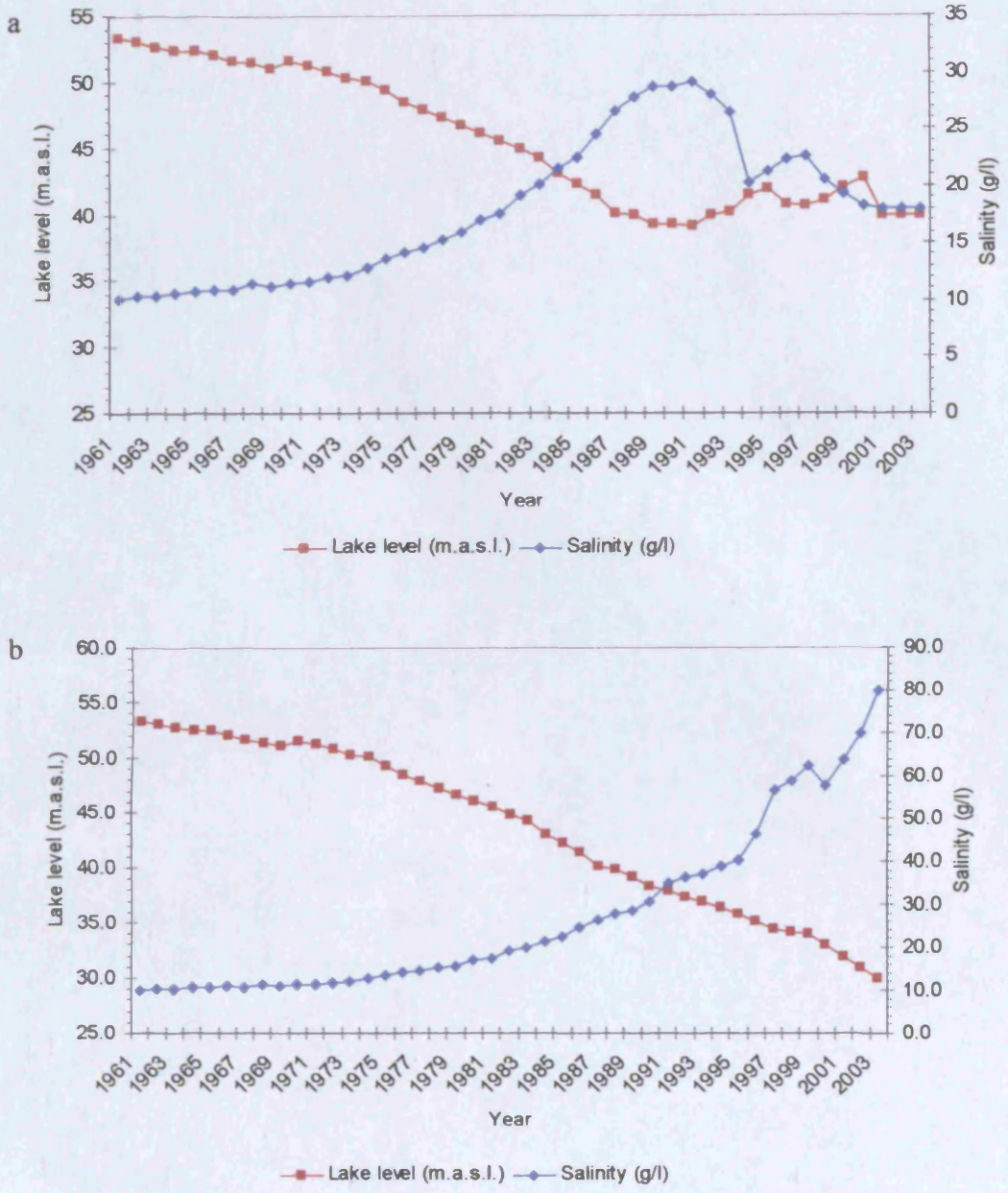

Figure 2.6. Lake level decline and corresponding salinity increase of the Small Aral Sea (a), showing recovery after the splitting of the lake into two waterbodies in 1989 and (b) lake level decline and salinity increase of the Aral Sea as a whole and the western basin of the Large Aral following separation. (Note axes are on different scales).

As the stability of the Small Aral has increased, the Large Aral continues to decrease in size and increase in salinity (Figure 2.6, table 2.3). At the time of writing, the surface area is just 17,350 km^2 and volume 109 km^3. Of this the shallow eastern basin has an area of 12,140 km^3 and volume of 32.8 km^3 while the western basin has an area of 5210 km^2 and a volume of 76.2 km^3. The current regression has led to increased continentality within the region with the expansion of desert zones on to the

former sea bed and into the deltaic regions of primarily the Amu Darya and Syr Darya (Saiko and Zonn, 2000). Local climatic conditions will now be considered in more detail

2.5 Local climate

2.5.1 Precipitation

Mean annual on lake precipitation ranges from just 105 mm to 150 mm and is greatest over northern areas (Letolle and Mainguet, 1993, Zavialov, 2005). Importantly no significant decline in overall precipitation has been observed during the present regression with mean values from 1960 – 2001 similar to those prior to the current period of extensive irrigation. Nor has the timing of precipitation changed, with highest values seen to occur during May and October (Figure 2.7). The contribution of precipitation to the hydrological balance has changed but this is due to the reduction of lake area (Zavialov, 2005).

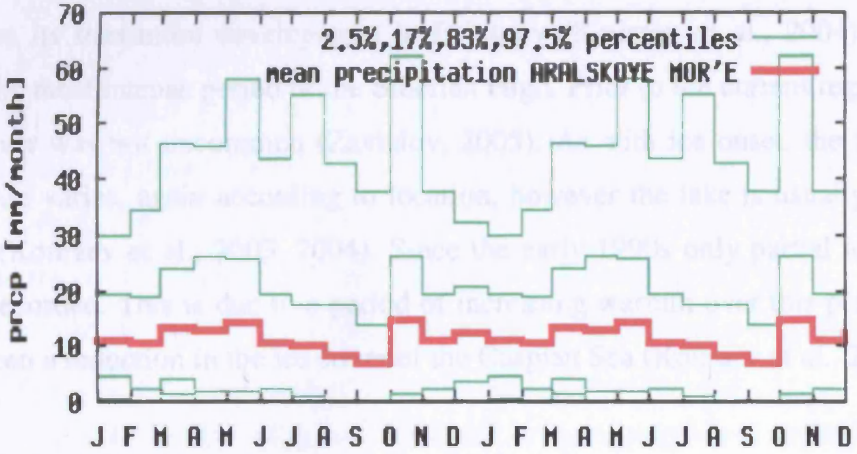

Figure 2.7. Monthly precipitation over a two-year cycle (averaged from records spanning 1906 – 1999) from Aralsk (46°47'N - 61°14'E) a former port on the shore of the Small Aral. Image created using data freely available on the Climate Explorer wesite (http://climexp.knmi.nl/start.cgi)

2.5.2 Temperature

Summer daytime temperatures in the Kyzylkum desert are often close to or over 40°C while those at night may fall as low as - 5°C (Letolle and Mainguet, 1993). Mean January air temperatures over the lake range from ca. - 6°C in the south to ca. - 12°C

in the north while in summer mean air temperatures are ca. 26°C, considerably less than the surrounding deserts and an excellent example of the ameliorating effects of a large body of water upon air temperature. Although there appears to be a general trend in increasing temperatures across Central Asia and indeed globally, it is suggested that mean, maximum and minimum temperature changes in the vicinity of the Aral Sea have changed by as much as 2 - 6°C with the current desiccation directly responsible for as much as 50% of that increase (Small et al., 2001a). By 2004, winter temperatures were thought to have fallen by 2 – 3°C (Zavialov, 2005).

2.5.3 Sea surface temperature and ice cover

Before the present low lake level stand SSTs averaged 11°C, varying between - 0.5°C in winter to 24 – 25°C in summer. Due to the extreme winter temperatures, ice cover is ususal on the lake, its duration varying according to location. Freezing commences in the north coastal regions by mid-November and the south by the end of November. Ice cover on the open water does not occur until the end of December and in the western coastal zone ice formation does not occur until January. Ice cover usually reaches its maximum development in February (Kouraev et al., 2004), coinciding with the most intense period of the Siberian High. Prior to the current regression 90% ice cover was not uncommon (Zavialov, 2005). As with ice onset, the timing of its break up varies, again according to location, however the lake is usually ice free by April (Kouraev et al., 2003, 2004). Since the early 1990s only partial ice cover has been recorded. This is due to a period of increasing warmth over this period that has also seen a reduction in the ice cover of the Caspian Sea (Kouraev et al., 2004).

2.6 Hydrology

From 1911 until the collapse of the fSU instrumental monitoring of the Aral Sea had been fairly rigorous. Since 1990 however, a combination of the breakdown of this network under the newly formed Central Asian States and the current regression which has left many former monitoring stations redundant, literally high and dry, has led to a decline in regular systematic instrumental observations. The last decade or so has seen data being derived from a combination of those monitoring stations which do remain, from several recent expeditions (Nourgaliev et al, 2003; Zavialov et al,

2003; Friedrich and Oberhaensli, 2004); satellite imagery (Kravtsova, 2001, Peneva et al, 2004) and mathematical modelling, (Salokhiddinnov and Khakimov, 2004).

Table 2.4. Hydrological inputs to the Aral Sea and surface evaporation since 1911.

Years	Combined river Runoff (km^3)	Precipitation (km^3)	Evaporation (km^3)
1911-1960	56.0	9.1	66.1
1961-1965	39.4	8.9	68.9
1966-1970	47.0	7.4	68.6
1971-1975	21.2	6.0	58.5
1976-1980	11.6	6.4	50.3
1981-1985	2.0	6.1	45.9
1987-1990	7.9	5.4	41.4
1991-2000	9	1-4	15-25

2.6.1 River discharge

The Amu Darya and Syr Darya rivers combine to provide the majority of the hydrological inputs to the lake (table 2.4) and are fed by snowfields and glacial meltwaters in the Pamir and Tien Shan. The Amu Darya with a catchment of 534,764km^2 (Figure 2.8) has its headwaters in the Pamir and runs through the mountainous regions of Tajikistan and the Karkum desert for a total of 2574 km before entering the southern section of the Aral. Much of the history of lake level fluctuations is intertwined with the Amu Darya. Not only does it provide the majority of water for irrigation but it has altered its course naturally. During the late Pleistocene, the Amu Darya is believed to have discharged directly into the Caspian Sea. By the start of the Holocene, flow was diverted northwards to the Aral Basin. The reasons for this are unclear. Nurtaev (2004) suggests that regional tectonics were responsible, whereas increased fluvial discharge associated with increased moisture availability at the beginning of the Holocene is considered to be the main factor (Rubanov, 1991; cited in Boomer et al., 2000). Throughout the Holocene, the Amu Darya has at times flowed directly towards the Caspian Sea, usually via the Sarykamysh depression only to divert northwards to the Aral Sea due to the excessive build up of alluvial deposits (Letolle and Mainguet, 1993; Glazovsky, 1995; Tsvetsinskiya et al., 2002). The Syr Darya, 2212 km in length and with a catchment

of 782,669km^2 (Figure 2.8) originates in the Tien Shan, crosses Kyrgyzstan and the Kyzylkum desert before entering the Aral Sea to the north.

The flow of both rivers is greatest during the summer months (JJA). However, as a result of evaporation, transpiration and bed filtration see their flows become substantially diminished before they discharge into the lake (Nezlin et, al., 2004). Although fresh at their headwaters, a combination of evaporation and the influx of salts (the latter a consequence of the salinisation of cultivated areas along their riverbanks) results in the discharge of oligosaline water into the lake (Letolle and Chesterikoff, 1999). The annual average combined river discharge to the Aral Sea from 1911-1960 was 56 km^3 (table 2.4) the inception of irrigation resulted in a rapid decline, so much so that for several years during the 1980s very little or no water from either river reached the lake (Figure 2.9).

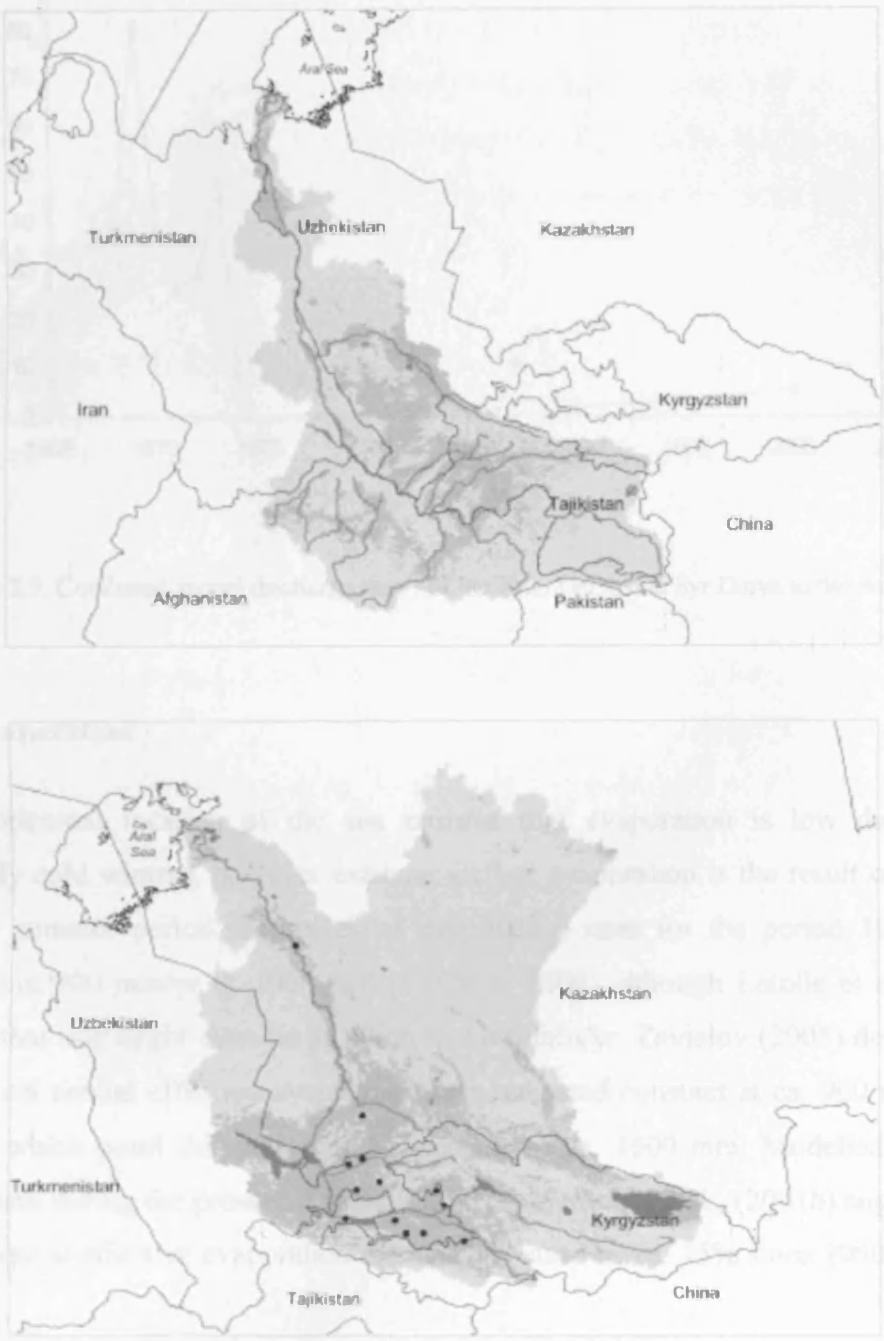

Figure 2.8. The Amu Darya (top) and Syr Darya drainage basins. Source; World Resource Institute. Image available Online at: http://earthtrends.wri.org/maps_spatial/maps_detail_static.cfm?map_select=343&theme=2 **Downloaded 01/05/05.**

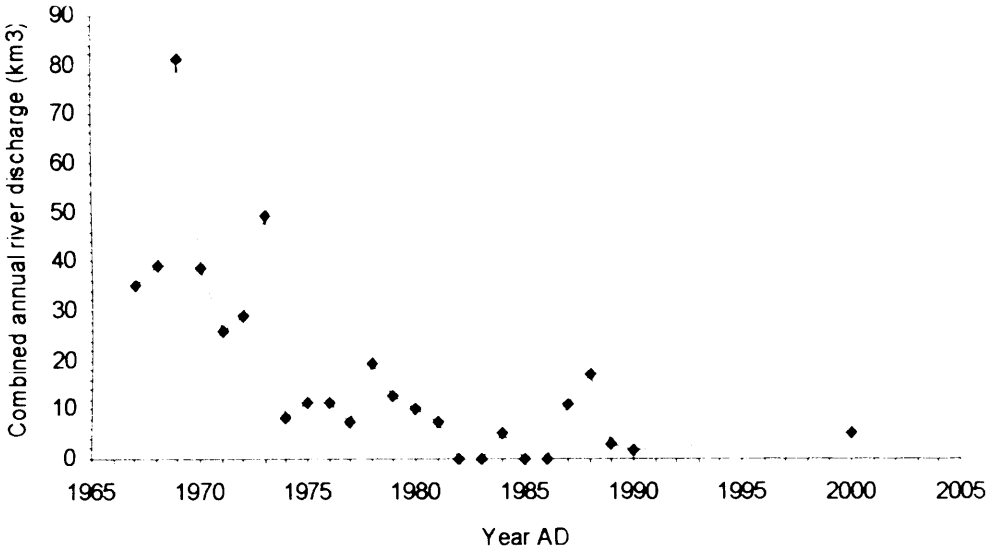

Figure 2.9. Combined annual discharge (km^3) of the Amu Darya and Syr Darya to the Aral Sea.

2.6.2 Evaporation

The continental location of the sea ensures that evaporation is low during the extremely cold winters, however extreme surface evaporation is the result of the hot and dry summer period. Estimates of evaporation rates for the period 1960-1990 range from 900 mm/yr to 1000 mm/yr (Chub, 2000) although Letolle et al (2004) suggest that this might even be as much as 1300 mm/yr. Zavialov (2005) determined that the net annual effective evaporation rate remained constant at ca. 900 mm until 1993 at which point this was seen to increase to ca. 1600 mm. Modelled rates of evaporation during the present desiccation phase by Small et al., (2001b) suggest that the net annual effective evaporation rate has increased by ca. 15% since 1960.

2.6.3 Groundwater input

Jarsjo and Destouni (2004) estimated that the pre 1960 groundwater input to the Aral Sea ranged between 0-5 km^3/yr and had the potential to account for ca. 12% of the total fluvial inputs. A combination of water balance expressions and hydraulic gradient analysis led them to suggest two groundwater scenarios dependant upon groundwater depth, one where the rate of input is unchanged and another where it may increase by as much as 200%. While this latter figure is the absolute upper limit,

it can be said with confidence that groundwater input is now more important to the hydyological balance of the lake than pre 1960. Even if unchanged, at a limit of 0-5 km^3/yr this has risen from 12% of the fluvial inputs to measuring at times 100% of the combined river discharge of recent years (table 2.4). The salinity of groundwater in the areas immediately surrounding the lake are seen to range from 1 – 15 g/l (Letolle and Mainguet, 1993).

2.7 Hydrochemistry

Pre 1960, the annual salt balance was controlled primarily by river discharge which accounted for a total of 29 million tonnes. Other sources include the atmospheric precipitation of salts which measured 4 million tonnes, whilst those derived from groundwater inputs ranged from 0.7-3.3 million tonnes (Glazovsky, 1995). Measured salinity for the period 1911-1960 averaged ca. 10 g/l, the ionic component being dominated by $Cl^- > SO_4^{-2} > Na^+$ (table 2.5). As river discharge declined, salinity increased exponentially reaching 30 g/l prior to the division of the lake (Letolle and Chesterikoff, 1999), being further aided by an increase in the rate of evaporation.

Table 2.5. Distribution of major anions and cations in the Aral Sea in the summer of 2002. (Friedrich and Oberhaensli, 2004); 1947 data from Blinov in Letolle and Mainguet, (1997); 1952 data from Bortnik and Chistayeva (1990)

	Anions and cations (g/kg)							
Location	Cl^-	SO_4^{-2}	HCO_3^-	Na^+	Mg^+	Ca^{+2}	K^+	Total
Tastubek Bay								
Small Aral	5.96	6.10	0.22	3.67	1.00	0.55	0.20	17.68
Tschebas Bay								
Large Aral (eastern basin)	31.59	24.10	0.43	18.60	5.26	0.75	1.11	81.83
Chernishov Bay								
Large Aral (western basin)	31.56	24.52	0.41	18.87	5.15	0.75	1.17	82.42
Aral 1947 (g/l)	3.50	3.31	0.19	2.26	0.49	0.56	0.08	10.39
Aral 1952 (g/l)	3.55	3.21	0.16	2.26	0.12	0.48	0.54	10.32

Friedrich and Oberhaensli (2004) report surface water salinity of the relatively stable Small Aral of 17-18 g/l. Salinity levels of the two basins of the Large Aral have increased rapidly since the division of the lake and the loss of inflow from the Syr

Darya. Surface water salinity values for the less studied shallow eastern basin are estimated to be between 155-160 g/l (Mirabdullayev et al., 2004) compared with 82 g/l in the western basin, (Zavialov et al., 2003; Friedrich and Oberhaensli, 2004). The increased salinity of the western basin is not simply a result of local evaporation but also due to the advection of salt (possibly as much as 900 million tonnes from 1990-2002) from the eastern basin (Zavialov, 2005). The surface water salinity of 82 g/l was found to be overlying bottom water with salinity of between 96 g/l (Zavialov et al., 2002) and 110 g/l (Friedrich and Oberhaensli, 2004). The increased salinity has resulted in the oversaturation of $CaSO_4$ and precipitation of gypsum and will, due to evaporative concentration, see the formation of other salts notably mirabilite, glauberite and epsomite. The pH of the lake is seen to vary from 8.0 – 8.5 both prior to and during the present regression.

2.8 Thermal stratification

Prior to 1960 density stratification of the water column is reported to have been minor (Zavialov et al., 2003). Consequently summer stratification would generally commence in May with the thermocline at a depth of 10 – 15 m (Ginzburg et al., 2003) by November the declining air temperatures and decreasing solar radiation would result in the loss of stratification (Letolle and Mainguet, 1993). The dramatic rise in salinity has seen the development of a strong density gradient in the western basin of the lake in particular (Bortnik, 1992, Zavailov et al., 2003; Friedrich and Oberhaensli, 2004) and resulted in effects on water circulation (Zavialov et al., 2003; Sirjacobs et al., 2004) and the vertical mixing of waters.

Zavialov et al., (2003) determined that during November 2002 in the western basin, the water column was thoroughly mixed at all stations measured with depths of less than 20m. In deeper waters (ca. 40 m) surface water temperatures and those in the water column were stable at ~10.6°C to depths of ca. 20 m after which point there was a temperature inversion and oxygen depleted bottom waters of >14°C. They hypothesise that these warmer bottom waters formed during the summer in the shallow Eastern basin and are flushed through the narrow channel that now separates the two basins of the Large Aral (Figure 2.3) and that the strong density gradient prevents the complete mixing of the water column. This corresponds with evidence

obtained from a water depth of 22 m by Friedrich and Oberhaensli (2004) in August 2002; while the water column was mixed with temperatures of ca 22°C to a depth of ca. 4-6 m, a cold intermediate layer (ca 12-16°C) was found to overlay the highly saline bottom waters (ca. 19°C) which was also depleted in oxygen (Figure 2.10).

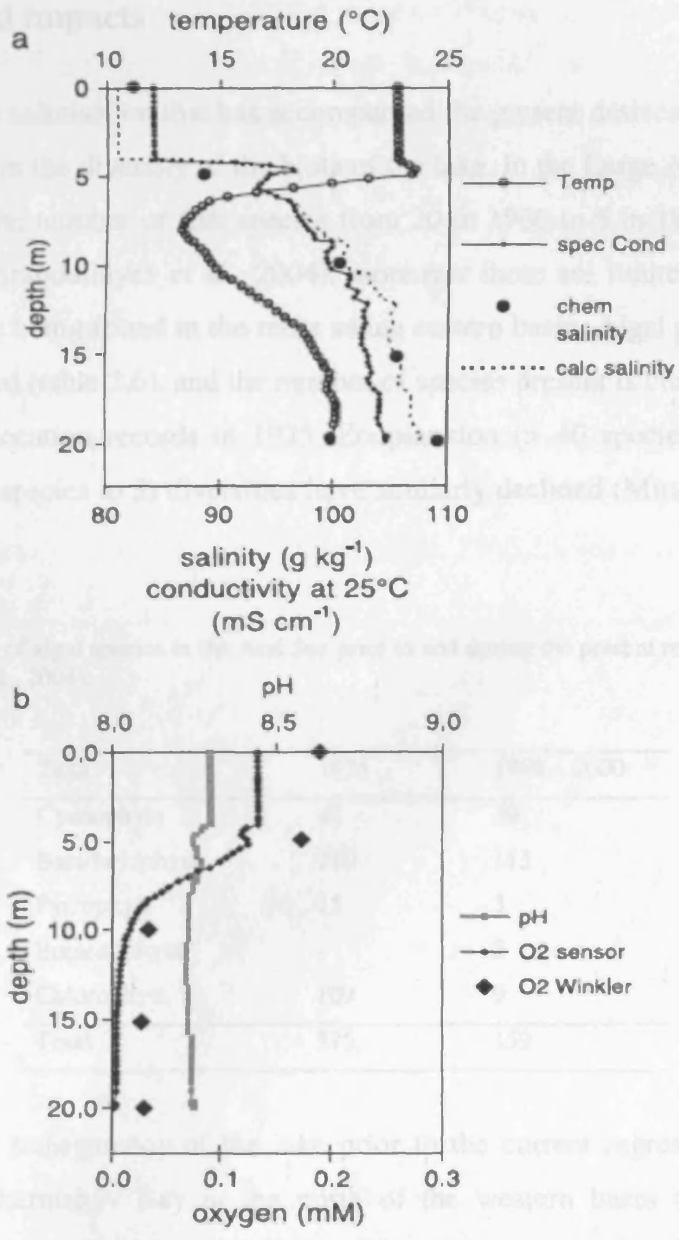

Figure 2.10. Vertical profiles of (a) temperature (°C), conductivity (mS cm^{-1}), chemically determined salinity (g kg^{-1}) and salinity calculated from conductivity (g kg^{-1}) and (b) pH and dissolved oxygen. (From Friedrich and Oberhaensli, 2004).

Friedrich and Oberhaensli (2004) suggest this cool intermediate layer and highly saline bottom layer is a result of the water column failing to mix completely in winter

and that complete autumnal overturn will be prevented by the strong density gradient leading them to conclude that the western basin has become meromictic. This state has led to the presence of hydrogen sulphide and anoxic bottom water conditions in the western basin.

2.9 Ecological impacts

The progressive salinisation that has accompanied the present desiccation has brought about a decline in the diversity of the biota of the lake. In the Large Aral this has seen a reduction in the number of fish species from 20 in 1960 to 5 in 1998 and just 2 in recent years (Mirabdullayev et al., 2004), moreover these are limited to the western basin, with none being found in the more saline eastern basin. Algal populations have similarly suffered (table 2.6), and the number of species present is currently only 50% that of pre desiccation records in 1925. Zooplankton (> 40 species to just 4) and zoobenthos (60 species to 3) diversities have similarly declined (Mirabdullayev et al., 2004).

Table 2.6. Number of algal species in the Aral Sea prior to and during the present regression (from Mirabdullayev et al., 2004).

Taxa	1925	1999 – 2000
Cyanophyta	41	30
Bacillariophyta	210	115
Pyrrophyta	15	3
Euglenophyta	-	2
Chlorophyta	109	9
Total	375	159

The high water transparency of the lake prior to the current regression [27 m was recorded for Chernishov Bay in the north of the western basin (Romashkin and Samoilenko, 1953 in Zavialov, 2005) and 24 m for an undisclosed location in the western basin (Zenkevitch, 1963)] allowed the development of large amounts of benthic vegetation in especially, *Tolypella aralica*, *Vaucheria dichotoma*, *Cladophora gracilis* and *Zostera nana*, by 2003 all of these had disappeared form the lake (Mirabdullayev et al., 2004) a combination of the hypersaline conditions and

reduced water transparency, the latter caused by the resuspension of sediments and increased phytoplankton productivity (Orlova and Rusakova, 1999).

2.10. Human activity in the Aral Sea Basin

Chapter one highlighted the internal and external forcing mechanisms that are capable of inducing climatic fluctuations and environmental change. In the Aral Sea Basin however, human activity particularly in the form of irrigation and military conflict leading to the destruction of these facilities is perceived as having direct consequences for lake levels during the late Holocene (Letolle and Mainguet, 1993, 1997; Kes, 1995).

Human habitation in the region stretches back into the Palaeolithic with new sites being recently discovered around the shorelines of the Small Aral (Boroffka et al., 2005). Many later Neolithic sites of the Kelteminar culture have been found to the south along the entire length of the now dry bed of the Uzboi River in modern day Tukkmenistan and Uzbekistan (Figure 2.11) (Letolle and Maiugnet, 1997; Letolle, 2000; Tsvetsinskaya et al., 2002).

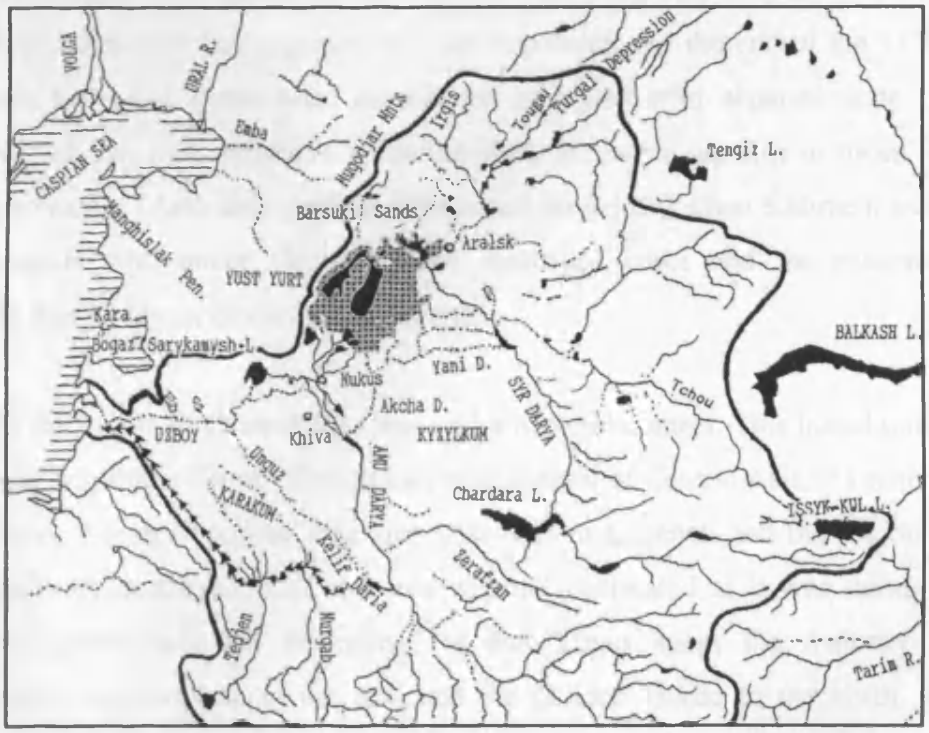

Figure 2.11. Sketch map of the Aral Sea Basin highlighting the Aral Sea pre 1960 (hatched) and during the present regression (solid), Lake Sarykamysh and the course of the Uzboi to the Caspian Sea. (Courtesy Rene Letolle).

Artefacts including small projectile and harpoon points belonging to this period indicate a fishing economy (Bajpakov et al., 2005; Boroffka et al., 2005). By the early Bronze Age the expansion of forest and forest steppe vegetation southwards from the Urals is indicated by increasing projectile point size and importantly abundant finds of horse bones, a species much more suited to a steppe environment than the semi arid desert zones in the region today (Boroffka et al., 2005). The changes witnessed during these periods may be ascribed to natural forcing mechanisms. It is not until the later Bronze and Iron Ages however and the creation of the Khorzem State centred around the city of Ugrench and the lower reaches of the Amu Darya, that irrigation practices and agricultural activities began in earnest. The development of irrigation in the region is seen to have reached a peak during the 7^{th} – 5^{th} centuries BC, a consequence of the movement of the Persians into the region and the accompanying technological advancements. This period also saw the start of irrigation along the Syr Darya (Andrianov, 1995). Khorzem was subject to both Greek and Roman influence until ca. 400 AD (along with that from East Asia due to the development of the Silk Route) at which point the Ephaplites (White Huns) invaded the region and many of its irrigation facilities were utterly destroyed (Letolle and Maigunet, 1997). There then followed a series of invasions of the region by the Turk empire (522 – 744 AD) bringing with them Islam and then a period of Arab expansion. By the end of the 11^{th} century AD Khorzem had once again been established as a powerful separate state ruled by the Khwarazmshahs, with extensive irrigation facilities much superior to those one thousand years previously (Andrianov, 1995). This lasted until 1220 when Khorzem was invaded by the Mongols who under Genghis Khan destroyed cities and the extensive irrigation facilities that had been developed at Urgench.

By 1223 the whole of Central Asia was under Mongol control. This lasted until 1370 when the similarly ruthless Timur (Tamerlane) took control of Central Asia. As with the Mongols before him, the all important irrigation networks in Urgench and the region south of the Aral Sea were destroyed. That the area was not decimated as it was during the Mongol interlude (particularly the beginning) is that Timur spent the majority of his time campaigning against Iran to the east and the Golden Horde to the north. This and the reluctance of his successors to engage in military campaigns resulted in a golden age for Central Asia in particular during the 15^{th} century AD when notably the city of Samarkand was seen to flourish (Soucek, 2004).

2.11 Holocene lake level fluctuations

A keen interest in the history of the Aral Sea and its former regressions developed at the end of the 19th century (e.g. Wood, 1875; Tillo, 1877). This was continued into the early 20th century notably by Berg (1908) who was the first to organise direct measurements of lake level in 1900. Since then a combination of archaeological, geomorphological and palaeolimnological studies have highlighted several phases of lake level fluctuations. These suggest that the current regression is just one of many to have occurred during the present interglacial as a consequence of natural and/or anthropogenic activity.

2.11.1 Former shorelines

The most obvious indicator of former lake levels is the presence of terraces representing former shorelines, eight of which have been discovered (Figure 2.12) at elevations of: 71-72 m, 57-58 m, 54-55 m, 53 m, 43-44 m, 40-41 m, 35-36 m and 31 m (Boomer et al., 2000). Towards the end of the Pleistocene/early Holocene the Amu Darya flowed directly into the Caspian Sea (Boomer et al., 2000). A shoreline thought to be representative of this period was found at 31 m a.s.l. in bottom sediments of what is now the Small Aral and the eastern basin of the Large Aral, indicating lake levels similar to those of the present day. The highest terrace of ca. 72 m, located principally on the west and north flanks of the lake, was until recently, thought to be representative of a period of prolonged increased moisture ca. 5 ka BP (uncalibrated), however, recently discovered in-situ palaeolithic artefacts have been found at an elevation of 60 m (Boroffka et al., 2004) appearing to rule out the existence of this terrace during the Holocene. Furthermore, at this elevation the Aral Sea would have stretched to the Caspian and left distinct traces of its coastline along all its shores. Consequently this terrace is more likely to be a remnant of an earlier Neogene transgression (Kes, 1995).

It would appear that the maximum sea level elevation during the Holocene is one of ca. 58 m (Kes, 1995; Boroffka et al., 2004). Radiocarbon dating of material from this shoreline has shown a wide range of (uncalibrated) dates; 12 ka BP, 5 ka BP, 3 ka BP and 2-3 ka BP suggesting that this level has been reached on numerous occasions.

Those terraces discovered that lie between the high and low stands are seen to indicate periods of stability during lake level fluctuations, the shoreline at 53 m representing the 1911-1960 phase.

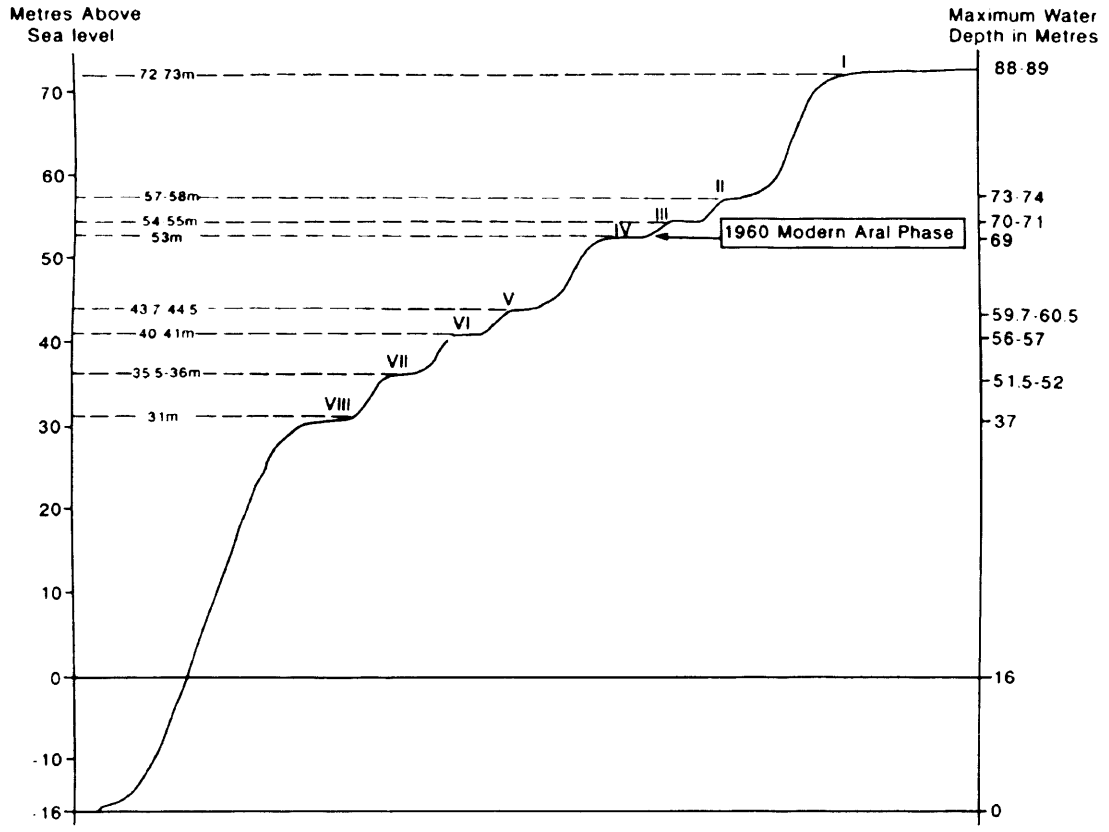

Figure 2.12. Summary diagram of eight Aral Sea lake levels and associated palaeoshorelines and corresponding maximium depth. From Boomer et al., (2000).

2.11.2 Palaeolimnology

Early investigations of sedimentation processes were undertaken by Zenkevitch (1953) who determined that transgressive phases were seen to result in predominantly terrigenous sedimentation, comprised mainly of suspended material brought in with the rivers but also some aoelian input. Authegenic and biogenic sedimentation was found to dominate periods of low lake level. More detailed analysis was possible due to the collection of almost 100 cores from the central part of the Aral Sea during the late 1970s, highlighting the episodic nature of the lake level changes. Rubanov (1982) noted the presence of 5 phases of gypsum deposition and one of peat like sediment in the eastern basin, all indicative of previous regressions. The first two gypsum

horizons were dated to ca. 6 ka BP and ca. 5 ka BP (uncalibrated), falling during the supposed pluvial phase of the Holocene climatic optimum before any irrigation was occurring, suggesting that this climatic episode in this region might not have been particularly stable. A third level is dated to ca. 3.6 ka BP and is thought to reflect an earlier period of irrigation (Letolle and Mainguet, 1997).

The deposition of peat like sediments is dated to ca. 1.6 ka BP and corresponds to low lake levels further to the south (Maev et al., 1999). Rubanov (1982) suggests that the peat layer extends for ca. 10, 000 km^2 in the centre of the eastern basin of the Large Aral and is concordant with the deposition of mirabilite in the western basin. Examination of diatoms, molluscs and ostracods within this horizon highlight a decline in brackish water species and a corresponding increase in those favouring shallow freshwater habitats (Aleshkinsaya et al, 1996; LeCallonnec et al., 2005). It is suggested that during this period the western basin was maintained as a shallow or series of shallow hypersaline lakes (Letolle and Mainguet, 1993) and that the peat-like deposits in the eastern basin were a result of the migration of the Syr Darya towards the centre of the lake and the maintenance of a small, shallow fresh/brackish water body (Boomer et al., 2000).

A fourth gypsum layer is dated to ca 1.0 ka BP and is felt to be concordant with the destruction of irrigation systems by the Mongols, while a fifth undated layer is felt to be contemporaneous with low lake levels during the 13^{th}-15^{th} centuries (Letolle and Mainguet, 1993a). Carbon and oxygen isotope analysis of ostracods from an undated 1.5 m core from the northern basin (Boomer, 1993) highlight three episodes of increased values and salinity. Chemical analysis (Mg/Ca and Sr/Ca) from this site and two others in the western basin suggest that during these phases salinity did not reach that of 1991 (35 g/l). Juggins, (1997) had to obtain estimates of salinity from ostracod remains due to the lack of preservation of diatom valves in sediments obtained from the northern basin, these indicate a low lake level stand at ca. 1485 AD.

Smaller scale fluctuations have been seen to occur since the early 1700s. Remains of Saxual (*Haloxylun aphyllum*) groves dated to 287 ± 5 ^{14}C yr BP (365 ± 65 cal. yr BP/1635 ± 65 AD) have been found at 40 m a.s.l. in the eastern basin and suggest by the early 1700s lake levels remained low. By 1790 levels were similar to those of

1960. Two fluctuations of ca. 3 m, thought to correspond with increased solar activity (Shermatov et al., 2004) are seen to occur at ca. 1830 and ca. 1890 after which, increased precipitation in the region is thought to account for the increased levels which were maintained, with slight fluctuations until 1960.

2.12 Aims, objectives and thesis outline.

This project forms part of the wider ranging CLIMAN project (CLImatic variability and the evolution of huMAN settlement in the Aral Sea Basin). This multiproxy undertaking by participants from Europe and the former Soviet Union and funded by INTAS (Project 00-1030), seeks to obtain a detailed data set from biotic (chironomids, diatoms, dinoflagellates, ostracods, organic isotopes and pollen) and abiotic (geochemistry, grain size analysis, lithological analysis mineralogy and palaeomagnetism) proxies contained within sediments in an 11.12 m core and other shorter cores, extracted from the Aral Sea. This is being supported by new archaeological and geomorphological investigations. The original aim had been to establish a record of lake level fluctuations during the late glacial and present interglacial. It was found however that the main core to be examined encompasses just the last two millennia. Consequently the objectives changed, the goal becoming the determination, at high resolution, of both the extent and the timing of climatic fluctuations in Central Asia and the impact of human activity and water related land-use change in order to add to the growing number of records documenting change across the globe during the climatically sensitive time period of the last 2000 years. This interaction between human activity, climate and environmental processes is currently a major focus of the IGBP-PAGES (Past Global Changes) programme (http://www.liv.ac.uk/geography/PAGESFocus5/aboutF5.htm) an important aspect of which is the determination of baseline conditions which may be subsequently used as a target when attempting to restore ecosystems damaged by anthropogenic activity to their natural state (Dearing et al., 2006).

The primary aim of this project is the determination of lake level fluctuations and the palaeoconductivity of the Aral Sea in both a qualitative and quantitative fashion. An age model will be constructed and the diatom flora contained within an 11.12 m core and a radiometrically dated surface sediment core will be examined at decadal to sub-

decadal resolution. A qualitative assessment of the flora and knowledge of their habitat requirements and known salinity preferences will allow the determination of episodes of high or low lake levels, high salinity or low salinity. A quantitative assessment of the salinity (in this case conductivity) history during the late Holocene will be derived by using a diatom based conductivity transfer function. The record of conductivity will then permit the determination between regressive and transgressive phases. Knowledge of the mean salinity (ca. 10 g/l) from 1911 – 1960 and subsequent well recorded exponential increase to the present day will allow the reliability of the transfer function and reconstructed conductivity to be assessed with the material from the short cores. This will be supported by the analysis of both stable isotopes ($\delta^{13}C$) and C/N of organic matter, the source of which may provide important information regarding the physical environment in and around the lake and its catchment at a given time.

In order to detect the extent of anthropogenic activity within the region, the concentrations of Cd, Hg and Pb will be ascertained in an effort to determine to what extent the region has suffered from trace metal pollution since the onset of the industrial period and earlier episodes of metal contamination observed in Europe and Scandinavia and South America. These will, of course, be dealt with in more detail in the relevant chapters.

The first chapter has dealt with climate change over the past 2000 years on both a temporal and spatial scale and the mechanisms that are seen to be responsible for these changes. The second chapter has introduced and dealt exclusively with the study site, the Aral Sea. The third will provide coring details and establish a chronology. The fourth, fifth and sixth chapters will deal with results from respectively: diatom analysis and the palaeoconductivity reconstruction, $\delta^{13}C$ and C/N of organic carbon and lastly trace element analysis. The final chapter, chapter 7 will provide a summary of the findings of this thesis, while also making recommendations for future work.

The Aral Sea is of course not a sea but a large, saline, inland lake and in this project is treated as such. Therefore terms such as lake level, lake bed etc are used. The Aral Sea is taken to be the name of the lake consequently when referring to the lake by name the term Aral Sea is used.

Chapter Three

Coring details and chronology

3.1 Site selection and coring details

Coring sites for the CLIMAN project were identified by a team from Kazan State University, Russia. Tectonic activity in the region is common, consequently, seismic profiling and echo sounding were undertaken in order to locate suitable sites. Three potential coring locations were identified: Tschebas Bay and Chernyshov Bay located in the east and western basins of the Large Aral, respectively, and Tastubek Bay in the Small Aral (Figure 3.1).

Figure 3.1 Coring sites at Chernyshov Bay and Tschebas Bay in the Large Aral and Tastubek Bay in the Small Aral. Also shown are the former ports of Aralsk (Kazakhstan) and Muynak (Uzbekistan).

As a result of the present regression and subsequent retreat of the lake from the former ports of Aralsk and Muynak (Figure 3.1), any scientific investigation of the lake is fraught with difficulties, primarily access to the lake itself. With no suitable vessels from which to core, material from all three sites was obtained using a Uwitec piston corer mounted on a jetfloat drilling platform (Figure 3.3). The Uwitec piston corer is rope operated and may be used in unlimited depths with coring being driven by a steel weight at the sediment surface. Core sections of up to either 2 m or 3 m in length and with a diameter of 59 mm within plastic tubing may be obtained. A 12 m core was recovered from Chernyshov Bay with coring to further depths being prevented by an impenetrable layer of gypsum. A Uwitec free-fall gravity corer was also used to obtain sediments for ^{210}Pb at AWI in Bremerhaven, Germany (Heim and Friedrich, in review). The details of the cores used in this study are given in table 3.1., it had also been hoped to investigate the core material from Tastubek Bay as well as that from Chernyshov Bay, a preliminary examination of the material collected from this site highlighted the total absence of diatoms. Consequently the analysis of sediment material in this investigation is limited to cores obtained from Chernyshov Bay (Figure 3.1). Here, echo sounding revealed the presence of a shallow shoreline followed by a sharp descent to the lake bottom at a depth of 22 m, where seismic profiles would appear to indicate sedimentation free from slumping, reworking and tectonic activity (Figure 3.2).

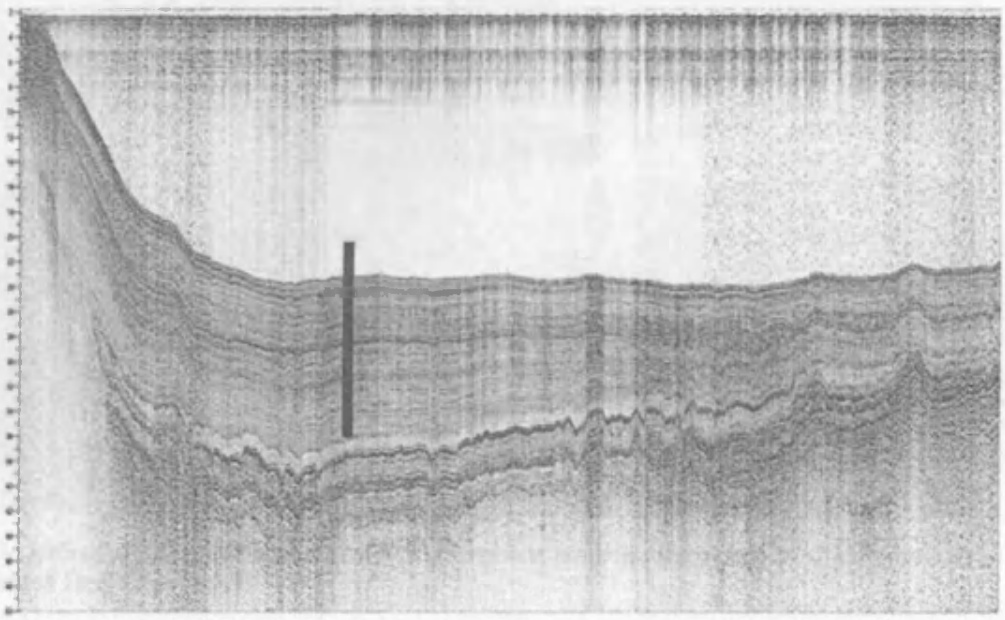

Figure 3.2. Scanning image of the Lake bed at Chernyshov Bay and location of coring site at a depth of 22 m. Image courtesy Danis Nourgaliev.

Upon retrieval, the cores were transported to Almaty in Kazakhstan and from there by rail to GFZ in Potsdam, Germany. When opened, (longitudinally by sawing through the plastic tubing), these were split into an archive and a working half. Both sections were photographed and described and kept refrigerated at 4°C. Magnetic susceptibility was also undertaken at a 3.5 mm resolution with a Bartington M.S.2.E-Sensor with a frequency of 5890 Hz.

Table 3.1. Cores collected from Chernyshov Bay during the CLIMAN campaign of 2002 used in this investigation.

Core location, code and type	Date	Water depth	Interval	Coordinates
Chernyshov Bay				
Ar-21-23	24/08/02	22m	0-650	N 45°58,581; E 59°14,461
Ar-27, 28	25/08/02	22m	600-1150	N 45°58,570; E 59°14,54
Ar-29	26/08/02	22m	1100-1200	N 45°58,512; E 59°14,438
Ar-9 (Gravity)	24/08/02	22m	0-60	N 45°58,616; E 59°14,44

Figure 3.3. Jetfloat drilling platform with UWITEC piston corer photographed at Chernyshov Bay. Image courtesy Hedi Oberhaensli

3.2 Core correlation

The correlation of features in time-series curves generated using the same technique on individual cores enables the overall correlation of the cores obtained from Chernyshov Bay. This may be achieved through sharp peaks in biotic proxies e.g. diatoms or pollen or similar peaks in geochemistry or magnetics (magnetic susceptibility or palaeomagnetism). For the Chernyshov Bay cores, magnetic susceptibility of the six coring sections was used to correlate the material. This resulted in a composite core with a total length of 11.12 m (hereafter referred to as CH-1) with a hiatus having been detected between cores Ar-28 and Ar-29 at 10.28 m. This hiatus was confirmed by magnetic susceptibility and diatom analysis of these sediments which indicate a contemporaneous shift in species composition, with small planktonic species notably *Thalassiosira proschkinae* and *T. incerta* at the top of Ar-29 being replaced by small benthic species in particular *Amphora pediculus* and *Cocconeis neodiminuta* in the basal sediments of Ar-28 (Figure 3.4).

3.3 Sedimentology

The lithology of the core has been described by Philippe Sorrel at GFZ (Sorrel et al., 2006). Most notable are the presence of two gypsum horizons and gypsum crystals and an episode of sub-mm laminations. With the exception of the hiatus between Ar-28 and Ar-29 the core appears to be free of disturbance from tectonic activity, slumping, turbidites or reworking. From 0 – 478 cm the sediments are comprised of dark grey and black silt to sandy clay interspersed with organic mud horizons. Small gypsum crystals were found dispersed within the sediment at 25 cm and 120 cm. From 478 – 501 cm, there is initially a 11.5 cm thick dark brown section of finely laminated sediments (Figure 3.5), underlying these is a further 11.5 cm of finely laminated yellowish-brown sediments. At the base of this zone is a 0.5 cm horizon of gypsum, interspersed with a narrow layer of grey silty clay. From 501 – 1028 cm the sediments are characterised by dark brown silt and sand, the material being interspersed with the remains of filamentous algae. In the lowermost zone from 1028 – 1112 cm (after the hiatus), the sediment consists of thinly laminated grey silty clays. At the base of this zone there is a 10 cm section of material that is characterised by a gypsum horizon which is interspersed by narrow bands of grey silty clay.

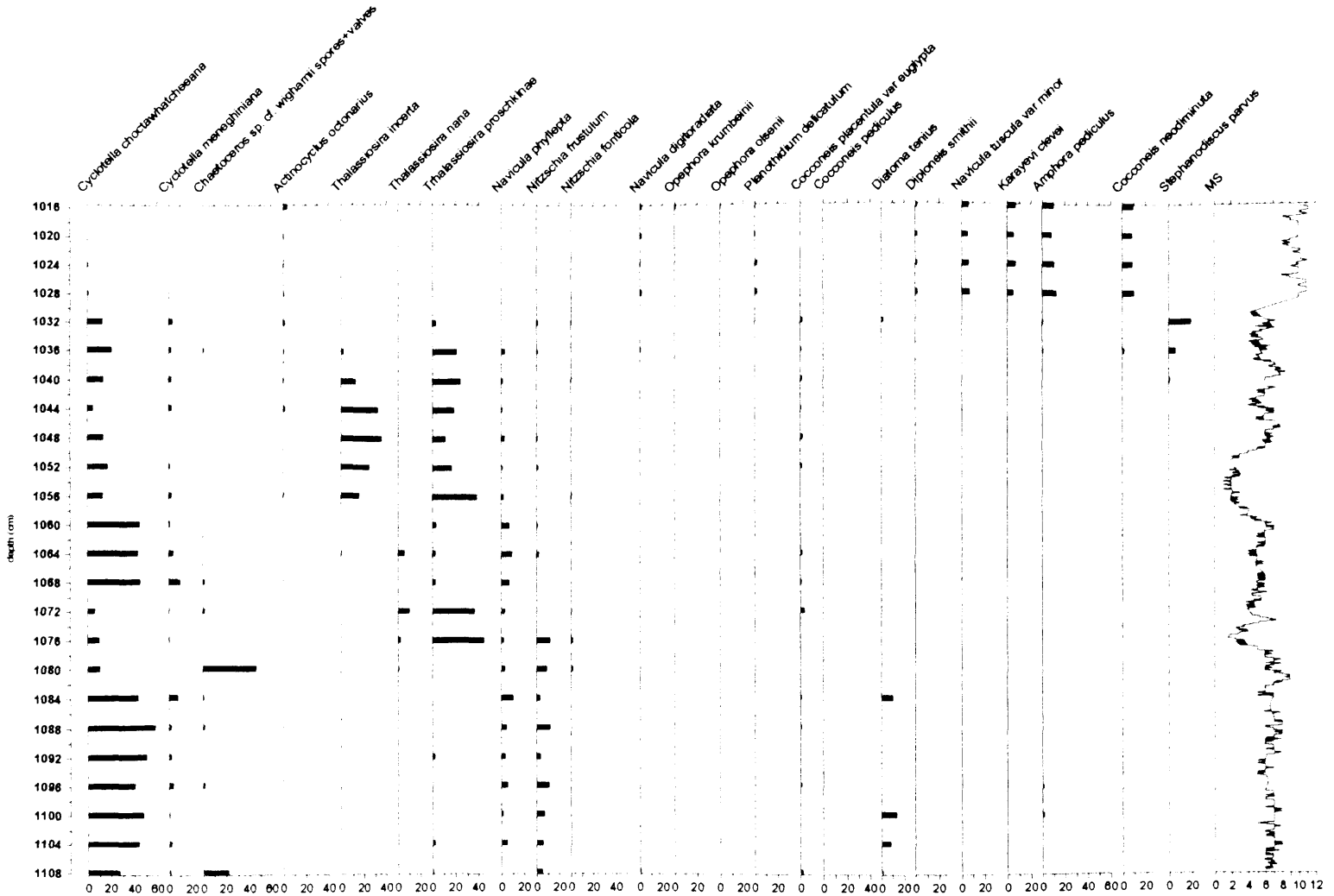

Figure 3.4. CH- 1 diatom flora (> 10%) and magnetic susceptibility from 1016 – 1108 cm. The red reference line at 1028 cm marks the hiatus between Ar-28 and Ar-29.

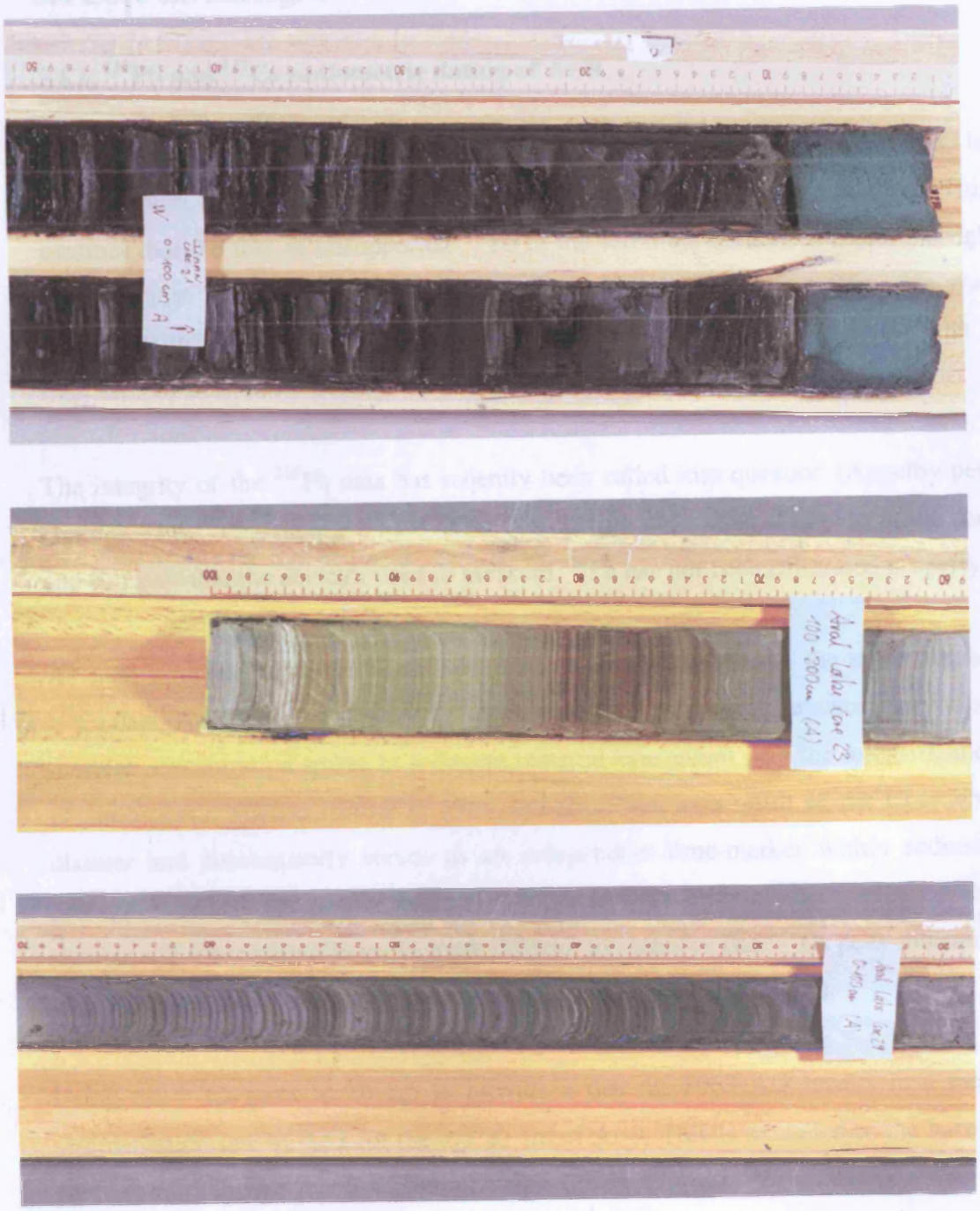

Figure 3.5 Photographic images of core sections discussed in the text. Top image shows the dark grey and black silt and silty sand material characteristic of the core between 0-479 cm. The middle image shows the laminated sediments and gypsum horizon between 479 and 501 cm. The lower image highlights the grey laminated sediments below the hiatus at 1028 cm.

3.4 Core chronologies

3.4.1. ^{210}Pb and ^{137}Cs radiometric dating of Ar-9

The short core, Ar-9, has been dated by Christine Heim and Jana Friedrich at AWI in Bremerhaven, Germany, using the constant rate of supply (CRS) method. This assumes that the flux of unsupported ^{210}Pb to the sediment remains constant through time but that the sedimentation rate may change (Appleby, 1997). The core was sampled at 0.5 cm intervals to a depth of 14 cm and 1 cm intervals to 30 cm with a final sample analysed at 38 cm.

The integrity of the ^{210}Pb data has recently been called into question (Appelby pers comm.). The ^{210}Pb data at the base of Ar-9 is comparable to that at the top of the core and suggests that the detector used to measure ^{210}Pb has not been calibrated properly.

As such it has been suggested to base the chronology of Ar-9 on the more reliable ^{137}Cs data (Appleby, pers. comm.).^{137}Cs is an artifical radionucleide which may show discrete concentration spikes in sediment material concordant with the intensification of atmospheric nuclear testing in 1963 and also 1986 as a result of the Chernobyl disaster and consequently serves as an independent time-marker within sediment profiles. Similar peaks may represent 1958/59 and 1971 although these are somewhat smaller and subsequentally prove more difficult to identify. The ^{137}Cs peak indicative of 1963 atomic weapons is seen to occur at 20 cm in Ar-9 (Figure 3.6).

Using the ^{137}Cs peak at 20 cm to provide a date of 1963 AD results in a mean sedimentation rate of 0.51 for the top 20 cm of Ar-9. This is extended to the base of the core and suggests that the material covers the time frame 1927 – 2002 AD

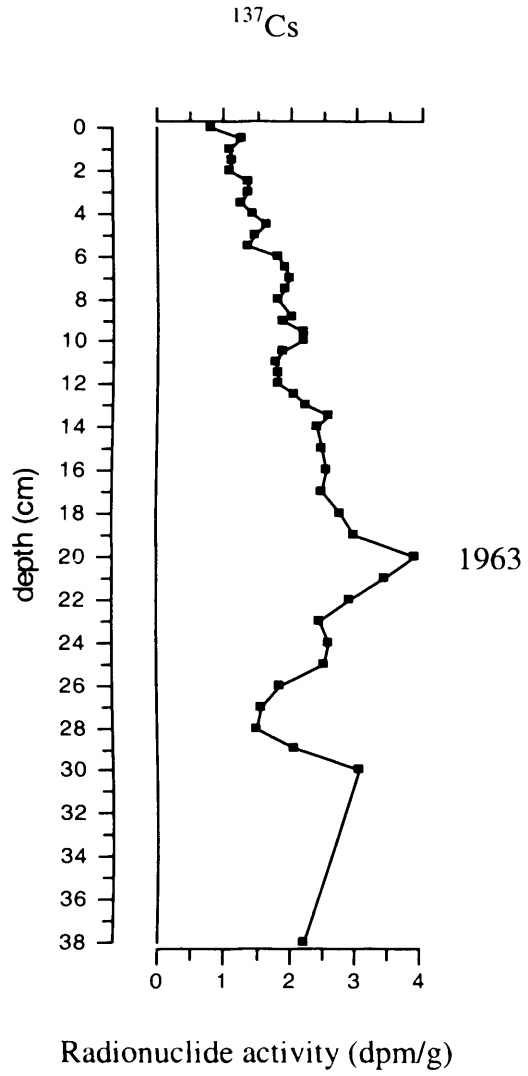

Figure 3.6. Ar-9 radionuclide activity of ^{137}Cs.

3.4.2 Radiocarbon dating of CH-1

The model for CH-1 has been developed using linear interpolation between ages which have been determined through a variety of techniques: ^{14}C AMS radiocarbon dating, correlation with other successfully radiocarbon dated cores from the same location and the correlation of gypsum deposits, (seen to reflect high conductivity and low lake levels) within the core with known regressions over the last 2000 years.

Table 3.2. Radiocarbon dates from Chernyshov Bay. Radiocarbon dates were calibrated using OxCal version 3.10 (Bronk Ramsey, 2005). The KSU code refers to dates obtained by Kazan State University. See Nourgaliev et al., (2003).

Laboratory code	Core	depth (cm)	Material	Age, ^{14}C yr B.P.	+/- (1 sigma)	Age, cal. yr B.P.	+/- (2 sigma)
KSU 1	k-Ar-8	100 cm	Algae	340	50	450	100
KSU 2	k-Ar-8	152 cm	Algae	435	50	480	120
KSU 3	k-Ar-8	480 cm	Algae	640	45	655	55
POZ 4753	Ar-21	55 cm	Algae	108.6	0.3	modern	
POZ 4750	Ar-22	124 cm	Algae	4320	80	4955	350
POZ 4756	Ar-23	593 cm	Algae	1650	30	1605	140
POZ 4758	Ar-23	604 cm	Algae	1225	30	1215	105
POZ 4759	Ar-27	617 cm	Algae	1655	30	1655	100
POZ 4762	Ar-27	720 cm	Algae	1395	30	1360	35
POZ 4764	Ar-28	763 cm	Algae	1600	40	1535	90
POZ 9962	Ar-28	788 cm	Mollusc	1480	30	1410	55
POZ 4760	Ar-28	860 cm	Algae	1515	25	1475	95

3.4.2.1 Chronology

In order to establish a secure chronology for the core, AMS radiocarbon dates were obtained from filamentous algae (*Vaucheria* spp.) and molluscs (Table 3.2). ^{14}C ages were transformed into calendar ages using OxCal v. 3.10 (Bronk Ramsey, 2005). Heim and Friedrich (in review) detail a peak in ^{137}Cs at 46 cm in Ar-21 representing the 1963 fallout maximum from atomic weapons testing. This date combined with similar trends in the $\delta^{13}C$ of organic material (see chapter 5) from a further radiometrically dated short core (Heim and Friedrich, in review) suggest that the uppermost sample of CH-1 contains modern day sediments. Two dates: 480 cal. yr BP at 152 cm and 655 cal. yr BP at 480 cm (Table 3.2) were obtained by correlating

the magnetic susceptibility record of CH-1 with the material recovered by Kazan State University (see Nourgaliev et. al (2003) for a description of this material). Two gypsum horizons at the base of the core and at 501 cm suggest episodes of high conductivity and low lake levels which may be used to verify the age model.

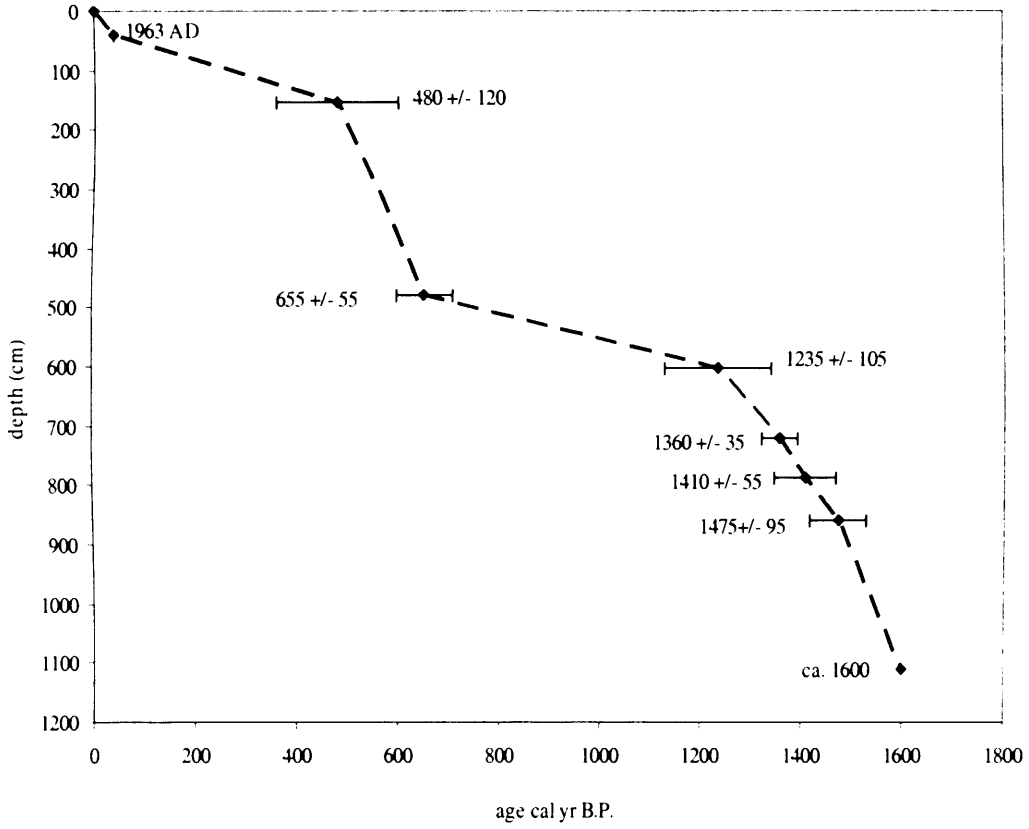

Figure 3.7. Age depth model for CH-1 from Chernyshov Bay. The error bars represent the 95.4% probability distribution for the calibrated radiocarbon dates. The ^{137}Cs peak of 1963 is also shown (see text for details).

A linear extrapolation from the lowermost radiocarbon date of 1475 ± 95 cal. yr B.P at 860 cm (Figure 3.7) provides a date of 1558 cal. yr B.P at 1028 cm at which point an abrupt transition in the diatom flora and magnetic susceptibility (Figure 3.4) reflects the hiatus within the material. High lake levels of the Aral Sea are indicated at ca. 200 AD (Borrofka et al., in press) and the basal gypsum layer correlates with a severe regression of the Aral Sea from ca. 1600 yr B.P. (Rubanov et al., 1987). Peat deposited in the lake's eastern basin has been dated to 1590 +/- 140 B.P (1600 ± 300 cal. yr B.P) and is believed to correspond with mirabilite deposition in the western basin (Letolle and Mainguet, 1997). On this basis, a date of ca. 1600 cal. yr BP,

thought to reflect the maximum regression of this period (Boomer et al., 2000), is ascribed to the base of the core at 1112 cm.

The sediment accumulation rates ranged between 0.21 and 2.01 cm yr^{-1}. One of the problems with linear interpolation models is that it is assumed that sedimentation rates change at the depth of a particular date. Telford et al., (2004) state that if changes in sedimentation rate can be successfully identified, linear interpolation models are probably the most appropriate. Assuming that the dates of 1475 +/- 95 (860 cm), 1410 +/- 55 (788 cm) and 1360 +/- 35 (720 cm) are realistic, evidence for such a change is provided by the second gypsum horizon at 501 cm. This is considered to correlate with a known regression of the Aral Sea initiated in 1221 AD (ca. 780 yr BP) due to the destruction of irrigation systems along the upper reaches of the Amu Darya by the Mongols and the subsequent diversion of the river away from the Aral Sea (Letolle and Mainguet, 1997), and with no sediment disturbance between 501 and 720 cm reflects a significant decline in the sedimentation rate. Furthermore, the model suggests that this horizon is dated to ca. 750 cal. yr B.P. (agreeing with the date of 1221 AD). This gypsum horizon is also overlain by fine laminations (Figure 3.5) which would preclude any major erosion event and subsequent hiatus similar to that detected at 1028 cm.

The dates 4320±80 yr BP, 1650±30 yr BP, 1655±30 yr BP and 1600±40 yr BP (Table 3.2) are seen to reflect the reworking of older material from the shoreline and is confirmed by the large number of reworked dinoflagellate cysts found in the sediments (Sorrel et al., 2006) These dates are consequently rejected.

Chapter Four

Diatom conductivity reconstruction of the Aral Sea and lake-level change since 400 AD

4.1 Introduction

Diatoms (Class Bacillariophyceae) are single celled siliceous alga with estimates of species numbers varying from 10^4 to 10^5, (Stoermer and Smol, 1999). They are abundant in all aquatic environments with sufficient light for photosynthesis. Their use as proxies for climate change and former environments is facilitated by their short generation times and an ability to respond quickly to changing ecological conditions (Dixit et al., 1992; Battarbee et al., 2001). Consequently, knowledge of diatom habitat requirements, survival strategies and their autoecology may be used to reconstruct climate variability (e.g. Bradbury et al., 1981; Smol, 1988; Wolin and Duthie, 1999; Bradbury et al., 2002).

More recently however, quantitative multivariate techniques have been used to reconstruct climatic variability. These reconstructions are commonly carried out using one of three methods: the indicator species approach, in which the knowledge of a particular species tolerance for an environmental variable is used to infer former conditions in the fossil samples in which it is present; the assemblage approach which considers the fossil assemblage as a whole and the proportions of taxa therein. This is commonly undertaken using the modern analogue technique (MAT) which will assign a value of an environmental variable to a particular sample based upon the mean value of a pre-determined number of sites that prove to be the closest analogue. Lastly the multivariate transfer function approach used in this study, which estimates an environmental variable by modelling the responses of those taxa present in a modern day calibration set which are also present within a fossil data set.

As such, diatoms have been used as a proxy for past climatic conditions through the establishment of transfer functions in order to infer former mean air temperature (e.g. Korhola et al. 2000; Rosen et al., 2000; Bigler et al., 2002; Weckstrom et al., 2006)

and summer surface water temperatures (e.g. Pienitz et al. 1995; Joynt and Wolfe, 2001). Transfer functions have also been used to reconstruct climate variability in an indirect fashion. This assumes that changes in a particular variable, e.g. ice cover (Overpeck et al., 1997; Smith, 2002) pH (Psenner and Schmidt, 1992; Sommaruga-Wograth et al., 1997, Koning et al., 1998) or snow cover (Mackay et al. 2005) will be linked to climate change.

4.1.2 Diatoms as indicators of palaeosalinity, lake level and environment change.

Diatoms have been used as palaeosalinity indicators since the end of the 19th century when workers in Scandinavia (e.g. Cleve, 1899) were investigating periods of land uplift and developmental stages of the Baltic Sea. The assumption when analysing diatoms in a qualitative fashion to undertake palaeoclimatic reconstructions of former salinity and lake level change, is that an assemblage dominated by species with a tolerance to high salinity levels will reflect either i) periods where surface water evaporation is greater than any hydrological inputs, consequently representing phases of low lake level or ii) marine incursions. Conversely, assemblages dominated by diatoms with a low tolerance for saline conditions reflect i) episodes where hydrological inputs are greater than surface water evaporation therefore indicating high lake levels or ii) no marine incursions.

As lake levels fluctuate so available habitats will vary, thus it is assumed that low lake levels will result in an increase in the proportion of benthic species while higher lake levels will give rise to a higher proportion of planktonic species. These lake-level changes may then be associated with either climatic change and/or anthropogenic activity. This may be the general rule however it should be treated with some caution particularly when dealing with large waterbodies which may have several distinct basins. (e.g. Stone and Fritz, 2004).

An excellent review of the classification of diatoms into particular salinity groups can be found in Juggins (1992). The early classification of Kolbe (1927) resulted in four catagories; polyhalobous (> 35 g/l), euhalobous (30 – 40 g/l), mesohalobous (5 – 20 g/l) and oligohalobous (< 5 g/l). This was revised by Hustedt (1953, 1957) and although being developed specifically for chloride waters, remains popular when using

diatoms to infer former salinity in a qualitative fashion although as many diatoms of saline environments are in fact euryhaline, i.e. found in waters of widely differing salinities, Simonsen (1962) argued the need to determine species tolerance ranges to provide a clearer understanding of former conditions.

In an effort to quantitatively infer former conditions in saline lakes, the last decade or so has seen the development of diatom salinity training sets and transfer functions. Weighted averaging (WA) techniques in which estimates of a reconstructed environmental variable are based upon the optima of taxa in common between the training set and fossil assemblages are used in order to address the question of salinity/conductivity change. These exist on a regional scale for Africa (Gasse et al., 1995), Antarctica (Roberts and Mcminn, 1998), Central Mexico (Davis et al., 2002), North America (e.g. Fritz, 1991; Wilson et al., 1996), South America (Servant-Vildary and Roux, 1990), Spain (Reed, 1998), Tibet (Yang et al., 2003) and West Greenland (Ryves et al., 2002). The European Diatom Database Initiative (EDDI), which is used to reconstruct conductivity in this project, has merged the dataset from Africa with those from Spain (Reed, 1998) and the Caspian region, resulting in a combined conductivity training set based on 604 species obtained from 387 lakes in order to reconstruct former chemical parameters including conductivity (Battarbee et al., 2000).

4.2 Conductivity reconstruction

The EDDI combined salinity training set (http://craticula.ncl.ac.uk/Eddi/jsp/index.jsp) has been used to reconstruct conductivity. Reconstructions are determined and results plotted using the C2 v. 1.4 computer programme (Juggins 2004) which allows both analysis and visualisation of palaeoenvironmental data and enables the estimation of sample-specific errors of prediction by bootstrapping (see section 4.7.3) for the individual fossil samples. Conductivity results are expressed as $\log_{10}$ μS/cm and are back transformed to mS/cm. The C2 programme enables modification of the original training set, thus due to the large number of species in the training set that are not observed in the fossil set (sections 4.7 and 4.9) it was decided to form three separate training sets from the original in an effort to determine whether a closer analogue between training set and fossil set improved results (Juggins, pers. comm.).

Consequently three reconstructions have been undertaken, using i) the entire EDDI training set; ii) a version of the training set in which all species with a maximum abundance of < 1% have been deleted so as to reduce their impact and iii) a final version in which all those species in the training set which are not represented in the fossil set have been deleted.

4.2.1 Evaluation and reliability of inferred diatom conductivity

All quantitative environmental reconstructions will produce a result (Birks, 1995). It is thus important to evaluate these results in terms of their reliability. As already stated the most obvious way is to compare instrumental observations of an environmental parameter against those inferred by the training set. If these observations exist, the chances are that they will not extend beyond the last 350 years (Jones and Thompson, 2003). Consequently when evaluating reconstructions over longer time scales it is important to assess the reliability of the reconstructed values for each fossil sample (Birks, 1995). In this project three methods are used to identify fossil samples where the reconstructed values may be poorly modelled.

i) Reconstructions are far more likely to be reliable if there are good analogues between the fossil assemblages and the modern calibration set. Here MAT is used to establish the minimum dissimilarity coefficient (minDC) of each fossil sample from its nearest analogue (chi-squared chord distance) within the modern calibration set. Any fossil samples with a minDC in the extreme 90% of the modern calibration set values are seen to have poor modern analogues.

ii) Canonical correspondence analysis (CCA) is used to evaluate the reliability of the reconstructed conductivity by fitting fossil samples passively on to the first axis of the environmental variable being reconstructed (i.e. conductivity) and the residual distance (square residual length, SqRL) of samples from that axis. This provides a 'goodness of fit' measure, fossil samples that have a low SqRL from the environmental variable axis are deemed as having a good fit to that variable. Alternatively samples in the extreme 90% of the SqRL of modern calibration samples

are regarded as having a poor fit to the environmental variable under investigation (see Birks, 1995, 1998 for a full review).

iii) A reconstructed environmental variable is likely to be more reliable if the fossil sample consists of species that are well represented in the training set, thus a simple percentage analogue between species in each fossil assemblage and the modern calibration set can provide extra information into the reliability of reconstructed values.

4.3 Diatom analysis and slide preparation.

Diatom analysis was undertaken at 4 and 8 cm resolution on CH-1 and at 2 cm intervals on core Ar-9. Slide preparation follows the methods outlined by Battarbee (1986). Approximately 0.1 g of wet sediment was measured into test tubes into which 5 ml of 30% H_2O_2 was added. These were then placed in a water bath and heated for up to 48 hours in order to destroy any organic material. After heating, several drops of 50% HCl were added to each sample in order to rid the solution of any carbonates and remaining H_2O_2. The supernatant was then decanted, samples topped up with distilled water and centrifuged at 1200 rpm for 4 minutes. This procedure was repeated three times with a weak ammonia solution added to each sample on each wash so as to suspend any clay particles and facilitate their removal. Distilled water was then added to the test tubes. As diatom concentrations were required (Battarbee and Kneen, 1982) between 0.1 and 2 g of microspheres (concentration 6.18 x 10^6/g) were then added to each sample. A suspension of the diatoms and microspheres was then placed on a cover slip and allowed to dry overnight. The dry coverslips were then mounted on to labelled slides using Naphrax™ and heated to 130°C for 30 minutes. Diatom species identification was then carried out using a x1200 Leitz Ortholux oil immersion light microscope with phase contrast.

A total of 300 valves were counted per slide except in those samples where diatom concentration was low or preservation was such that there were insufficient diatom numbers. The differential preservation of diatom valves in highly saline and alkaline waters may bias conductivity reconstructions towards those species more resistant to dissolution (e.g. Ryves et al., 2001). This was assessed by using a simple index of

preservation (*F* index) in which valves with no indication of dissolution are expressed as a ratio of all valves counted where 0 = all valves partly dissolved and 1 = all valves pristine (Flower, 1993). Valve preservation in both cores was generally good, possibly due to the high sedimentation rate and their subsequent rapid removal from the water column. However between 96 – 136 cm and 840 – 892 cm in CH-1 it was not possible to count 300 valves although this is thought to reflect low concentration rather than extreme dissolution. Diatoms were absent in the basal sample at 1112 cm. The problems of differential diatom dissolution in general and with respect to the material from the Aral Sea are discussed further in section 4.11.

Diatom diagrams were plotted against both depth and age using the C2 v. 1.4 programme (Juggins, 2004). Constrained instrumental sum of squares cluster analysis was used to zone the diatom diagrams using CONISS (Grimm, 1987). For both stratigraphic and ordination plots only species occurring > 5% in Ar-9 and > 10 % in CH-1 were included.

4.4 Diatom taxonomy

The identification of many species (e.g. *Actinocyclus octonarius*, *Amphora pediculus*, *Cocconeis neodiminuta*), was straightforward. SEM micrographs of selected common species are shown in figure 4. 1. The identification of Aral Sea flora has been determined using a wide range of literature, the main texts being, Cooper (1995), Gasse (1986), Germain (1983), Gleser et al. (1974; 1988; 1992), Krammer and Lange-Bertalot (1986 - 1991), Lange-Bertalot (2001), Snoejis et al. (1993 - 1996), Witkowski (1994) and Witkowski et al. (2000) along with other individual papers referred to in the text.

The characteristics of *Cyclotella choctawhatcheeana* (the most common taxon) which has in the past and still continues to be wrongly identified as *Cyclotella caspia* (e.g. EDDI, 2000) have been reviewed by Hakannson (1993) and Carvalho et al., (1995). The identification of this species (Figure 4.1a) was made on the basis of its small valve diameter (4 – 7 μm), a colliculate and undulate central zone, on the uplift portion of which were 1 – 3 valve face fultoportulae, and the presence of ca. 20 – 25 striae in 10 μm, which corresponds with valves of *C. choctawhatcheeana* found at its

type site in Choctawhatchee Bay, Florida (Prasad et al., 1990), the Baltic Sea (Hakansson, 1993) and the Zrmanja River estuary, Croatia (Keve Kiss, personal communication). Several valves of *C. caspia* were observed, however these differed from *C. choctawhatcheeana* by their larger diameter (> 12 μm) and the presence of many more valve face fultoportulae (> 10) on a smooth central zone in common with observations by Håkansson (1993).

Nitzschia fonticola and *N. frustulum* are two very similar species that occurred together during low lake level stages. Krammer and Lange-Bertalot (1988) report that both of these species may reach up to 65 μm in length. This was not the case in the Chernyshov Bay sediments where valves were between 5 – 20 μm. The striae and fibulae density of both species are overlapping therefore separation of the two species is difficult and was made on the basis of valve length and overall shape. Valves of *N. frustulum* were very rounded with no discernable valve endings (almost oval in shape) and never more than 10 μm in length. This contrasts with *N. fonticola* which were always longer than 10 μm and more distinct drawn out endings (Figure 4.1b). Both species have a central node, however when two valves of *N. fonticola* occurred together it was common for only one valve to exhibit this characteristic.

One surprising aspect was the presence in some cases of large numbers of vegetative cells of *Chaetoceros* sp. cf. *wighamii*. Valve length was variable, generally between 10 – 30 μm, although these were the extremes of the range. The surfaces of some valves, although not all, was characterised by a single process. Resting spores were less common than valves in all samples where identified. When present these usually consisted of a primary convex valve that was either smooth or characterised by the presence of short spines. The secondary valve was however always truncated to varying degrees and always smooth.

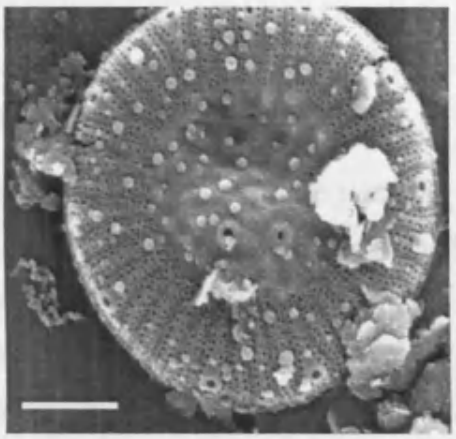

A. *Cyclotella choctawhatcheea*. Scale bar = 1μm

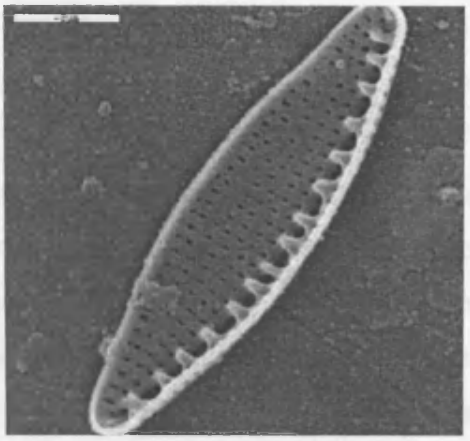

B. *Nitzschia fonticola* . Scale bar = 2μm

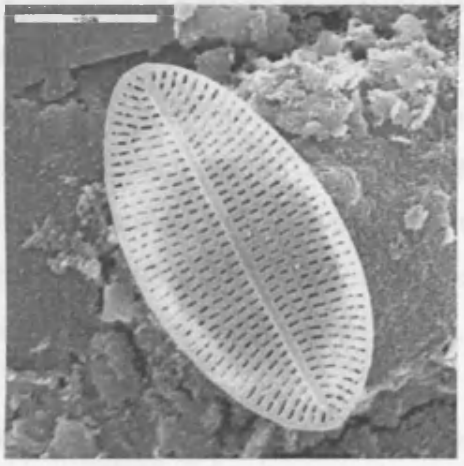

C. *Cocconeis placentula* var. *euglypta* Scale bar = *5* μm

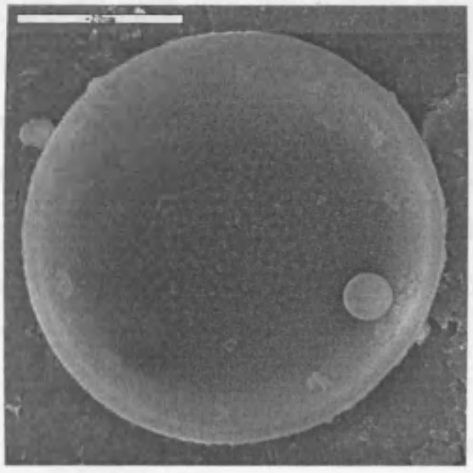

D. *Actinocyclus octonarius*. Scale bar = 20 μm

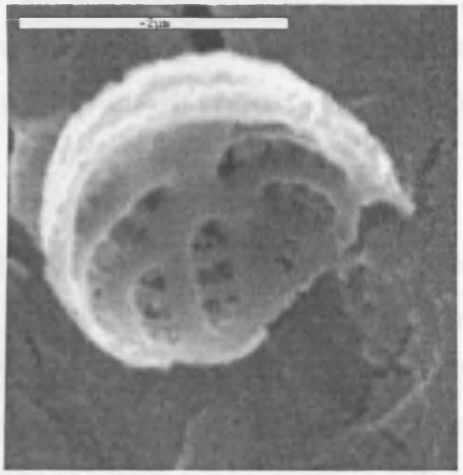

E. *Opephora krumbeinii.* Scale bar = 2 μm

Figure 4.1. SEM images of some of the common diatom species from Chernyshov Bay. Note the different scales.

4.5 Numerical analysis.

4.5.1 Ordination.

Ordination is the collective term for multivariate techniques that arrange sites along axes on the basis of data obtained on the species composition of a biological community (ter Braak, 1999). Palaeoecological data are predominantly multidimensional, containing many species and samples. Ordination reduces this dimensionality providing a visual means of assessing the trends exhibited in a dataset (Kovach, 1995).

Any change in the composition of a biological community (terrestrial or aquatic) may often, but not always, be related to changing environmental variables and the ability of species within the community to adapt to a new set of conditions. The variation in biological communities may be summarised using any one of a wide range of statistical techniques. However if the analysis and description of the continuity of change within a community is desired then the method most appropriate is that of ordination (Lepš and Šmilauer, 2003).

Ordination is generally presented visually as a two-dimensional scatterplot where similar species, samples or environmental variables are plotted close together while those with little similarity are plotted further apart. The majority of ordination methods are based upon the extraction of axes through a process of eigenanalysis with each new axes summarising as much of the data as possible. In order to determine the importance of any individual axis an eigenvalue is generated. The most important axes will have the highest eigenvalues.

Four basic ordination methods may be distinguished, based upon the underlying species response model and whether the ordination is constrained (direct gradient analysis or simply, direct) or unconstrained (indirect gradient analysis/indirect) (Lepš and Šmilauer, 2003). The species response model may be either unimodal or linear. In the case of the former, taxon will have a maximium abundance at a particular value of an environmental variable and declining abundances either side of this maximum, similar to a Gaussian species response (Birks, 1995), where an individual taxa has a

maximum abundance, a specific tolerance range for an environmental variable and an optima (Ter Braak and Looman, 1999). A linear response assumes that as the value of an environmental variable is seen to increase so to will the abundance of a particular species. Of the two, unimodal responses are generally the more common in biological communities (Birks, 1995).

Constrained or direct analysis may be used if an explanatory variable is obtained at the same location as the species data, and will display the distribution of taxa along the gradient of this variable (Gauch, 1982). By comparison, unconstrained or indirect methods are interpreted by assuming that the result is a response to an environmental variable which has been previously determined using ecological knowledge (ter Braak, 1995).

The gradient length of the first axis will help to determine whether linear or unimodal methods should be applied. If gradient length is less than ca. 2 SD units, taxa are seen to be behaving monotonically and a linear response is indicated. Over a longer gradient (> 2 SD) taxa are seen to respond in a non-linear, unimodal fashion. The exact length is, however, difficult to define with linear techniques suggested for axis 1 values of < 1.5 SD (Kent and Coker, 1996), to < 3 SD (Lepš and Šmilauer, 2003).

Detrended correspondence analysis (DCA) is an unconstrained unimodal method which is used, with rare species downweighted, to determine the gradient length of the first axis. If gradient lengths are found to indicate a linear response, subsequent analysis is undertaken using Principal Components Analysis (PCA), which provides an indirect ordination technique for obtaining a low-dimensional representation of multivariate data. Conversely gradient lengths suggesting a unimodal response may be further analysed using Correspondence Analysis (CA), a unimodal based equivalent of PCA. This may however, result in an 'arch effect' which causes compression of points at the end of the gradient during data reduction and is a '*mathematical artefact corresponding to no real structure in the data*' (Hill and Gauch, 1980). Consequently the second axis is seen as an artefact of the first and is thus not easy to interpret, while the compression of samples (or species) along the first axis is not necessarily related to the amount of change along the primary gradient.

This effect may be corrected for by using DCA which divides the first axis into segments while centering the second axis on zero.

Numerical analysis on the diatom data of Ar-9 and CH-1 was undertaken using CANOCO v. 4.5 (Ter Braak and Šmilauer, 2002). The transformation of data into a format suitable for this programme was carried out using WINTRAN v. 1.5 (Juggins, 2002).

4.6 Aims and objectives

In this chapter the methods discussed above will be applied to the two cores Ar-9 and CH-1 obtained from Chernyshov Bay. A conductivity and lake level history over the last ca. 100 years from Ar-9 will initially be inferred. This material has been accurately dated at high resolution (section 3.4.1) thus enabling a comparison between reconstructed conductivity and instrumental records of salinity over a period in which lake levels and salinity were stable until the inception of mass irrigation in 1960.

This will then provide an assessment of the reliability of the conductivity reconstruction and a picture of how the diatom flora respond to changes in the Aral Sea during a period of well monitored change. This will also help to distinguish, along with other numerical methods (section 4.4.1), the reliability of reconstructed conductivity and inferred lake level change in CH-1 spanning the last ca. 1600 cal. yr BP.

The timing and severity of any fluctuations in lake level will then be compared with records of climate change in the region and archaeological and historical evidence for anthropogenic activity, in particular irrigation, in an effort to determine whether climate or human activity is the principal driving force behind lake level change.

4.7 Ar-9

4.7.1 Diatom stratigraphy

Figure 4.2 shows the percentage abundance of species appearing > 5% on one occasion or more and is plotted against depth and age as determined by ^{137}Cs (Heim

and Friedrich, in review). They are ordered on the basis of conductivity optima (declining from the left) as determined by the EDDI training set and optima (conductivity and salinity) determined from literature cited within the text (e.g. Fritz et al., 1991; Gasse et al. 1995; Reed 1998; Snoejis et al., 1996; Wilson et al., 1996; Yang et al., 2003). Figure 4.3 shows individual species concentrations. Of the 79 species identified just 6 were planktonic and tychoplanktonic. Also shown are diatom concentration, PCA axis one scores, the percentage abundance of planktonic species and the F-index of dissolution. The three zones (Ar9-z1 to Ar9-z3) shown are those determined by CONISS (Grimm, 1987).

The lowermost zone **Ar9-z1** from 38 – 24 cm (ca. 1925-1955 AD) is dominated by *C. choctawhatcheeana*, the abundance of which fluctuates between 45 – 60%. Also present in values around 5 – 10% for most of the zone is the planktonic *Actinocyclus octonarius* and three benthic species, *Diploneis smithii*, *Navicula perminuta* and *Navicula phyllepta*, the latter increasing its abundance to 17% at 28 cm (ca. 1945 AD). *P. delicatula* is also present in small numbers. Diatom preservation is generally good with planktonic diatoms accounting for on average ca. 60% of the assemblage. The mean diatom concentration within this zone is 7.19 x 10^6 valves/g dry sediment.

The overlying zone **Ar9-z2** from 24 – 8 cm (ca. 1955 – 1985 AD) is characterised by an initial decline in the abundance of *C. choctawhatcheeana*, although values still remain > 30% and the first appearance of the tychoplanktonic *N. fonticola*. Low values (20%) of *C. choctawhatcheeana* are seen to occur with a peak in the abundance of *Nitzschia coaractata* which reaches almost 20% and the presence, for the first time, of *Nitzschia compressa* at 20 cm (ca. 1965 AD). Throughout most of this zone *N. phyllepta* has been present in small numbers, there is however a small increase to around 15% at 10 cm (ca. 1985 AD). The planktonic flora account for around 55% of the assemblage and as with the underlying zone diatom preservation is high. Concentration however is lower than that of Ar9-z1, averaging 4.47 x 10^6 valves/g.

The uppermost zone **Ar9-z3** from 0 – 8 cm (ca. 1985 - 2002 AD) is again dominated by *C. choctawhatcheeana* which has both its highest values (75%) and lowest (6%) within the core. *N. fonticola* exhibits an increasing trend throughout this zone,

attaining an abundance of almost 50% in the uppermost sample. *N. phyllepta* and *N. compressa* also increase their abundance, while *Nitzschia frustulum* appears in significant numbers for the first time in the uppermost sample in which the values of *C. choctawhatcheeana* have fallen to just 6%. The planktonic to benthic ratio remains high, however it is driven by the tychoplanktonic *Nitzschia* species rather than *C. choctawhatcheeana* as has been the case for the vast majority of the core. The average diatom concentration is 10.36 x 10^6 valves/g of dry sediment, with the highest values within the core of 19.62 x 10^6 occurring at 6cm (ca. 1990 AD).

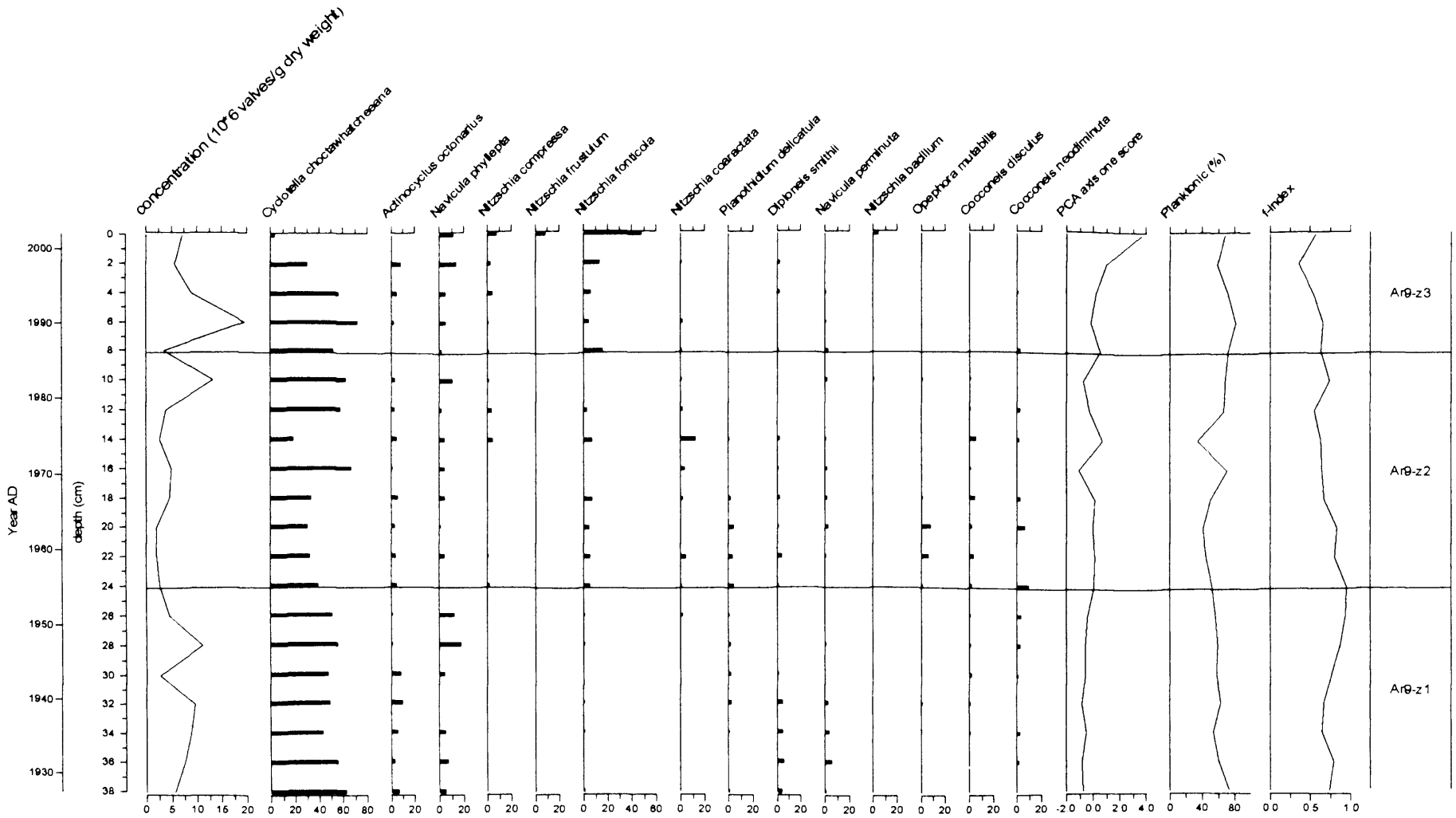

Figure 4.2. Diatom stratigraphy of Ar-9. Species shown are those appearing > 5% abundance on one occasion or more and are ordered on the basis of the conductivity/salinity optima. Also shown are the PCA axis one scores, the percentage abundance of planktonic species, the f-index of diatom dissolution and diatom concentration.

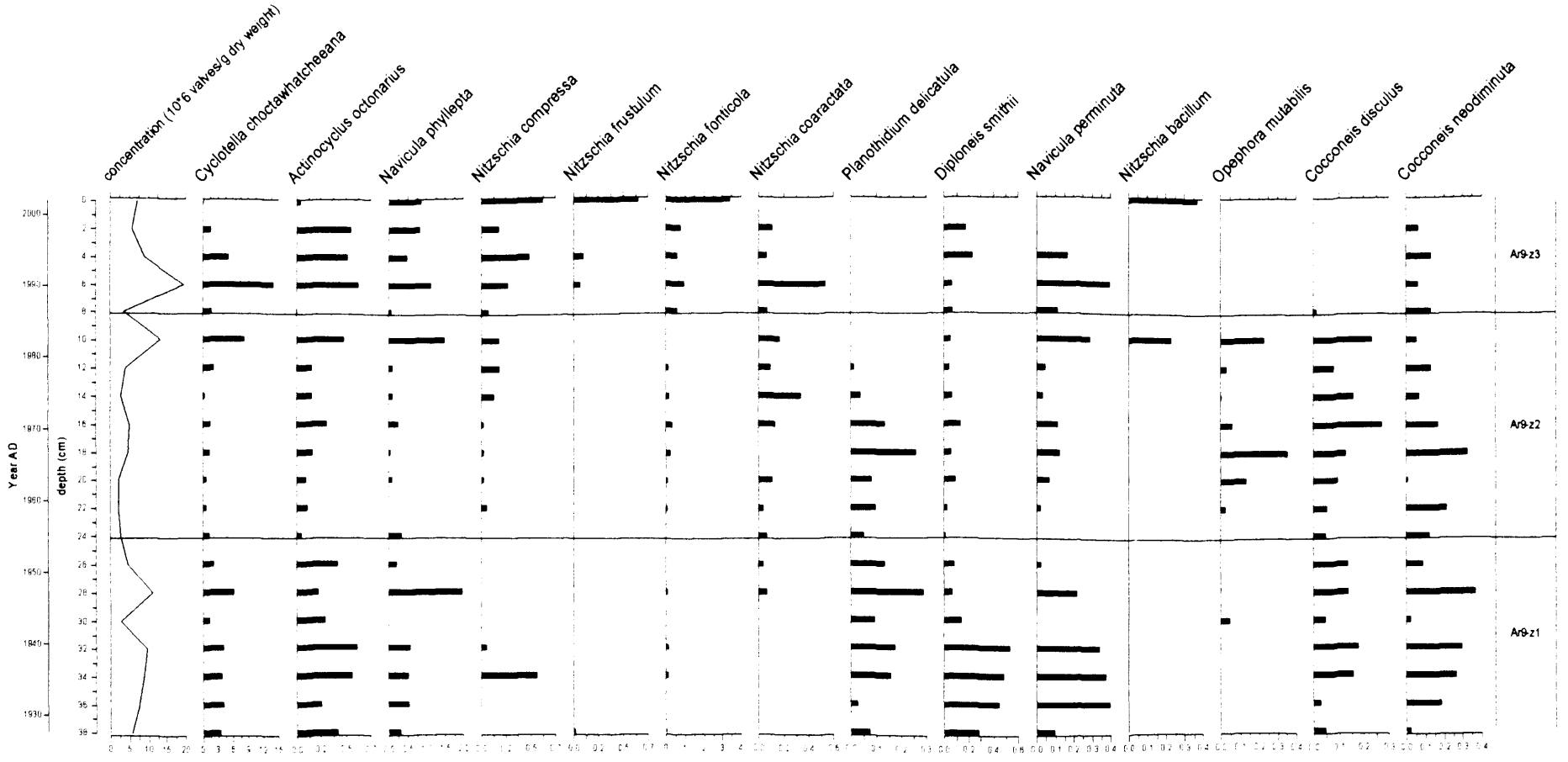

Figure 4.3. Concentration (x10^6 valves cm^2 yr^{-1}) of individual diatom species in Ar-9, occurring with abundances of > 5% on one occasion or more, plotted against age and depth. Note that axes are on different scales.

4.7.2 Ar-9 diatom data ordination

Initial DCA analysis of species occurring > 2% (32) in any one sample resulted in eigenvalues for the first two axes of $\lambda_1 = 0.180$ and $\lambda_2 = 0.057$ and gradient lengths of 1.873 and 0.875 respectively. The two axes together account for 58.2% of the cumulative variation within the species data (table 4.1). The short gradient length of 1.873 SD units indicates a linear response consequently PCA (table 4.2) is used.

Table 4.1. DCA results for species occurring > 2% in any one sample of Ar-9.

DCA axes	1	2	3	4	Inertia
Eigenvalues	0.180	0.057	0.016	0.009	
Lengths of gradient	1.873	0.875	0.770	0.638	
Cumulative % variance of species data	44.2	58.2	62.0	64.1	
Sum of all unconstrained eigenvalues					0.407

Table 4.2. PCA results for species occurring > 2% in any one sample of Ar-9.

PCA axes	1	2	3	4	Inertia
Eigenvalues	0.420	0.124	0.08	0.062	
Cumulative % variance of species data	42.0	61.5	70.9	79.2	
Total inertia					1.00

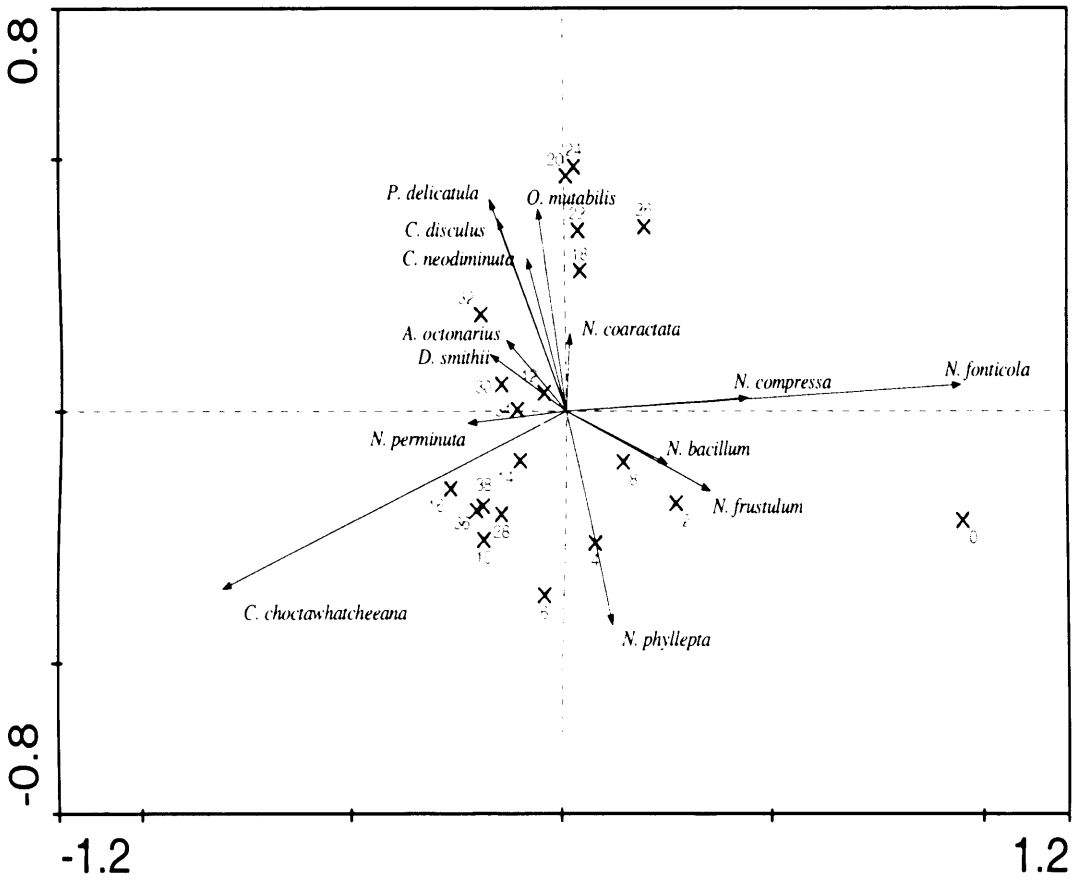

Figure 4.4. PCA biplot of axis 1 and axis 2 scores for those species occurring > 2% in any one sample. of Ar-9. The species data were squareroot transformed and rare species downweighted with focus on inter species distances. The graph is centred by species. For ease of interpretation only those species occurring > 5% are shown along with sample depths.

PCA axes 1 and 2 are seen to account for 61.5% (42.0% and 19.5% respectively) of the variance in species data. The first axis would appear to be dominated by the relationship between *N. fonticola* and *C. choctawhatcheeana* (although the positioning of *C. choctawhatcheeana* would appear to suggest that it might also be influenced by the second axis). This is clearly seen in figure 4.2 where the uppermost sample contains a high abundance of *N. fonticola* (48%) compared with only 5% abundance of *C. choctawhatcheeana*, a situation which is reversed for the remainder of the core. *C. disculus*, *C. neodiminuta*, *O. mutabilis* and *P. delicatulum* are small benthic species all common in fresh and brackish environments and have positive axis 2 scores, compared with *N. phyllepta*, a benthic diatom characteristic of more saline environments.

4.7.3 Ar- 9 Diatom inferred conductivity reconstruction

This study employs weighted averaging (WA) in which estimates of a reconstructed environmental variable are based upon the optima of taxa in common between the training set and fossil assemblages, consequently this technique is seen to perform well when fossil assemblages have poor analogues within the modern calibration set (Birks, 2003). WA also assumes a unimodal species response along an environmental gradient as is more often the case in nature. One of its main disadvantages, however, is that it disregards correlations in the biological data that may remain after fitting the environmental variables of interest (Birks, 2003). Consequently weighted averaging partial least squares, WA-PLS (Ter Braak and Juggins, 1993) was developed in order to take in to account these relationships while also reducing edge effect problems inherent in WA leading to over and under estimation of optima at the low and high ends of the environmental gradients of interest.

Estimates of the error in the predictive ability of the models are determined by bootstrapping in which a 'new' independent test set is created randomly with replacement from the full data set (Birks, 2003). Those samples not selected for the 'new' training set go on to form a separate test set. This procedure is commonly repeated 1000 times with the average of all results providing: i) the root mean square error of prediction (RMSEP), a combination of the error due to variability in the estimation of species parameters in the training set and that caused by the variation in species abundance at a particular environmental value and ii) the r^2 value of the relationship between the observed values and the predicted values.

Racca et al., (2003) determined that just 15% of taxa from the Surface Water Acidification Project (SWAP) pH diatom data set were required to provide a robust pH reconstruction. This contrasts with the results obtained here, where of all the models tested it was WA with inverse deshrinking, using all species in the data set that proved the most robust (table 4.3) with an RMSEP of 0.468 log10 μS/cm and an r^2_{boot} of 0.767 log10 μS/cm, this latter value indicating the robust nature of the model (Prairie, 1996). Use of the entire data set including those taxa with limited occurrences is seen to perform best, and is in common with the findings of others (Birks, 1994; Wilson et al. 1996; Cameron et al. 1999) and may be a consequence of

rare taxa contributing some ecological information or signal to the model rather than having no, or indeed a negative effect on the outcome (Birks, 1994). Plots of observed conductivity against that predicted by the training set and the observed values against the residuals (the difference between observed and predicted values) are seen in figure 4.5, the latter indicating that the model performs best between 2.6 – 3.8 $\log_{10}$ µ/S with most bias found at the lowest and highest values.

Table 4.3. WA and WA-PLS model performances for reconstructed conductivity of Ar-9 using the Complete EDDI combined salinity training set.

	WA inverse deshrinking	WA classical	WA Tol. inverse deshrinking	WA Tol Classical	WA-PLS 1
RMSE	0.359	0.389	0.3	0.316	0.359
R^2	0.851	0.851	0.896	0.896	0.851
RMSEP					
$R^2_{(boot)}$					
Boot ave bias	0.025	0.029	0.038	0.041	0.024
Boot max bias	0.924	0.732	1.028	0.923	1.033

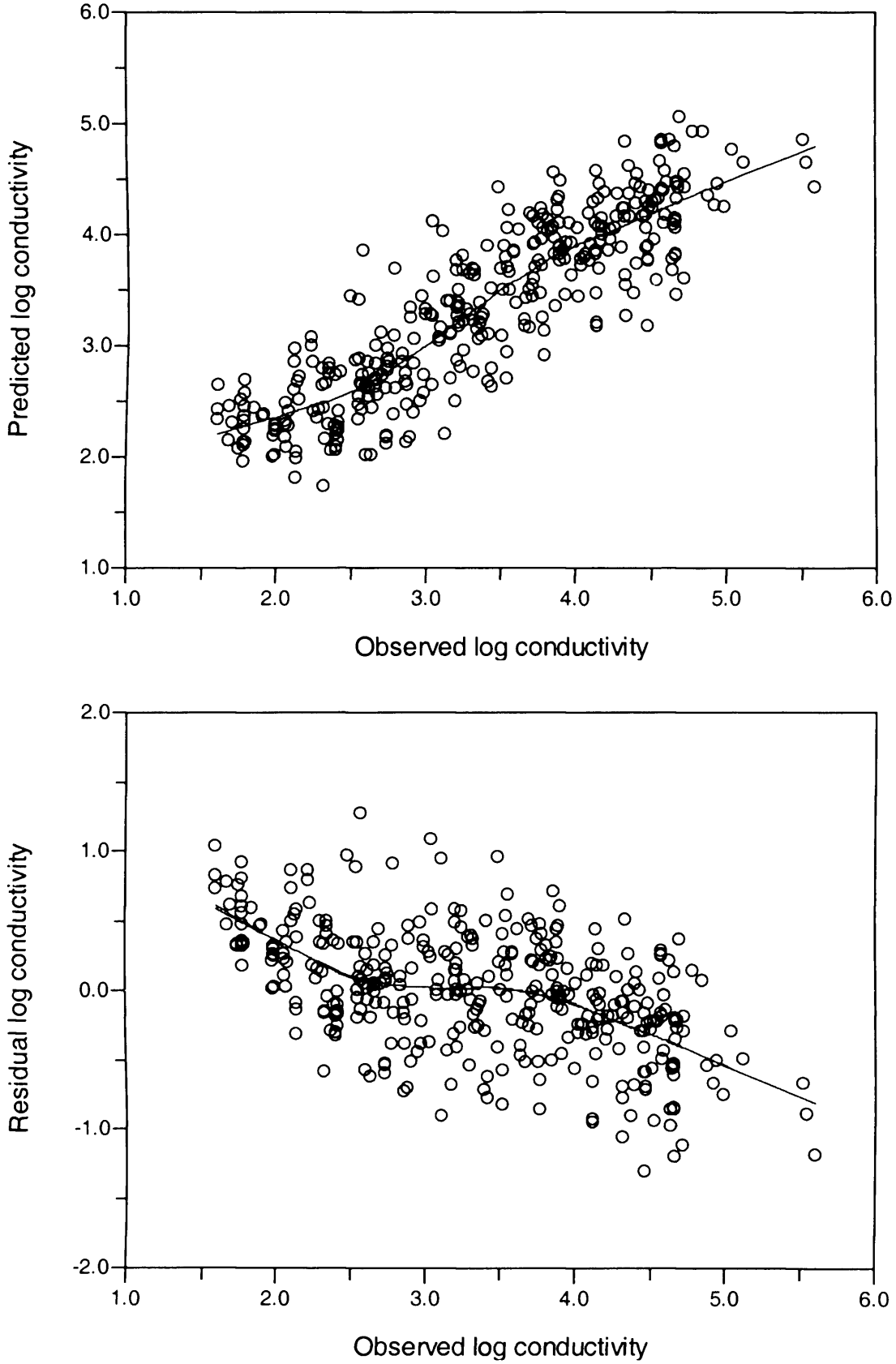

Figure 4.5. Scatterplots of observed conductivity against predicted conductivity (top) and observed conductivity against residual conductivity (bottom) using the entire EDDI training set. A LOWESS smooth line is fitted to illustrate the values where most bias is seen to occur. All units are in $\log_{10}$ μS/cm.

Racca and Prairie (2004) have recently argued that when estimating the prediction biases of the *model*, it is in fact more useful to look at the predicted (rather than observed) values against residual values. This will help to understand whether predictions are biased where the model predicts high or low values and that only plots of predicted against residual values are useful when evaluating the general tendency of numerical models. As such residual conductivity against predicted conductivity is seen in figure 4.6 where $r^2 = 0.211$ compared with $r^2 = -0.287$ for the residual conductivity plotted against observed conductivity indicating little bias where the model predicts high and low values.

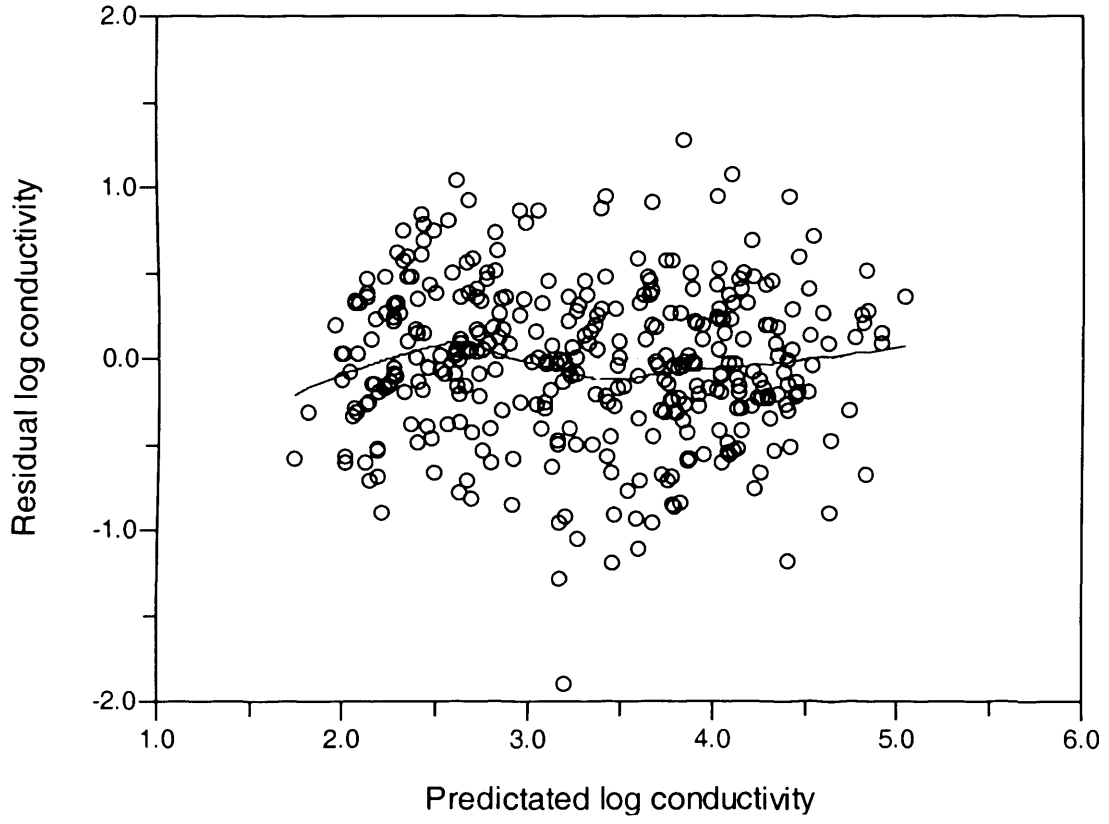

Figure 4.6. Scatterplot of predicted conductivity against residual. A LOWESS smooth line is fitted to illustrate the values where most bias is seen to occur. All units are in log10 μS/cm.

4.8 Reconstructed conductivity of Ar-9 (1905 – 2002 AD)

Of the 79 species identified in Ar-9, 41 were found in the training set. Reconstructed conductivity of Ar-9 (in both log10 μS/cm and back transformed to mS/cm) covering the last century is illustrated in figure 4.7. The zones shown are those determined by CONISS on the percentage diatom data (figure 4.2) Also shown is the measured record of salinity for that period; the abundance of *C. choctawhatcheeana* and *N. fonticola*, the dominant diatom species within the core; the square residual length (SqRL) of the fossil samples; the chi-squared chord distance (minDC) from an individual sample's nearest analogue within the calibration set and the percentage of taxa in fossil samples that feature in the calibration set. The conductivity values have also been converted into salinity (http://www.fivecreeks.org/monitor/sal.html) in order to enable comparison with the instrumental observations.

4.8.1. Reconstructed conductivity and reliability.

Between ca. 1925 and 1955 in Ar9-z1, mesosaline conditions persisted with conductivity values fluctuating between 15 – 25 mS/cm. By ca. 1955 at the start of Ar9-z2 values of 10 mS/cm are inferred. This zone sees a steady increase in conductivity so that by ca. 1970 values of 30 mS/cm and polysaline conditions are inferred. By ca. 1975 values have more than halved to 12 mS/cm and are then seen to rise once again, so that by ca. 1985 conductivity has reached 22 mS/cm. The uppermost zone, Ar9-z3 is characterised by increasing conductivity to values of 31 mS/cm by ca. 1990 at which point conductivity declines, falling to 14 mS/cm in the surface sediments representing 2002 AD.

The methods used to evaluate the above reconstruction provide contrasting results. The minDC determined that only two samples (0 and 14 cm) had poor analogues (minDC > 114) within the training set. Conversely the square residual length as determined by CCA resulted in 19 out of 20 fossil samples falling in the extreme 10% of the modern squared residual length (> 42). The only exception was the uppermost sample at 0 cm suggesting that reconstructed conductivity for this sample is statistically reliable (even though the minDC value indicates that it has no close analogue within the training set) while others must be treated with caution. The

overlap between species in individual fossil assemblages and the modern calibration set is over 75% in all samples, over 80% in all but four (18, 20, 30 and 32 cm) and over 90% in eight samples (0, 4, 6, 8, 10, 12, 14 and 26 cm).

Both minDC and the analogue of species in individual fossil assemblages and the calibration set suggest the reconstructed values are reasonably reliable. However, as already stated, one of the surest ways to validate a reconstruction of any environmental parameter is to compare the results generated with reliable instrumental records from the site in question. As is clearly seen in figure 4.7 there are problems with the reconstructed values when compared with the observational records ($r = 0.181$). Firstly instrumental observations highlight the stable conditions observed in the Aral Sea from 1927 – 1969 when salinity was generally around 10 – 11 g/l and lake levels were high. During this period no such stability is predicted in the reconstruction where values fluctuate between 9 – 28 mS/cm (6 – 19 ppt) although the average value for this period of 18 mS/cm (12.33 ppt) is close to that of the instrumental measurements. The correlation between PCA axis 1 scores and reconstructed conductivity is low ($r = 0.35$) suggesting that conductivity is poorly correlated with the distribution of species throughout the core and that other factors may be responsible.

This might be explained by the abundance of *N. fonticola* within Ar-9. Between ca. 1925 – 1985 AD, this species has an average abundance of just 3% compared with 18% from ca. 1990 – 2003. The overall abundance of *N. fonticola* correlates well ($r = 0.77$) with the measured salinity over the last ca. 100 years (Figure 4.7). Rather than reflecting the dissolution of *C. choctawhatcheeana*, (the valves of which are generally well preserved throughout this period), this correlation is possibly a consequence of the increased proximity of the coring site to a muddy foreshore as lake levels decline and as a result, increased abundance of *N. fonticola* and other small *Nitzschia* spp which are tychoplanktonic and often found in the epipelon (Ben Goldsmith pers. comm.). Furthermore, *C. choctawhatcheeana* dominates fossil assemblages for much of the profile while *N. fonticola* and measured salinity are seen to correlate, the reconstructed conductivity displays a remarkable similarity ($r = 0.81$) to the abundance of *C. choctawhatcheeana* throughout the core. Any over estimation of conductivity from 1905 – 1969 is in all probability a result of the high conductivity

optimum that *C. choctawhatcheeana* exhibits in the training set (4.29 log10 µS/cm/19 mS/cm) with conductivity fluctuations clearly linked to its abundance. It also has an n2 value of 2.26 compared with an average of 9.26 for the dominant species in Ar-9 which figure in the modern calibration set. This suggests that in terms of the calibration set at least, its ecology is poorly circumscribed. This species would appear to favour mesosaline conditions, (e.g. Wilderman, 1987; Prasad, 1990; Hakannson et al. 1993) however, a bimodal distribution is observed in the Baltic (http://craticula.ncl.ac.uk/Molten/jsp/index.jsp) and it has been found in hypersaline conditions (e.g. Lange and Tiffany, 2003; Flower et al., 2005) suggesting that it may in fact be euryhaline and as such the reconstruction of the Aral Sea conductivity during the stable phase prior to the present regression is hampered by the training set optima of this species.

From 1970 to the present day the instrumental records show ever increasing salinity in accordance with lake level decline. Conversely the diatom inferred conductivity fluctuates albeit with an increasing trend, the trend from ca. 1975 – 1990 in particular having a good correlation with the instrumental record (r = 0.82). From ca. 1990 to the present day, instrumental salinity of the western basin of the Aral Sea increases to 82 g/l reflecting low lake levels while reconstructed conductivity falls to 14 mS/cm (8 ppt) implying a return to more dilute conditions and high lake levels. The obvious discrepancy in the reconstruction of the uppermost samples is the decline in diatom inferred conductivity/salinity observed from 1990 to the present day in contrast with the instrumental record. If one looks at the uppermost sample where both the SqRL and species analogue between the fossil assemblage and calibration set (98%) suggest a reliable reconstruction, the value of just 14 mS/cm (8 ppt) falls way short of 82 g/l recorded at the time of coring in 2002. Again the optimum conductivity of 3.87 log10 µS/cm (7.40 mS/cm) of *N. fonticola* the dominant taxa in this sample accounting for 48% of the assemblage would appear to draw the reconstructions to lower values.

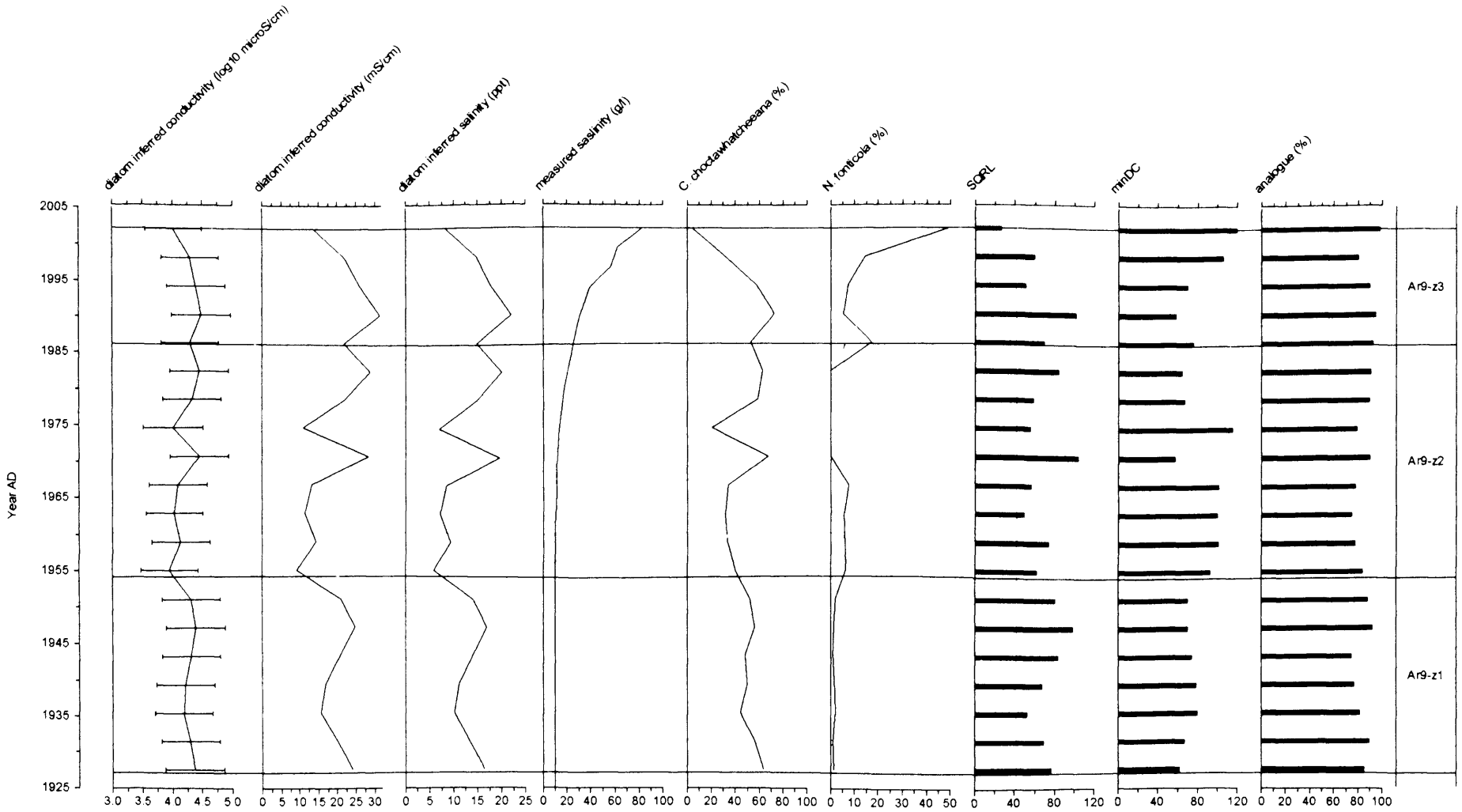

Figure 4.7. Diatom-inferred conductivity of Ar-9 plotted against age (year AD). Also shown is diatom-inferred conductivity transformed into salinity (ppt), the percentage abundances of *C. choctawhatcheeana* and *N. fonticola* and results of the various techniques used to evaluate the reliability of the conductivity reconstruction. The y-axis reference line at 1960 indicates the point at which the current regression was initiated. The x-axis reference lines indicate the extreme 90% of the training set SqRL and minDC values.

4.9 CH-1 (ca. 400 AD – present day).

4.9.1 CH-1 Diatom stratigraphy.

A total of 335 species were identified, the majority of which are benthic. Figure 4.8 shows the percentage diatom abundance for species occurring in any one sample > 10%. Also shown is diatom concentration, the percentage abundance of planktonic diatoms, CA axis one sample scores and the F-index of dissolution. The seven diatom zones shown (CH1-z1 to CH1-z7) have been independently determined using the clustering technique, constrained instrumental sum of squares (CONISS). Individual species concentrations are seen in figure 4.9. As with Ar-9, the diatom flora are ordered on the basis of conductivity optima in the EDDI training set and other estimates of conductivity and salinity.

CH1-z7: 1112.0 – 1032.0 cm (ca. 400 – 440 AD)

Diatoms are absent from the basal sample of the core at 1112 cm (which is composed of gypsum), appearing for the first time at 1108 cm. The assemblage found in this zone is dominated by planktonic species some of which are unique to the core, such as *Stephanodiscus parvus* and *Thalassiosira incerta*. These species have well defined peaks of 20% at 1032 cm and at 1048 cm respectively, occurring after a decline in *C. choctawhatcheeana*, the dominant species in the lower part of this zone, which reaches a maximum value of 58% at 1088 cm. Also present throughout is *Thalassiosira proschkinae* with three notable peaks in the upper half of the zone and valves and spores of *Chaetoceros* cf. *wighamii*, which peak at 47% at 1080 cm. Other common species include *A. octonarius*, *N. phyllepta*, *N. frustulum* and *D. smithii*. The preservation of species in this zone is variable, with F-index values ranging between 0.56 and 0.91 (mean 0.74) the valves in the lowermost samples being the best preserved. Concentration ranges from 5.47×10^6 – 3.09×10^7 valves/g, while planktonic flora make up 60% of the assemblage.

CH1-z2: 1028.0 – 812.0 cm (ca. 445 – 570 AD)

The start of this zone occurs at the hiatus detected within CH-1. The dominant species are the small benthic *Amphora pediculus* and *Cocconeis neodiminuta* both of which

were all but absent from the previous zone and have relatively constant values of between 15 – 20%. The planktonic element which dominated the underlying zone has all but disappeared with *C. choctawhatcheeana* reduced to values of between 5 – 10% a result of both low concentration and the increased concentration of *A. pediculus* and *C. neodiminuta* (Figure 4.9). Other small benthic species include; *Karayevi clevei*, *Fragilaria atomus*, *Navicula tuscula* var. *minor*, *Opephora olsenii* and *Planothidium delicatulum*. As with the previous zone, preservation is variable with F-index values between 0.30 and 0.83 (mean = 0.56). Overall diatom concentrations are lower than the previous zone, ranging from just $5.23x10^5$ to $2.31x10^7$ valves/g. In contrast with the underlying zone the planktonic element has declined to just 12% of the assemblage.

CH1-z3: 808 – 516 cm (ca. 575 – 1175 AD)

The overall abundance of planktonic species remains low (15%) and the species composition is relatively similar to the underlying zone although both *A. pediculus* and *C. neodiminuta* exhibit a declining trend, all but disappearing by the top of this zone. One notable change is the presence of *Opephora krumbeinii* throughout the zone, reaching a maximum abundance of 28% at 566 cm. Several species have short well-defined peaks; *C.* cf. *wighamii* reaches 9% at 712cm while *Navicula digitoradiata*, present throughout the zone in small numbers reaches 17% at 514 cm. Diatom concentration is between $1.02x10^6$ - $2.94x10^7$ valves/g and as is the case with the previous zones the F-index values range between (0.30 – 0.85, mean = 0.70).

CH1-z4: 512 – 462 cm (ca. 1195 – 1355 AD)

The lower part of this zone sees an increase in diatom concentration reaching highest values within the entire core of $6.36x10^7$ at 498 cm. This is accompanied by a an abrupt decrease in the small benthic species which dominated the underlying zone. The small planktonic component of the previous zone of *A. octonarius* and *C. choctawhatcheeana* has been replaced by the tychoplanktonic *N. fonticola* and *Nitzschia liebetruthii* var. *liebetruthii* which dominate the assemblage between 510 – 498 cm, the latter having a maximum abundance of 56% at 506 cm yet contributing just 1% to the assemblage by 498 cm. The second half of this zone sees a switch from

the domination of the small *Nitzschia* spp. to one which at 494 cm contains 35%. This is immediately followed by a peak of *Cocconeis pediculus* of 32% and abrupt increases in the abundance of four planktonic species all exhibiting well defined peaks within the zone; *A. octonarius* which reaches 34% at 490 cm, *C. choctawhatcheeana* (24% at 486 cm), valves of *C.* cf. *wighamii* (52% at 474 cm), and *T. proschkinae* (14% at 478 cm). By the top of this zone, diatom concentration has once again declined. The varying F-index of preservation values are consistent with the previous zones (0.47 – 0.87, mean = 0.67). The overall proportion of planktonic species has increased in this zone, averaging around 55%.

CH1-z5: 458 – 276 cm (ca. 1360 – 1455 AD)

The start of this zone sees an increase in small benthic flora, initially *C. neodiminuta* which is then replaced by *A. pediculus*, having a maximum abundance of 58% at 380 cm and then exhibiting a declining trend throughout the rest of the zone but is nevertheless still present at values above 25% and often in excess of 30%. These trends are seen in the concentrations of these two species (Figure 4.9). Other important species are *D. smithii* which attains 21% in the early part of the zone and *N. tuscula* var. *minor* which appears in the middle of the zone, peaks at 20% at 308 cm and returns to low values at the top of the zone. Overall planktonic abundance is the lowest in the entire core, at no time attaining values in excess of 5%. Diatom concentration within this zone fluctuates between 2.34×10^6 – 3.95×10^7 and as with the underlying material the preservation varies from 0.35 to 0.87 (mean = 0.60).

CH1-z6: 272 – 92 cm (ca. 1460 – 1765 AD)

The dominant species of the underlying zone *A. pediculus* and *C. neodiminuta* continue to feature, although both decrease in abundance throughout this zone. *K.. clevei* also makes a return to the assemblage peaking in the middle of the zone as does *O. krumbeinii*, both reaching maximum values of 18%. *P. delicatulum* increases in abundance throughout this zone, reaching a maximum of 22% at 112 cm. The planktonic species increase in abundance, notably valves of *C.* cf. *wighamii*, which has several well defined peaks (the highest of which is 23% at 188 cm). Diatom concentration fluctuates between 1.46×10^6 and 5.38×10^7, exhibiting two large peaks in

the lower half and middle of the zone, and is particularly low between 96 – 112 cm. Valve preservation once again is seen to vary, the F value ranging from 0.31 – 0.81 and having a mean of 0.62. This zone is notable for exhibiting a clear decline in F-index values, some of the lowest within the core seen at the top of this zone. As with the underlying zone the planktonic element is low (ca. 10%).

CH1-z7: 88 – 0 cm (ca. 1780 AD – present)

This uppermost zone is marked by an overall decline in species numbers and an increase in the proportion of planktonic and tychoplanktonic species which reach 70% in the uppermost sample. *C. choctawhatcheeana* appears at abundances of > 20% in almost all samples with a maximum of 38% at 20 cm. The low values seen in the uppermost sample are a reflection of the increased concentration and subsequently abundance of *N. fonticola* (Figures 4.8 and 4.9) the values of which rise throughout the zone reaching 23% at 4 cm and then doubling in abundance to 46% in the uppermost sample. Valves of *C.* cf. *wighamii* are also present in low numbers with one exception at 36 cm and a peak of 28%. The small benthic flora that characterised the underlying zone declines, while *N. phyllepta* appears at higher values reaching 12% at 24 cm. Diatom preservation varies from 0.37 – 0.81 (mean = 0.62) and as with the previous zone, there is a gradual decline in valve preservation from 32 cm. Diatom concentrations range from 2.15×10^6 to 3.57×10^7 valves.

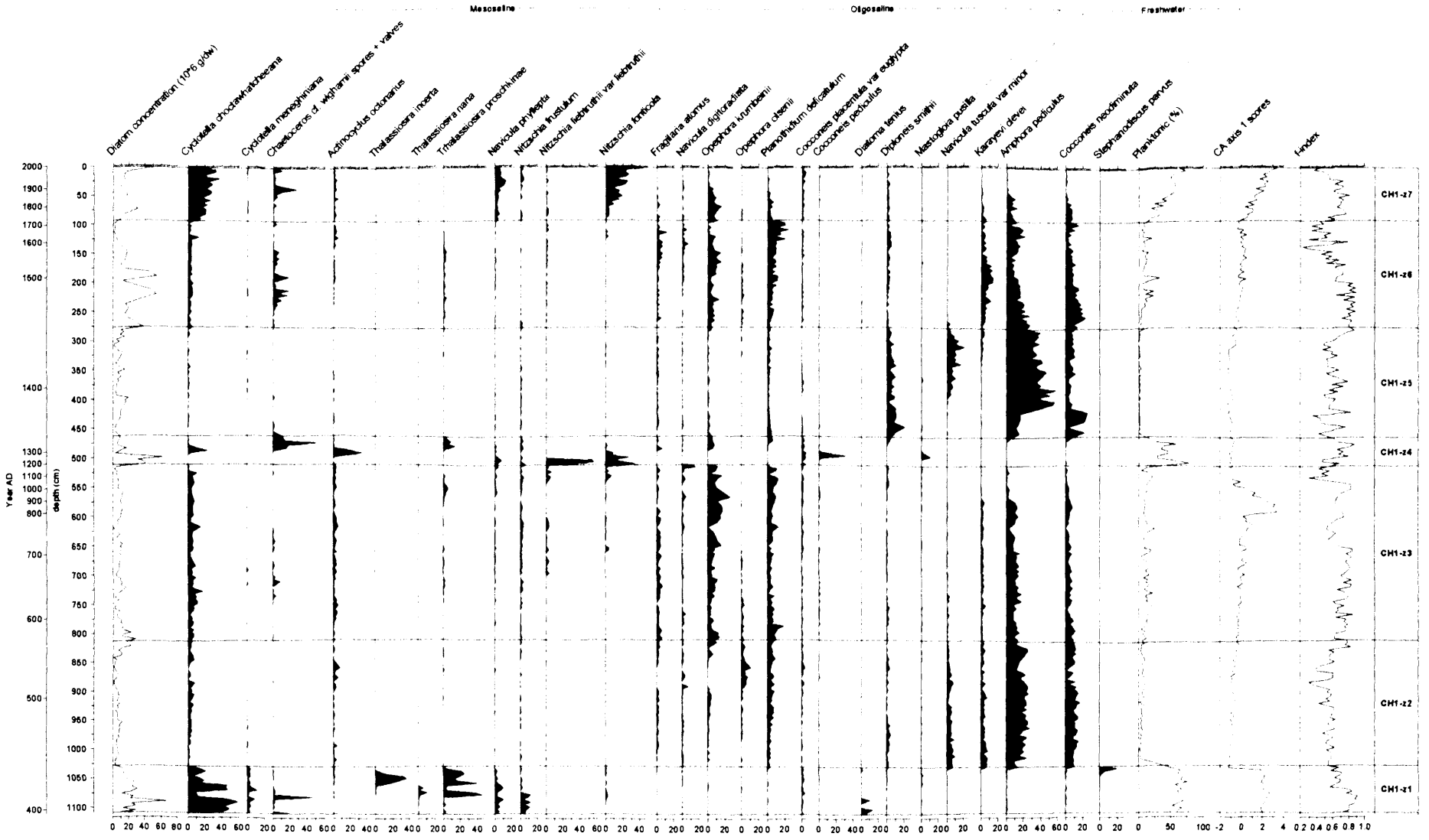

Figure 4.8. Diatom stratigraphy of CH-1. Species shown are those appearing > 10% abundance on one occasion or more, plotted against age and depth. Also shown is diatom concentration, CA axis one scores, the percentage abundance of planktonic species and the F-index of diatom dissolution.

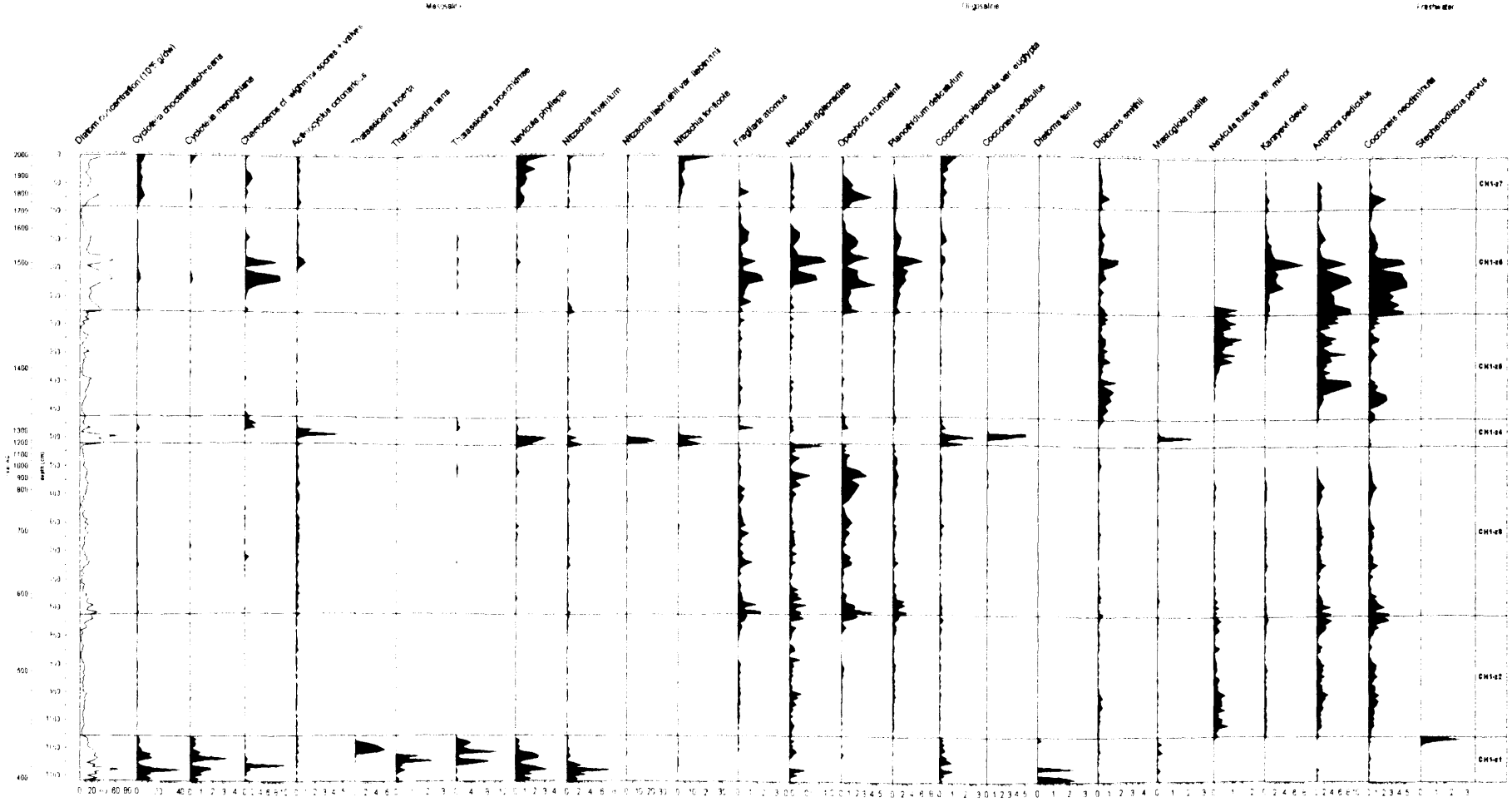

Figure 4.9. Concentration (x10^6 valves cm^2 yr^{-1}) of individual diatom species in CH-1, occurring with abundances of > 10% on one occasion or more, plotted against age and depth. Note that axes are on different scales.

4.9.2 CH-1 ordination

Initial DCA analysis of species occurring > 2% (171) in any one sample resulted in eigenvalues for the first two axes of $\lambda_1 = 0.294$ and $\lambda_2 = 0.112$ and gradient lengths of 2.889 and 1.687 respectively. The two axes account for 19.8% of the cumulative variation within the species data (table 4.4). The gradient length of 2.889 SD units suggests a unimodal response and consequently CA (table 4.5) is used to ordinate the data. This results in eigenvalues for the first two axes of $\lambda_1 = 0.294$ and $\lambda_2 = 0.154$ respectively, with both axes combining to account for 21.3% of the cumulative variance of species data. As discussed in section 4.2.1., CA may result in an 'arch effect' and subsequent misinterpretation of the data. None was apparent in this case and the first two ordination axes are seen in figure 4.10.

Table 4.4. DCA results for species occurring > 2% in any one sample of CH-1

DCA axes	1	2	3	4	Inertia
Eigenvalues	0.294	0.112	0.086	0.055	
Lengths of gradient	2.889	1.687	2.117	1.988	
Cumulative % variance of species data	14.0	19.8	23.9	26.5	
Sum of all unconstrained eigenvalues					2.104

Table 4.5. CA results for species occurring > 2% in any one sample of CH-1

CA axes	1	2	3	4	Inertia
Eigenvalues	0.294	0.154	0.122	0.114	
Cumulative % variance of species data	14.0	21.3	27.1	32.5	
Total inertia					2.104

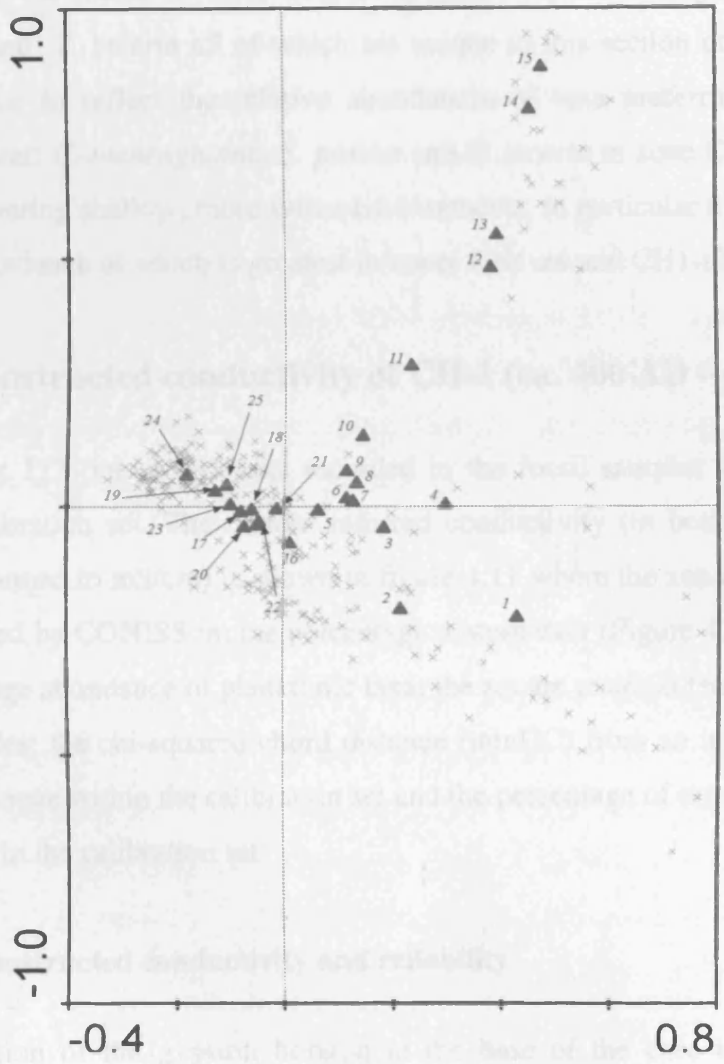

Figure 4.10. CA ordination biplot of species occurring > 2% on one occasion or more with those species occurring > 10% shown. The species data were square root transformed and rare species downweighted. 1 = *N. fonticola*, 2 = *N. liebetruthii*, 3 = *C.* cf. *wighamii* spores + valves, 4 = *N. phyllepta*, 5 = *A. octonarius*, 6 = *C. placentula* var *euglypta*, 7 = *C. pediculus*, 8 = *C. choctawhatcheeana*, 9 = *N. frustulum*, 10 = *M. pusilla*, 11 = *T. proschkinae*, 12 = *C. menenenghiana*, 13 = *D. tenue*, 14 = *S. parvus*, 15 = *T. incerta*, 16 = *O. krumbeinii*, 17 = *C. neodiminuta*, 18 = *D. smithii*, 19 = *P. delicatula*, 20 = *K. cleveii*, 21 = *N. digitoradiata*, 22 = *F. atomus*, 23 = *A. pediculus*, 24 = *N. tuscula* var. *minor*, 25 = *O. olsenii*

Many species are tightly clustered around the centre of the diagram (Figure 4.10) and as such cannot be readily assigned to any particular part of the core. *N. fonticola* and *N. liebetruthii* are oriented towards the topmost sediments and those from 486 – 510 cm situated on the right of axis 1, which mainly reflects conductivity. Those towards the left are benthic species more likely to represent high lake levels and lower

conductivity. The isolated cluster of samples at the top of the diagram are those which occur below the hiatus in zone CH1-z1 (Figure 4.8) containing *C. menenghiana*, *S. parvus* and *T. incerta* all of which are unique to this section of the core. Axis 2 would appear to reflect the relative abundances of taxa preferring deep fresh or brackish water; *C. menenghiana*, *S. parvus* and *T. incerta* in zone CH1-z1 with those species favouring shallow, more saline environments, in particular the small *Nitzschia* spp, the abundance of which is greatest in zones CH1-z4 and CH1-z7 (Figure 4.8).

4.10 Reconstructed conductivity of CH-1 (ca. 400 AD – present)

Overall, just 113 out of 335 taxa recorded in the fossil samples were found in the modern calibration set. The diatom inferred conductivity (in both log10μS/cm and back transformed to mS/cm) is shown in figure 4.11 where the zones shown are those as determined by CONISS on the percentage diatom data (Figure 4.8). Also shown is the percentage abundance of planktonic taxa; the square residual length (SqRL) of the fossil samples; the chi-squared chord distance (minDC) from an individual sample's nearest analogue within the calibration set and the percentage of taxa in fossil samples that feature in the calibration set.

4.10.1 Reconstructed conductivity and reliability

The deposition of the gypsum horizon at the base of the core is an independent indication of high salinity and low lake levels. This is supported by the diatom-inferred conductivity values (9.64 – 16.12 mS/cm) reflecting mesosaline conditions in zone **CH1-z1** between 1108 – 1032 cm (ca. 400 – 440 AD). There is a rapid reduction in diatom inferred conductivity to 0.60 mS/cm at the start of the overlying zone **CH1-z2**, 1028 – 812 cm (ca. 445 – 570 AD), however it is impossible to state whether this is a true reflection of events due to the sediment hiatus at this point. Conductivity fluctuates between 1.94 – 0.57 mS/cm, these lower values reflecting oligosaline conditions and higher lake levels. In zone **CH1-z3** from 808 – 516 cm (ca. 575 – 1175 AD) diatom inferred conductivity values are slightly higher than in the underlying zone, fluctuating between 1.29 – 9.82 mS/cm. This zone is characterised by initial oligosaline values reflecting high lake levels, there is, however, a gradual shift to mesosaline conditions and declining lake levels by the top of this zone at ca. 1050 AD.

Between 512 – 462 cm (1195 – 1355 AD) in zone **CH1-z4** a second severe episode of reduced lake levels occurs with conductivity values reaching a maximum of 27.86 mS/cm at ca. 1320 AD. In zone **CH1-z5** from 458 – 276 cm (ca. 1360 – 1455 AD), a return to high lake levels and fluctuating fresh and oilgosaline (0.41 – 2.40 mS/cm) conditions are inferred. The training set indicates that the dilute conditions persist throughout the overlying zone **CH1-z6** from 272 – 92 cm (ca. 1460 - 1765) values ranging from 0.50 – 4.61 mS/cm, the higher values towards the top of this zone. An increase in conductivity is highlighted in the uppermost zone, **CH1-z7**, between 88 – 0 cm (ca.1780 AD - present), with values between 1.39 – 19.60 mS/cm. Initially values fluctuate around oligosaline and mesosaline values, however by ca. 150 cal. yr BP values are at the high end of the mesosaline range.

The determination of the chi-squared chord distance of samples from their nearest analogue within the training set highlighted just 26 fossil samples (minDC < 114) deemed to have a suitable analogue (4 – 56 cm, 474, 486, 494, 1060, 1064, 1068 cm and 1080 – 1108 cm). The SqRL of fossil samples resulted in 137 having a poor fit to the reconstructed conductivity values (SqRL > 42). The distribution throughout the core of those samples regarded as having a good fit to conductivity are found in the uppermost 92 cm, from 462 – 510 cm and 1032 – 1108 cm and fit in broadly with those samples with a suitable analogue as determined by their minDC, suggesting that reconstructions from these samples are statistically reliable. The overlap between species in fossil samples that are represented in the calibration set averaged just 65% however those samples where the highest conductivity is inferred fared rather better with values often in excess of 80%.

All three methods used to evaluate the reconstruction would appear to suggest that reconstructed conductivity values are most reliable in episodes of high conductivity which are dominated by *C. choctawhatcheeana* and/or *N. fonticola* and *N. liebetruthii* var. *liebetruthii.* Conversely samples where reconstructions are deemed unreliable are those indicative of dilute conditions and high lake level phases with species such as *F. atomus*, *O. krumbeinii* and *N. tuscula* var. minor which are absent from the training set, or fossil assemblages where species are rare in the training set e.g. *K. clevei*, *C. neodiminuta*, *D. smithii*, and *P. delicatulum.* While not having instrumental records with which to compare these reconstructions from 400 AD, the highest

inferred values are seen to correspond with geochemical, biological and historical evidence of severe regressions of the Aral Sea over the last ca. 1600 years (section 2.10) Conversely the prolonged episodes of low reconstructed conductivity are concordant with high lake level stands over the same period where more stable conditions are inferred in CH-1 than the 65 year period leading up to the current regression recorded in Ar-9. Using this stability prior to the current regression as an analogy for those recorded over the last ca. 1600 years then one might expect salinity of the Aral Sea to be in the region of 10-11 g/l. Thus conductivity is being underestimated, due to; a) the unreliable nature of the reconstructions during these episodes and b) the high abundance of *A. pediculus* in these samples. This species has a training set optimum of just 2.63 log10 μS/cm (0.453 mS/cm) indicative of fresh conditions, combined with the lack of species such as *O. krumbeinii* from the training set which on occasion accounts for > 20% of the assemblage and is commonly found in water ca. 8 g/l (see section 4.1).

To summarise, it would appear that the reconstruction of conductivity in Ar-9 is too closely linked to the training set optima and fluctuations of certain species (*C. choctawhatcheeana* and *N. fonticola*) to provide a reliable indication of conductivity over the period for which instrumental observations exist. The reconstruction of CH-1 is however more successful. The measures undertaken to evaluate the reliability of inferred conductivity over the past ca. 1600 years suggest that the episodes of high conductivity and accompanying low lake levels are modelled with more precision than inferred dilute conditions and high lake levels. Although underestimating conductivity in both cases and perhaps not being able to infer minor shifts in lake level, the transfer function clearly enables the distinction of major regressions and transgressions, the finer points of which may be improved upon by taking into account the autoecology of the main diatom species.

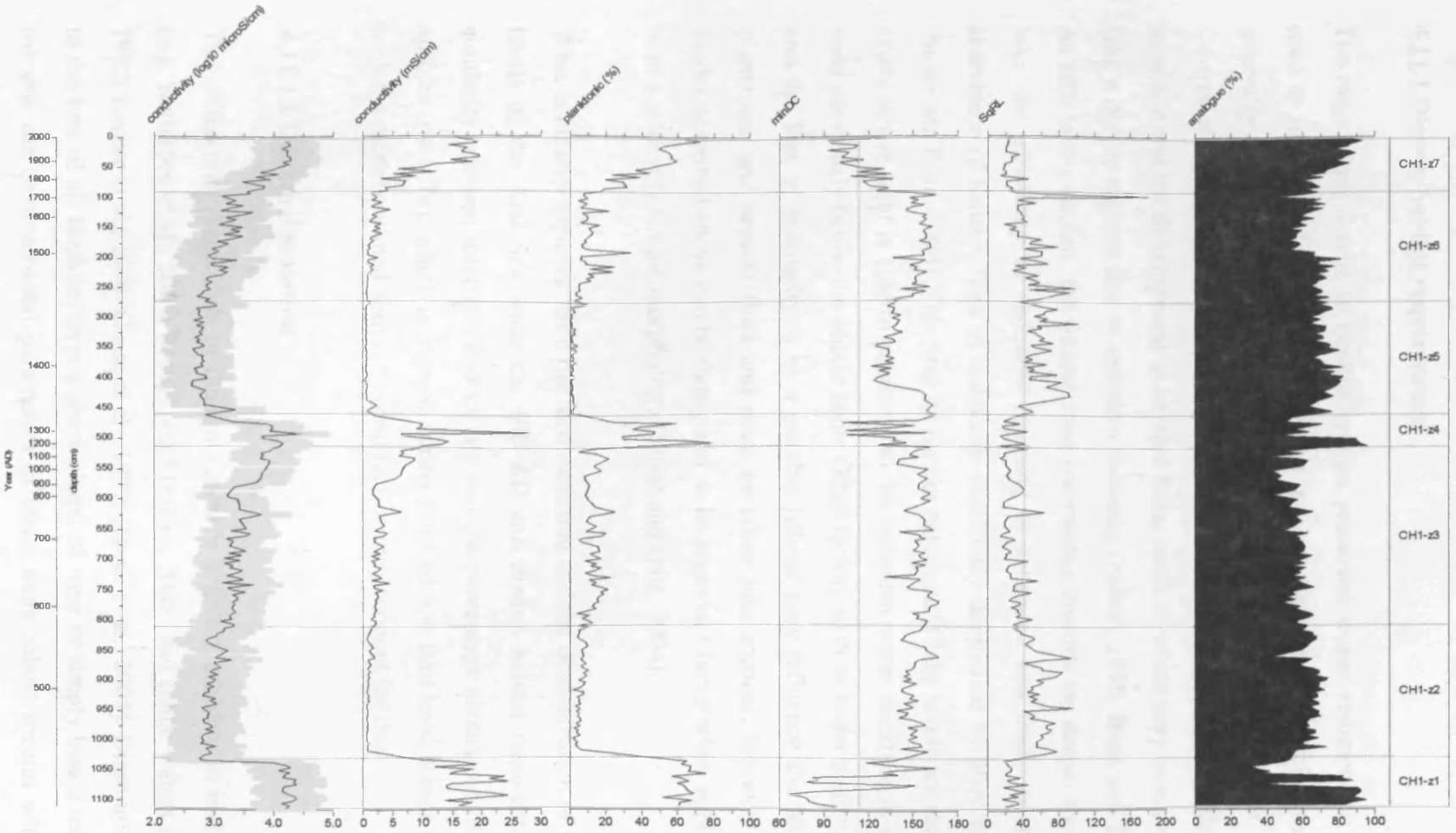

Figure 4.11. Diatom-inferred conductivity of CH-1 plotted against age (cal. yr BP) and depth. Also shown is the percentage abundance of planktonic species and the results of the various techniques used to evaluate the reliability of the reconstructed conductivity. The x-axis reference lines indicate the extreme 90% of the training set minDC and SqRL values.

4.11 Discussion

4.11.1 Diatom habitat requirements

The ratio of planktonic to benthic species preserved within sediments is commonly used to infer lake level history, with an increased abundance of planktonic species generally indicative of high lake levels (e.g. Stager, 1997; Tapia et al., 2003). Conversely, shallow littoral zones allow light penetration to the sediment-water interface and the development of benthic flora, some of which may be transported to a lake's deeper regions due to sediment focusing (Hilton, 1985; Blais and Kalf, 1995). As lake levels decline, the littoral zone encroaches towards the deeper sections of the lake, the efficiency of sediment focusing is enhanced and leads to an increased abundance of benthic flora in sediments previously dominated by planktonic species (Stone and Fritz, 2004). This may be further enhanced if lake levels are reduced to the extent where light is able to penetrate to the sediment-water interface in areas which were previously below the photic zone. Other factors such as water clarity, turbulence and the loss of macrophytes as a suitable habitat may influence the abundance of planktonic and benthic flora and must be taken into account, however the simple model described above can be thought of as an important factor when applied to lakes with a relatively simple morphology (Stone and Fritz, 2004).

What is clearly apparent from the reconstruction and the determination of former lake levels of the Aral Sea since ca. 400 AD and diatom habitat requirements, is the similarity between inferred conductivity and the percentage abundance of planktonic species ($r = 0.74$), which is highest during inferred low lake level stands and at odds with the model outlined above. Several factors may account for this:

4.11.1.1 Diatom dissolution

The differential dissolution of diatom valves is a severe problem in both freshwater (e.g. Battarbee et al., 2005; Rioual and Mackay, 2005) and saline waters (e.g. Barker, 1992; Barker et al., 1994; Gasse et al., 1997; Ryves et al., 2001). Dissolution may lead to the loss of all frustules over a short period of time or simply bias a reconstruction towards the environmental parameters of those more robust species which are less

susceptible to dissolution. Gasse et al (1997) noted that after 46 days immersion in an Na_2CO_3 solution the initial abundance (12%) of *Stephanodiscus neostraea* was increased to 80% following the dissolution of *Fragilaria* spp. that had originally dominated the sediments. Similarly experimental work undertaken by Ryves (2001) showed that over a period of 1200 hours *Mastogloia elliptica* var. *dansei* increased its representation within an assemblage from 20-70%. One of the most important factors affecting the rate of dissolution is pH. The dissociation of silicic acid above pH 9.0 results in the exponential increase of diatom dissolution with substantial dissolution suggesting strongly alkaline waters with a pH well in excess of 9.0 (Barker, 1990, 1992). This may occur either within in the water column or on the sediment surface if exposure to the aquatic environment as a result of a low sediment accumulation rate is prolonged. This misrepresentation of the original assemblage will obviously hamper any successful palaeoenvironmental reconstruction using diatoms. Conversely a high accumulation rate and pore waters saturated with silica will heighten the chances of diatom preservation (Flower, 1993), which is also thought to be improved in the presence of organic matter (Hinman, 1990).

In the sediments from Chernshov Bay, dissolution is not thought to have had a major influence on the composition of the fossil assemblages. *C. choctawhatcheeana* is a species which is particularly susceptible to dissolution (Ryves et al., 2001) and yet it is present in most samples, and is one of the dominant species during low lake level phases and high conductivity. This can be explained by the high sedimentation rate (0.21 – 2.01 cm yr^{-1}) at Chernyshov Bay and a pH of between 8 – 8.5. A possible candidate for severe dissolution is *Sceletenoma costatum* which is a lightly silicified planktonic diatom found to be abundant in the Aral Sea plankton during all seasons when studied between 1967 – 1972 (Anon, 1975) during which time recorded salinity was ~11 g/l and lake level ~51 m.a.s.l (Aladin pers. comm.). *S. costatum* is however completely absent from the sediment records of both Ar-9 and CH-1, thus while it might possibly have been the dominant species during earlier high lake level phases, its dissolution may have skewed the fossil assemblage composition towards the benthic species. However the low abundance of planktonic species during high lake level stands may well be due to physical rather than chemical characteristics of the Aral Sea.

4.11.1.2 Lake Morphology

The morphology of the Aral Sea is thought to play an important role in the distribution of diatom species. Stone and Fritz (2004) determined that the dominance of planktonic species in Lake Foy, Montana, during known episodes of lake level decline was due to the rapid increase of lake mean depth as overall lake level declined and the subsequent isolation of the deeper basin and reduction in littoral habitat. Although the present mean lake depth (6 m) of the Aral Sea has decreased since 1960 (16 m), the morphology of the lake bed is such that high levels result in a lake with a deep, steep sided western basin and a large, shallow eastern basin (Figs. 4.12 and 4.13)

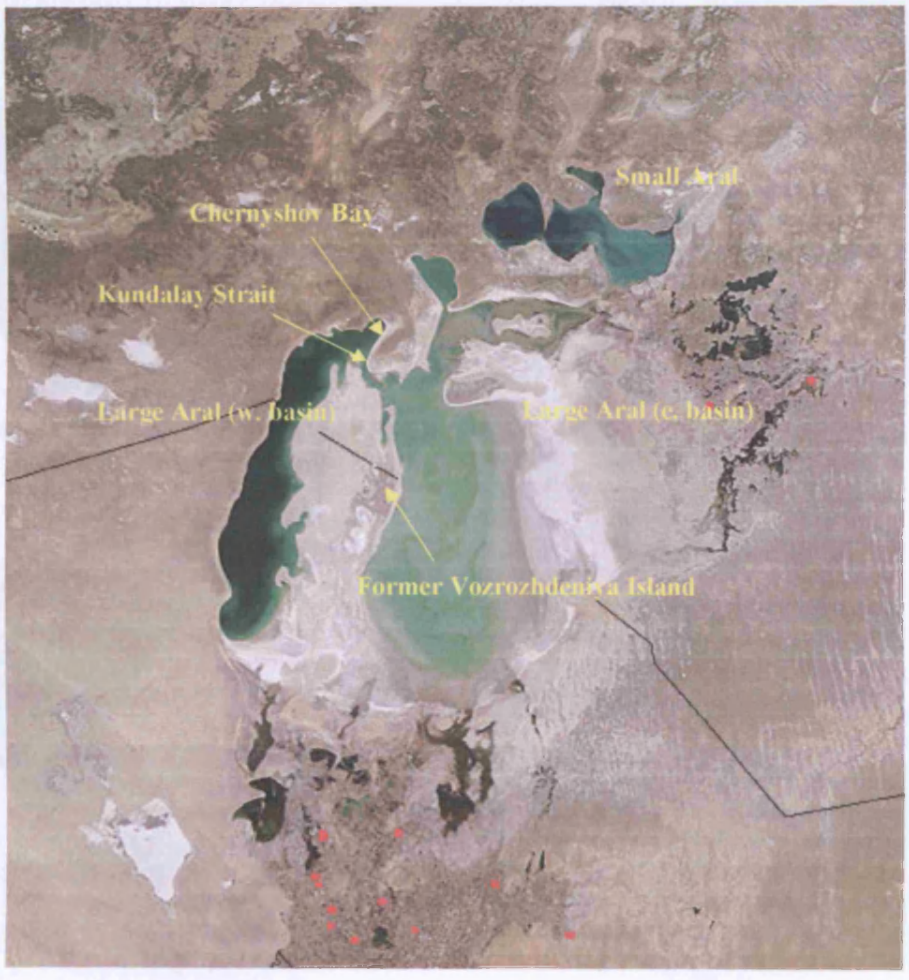

Figure 4.12. Satellite image of the Aral Sea, highlighting the location of Chernyshov Bay and the dried up former seabed of the eastern basin and the shallows north and east of the former Vozorhdeniya island. Also shown is the location of the recently discovered channel in the Kundalay Strait through which benthic flora may be transported from the eastern basin.

The Aral Sea is known to have remarkable transparency during high lake level phases, with visibility, on occasion, extending to depths of > 20 m in the western basin (Zenkevitch, 1963, Zavialov, 2005) permitting the development of benthic flora at considerable depths. Consequently, sediment focusing from the former eastern basin and the shallow regions that surround the former Vozrozhdeniya Island (Figure 4.12) will invariably result in the transport of benthic diatoms to the deeper parts of the lake in the western basin. Stone and Fritz (2004) suggest that these processes will be limited in large shallow lakes such as the Aral Sea, however, the recent discovery of a narrow channel, which is in places 8 m deep, on the otherwise shallow lake bed (1.5 m) of the Kundalay Strait, presently separating the eastern and western basin near Chernyshov Bay (Figure 4.12) suggests the possible re-suspension and transport of sediment to the western basin (Zavialov, 2005).

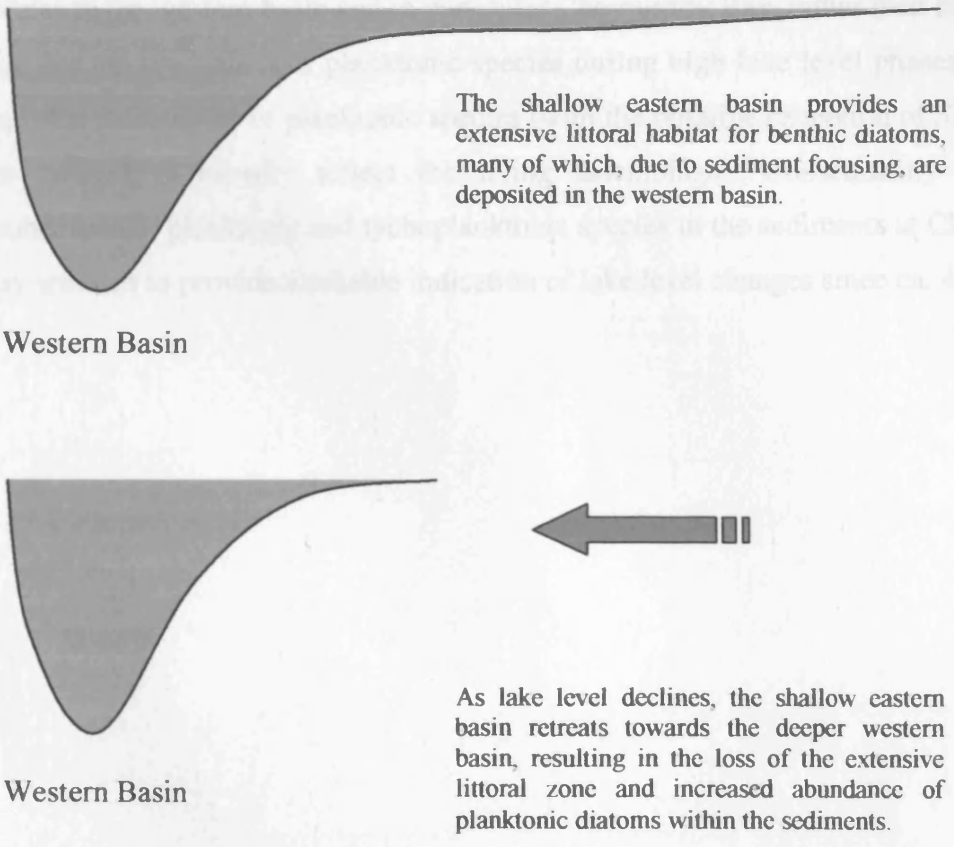

Figure 4.13 Cartoon depicting the extensive littoral habitat of the eastern basin during episodes of high lake level (top) and below, the reduction of the littoral zone and the subsequent confinement of lake water to a steeper sided lake with reduced habitat for benthic flora.

Conversely where diatom inferred conductivity over the last ca. 1600 cal. yr BP is highest and lake levels low, assemblages are dominated by planktonic and tychoplanktonic species (Figure 4.14). Again this may be a consequence of several factors; i) a reduction in the transparency of water and consequently the inability of benthic species to photosynthesise at relatively shallow depths, due to the increased turbidity and productivity of planktonic algal species which is seen in the current regression (Orlova and Rusakova, 1999) and in earlier regressions indicated by positive shifts in $\delta^{13}C$, C/N < 10, (chapter 5); ii) as levels decline the extensive habitat for benthic flora provided by the eastern basin is dramatically reduced, the lake gradually becoming confined to the deep, steeper sided, western basin (Figs. 4.12 and 4.13) in which one would expect planktonic species to dominate.

As such it is felt that the increased influence of the littoral zone and influx of benthic species to the western basin and in particular Chernyshov Bay, rather than dissolution, explains the low values of planktonic species during high lake level phases in which recorded abundances of planktonic species (with the possible exception of *S. costatum*) are thought to broadly reflect the living assemblages. Consequently increased abundances of planktonic and tychoplanktonic species in the sediments at Chernyshov Bay are seen to provide a reliable indication of lake level changes since ca. 400 AD.

4.11.2 Lake level fluctuations since ca. 400 AD

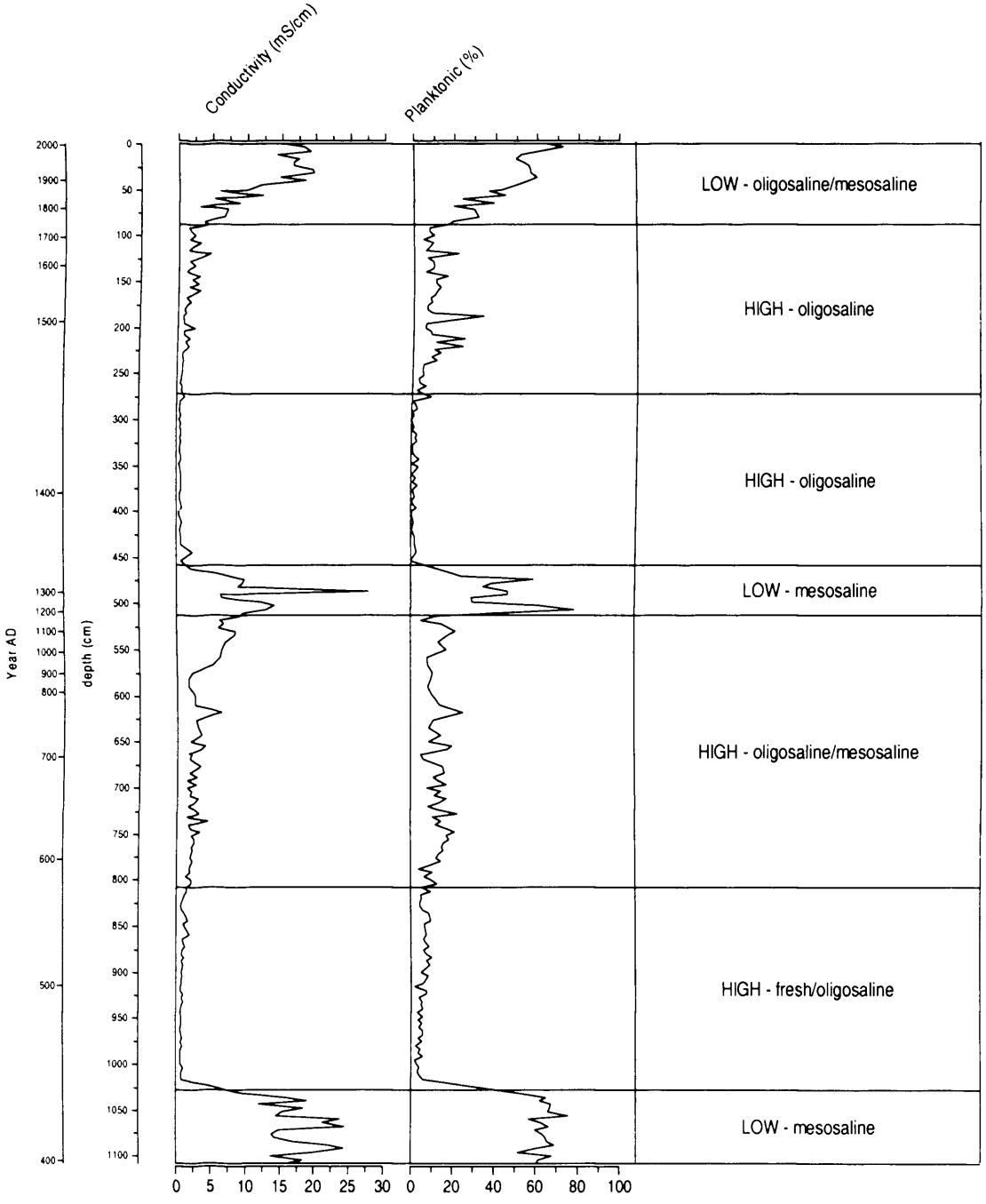

Figure 4.14. Diatom-inferred conductivity (mS/cm), overall abundance of planktonic species (%) and lake level status plotted against age (year AD) and depth.

The almost complete dependence on river discharge for hydrological inputs means that any regressions of the Aral Sea are inextricably linked to fluctuations in their flow, in particular that of the Amu Darya which accounts for ~ 80% of the total fluvial input. A close correlation has been shown to exist between the discharge rate of the Amu Darya and solar activity, leading to several regressions of around 3 m during the last ~ 200 years (Shermatov et al., 2005). When trying to ascertain a climatic connection to more severe regressions however, it is necessary to look at events in two distinct geographical regions where increased aridity may have contributed to low lake level stands. Isotope data from all GNIP stations indicate that the Indian Monsoon has little or no influence on precipitation in Central Asia (Kreutz et al., 2003), consequently the majority of precipitation is derived from the Eastern Mediterranean (EM), where depressions form, are transported across Central Asia by the westerly jet stream to the Pamir and Tien Shan mountains where moisture condenses and falls as snow. Secondly climatic events in the montane regions themselves need to be considered, where conditions will control the rate at which melting glaciers and snowfields feed the Amu Darya and Syr Darya. Importantly, severe regressions may not only be linked to overall moisture availability across the region and the subsequent flow rate of the Amu Darya but also its direction of flow, which since the late Pleistocene has been subject to change (Kes, 1995; Boomer et al., 2000) due to three possible factors: i) the natural build up of sediment within its bed which may alternately divert the river away from and towards the Aral Sea (Yagodin accepted) ii) human activity, in particular irrigation and military conflict, both of which have previously diverted discharge away from the lake (Letolle and Mainguet, 1997; Letolle, 2000) and iii) tectonic activity (Nurtaev et al., 2004). This section will attempt to identify the causes behind the three low lake level stands detected since 400 AD.

4.11.2.1 Regression ca. 400 AD

Lacustrine sediments indicative of high levels of the Aral Sea are dated to ca. 200 AD (Boroffka et al., in press) and correspond with increased moisture availability and lower temperatures across much of the EM. This is reflected in increased moisture availability in the Judean Desert (Yakir et al. 1996), high levels of the Dead Sea recorded between ca. 2100 – 1550 yr B.P/100 BC – 450 AD (Frumkin et al. 1991,

1999; Yechieli et al. 1993; Enzel et al. 2000; Klinger et al. 2003, Bookman et al., 2004) and archaeological investigations that indicate humid conditions around 1700 yr BP/300 AD (Hirschfeld, 2004). A similar pattern is observed in the Tien Shan where high levels of Lake Issyk-Kul are believed to have occurred from ca. 2200 – 1900 yr B.P/200 BC – 100 AD (Aleshkinsaya et al., 1996b). This is contemporaneous with glacier expansion between ca. 2100 – 1700 (L) yr B.P /100 BC – 300 AD in the northern and western Tien Shan (Savoskul and Solomina, 1996) and in the Pamir (Zech et al. 2000).

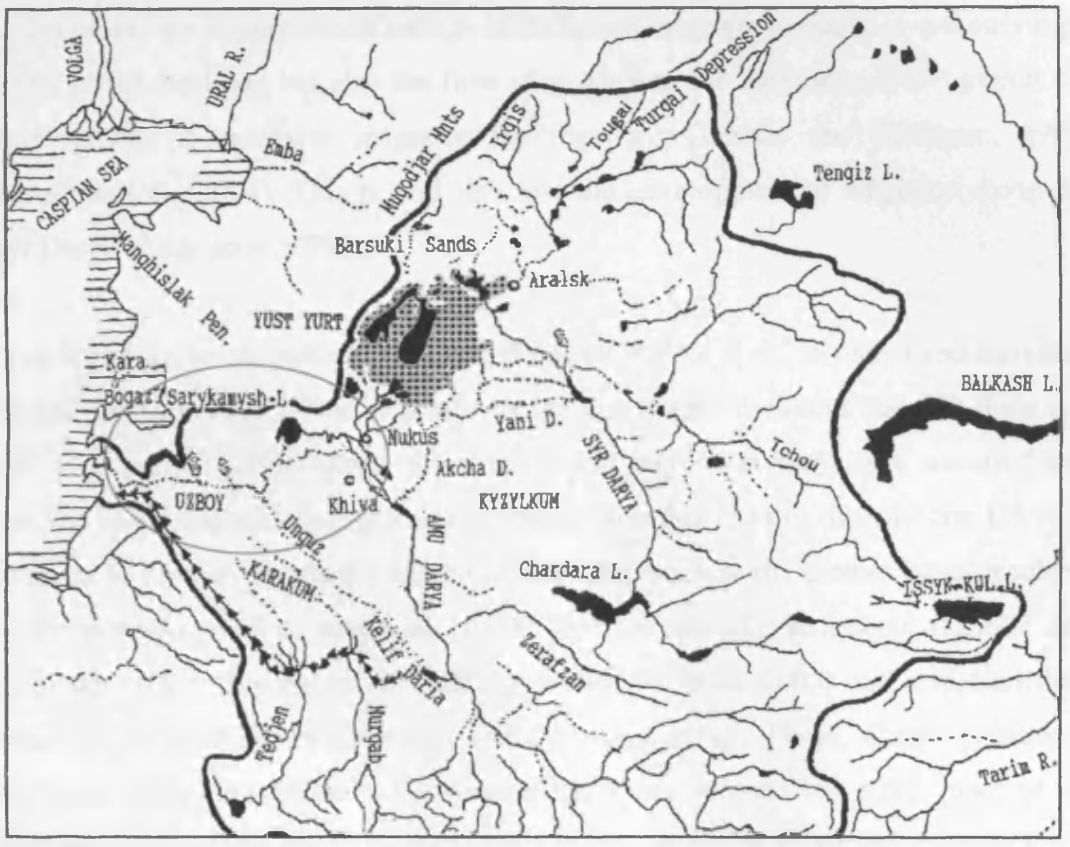

Figure 4.15. Sketch map of the Aral Sea Basin highlighting the Aral Sea pre 1960 (hatched) and during the present regression (solid), Lake Sarykamysh and the course of the Uzboi to the Caspian Sea, highlighted in the red ellipse. (Courtesy Rene Letolle).

At this time a large area to the southwest of the Aral Sea, the Prisarykamysh (Figure 4.16) was also believed to have been in receipt of a stable water supply, resulting in high levels of Lake Sarykamysh and at times flow through the Uzboi Channel to the Caspian Sea (e.g. Letolle 2000; Tsvestkinsaya et al., 2002). During wet episodes it has been suggested that the Amu Darya is naturally diverted away from the Aral Sea towards Lake Sarykamysh, or that it may form several deltas discharging into both

lakes (Shnitnikov, 1969, cited in Boomer et al., 2001). Letolle et al (in review) have determined that the Uzboi does not have the capacity to transport the entire flow of the Amu Darya, suggesting that on occasion it may form different branches when diverted from the Aral Sea, with a portion of the flow simply terminating in the desert. During this episode of high lake levels at around 200 AD, it is thought that control of irrigation systems was sophisticated to such an extent that discharge of the Amu Darya was maintained to both the Aral Sea and the Sarykamysh (Letolle and Mainguet, 1997; Boomer et al, 2000). Subsequently it would appear that prior to 400 AD and definitely around 200 AD when high lake levels are recorded by Boroffka et al. (in press) the region was in receipt of sufficient moisture to maintain not only high levels of the Aral Sea but also the flow of water into the Sarykamysh and permit the development of extensive irrigation facilities (e.g. Letolle and Mainguet, 1993; Boroffka et al., 2004). This period also saw the development of irrigation along the Syr Darya (Andrianov, 1995).

With high lake levels indicated at ca. 200 AD (Boroffka et al., in press) and increased fluvial input to the Aral Sea indicated by the age model at around 400 AD there is a 200 year period during which this first severe regression may have occurred and resulted in the deposition of gypsum at Chernyshov Bay. At this time the Syr Darya is believed to have maintained a shallow freshwater body in the eastern basin resulting in the deposition of as much as 10,000 km^2 of peat-like sediments (Letolle and Mainguet, 1997; Boomer et al. 2000; Le Callonnec et al. 2005) and a diatom flora indicative of such an environment (Aleshkinsaya et al., 1996). Contemporaneous discharge of the Amu Darya to the western basin was limited (Kes, 1995) much of the flow believed to have been diverted in a westerly direction along old river beds and irrigation channels towards Lake Sarykamysh (Figs. 4.15, 4.16) and on to the Caspian Sea through the now dry Uzboi river bed (Letolle 2000; Tsvetsinskaya et al. 2002).

The diversion of the Amu Darya away from the Aral Sea resulted in the deposition of mirabilite in some parts of the western basin which in all probability existed as either a single or a series of shallow hypersaline lakes. Letolle et al. (2004) have suggested that a salinity of 150 g/l would be required for the precipitation of mirabilite and that this would equate to a lake level of ~23 m a.s.l., making this regression more severe than the current low stand.

In the EM levels of the Dead Sea are believed to have been in decline from ca 300 AD (Heim et al., 1997; Frumkin et al., 2001) to as late as ca. 450 AD (Bookman et al., 2004). This range of dates certainly corresponds with the potential timing of the low levels of the Aral Sea at 1600 +/- 300 cal. yr BP. Enzel et al., (2003) suggest that dry episodes and low lake levels of the Dead Sea are characterised by the failure of cyclones to penetrate into the EM and/or the displacemet of storm tracks farther north. This would similarly have the effect of reducing overall moisture availability in those continental regions of Central Asia which are reliant upon the westerly transport of these cyclones. However as the Syr Darya was able to maintain significant discharge into the lake's eastern basin, increased aridity as the sole cause of this regression, is open to question.

This period coincides with the westward expansion and destruction of settlements along the Amu Darya by the Ephalites (White Huns) in the early 5th century AD, one consequence being the diversion of the Amu Darya towards Lake Sarykamysh (e.g. Klige et al., 1996; Letolle and Maiugnet, 1997; Tsvestkinsaya et al., 2002; Yagodin, in press). Whether fluvial inputs to Lake Sarykamysh itself were maintained at this time is debated however archaeological data from the region indicate that water was, at the very least, still flowing towards its delta (Klige et al. 1996). Discharge may also have been diverted into the desert as suggested by Letolle et al., (in review). Thus differentiating between the two forcing factors is difficult. It is conceivable that an episode of increased aridity across the region may have been responsible for the onset of a low lake level stand, the severity of which was ultimately enhanced by human activity.

Immediately overlying the gypsum deposit, the diatom inferred conductivity in CH1-z1 indicates mesosaline conditions and low lake levels. Planktonic lifeforms dominate, in particular *C. choctawhatcheeana*. Although generally considered to favour mesosaline conditions (Wilderman, 1987; Prasad, 1990; Hakannson et al. 1993; Prasad and Nienow, 2006), *C. choctawhatcheeana* has been reported from the Aral Sea and the Syr Darya delta at salinities of 36 g/l and 5 – 7 g/l respectively (Rusakova, 1995) and a range of other environments, including the Danube (Kiss et al., 1988) and the hypersaline waters of the Salton Sea, California (Lange and Tiffany 2002) and Lake Quarun, Egypt (Flower et al, 2005). As the abundance of this species declines,

others indicative of more dilute conditions increase (Figure 4.8) e.g. *T. incerta*. This species is found in the plankton of the Volga and is common in the Caspian Sea, leading Hasle (1978) to suggest that it is essentially a freshwater species capable of tolerating brackish conditions. The uppermost samples of CH1-z1 are notable for the presence of *S. parvus* a species found in fresh and oligosaline conditions (Snoejis et al. 1993; Yang et al. 2003) and in the plankton of large rivers (Kiss and Genkal, 1993). This flora combined with the presence of other freshwater algae and dinoflagellates (Sorrel et al., 2006) suggests that this zone reflects a period of lake level rise and the progressive dilution of the western basin as flow from the Amu Darya returned to the Aral Sea. According to the age model, this was a rapid event occurring in under 10 years, and confirms the opinion that the preservation of mirabilite in the western basin was made possible by rapid fluvial input with a heavy sediment load thereby preventing dissolution (Letolle and Maiugnet, 1997; Letolle et al. 2004). This process is also likely to be responsible for the preservation of the gypsum horizon in Chernyshov Bay.

Archaeological investigations show that after the 4^{th} – 5^{th} centuries AD the area southwest of the Aral Sea dried up completely (Tsvetsinskaya et al., 2002). The Amu Darya has a sediment load of between 1 – 4 g/l (Froebrich and Kayumov, 2005) and a tendency to naturally divert its course due to the accumulation of sediment within its bed. This was particularly evident during both the Neolithic and the Bronze Age with flow being diverted in a westerly direction towards Lake Sarykamysh and subsequent sediment build up then re directing the river northwards to the Aral Sea (Klige et al., 1996; Letolle and Maiugnet, 1997; Boroffka et al., in press; Yagodin in press). The development of irrigation facilities is thought to control this tendency, consequently one might hypothesise that the lack of water management after the destruction of irrigation systems by the Huns led to sediment build up within the bed of the Amu Darya and its natural diversion, this time away from the Sarykamysh and north towards the Aral Sea, bringing what would appear to be a swift end to a major regression. Tectonic activity must also be taken into account. When flowing in an East – West direction towards the Sarykamysh, the Amu Darya crosses a region with an annual uplift rate of ca. 6 mm (Nurtaev, 2004; Jaboyedoff et al., 2005), compared with a region of negligible uplift when flowing in a southeast – northwest direction towards the Aral Sea thus it is conceivable that anthropogenic activity and natural

processes in particular the deposition of alluvial sediments and tectonic activity all combined to redirect the flow of the Amu Darya towards the Aral Sea.

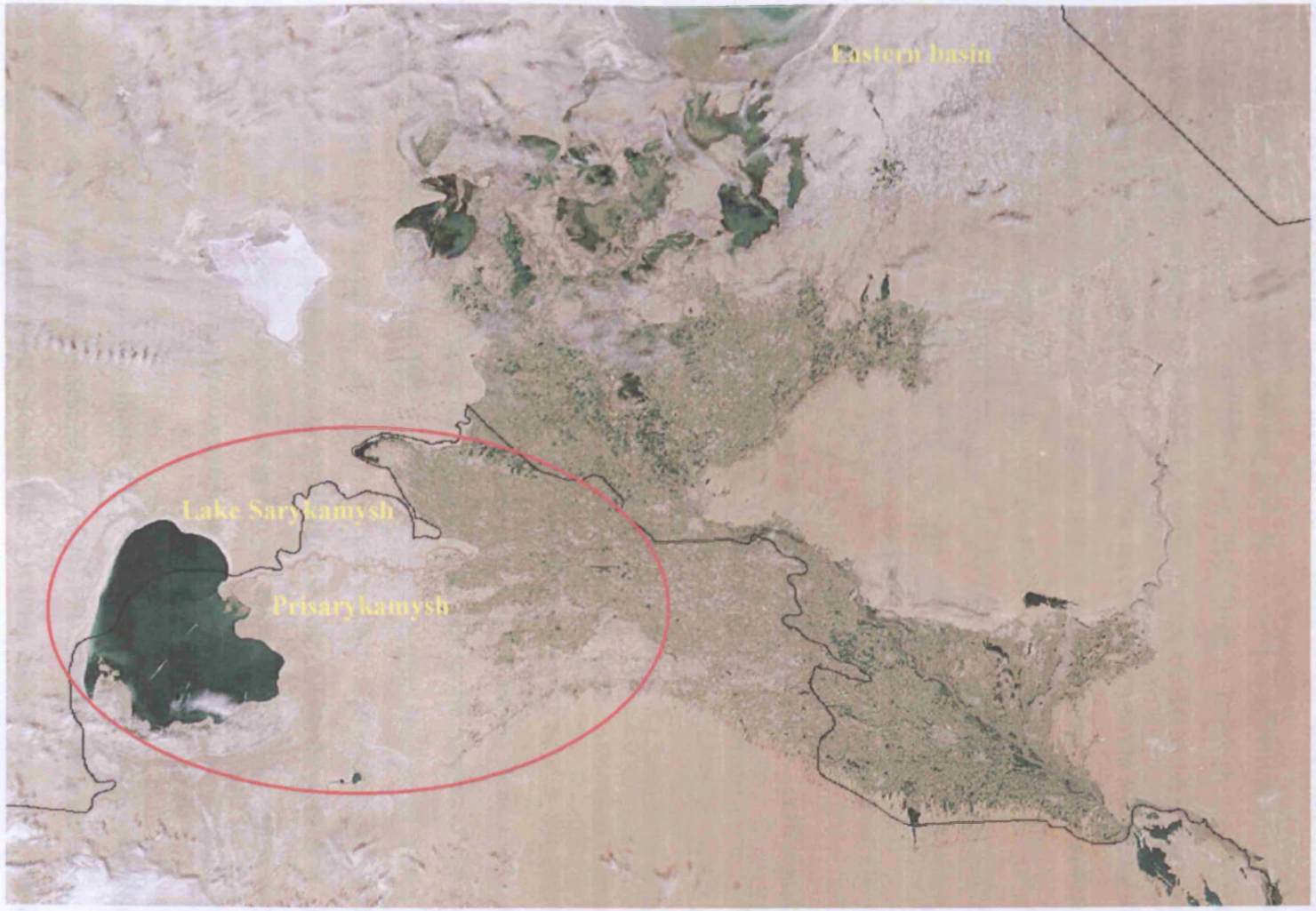

Figure 4.16. Satellite image of the upper reaches of the Amu Darya. The extensive irrigation along its course in an otherwise arid landscape can clearly be seen. The Prisarykamysh region and the Sarykamysh Lake (see text for details) are highlighted in the red oval. Image available online at http://rapidfire.sci.gsfc.nasa.gov. Downloaded 09/03/06.

4.11.2.2 High to intermediate levels ca. 440 – 1195 AD

These high lake levels and oligosaline conditions persisted throughout CH1-z2 from 440 – 570 AD. The decline in the planktonic element of the fossil assemblages and the dominance of *A. pediculus*, a benthic species common in freshwater environments (Gasse et al., 1986; Snoejis et al., 1996) but also found in brackish conditions (Vos and de Wolf, 1993; Witkowski, 1994) is a consequence of rising lake levels and the incorporation into the Chernyshov Bay sediments of flora from the increasing littoral zone as a result of sediment focusing. (section 4.11.1) Furthermore, Andren et al (1999) state that *C. neodiminuta*, generally regarded as a freshwater species is able to survive in brackish water conditions near freshwater discharges, strengthening the argument for renewed fluvial input to the lake and the transport of diatoms from shallower regions.

At around this time, the Levant experienced increased humidity, (Schilmann et al. 2001) as did the Aral Sea Basin (Sorrel et al. in review1), suggesting that increased moisture availability over the region may also have been contributing to the rise in lake levels. Similar conditions are observed in CH1-z3 in which conductivity gradually increases from about 600 AD until at ca. 985 AD when mesosaline conditions suggest the inception of a second regression. Yagodin (in press) has suggested that the natural build up of sediment in the bed of the Amu Darya and its delta during the 8^{th} and 9^{th} centuries AD led to its diversion westward towards the Sarykamysh, where, by the 10^{th} century AD, the region was once again being exploited (Tsvetsinskaya et. al. 2002). This period also coincides with the introduction of new irrigation laws, written in the 'Book of Canals' (*Qitab al-Quiny*), along the entire lower reaches of the Amu Darya (Blanchard, 2002) which may well have allowed discharge of the Amu Draya in to both lakes.

During this period the signal from the Eastern Mediterranean is somewhat mixed; high levels of the Dead Sea at around 1000 yr BP/1000 AD (Frumkin et al. 1991) coincide with both marine and terrestrial $\delta^{18}O$ values indicative of dry conditions between 1300 – 900 yr BP/700 – 1100 AD (Schilman et al. 2002). This is similarly a period of increased temperatures and favourable conditions for the growth of Juniper in the Karakorum and Tien Shan, where Esper et al. (2002) suggest a 'Medieval

Warm Period' between 800 – 1000 AD. In the Pamir, Zech et al. (2002) attribute soil development at around 1000 yr B.P/1000 AD to increased warmth, conditions which may also have been responsible for the contemporaneous peat bog formation on a former glacier bed in the Tien Shan (Savoskul and Solomina, 1996) and high levels of Lake Issyk-kul between 1000 and 1180 AD (Giralt et al, 2003). Precipitation in the Issyk-Kul region is believed to have steadily declined throughout this period (Giralt et al, 2003) concurring with results of Sorrel et al. (in review1) suggesting increased aridity across the Aral Sea Basin.

It is thus possible to conclude that this period of high followed by declining lake levels was a result of the natural diversion of the Amu Darya and increased irrigation and that while increased aridity across the region may have been a contributing factor it is impossible to ascertain with any confidence whether it contributed significantly to lake level decline let alone determine whether it was the main driver of lake level change during this period.

4.11.2.3 Regression ca 1195 – 1355 AD

A second severe regression is inferred throughout CH1-z4 from 1195 - 1355 AD and is almost certainly responsible for the deposition of a gypsum horizon at around 1250 AD. This episode of low lake levels corresponds with a date of 970 +/- 140 yr BP (1000 +/- 300 cal. yr BP) obtained from the remains of saxaul (*Haloxylun aphyllum*) groves found below the 1960 lake level (Rubanov et al., 1987) and geochemical analysis which indicates that discharge to the lake at this time was dominated by the Syr Darya (LeCallonnec et al., 2005).

Stevens et al., (2006) use the model proposed by Stone and Fritz (2004) to interpret increased abundance of planktonic species as being indicative of low lake levels and the separation of basins at Foy Lake in Montana from 800 – 1200 AD (see section 4.11.1). The diatom flora overlying the gypsum horizon is dominated by saline planktonic and tychoplanktonic species (Figure 4.8) indicating increased conductivity and similarly low lake levels of the Aral Sea. Both *N. liebetruthii* var. *liebetruthii* and *N. fonticola* are also common in epipelic environments (Ben Goldsmith pers. comm.) and as such their presence suggests that the shoreline surrounding Chernyshov Bay

consisted of extensive mudflats as is the case today (Figure 3.3). Whether the western basin had become isolated from the eastern basin at this time is uncertain, however, assemblages dominated by small *Nitzschia* spp. would appear to indicate a major regressive episode similar to that occurring presently. The gypsum horizon is overlain by varve-like laminae (Figure 3.5) suggesting anoxic bottom water and possible meromictic conditions due to a density gradient as is the case today.

During this second regression, high levels of the Dead Sea (Bookman et al., 2004) are accompanied by humid conditions and a possible MWP across the EM (Schilman et al., 2002). Pollen evidence points to a period of increased precipitation in the Aral Sea basin (Sorrel et al., in review1) although this shift in vegetation types was not registered in the C:N ratio of organic isotopes (< 10) from Chernyshov Bay (see chapter 5). Similarly archaeological evidence close to Lake Sarykamysh indicates a humid environment (Tsvestkinsaya et al., 2002). In contrast arid conditions are recorded in the Karakorum and Tien Shan (Esper et al., 2002; Treydte et al., 2006) where levels of Lake Issyk-Kul are also low (Giralt et al., 2004). As with the previous regression, cyclonic activity may have been concentrated in the EM, possibly extending as far as the Aral Sea but failing to reach the Pamir and Tien Shan. Any increase in precipitation to the hydrological inputs of the lake however, is unlikely to have offset the reduced discharge of both the Amu Darya and Syr Darya that will have accompanied an extended dry episode in their headwaters.

In common with the previous regression, human intervention in the flow of the Amu Darya is also likely. This was a time of immense social upheaval in Central Asia, and while this regression is synchronous with increased aridity in the Pamir and Tien Shan it also coincides with the westward expansion of the Mongols led by Genghis Khan. In one particularly devastating encounter in 1221 AD they are known to have destroyed irrigation facilities and flooded the Khwarzem capital of Urgench resulting in the diversion of water towards Lake Sarykamysh (e.g. Kes, 1995; Letolle and Mainguet, 1997; Boroffka et al., 2005). Irrigation canals are believed to have been swiftly repaired (Yagodin, in press) and the age model suggests that by 1360 AD in CH1-z5, dilute conditions and high lake levels had returned.

4.11.2.4. High levels ca. 1360 – 1780 AD

High lake levels and dilute, oligosaline conditions persist throughout CH1-z5, from ca. 1360 – 1560 AD and contrasts with archaeological and historical evidence. For example, two recently discovered settlements in both the eastern and western basins at ca. 32 m a.s.l., point to a severe regression between the late 14th and 16th/17th centuries AD (Boroffka et al. 2005; Yagodin, in press), and is further supported by *Saxual* remains uncovered at about 40 m a.s.l. and dated to 287 ± 5 yr BP (415 ± 65 cal. yr BP/1585 ± 65 AD). This regressive phase was believed to have been brought about by the further destruction of irrigation systems by Tamerlane in the late 14th century which again led to the diversion of the Amu Darya towards to the Sarykamysh and intermittently through the Uzboi to the Caspian. From detailed historical records it is known that it was not until the late 16th century that discharge from the Amu Darya once again entered the Aral Sea (Letolle and Maiugnet, 1997; Boomer et al. 2001). Furthermore there is no mention of the existence of the Aral Sea in texts or maps of this period, (see Letolle and Maiugnet, 1993 for a full review). It must therefore be assumed that Chernyshov Bay at least, was receiving some form of hydrological input during this period and may have existed in isolation as a fresh/brackish waterbody. This period coincides with maximum humidity in the Aral Sea basin as inferred by Sorrel et al. (in review1) and for a settlement to have existed at 32 m a.s.l. in the eastern basin, freshwater must have been available. Boroffka (personal communication) states that the settlement was almost certainly abandoned as a result of Tamerlane's activities rather than reduced water supply. One might thus conclude that some form of fluvial input was reaching Chernyshov Bay.

The presence of valves of *Chaetoceros* cf. *wighamii* around 500 yr BP suggest an episode of increased salinity. *Chaetoceros* spp. valves are generally very finely silicified and hence susceptible to dissolution. The age model indicates a high sedimentation rate during CH1-z5 (1.87 cm/yr) thus the rapid burial of valves may have prevented their dissolution. This also corresponds with a significant positive shift in the values of $\delta^{13}C_{org}$, (C:N < 10, chapter 5) which may indicate increased conductivity and algal productivity, enhanced by the deposition of Si and other nutrients by dust transport from the former seabed. Johnson et al. (2001) suggest that increased productivity during low lake level stands may be due to the in-wash of

material, particularly Si, from a newly exposed lake bed. Although in the case of the Aral Sea input is more likely to be a consequence of dust storms, the frequency of which has increased during the present regression with as much as 140 – 150 million tonnes deflated annually from the former seabed (Glazovsky, 1995), much of which is carried west and south west. This will have also resulted in the input of nutrients to the surface waters a process expected to generate a phytoplanktonic biomass increase (Ridame and Guieu, 2002).

High lake levels and dilute conditions continue into CH1-z6 from 1460 – 1730 AD. Decreasing abundances of *A. pediculus* and *C. neodiminuta* appear to suggest increasing conductivity and declining lake levels throughout this zone although not on the scale witnessed previously. This period coincides with the coldest conditions of the last 1300 years seen in the Karakorum and Tien Shan between 1600 – 1800 AD (Esper et al., 2002b, 2003) with advancing glaciers also recorded in the Tien Shan at 1700 AD (Yafeng and Jiawen) and 1750 AD (Savoskul and Solomina, 1996). A concordant lowering in the limit of permafrost of 300 – 400 m has also been estimated, with temperatures an estimated 2 - 3°C lower than the present day (Gorbunov, 1996). It is also estimated that irrigation in the Aral Sea Basin at this time totalled ca. 1.9 million ha (Tolstoy, 1962 cited in Boomer et al., 2000). The high lake levels recorded throughout this period appear to suggest that any decreases in temperature in the Pamir and Tien Shan and accompanying reduction in the contribution of summer meltwater to the hydrological balance of the lake, or increased aridity were insufficient to cause as severe a regression as those witnessed earlier.

4.11.2.5. Regression ca. 1780 AD – present

Fresh and oligosaline conditions and high lake levels persist until ca. 1780 AD in CH1-z7, at which point there is a shift to mesosaline conditions and the inception of what would appear to be a third major regression. The high percentage abundance of planktonic and tychoplanktonic species in the uppermost zone (Figure 4.8) has so far only been seen during episodes of low lake level. Interestingly, in CH-1 the abundance of *C. choctawhatcheeana* declines in the uppermost sample, however its concentration within the sediments exhibits a small increase (Figure 4.9). The decline in abundance is explained by increased numbers of *N. fonticola*, which, in common

with the regression at ca 1250 AD is possibly due to the availability of muddy littoral zones in the proximity of the coring site. The high values of *C. choctawhatcheeana* are also observed over the last 100 years in Ar-9 and not just during the present regression as one might expect. As previously discussed (section 4.10.1) diatom inferred conductivity in Ar-9 is linked to the abundance of *C. choctawhatcheeana*. This would also appear to be the case in the past 220 years or so in CH-1. Over the last 260 years, lake levels are generally considered to have been high (Shermatov et al 2004). This episode of low lake levels occurs much earlier than expected and clearly contrasts with historical and documentary evidence which indicate high lake levels with minor fluctuations and dilute conditions until 1960 (Figure 4.17). Interestingly the increase in conductivity is concordant with the ~ 3 m decline in lake levels initiated in 1790 AD. A decline of this magnitude will result in the loss of ca. 9000 km^2 of the littoral zone, this is thought to have resulted in the increased abundance of planktonic species which was maintained as a result of these minor fluctuations into the current regression.

During this period, pollen and geochemistry records from the KaraBogozGol (KBG) in the Caspian Sea (Gilat et al, 2004; Leroy et al, 2006) indicate high lake levels and enhanced moisture from 1817 – 1878 AD followed by reduced precipitation and arid conditions between 1878 – 1913 AD. As can be seen from figure 4.17 the episode of increased moisture recorded from the KBG does not manifest it self as clearly in the levels of the Aral Sea, which fluctuate over this period. Conversely the arid episode detected across the KBG does coincide rather better with reduced levels of the Aral Sea.

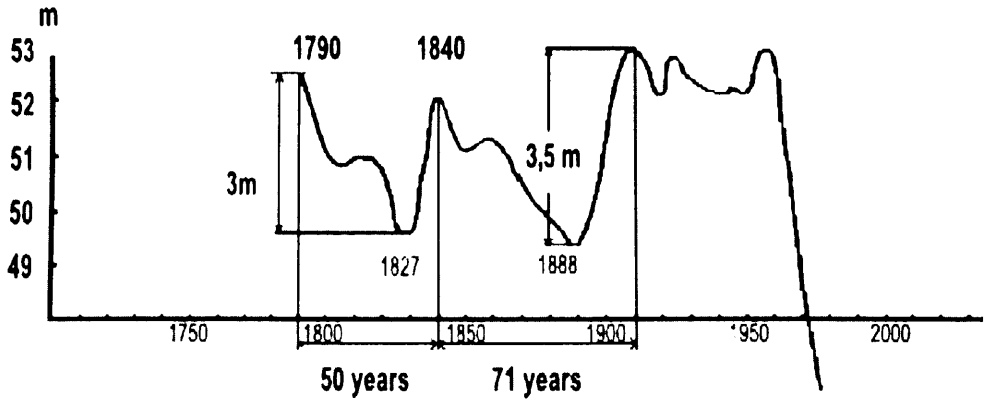

Figure 4.17. Fluctuations of the Aral Sea from 1790 – 1960 AD. From Shermatov et al., (2004).

Leroy et al (2006) point to a period intense evaporation between 1913 and 1955 and reduced precipitation in the region of the KBG from 1955 to 1998. Although the instrumental records of the levels of the Aral Sea (Figure 4.18) only extend as far back as 1942 it can be seen that lake levels show an increasing trend until the inception of irrigation in 1960 AD. Consequently over this period the lake appears unaffected by climatic factors influencing the level of the KBG and its surrounding vegetation.

It has been suggested that the NAO or its related phenonema the AO may be linked to climatic conditions across Central Asia (Kreutz et al., 2001; Small et al., 2001; Giralt et al., 2003; Todd and Mackay, 2003; Yousef, 2006). The shift to a positive NAO state since the early 1970s and the switch from meridional to zonal atmospheric circulation allowing the movement of relatively warm, moist air across northern Europe has resulted in an increase in the levels of the Caspian Sea, not as a consequence of increased on lake precipitation, which is likely to have declined during an episode of high NAO index along with that of the Mediterranean (Hurrell, 2000), but due to increased humidity in Eurasia and subsequent runoff from the Volga (Kaplin, 1995) despite large withdrawls for irrigation (Shermatov et al., 2004). Positive phases of the NAO are however associated with increased aridity across the Aral Sea and the Pamir and Tien Shan (Aizen et al., 2001) and subsequently a reduction in the levels of the Aral Sea.

Monthly precipitation and temperature records spanning 1906 – 1999 from Aralsk (a former fishing port on the coast of what is now the Small Aral) show no significant correlation with the NAO for the same period ($r = -0.024$ and -0. 013 respectively). There is however a weak relationship ($r = 0.25$, $p = 0.17$) between the annual average flow rate of the Amu Darya recorded at Chatly, 300 km upriver from the Aral Sea in Uzbekistan between 1931 and 1960 AD, a period during which the NAO fluctuated between both negative and positive phases.

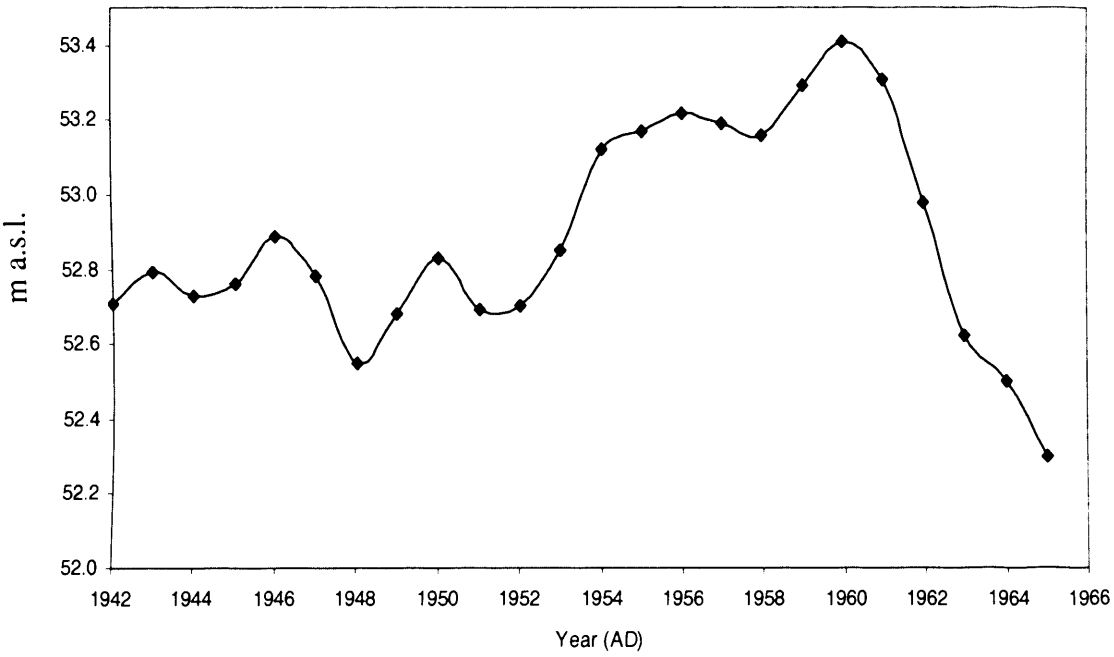

Figure 4.18. Annual fluctuations of the Aral Sea from 1942 – 1965 AD.

Shermatov et al (2004) have linked the ~3 m fluctuations in the level of the lake to solar activity. They suggested that these minor regressions are a consequence of a reduction in the flow of the Amu Darya during periods of high solar activity and have concluded that a natual reduction in lake levels of around 3 m would have occurred ca. 1962 AD regardless of the initiation of irrigation. They hypothesise that the forthcoming solar cycles 24 (2008 – 2018) and 25 (2019 – 2030) will see a natural increase in the of the Amu Darya and a potential 3 m rise in lake levels.

4.12 Conclusion.

The diatom record of conductivity and lake level change as recorded in the sediments of Chernyshov Bay provide evidence of three severe regressions of the Aral Sea during the past ca. 1600 years. The high resolution nature of the record serves to confirm the timing of these regressions established by other workers and discussed in the text. During this time frame it is essential to differentiate between environmental changes that are brought about by natural factors (i.e. fluctuations in aridity that are largely influenced by conditions in the EM and the natural shifts in the direction of flow of the Amu Darya) and, anthropogenic activity (i.e. irrigation and military conflict) or indeed a combination of the two.

The return to high lake levels at ca 400 AD would appear to follow a period during which there was sufficient moisture across the region to maintain high levels of both the Aral Sea and Lake Sarykamysh (i.e. at 200 AD). That the EM was also undergoing a period of enhanced moisture supply suggests climatic teleconnections between that region and Central Asia.

The timing of the lake level decline prior to ~ 400 AD is synchronous with increased aridity across the EM but also corresponds with an episode of social upheaval in Central Asia, the destruction of irrigation facilities and the subsequent diversion of the Amu Darya westwards towards Lake Sarykamysh. The build up of sediment within the Amu Darya and a lack of water management resulted in its diversion to the Aral Sea at ca. 400 AD.

The second regression at ca. 1250 AD would appear to have followed a period during which some of the Amu Darya was being naturally diverted towards Lake Sarykamysh. Increased moisture availability in the EM and Aral Sea basin at this time contrasts with aridity in the Pamir and Tien Shan and maybe a consequence of the failure of cyclones formed in the EM to penetrate the montane regions of Central Asia, indicating a breakdown of the climatic teleconnections that existed around 200 AD when levels of both the Aral and Dead Sea were high. However as with the earlier regression anthropogenic activity and in particular the destruction of irrigation facilities by the Mongols diverted the Amu Darya away from the Aral Sea.

Consequently stating with any certainty whether natural processes were ultimately more responsible than human activity is difficult. It is possible to say however, that while natural processes probably had a role in these regressions, historical evidence indicates that human activity, in common with the present day, almost certainly contributed to the low lake level stands and was in all probability responsible for the severity of these regressions, in common with present events.

Chapter Five

Aral Sea organic carbon isotope records ($\delta^{13}C_{org}$) and C/N ratios

5.1 Introduction

An isotope of an element has the same chemical properties and number of protons as the original element but differs in the number of neutrons. A well established technique when undertaking palaeoenvironmental reconstructions is the determination of the oxygen isotope ($\delta^{18}O$) composition of calcareous sediments and in particular authigenic carbonates, which are precipitated by the photosynthetic utilization of CO_2, and the resultant calcium carbonate supersaturation (Leng et al., 2001; Leng, 2003). However one of the pitfalls of this method is the difficulty encountered when attempting to distinguish between authegenic and allogenic material.

Exposed river banks believed to contain Neogene carbonate material have been observed close to the Aral Sea (Hedi Oberhaensli, pers. comm.). This gives rise to the potential contamination of sediments, consequently rather than the establishment of $\delta^{18}O$ from this material, the isotopes of concern in this study are those of carbon and in particular the ratio of $^{13}C/^{12}C$ (expressed as $\delta^{13}C$), which is subject to change by a process of fractionation, in which different rates of reaction for molecular species results in a disproportional concentration of one isotope over the other (Leng, 2003).

The analysis of $\delta^{13}C$ of bulk organic material ($\delta^{13}C_{org}$) preserved within lake sediments provides important information on the physical environment in and around the lake at a particular time, from which it is possible to distinguish episodes of anthropogenic disturbance within the catchment i.e. deforestation (e.g. Kaushal and Binford, 1999), climatic induced changes reflected by the in-wash of terrestrially derived organic matter (e.g. Valero-Garces et al., 2000; Battarbee et al., 2001; Lamb et al., 2004) and/or a history of within-lake productivity (e.g. Hodell and Schleske, 1998; Wolfe et al., 1999; Leng et al., 2005).

5.2 Controls on $\delta^{13}C$

The carbon isotope composition of lake waters total dissolved inorganic carbon (TDIC) is measured as the ratio of $^{13}C/^{12}C$ per mil ($\delta^{13}C$ ‰) and is controlled mainly by three processes; 1) the C isotopic composition of inflowing waters; 2) the exchange of CO_2 between the atmosphere and the TDIC of the lake waters; and 3) photosynthesis and respiration within the lake (McKenzie, 1985; Leng and Marshall, 2004). All of these factors are in some way connected to climate, nutrient availability and water residence time (Leng, 2004).

The TDIC within lake waters generally have a $\delta^{13}C$ value of ca. –7‰. In hydrologically closed lakes, however, where residence times are increased, this value is subject to change, reaching between +1 to +3‰ (unless altered by within lake photosynthesis and respiration) as lake water pCO_2 rises reaching isotopic equilibrium with atmospheric CO_2. Photosynthetic activity and respiration are the dominant control on the lake water values of TDIC (McKenzie, 1985); isotopic fractionation during photosynthesis results in the preferential uptake of the lighter ^{12}C isotope and

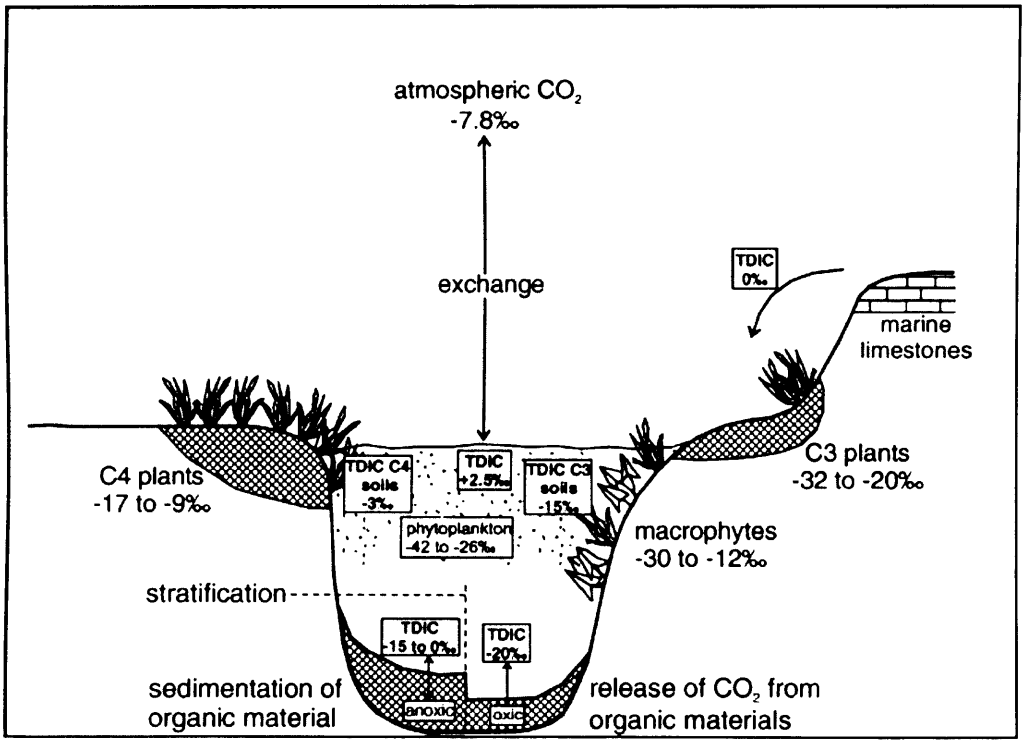

Figure 5.1. Carbon isotope values for the major sources of carbon into lakes and examples of the range of resulting $\delta^{13}C$. From Leng and Marshall (2004).

the carbon pool subsequently becoming enriched in ^{13}C. This process will continue if there is increased algal productivity and/or anoxic bottom waters where the breakdown of organic matter and subsequent release of ^{12}C is restricted. Alternatively, well aerated bottom water results in the oxidation of organic matter at the sediment-water interface and the subsequent release of ^{12}C thus reducing the effects of photosynthesis on the carbon pool. Stratification of the lake may even result in an isotopic gradient. For example, McKenzie (1985) reported surface waters of Lake Greifen, Switzerland, in the summer months as having a $\delta^{13}C$ value of –7.5‰ while those of the bottom waters neared –13‰.

5.2.1 Carbon isotopes in organic matter

The particulate detritus of plant material constitutes the primary source of organic matter to lake sediments (Meyers and Lallier-Verges, 1999). The origin of this matter may be from either the lake itself, its catchment or a combination of the two (Figure 5.1). These plants may be divided into separate groups.

- Vascular plants such as grasses shrubs and trees, containing large amounts of carbon-rich cellulose and lignin which may be found not only proximal to the lake but in shallow littoral areas as bottom rooted emergent vegetation.

- Non-vascular plants such as algae containing much less carbon-rich material, found attached to a substrate or living freely in the water-column.

The range of $\delta^{13}C$ values of a particular plant is governed by the photosynthetic pathway used to incorporate CO_2 from the atmosphere. Early examinations of the $\delta^{13}C$ values of plants (Wickman, 1952; Craig, 1953, 1954) highlighted a relatively constant value of –27‰ for most of those investigated. Termed C_3 plants and including algae, these incorporate atmospheric CO_2 through carboxylation of ribulose biophosphate, resulting in the preferential uptake of ^{12}C with an isotopic discrimination of ca. –20 ‰ from the $\delta^{13}C$ of the inorganic carbon source.

Later investigations in the 1960s (Hatch and Slack, 1968) revealed the presence of a second pathway, the C_4 Hatch-Slack pathway in which plants incorporate CO_2 by the

carboxylation of phosphenolpyruvate resulting in an isotopic discrimination of between –4 to –6‰ and a subsequent average $\delta^{13}C$ value of ca. –14‰ (Meyers and Lallier-Verges, 1999). Smith and Epstein (1971) determined that this pathway was utilised by a whole host of species, particularly grasses and those living under water stress in arid and semiarid environments. It was later discovered that some plants (primarily succulents in arid zones) are able to fix atmospheric carbon by using the CAM (crassulacean acid metabolism) pathway in which CO_2 is incorporated at night by either the C_3 or C_4 pathway (O' Leary, 1981). Isotopic discrimination in this latter group is between –4 to –20‰ and is dependent upon the photosynthetic pathway being utilised.

However, one of the main controls on the carbon isotope composition of lacustrine plants is the type of carbon available. In addition to dissolved CO_2 carbon is also available in the form of bicarbonate (HCO_3^-), some carbonate (CO_3^{2-}) and small amounts of carbonic acid (H_2CO_3), this latter carbonate species contributing just ~0.1% the value of CO_2 (Zeebee, 1999). The ratio between the three is a function of temperature and particularly pH (Figure 5. 2).

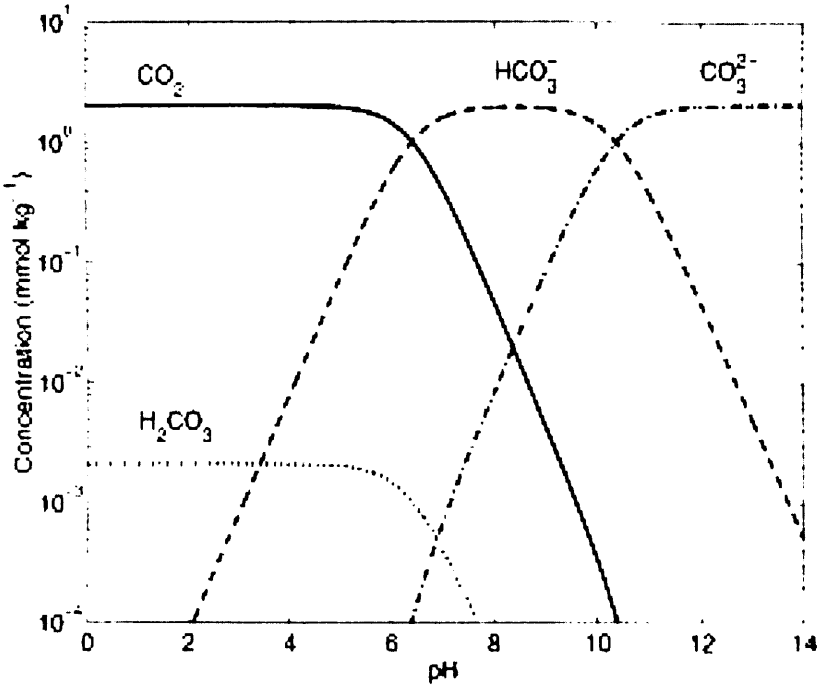

Figure 5.2. The concentration of dissolved carbonate species as a function of pH. From Zeebee (1999).

In waters with a pH of 5.5, 80% of the inorganic carbon is found as dissolved CO_2 whereas in a pH of 8.5 dissolved CO_2 may be less than 1% (Keeley and Sandquist, 1992, Hassan et al. 1997). When interpreting the $\delta^{13}C_{org}$ values obtained from lake sediments particular attention needs to be paid to this form of carbon assimilation as values of HCO_3^- are between 7 to 11‰ higher than the values obtained when utilising dissolved CO_2 (Mook et al. 1974). This discrepancy may result in the $\delta^{13}C$ values of algal organic matter, which uses the C_3 pathway and generally has a $\delta^{13}C$ value of between –30 to –25‰, reaching $\delta^{13}C$ values of ca. –9‰ which is in the range of C_4 plants (Meyers and Teranes, 2001).

5.2.2 C/N ratios

While the different isotopic values of C_3 and C_4 plants allow one to distinguish which may have provided the greater contribution to the lacustrine organic matter, algae produced within the lake using the C_3 pathway has overlapping $\delta^{13}C$ values (Figure 5.3) and cannot be easily differentiated (isotopically) from allochthonous material derived from C_3 plants. In order to help discern between an aquatic or terrestrial source, the ratio between carbon and nitrogen (C/N) contained within organic matter may be used as an additional indication of the relative contributions of organic matter from differing sources (Figure 5.3).

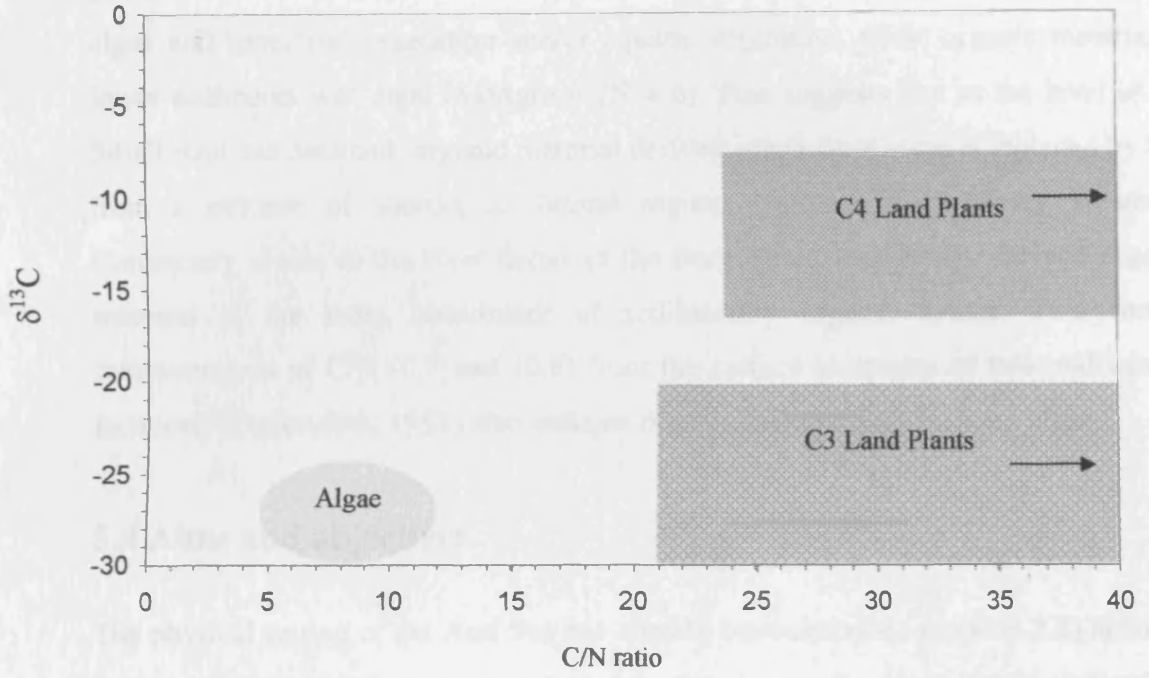

Figure 5.3. Representative elemental and carbon isotopic compositions of organic matter from lacustrine algae, C_3 land plants and C_4 land plants that use CO_2 as their source of organic carbon during photosynthesis. From Meyers and Lallier – Verges (1999).

The C/N ratios of lacustrine algae are generally low ca. < 10 – 12, with most diatoms varying between 5 and 8 (Lamb et al., 2004). Values between ca. 12 – 20 will often reflect organic material dominated by submergent and floating macrophytes, or a mixed source, while values > 20 are more typical of emergent macrophytes and terrestrial plants (Meyers and Lallier- Verges, 1999; Leng and Marshall, 2004). There may be some degradation of both carbon and nitrogen during the early stages of diagenesis; however any compositional alteration undergone does not cancel out the large differences in C/N between material derived from vascular land plants and non-vascular algae (Meyers and Lallier - Verges, 1999)

5.3 The Aral Sea, C/N and $\delta^{13}C_{org}$

There are to date, no published records of $\delta^{13}C_{org}$ from the Aral Sea. C/N ratios however have been recorded up to a depth of 10 cm from several locations in the Berg Strait near the Syr Darya delta (Figure 5.4) and Tastubek Bay, in the Small Aral, (Maeda et al. 1996). Results indicate that those sites near the river mouth (C/N 22 – 63) have organic material derived principally from terrestrial vegetation and aquatic

plants. At Tastubek Bay, surface sediment C/N ratio was 17, suggesting a mixture of algae and terrestrial vegetation and/or aquatic vegetation, while organic material in lower sediments was algal in origin (C/N = 6). This suggests that as the level of the Small Aral has declined, organic material derived solely from algae is replaced by that from a mixture of sources as littoral regions encroach upon coring locations. Conversely closer to the river deltas in the Berg Strait, terrestrially derived organic material is the main constituent of sedimentary organic matter. Two further measurements of C/N (6.7 and 10.6) from the surface sediments of two undisclosed locations (Zenkevitch, 1953) also indicate organic material derived from algae.

5.4 Aims and objectives

The physical setting of the Aral Sea has already been described (section 2.2) however it is to all intents and purposes situated in the centre of a large desert with sparse vegetation cover. Any significant increase or changes in this cover brought about by shifts in the regional moisture regime may possibly be detected in the $\delta^{13}C_{org}$ and C/N values of organic matter if it becomes incorporated into the lake sediments. Increased localised vegetation cover will generally be a consequence of higher moisture availability and this should result in the enhanced in-wash of terrestrially derived organic material to the lake. Any wider scale vegetation changes in the catchment due to natural factors or anthropogenic activity, principally an increase in the area of land under cultivation, may possibly be reflected in the $\delta^{13}C$ and C/N ratio of organic material entering the lake via the Amu Darya and Syr Darya. The establishment of the $\delta^{13}C_{org}$ history and C/N ratio of the Aral Sea will help to estimate the extent to which vegetation in and around the lake has been subject to change over the last ca. 1600 cal. yr BP. This will then help to determine whether the lake level changes established in the previous chapter, are driven by episodes of natural climatic variability and/or anthropogenic activity.

Figure 5.4. Location of the present study site at Chernyshov Bay and the former Berg Strait and Tastubek Bay, the sediments of which have been analysed for C/N ratios by other workers (see text for details).

5.5 Methods

Ar-9 and CH-1 were measured at 2 cm (20 samples) and 4 cm (275 samples) intervals respectively. In order to remove any carbonate material, samples were placed in ca. 100 ml of 5% HCl in glass beakers for 12 hours. Following acid treatment these were washed three times in de-ionised, distilled water and allowed to dry at 40°C in a drying cabinet. After drying, samples were ground to a fine powder and stored in plastic vials. Measurements for carbon isotope of organic material ($\delta^{13}C_{org}$), total organic carbon (TOC%) and total nitrogen (TN%), from which C/N is derived, were

performed at the NERC Isotope and Geosciences Laboratory at the British Geological Survey by combustion in a Carlo Erba 1500 on-line to a VG TripleTrap and Optima dual-inlet mass spectrometer. $\delta^{13}C_{org}$ values were converted to the VPDB (Vienna – PeeDee Belemnite) scale using a within-run laboratory standard calibrated against NBS-19 and NBS-22. C/N ratios were calibrated against an acetanilide standard. Replicate analysis of well-mixed samples indicated a precision of $\pm$ <0.1‰ for $\delta^{13}C_{org}$ and $\pm$ <0.1 for C/N.

5.6 Results

5.6.1 Ar-9 (1925 – 2002 AD)

The $\delta^{13}C_{org}$, percent total organic carbon and nitrogen (TOC, TN) C/N ratios and diatom concentration are shown in figure 5.5 plotted against depth and age (year AD). Also illustrated is measured salinity. Those zones shown are those determined by CONISS on the percent diatom abundance (Figure 4.2). The values of $\delta^{13}C_{org}$ for the last ca. 75 years within the Chernyshov Bay sediments range from –28.0‰ to –20.8 ‰, with a mean value of –21.8 ‰ (s.d. 1.46‰). The C/N ratio has values ranging from 7.7 – 9.3 (mean = 8.2, s.d. 0.34) while that of total organic carbon (TOC) fluctuates between 1.3 and 12.4% (mean = 3.0%, s.d. 2.4%).

Values of $\delta^{13}C_{org}$ in the basal sample of **Ar9-z1** from ca. 1925 are –22.0‰. Values remain constant, although at the top of this zone in ca. 1955 these have increased to –20.8‰. C/N values are ca. 8 for much of this zone however from ca. 1945 to ca. 1955 there is an increasing trend with values of 9 in the uppermost sample. TOC is low (~ 2%) throughout. Values of $\delta^{13}C_{org}$ are around –22.0‰ throughout **Ar9-z2**, while C/N values of ~ 8 are typical for the rest of this zone. TOC shows a gradually increasing trend, reaching a peak of 5% in ca. 1975 but declines to 3% at the top of this zone by ca. 1985. The uppermost zone, **Ar9-z3**, has $\delta^{13}C_{org}$ values of around –22‰ until the surface sediment in 2002 when values decrease to –28‰. TOC shows an increasing trend in this zone, with surface sediments having a value of 12.4%. The C/N ratio however remains unchanged at ~ 8.

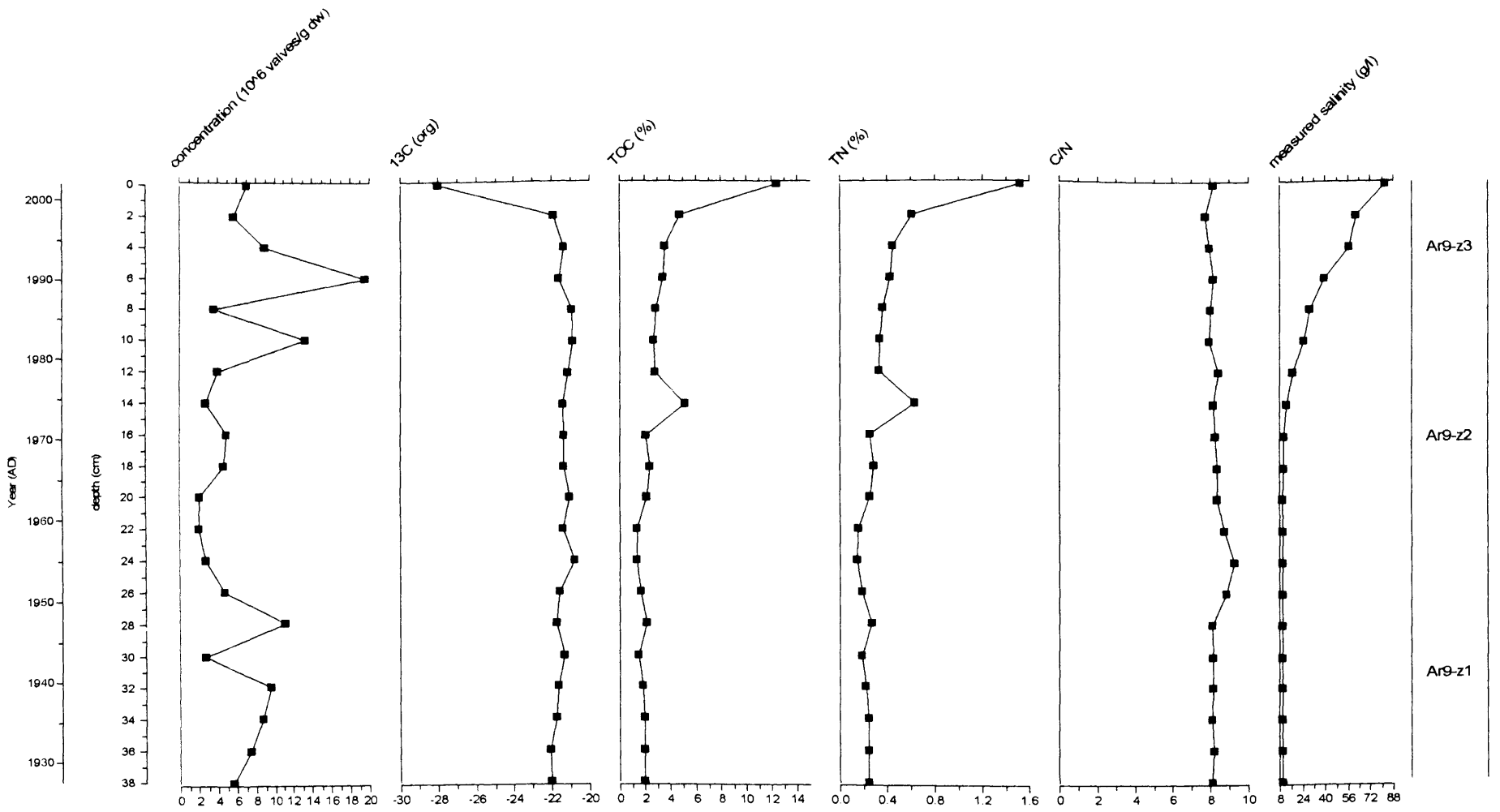

Figure 5.5. $\delta^{13}C_{org}$ vs. PDB, C/N ratio and percentage total organic carbon (TOC), total nitrogen (TN) and diatom concentration plotted against age (^{137}Cs) and depth for core Ar-9 from Chernyshov Bay those determined by CONISS on the percent diatom abundance. Also shown is measured salinity.

5.6.2. CH-1 (ca. 400 AD - Present)

The $\delta^{13}C_{org}$, C/N, percent total organic carbon (TOC) and nitrogen (TN) are shown in figure 5.6, plotted against both depth and age (year AD). The zones shown are those determined by CONISS on the percent diatom abundance (Figure 4.8). The values of $\delta^{13}C_{org}$ range from –26.9 ‰ to –17.4 ‰ with a mean value of –23.5‰ (s.d. 0.99‰). The C/N ratio has values between 4.5 – 10.1 (mean = 7.6, s.d. 0.74) while that of total organic carbon (TOC) fluctuates between 22.8 and 0.1 % (mean = 1.4 %, s.d. 1.12%).

The basal unit of the core, **CH1-z1** has C/N values of 9.5 in the lowermost sample at 1112 cm (ca. 400 AD) decreasing to 8.4 by 1032 cm (ca. 440 AD). TOC is generally low exhibiting a similar trend, declining from 2.4% to 1.0%. The $\delta^{13}C_{org}$ values of –23.1‰ at the base of the core rapidly decrease to –26‰ at 1100 cm (ca. 405 AD). There then follows a shift to higher values of –24.1‰ at the top of this zone. In zone **CH1-z2**, both C/N ratios and TOC remain around the values exhibited in the underlying zone, while $\delta^{13}C_{org}$ fluctuates between –24‰ and –23‰, with one excursion to –25.8‰ at 892 cm (ca. 510 AD) and a further excursion to higher values of –21.9‰ at 860 cm (ca 525 AD). In the overlying unit **CH1-z3**, C/N values remain < 10; TOC fluctuates between 1.5 and 2.5 % for the majority of this zone, reaching 7% in the uppermost sample. The $\delta^{13}C_{org}$ values of around –24‰ gradually increase, to values of –21.8‰ at the top of this zone. In zone **CH1-z4**, TOC increases to 10% at 498 cm (ca. 1260 AD) and 494 cm (1280 AD) corresponding with $\delta^{13}C_{org}$ values of –17.5‰, the highest obtained in the entire core. By 490 cm (ca. 1300 AD) these values have fallen sharply to –20.9‰ and TOC to 4%. By the start of **CH1-z5** at 462 cm (ca. 1360 AD) values have fallen to –23.6‰ and continue to show a decreasing trend reaching –25.7‰ at 326 cm (ca. 1430 AD) from which point $\delta^{13}C_{org}$ begins to increase with values of –23.5‰ at 256 cm (ca. 1465 AD). C/N continues to remain below 10 while TOC fluctuates at around 3%. Increasing values of $\delta^{13}C_{org}$ continue into the overlying **CH1-z6**, reaching –22.8‰ at 200 cm (ca. 1500 AD) from which point there is a gradual decline to –25.4‰ at 100 cm (ca. 1725 AD). As with the rest of the core, this zone is characterised by low C/N (<10) and TOC values (< 3%). **CH1-z7** sees a steady increase in TOC reaching 10% in the uppermost sample. C/N values remain < 10, $\delta^{13}C_{org}$ values of –23.9‰ at the bottom of this zone increase reaching –21.6‰ at 4 cm while in the uppermost sample values fall to –26.9‰.

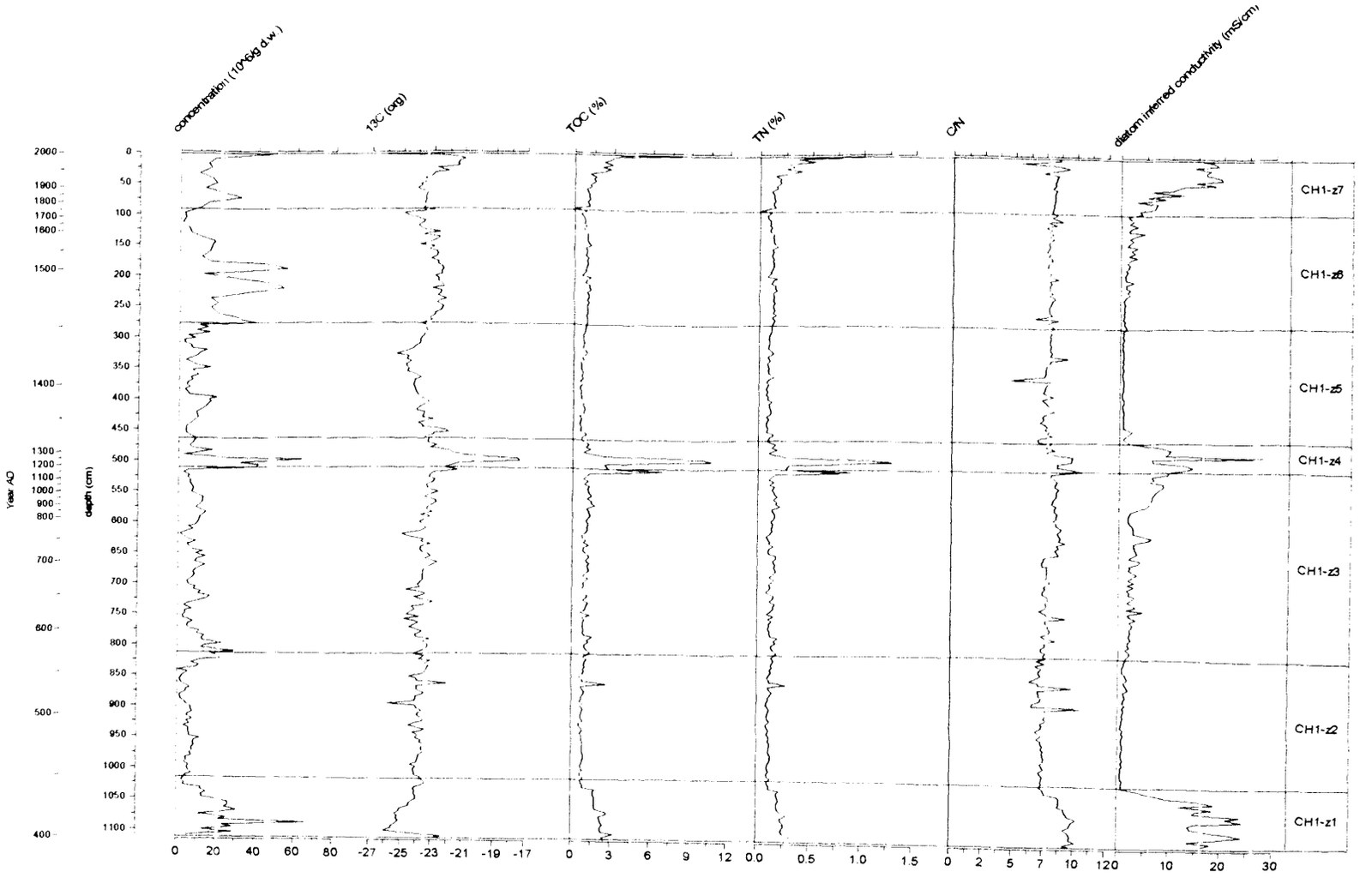

5.6. $\delta^{13}C_{org}$ vs. PDB, C/N ratio and percentage total organic carbon (TOC) total nitrogen (TN) and diatom concentration plotted against age (year AD) of CH-1 from Chernyshov Bay. The zones are those determined by CONISS on the percent diatom abundance. Also shown is diatom inferred conductivity.

5.7 Discussion

As previously discussed, the C/N ratio of organic material deposited within lake sediments is an important tool in determining its source. Its reliability may however be called into question if TOC is particularly low (< 1%) due to increases in inorganic nitrogen relative to that of organic carbon (Sampei and Matsumoto, 2001). In CH-1, 153 out of 275 samples fall into this category (mean = 0.8%). In these samples the mean C/N value is 7.3 which compares favourably with the mean C/N values (8.0) of the remaining 125 samples where TOC is > 1% (mean = 1.8%). Consequently it is felt that in this instance the C/N ratios accurately reflect the source material since ca. 400 AD and that any increases in inorganic nitrogen, while possibly lowering the C/N ratios, are not doing so to such an extent that the recorded values are unreliable. This potential pitfall does not arise in Ar-9 as all samples have TOC in excess of 1%.

The nature of the C/N ratios in both Ar-9 and CH-1 (< 10) rule out any significant contribution from terrestrially derived organic material in the sediments at Chernyshov Bay (Figure 5.7). Aquatic vegetation generally has C/N ratios from 12 – 20 (Tyson, 1995), some however, may have lower values in the range of algae (e.g. Muller and Mathesius, 1999). However, differentiating between organic material derived from algae and aquatic vegetation without measuring contemporary plant material is difficult. Pollen analysis highlights the paucity of aquatic pollen within the sediments of Chernyshov Bay (Sorrel et al. in review1) when compared with that derived from terrestrial vegetation. Vegetation cover in the region is particularly sparse but terrestrial vegetation pollen still manages to overwhelm the pollen production of aquatic vegetation. Consequently, the C/N ratio at Chernyshov Bay is thought to reflect algal productivity by diatoms and other algae, rather than being indicative of aquatic vegetation with low C/N ratios. As such the $\delta^{13}C_{org}$ values are thought to provide a record of within-lake productivity rather than switches between vegetation types. Additional evidence for a primarily autochthonous source of organic matter in both Ar-9 and CH-1 is reflected by the lack of correlation of the $\delta^{13}C_{org}$ values with the C/N ratios and consequently different controlling mechanisms (Figure 5.8)

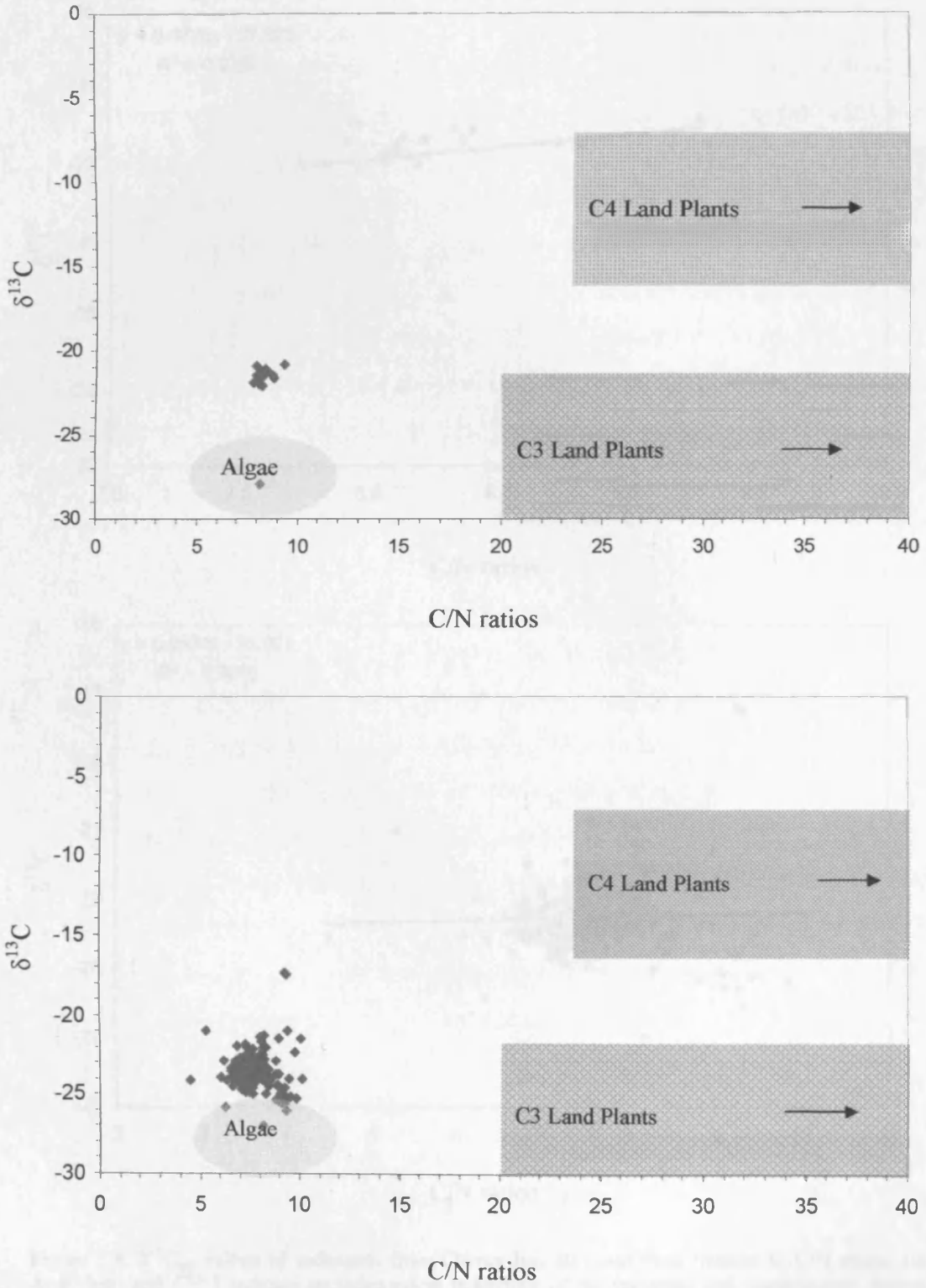

Figure 5.7. Distribution of $\delta^{13}C_{org}$ and C/N ratios of Ar-9 (top) and CH-1 (below). See text for details.

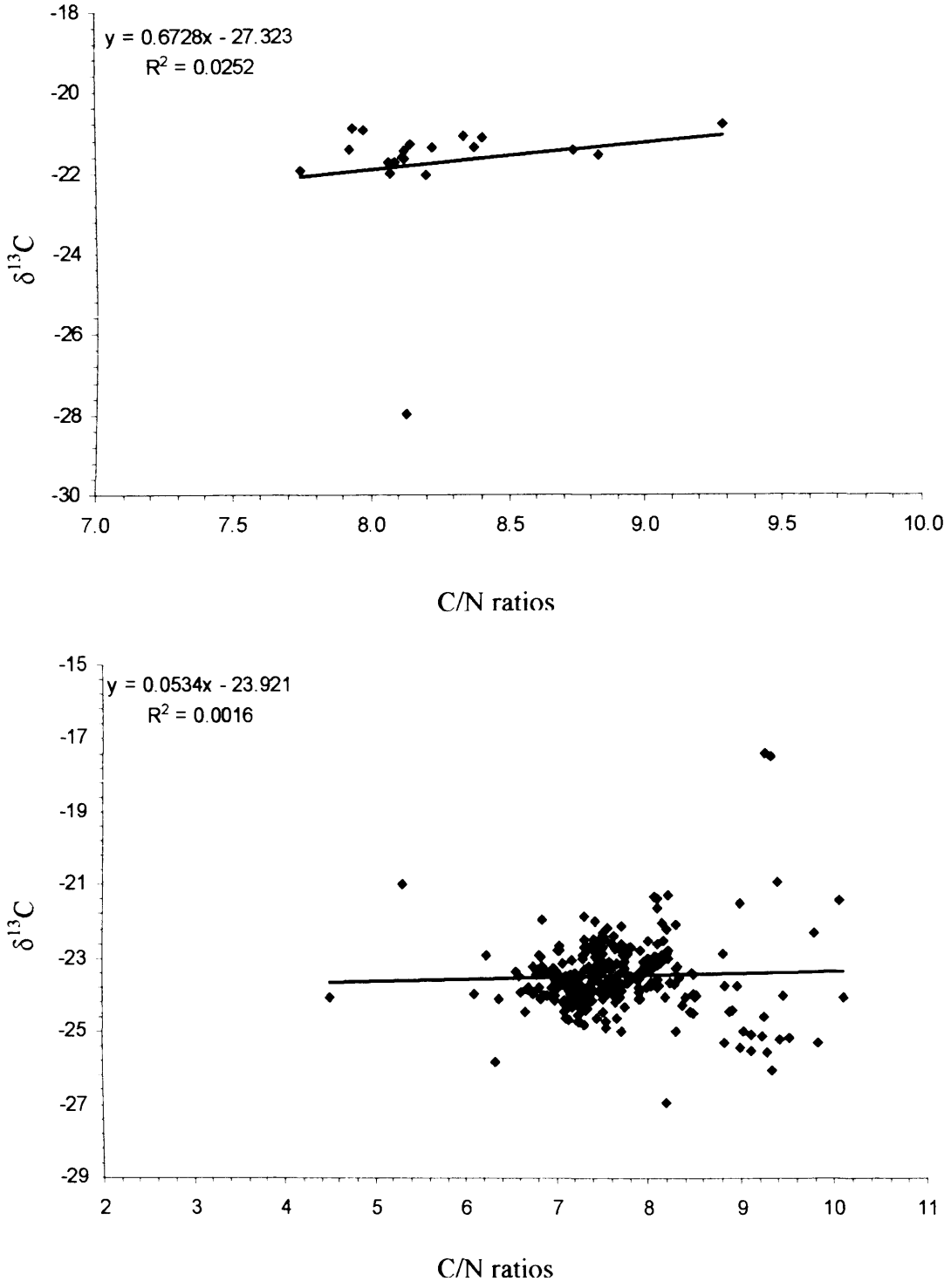

Figure 5.8. $\delta^{13}C_{org}$ values of sediments from Chernyshov Bay and their relation to C/N ratios. Both Ar-9 (top) and CH-1 indicate an independent behaviour of the variables and consequently different controlling mechanisms.

5.7.1 Ar-9 (ca. 1925 – 2002 AD)

From ca. 1925 to the inception of the present regression in 1960, lake level and salinity have remained stable, (Zavialov, 2005). Consequently it may be assumed that for Chernyshov Bay at least, the $\delta^{13}C_{org}$ values of around –22‰ from ca. 1925 – 1960, represent the stable nature of this phase as do C/N and TOC, the low values of the latter reflecting low within-lake productivity at this site. The recession of the shoreline has not been as great at Chernyshov Bay as other areas, particularly those in the eastern basin (Kravatsova et al., 2002). It is therefore assumed that over this period there has been very little incorporation of land derived organic material at this site. Reasons for this include the general paucity of terrestrial vegetation in this semi-arid region and the low rates of precipitation, which naturally contribute to the sparse vegetation cover and would result in low in-wash of terrestrial organic matter.

The $\delta^{13}C_{org}$ values around –22‰ for the majority of the core correlate well with measured salinity ($r = -0.65$, $p < 0.05$) and are somewhat higher than would be expected for algae (Figure 5.7) however the range shown is that of freshwater algae. Marine algae and algae from alkaline lakes tend to have generally higher $\delta^{13}C_{org}$ values, although range from ca. –24 to –16‰ (Lamb et al. 2006). Much of this is due to the uptake of carbon in the form of bicarbonate (HCO^{-}_{3}) rather than dissolved CO_2 (section 5.2.1). As the availability of the carbon species is a function of pH, that of the Aral Sea (pH ~ 8.5) results in the small amount of carbon from dissolved CO_2 being quickly utilised leaving only that available from bicarbonate, the uptake of which results in higher values of $\delta^{13}C_{org}$ of algal material than would otherwise be expected.

The minor increase in TOC since the diversion of the Amu Darya and Syr Darya in 1960 is consistent with a lake undergoing a regression, during which time organic material associated with clay sediments in the lake's littoral regions may be re-suspended and deposited in deeper waters (Benson et al. 1991; Meyers et al. 1998). The rapid decline in values of $\delta^{13}C_{org}$ from ca. –21 to –27‰ (C/N = 8, TOC = 12%) in the space of just a few years at the top of Ar-9 may be due to several factors, the most important being declining productivity. Orlova et al., (1995) have however suggested a period of increased productivity associated with latter stages of the current regression, which would lead to an increase in the values of $\delta^{13}C_{org}$. It is more likely

that the meromictic nature of Chernyshov Bay at the time of coring is the cause of the decline of $\delta^{13}C$. Zavialov et al. (2003) discovered that below a water depth of 20 m much of the western basin contained hydrogen sulphide (H_2S).

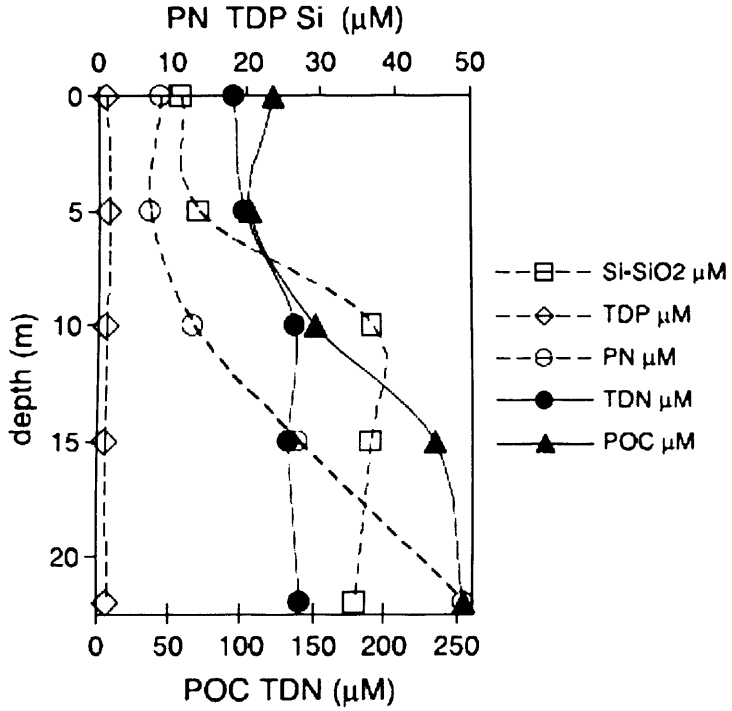

Figure 5.9. Large Aral, Chernyshov Bay. Vertical distribution of dissolved and particulate nutrients. (Friedrich and Oberhaensli, 2004).

In Chernyshov Bay similar conditions were observed at the time of coring in August 2002, with anoxic conditions and H_2S found below 10 m. Increased levels of particulate organic carbon (POC) were observed below the chemocline (Figure 5.9) and were most likely a result of the development of chemoautotrophic bacteria (Friedrich and Oberhaensli, 2004). These observations are consistent with evidence from Soda Lake in Nevada, where Cloern et al. (1983) demonstrated that productivity during periods of meromixis was dominated by chemoautotrophs rather than oxygenic photosynthesis by phytoplankton. Bacterial blooms may significantly reduce values of $\delta^{13}C_{org}$, even in areas where terrestrial or aquatic vegetation is found to dominate (Cloern et al. 2002). This may be the explanation for the depletion in values of $\delta^{13}C_{org}$ in the uppermost sample. The occurrence of bacteria below the chemocline and their presence in the upper sample suggests that the meromictic conditions observed at

Chernyshov Bay is a recent development which may even be intermittent or seasonal (Zavialov, 2005).

There is no significant correlation between reconstructed conductivity and TOC, however TOC is well correlated with measured salinity throughout Ar-9 ($r = 0.81$, $p < 0.05$) with highest values (12%) occur during hypersaline conditions in the uppermost sample (Figure 5.5). Jellison et al., (1996) also found a positive correlation between increased conductivity and organic matter content deposited in the sediments of the hypersaline Mono Lake in California. In Mono Lake this is not thought to be a consequence of increased productivity rather due to the decline in the rate of microbial decomposition of organic matter in hypersaline conditions. This is a process which may have been in operation in the Aral Sea during the summer of 2002 AD.

5.7.2 CH-1 (ca. 400 AD - present)

The decrease in $\delta^{13}C_{org}$ from around –22‰ to –26‰ at the base of the core appears to confirm the rapid changes occurring within the lake inferred by the diatoms (i.e. rising levels and declining conductivity) at ca. 400 AD. According to the age model, this 4‰ shift occurs in under 10 years and might be explained by one or a combination of the following factors:

1. A rapid reduction in productivity, this however would appear to be unlikely as diatom concentration (Figure 5.6) is high.

2. As already suggested (section 4.11) some form of enhanced fluvial input seems probable during this period and many accompanying factors may ultimately effect the $\delta^{13}C$ of organic material; i) The TDIC of the river waters whilst not being known, will probably be lower than that of the lake (Melanie Leng, pers. comm.) hence more of the lighter ^{12}C isotope will become available for photosynthesis; ii) any allochthonous algae brought in with the rivers and incorporated into the lake sediment will similarly have a lower $\delta^{13}C_{org}$ value than that contained within the lake and iii) the addition of freshwater will subsequently enable algae to better discriminate between the ^{12}C and ^{13}C isotopes. Potentially all of the above factors have played a role in

the lower isotopic value for this period, thus strengthening the diatom argument and that of dinoflagellates (Sorrel et al. 2006) for rapid lake level rise due to the redirection of the Amu Darya.

The steady increase in $\delta^{13}C_{org}$ from –26‰ to –23.5‰ observed over a ca. 35 year period through the rest of CH1-z1 is envisaged to be a result of algal productivity causing an increase in the $^{13}C/^{12}C$ ratio after the diversion of river water back into the lake. This may also have been enhanced by gradually increasing lake water residence time, resulting in increased TDIC equilibration with atmospheric CO_2. In CH1-z2, $\delta^{13}C_{org}$ fluctuates around –24‰. Two excursions seen at 892 cm and 860 cm to ca. –26 ‰ and –22 ‰ respectively, both of which accompany increases in C/N from ca. 7 to around 10 (still indicative of algal derived organic matter) are short lived events that might indicate episodes of increased and decreased productivity. The stable nature of the isotopic record in this zone corresponds to a period of low conductivity and high lake levels (section 4.11). $\delta^{13}C_{org}$ values are seen to fluctuate around –24‰ throughout CH1-z3 until ca. 700 AD when a trend towards higher values is observed, reaching around –21 ‰ at ca. 1130 AD. This overlaps with the gradual decline in lake levels and increased conductivity inferred by the diatoms (Figure 5.6).

This shift to higher $\delta^{13}C_{org}$ values during decreasing lake levels and increased conductivity was noted in Walker Lake, Nevada (Benson et al., 1991) and may reflect numerous processes working together. For example, increased algal productivity, increased conductivity (Figure 5.6) and subsequently less isotopic discrimination by algae under physiological stress and increased lake water residence time resulting in elevated $\delta^{13}C$ values of TDIC. By ca. 1210 AD, $\delta^{13}C_{org}$ has reached –17.5‰, and is accompanied by an increase in TOC from ca. 3% to 11%. Concordant with this increase in $\delta^{13}C_{org}$ is the presence of the epiphytic diatom *C. pediculus* (Figure 4.8). This shift to higher isotopic values may reflect increased productivity of not only diatoms but other algae such as *Cladophora* spp. upon which Germain (1981) found *C. pediculus* to be particularly prevalent. The extreme shift in $\delta^{13}C_{org}$ values may also be enhanced by anoxic bottom water conditions at this time (section 4.11.2), preventing the decomposition of organic material and causing ^{12}C to be retained within the sediments and increasing the $\delta^{13}C$ of the carbon pool (Leng and Marshall, 2004). TOC is around 10% and the source of the organic material is clearly having a

significant effect on the values of $\delta^{13}C_{org}$ which should be reflected in the C/N ratios. These have increased from ~7 to ~9 suggesting that algal derived organic material still dominates the sediments although a minor component may be from aquatic macrophytes (which may similarly serve as a substrate for *C. pediculus*) and are, potentially, more easily incorporated into the sediments during low lake levels and the subsequent encroachment of the littoral habitat to the coring site (Meyers and Teranes, 2001; Haberzettel et al., 2005).

Krishnamurthy et al., (1995) have suggested that an increase in the $\delta^{13}C_{org}$ value of the magnitude exhibited here, when C/N ratios indicate the dominance of algal derived organic matter, is unlikely to be a result of increased algal productivity alone. They suggest that a period when inflows and outflows to a lake are negligible (or even when a lake is hydrologically closed) may strongly influence the isotopic balance of lake water TDIC and as such, the shift from around –21 to –17‰ may indicate a minimal fluvial input to the lake and corresponds with the regression brought about by the destruction of irrigation systems by the Mongols and the diversion of the Amu Darya to the Sarykamysh and a period of increased conductivity and low lake levels inferred by the diatom flora and the reconstructed conductivity values.

The high $\delta^{13}C_{org}$ values of around –17‰ are seen to persist until ca. 1250 AD after which time, declining $\delta^{13}C_{org}$ values, characterise the remainder of CH1-z4 and continue into the overlying zone, CH1-z5 to ca. 1380 AD where values are around –25‰. Over the next ca. 45 years to ca. 1425 AD $\delta^{13}C_{org}$ values increase to around –22‰. This is concordant with an episode of low lake levels due to the further destruction of irrigation systems by Tamerlane in 1388 AD (Yagodin, in press). Diatom inferred conductivity values are seen to increase marginally at this time, (Figure 5.6) there is also an increase in the overall abundance of planktonic species and diatom concentration (Figure 4.8) which potentially serve as an independent indication of increased conductivity and low lake levels (section 4.11.1). The presence of high numbers of valves of *Chaetoceros* cf. *wighamii*, (an extremely delicate planktonic diatom particularly susceptible to dissolution and one that would indicate increased conductivity), suggest that silica redissolution was prevented by either the high sedimentation rate at this time (1.87 cm/yr) and its rapid removal from the water column or that the lake water was saturated with silica. Johnson et al. (2001) have

suggested that increased algal productivity during low lake level phases may be enhanced by the in-wash of material, particularly Si, from the newly exposed lake bed. Although, in this instance, this is more likely to be a consequence of input through the increasing number of dust storms in the region (Zavialov, 2005). This process will have also resulted in the input of nutrients to the surface waters a mechanism expected to generate a phytoplankton biomass increase (Ridame and Guieu, 2002). Thus, where the diatom inferred conductivity fails to clearly determine a known regression, the $\delta^{13}C_{org}$ is possibly reflecting increased nutrient availability at a time when the levels of the lake are known to be low.

This interval of increased $\delta^{13}C_{org}$ values around –22‰ persists until ca 1500 AD at which time a shift towards lower values is seen to occur, reaching –25‰ by ca. 1760 AD. After the destruction of irrigation systems by Tamerlane, it was not until the second half of the 16th century that water from the Amu Darya was diverted away from the Sarykamysh and back towards the Aral Sea (Yagodin, in press). The isotopic evidence and that from the diatoms suggests that some flow of water might have been reaching the Aral Sea prior to this. As discussed in the previous chapter, for the settlement at Kederi to have been located at 33 m a.s.l in the eastern basin, there must have been a freshwater supply. Borroffka et al., (2004) state that the Small Aral probably existed as a separate lake at this time and that a branch of the Syr Darya may have been flowing in to the eastern basin, it is possible that some fluvial input was maintained to Chernyshov Bay which may have existed as a separate fresh/brackish waterbody.

The rise in $^{13}C_{org}$ at ca. 1780 AD is followed by a century long episode of values around –23.5‰ until ca 1880 AD and a small increase in TOC. According to the age model by ca. 1925 AD $\delta^{13}C_{org}$ values of around –24‰ begin to increase, reaching –21‰ by 1994 AD. As with other shifts to higher values, this may again represent increased productivity as recorded by Orlova et al., (1995) as lake levels declined and by the small increase in TOC. The low values at the top of the core would appear to reflect the presence of bacteria in the uppermost sample as was the case in Ar-9.

What is apparent over the last 100 years (and in keeping with the diatom inferred conductivity records in chapter 4) is the discrepancy in the $\delta^{13}C_{org}$ record in Ar-9 and

CH-1. Values in Ar-9 are relatively constant over this period when compared with those from CH-1 which exhibits a significant increasing trend in $\delta\,^{13}C_{org}$, one which mirrors the increasing trend observed in the diatom inferred conductivity record and the known decline in lake levels. Despite these separate cores being taken from nearby locations, the observed $^{13}C_{org}$ record highlights the differences that can occur over short distances and characterise this particular location.

5.8 Conclusion

The first late Holocene record of $\delta^{13}C_{org}$ and C/N from Chernyshov Bay in the Aral Sea provides a record of within-lake productivity rather than reflecting any significant climatic shifts in the region that may have been manifested in the form of changing vegetation in the immediate vicinity of the lake and its wider catchment. That this should be the case is hardly surprising as the lake is to all intents and purposes located in the middle of a large desert and the moisture fluctuations detected by Sorrel et. al. (in review1) and the subsequent implications for the development of terrestrial organic material were minor. That said, Chernyshov Bay is located some distance from the deltas of the Amu Darya and Syr Darya consequently any vegetation changes along their courses in the form of cultivation might only be picked up at locations closer to the points of fluvial input.

It is probable that a range of factors contributed to the observed shifts in the $\delta^{13}C_{org}$ values of algae over the last ca. 1600 years. Despite a poor correlation between $\delta^{13}C_{org}$ and conductivity ($r = 0.06$) throughout the entire core, broad shifts in the organic isotope record are seen to correspond with the diatom inferred record of conductivity and lake level changes (Figure 5.6) and consequently provide an independent record of these fluctuations. In the case of the regression initiated by Tamerlane and known to have persisted from ca. 1380 – 1600 AD, the $\delta^{13}C_{org}$ record would appear to provide evidence for this change, while that obtained from the diatom inferred conductivity record is less conclusive.

Chapter six

Trace metal (Cd, Pb and Hg) contamination of the Aral Sea since 400 AD.

6.1 Introduction

As if the present regression, increased salinity and loss of habitat had not been enough to contend with, the problems facing the Aral Sea have been compounded by pollution from a range of sources, including: PCB compounds, fertilizers and in particular, high amounts of organochlorine pesticides (Jensen et al., 2004). In an effort to secure cotton harvests, pesticide application upstream of the lake in Central Asia has been up to 10 times the levels used in the rest of the former Soviet Union and the United States (Glantz et al., 1993). Runoff of these pesticides to the Amu Darya and Syr Darya then results in their deposition and subsequent accumulation within the sediments of the Aral Sea. As a consequence of this excess application water resources in the area are highly contaminated, with ca. 65% failing to reach accepted standards (Small et al., 2001). Furthermore, the exposed lake bed and the increased frequency of dust storm activity results in the dispersal of contaminated dust over a wide area, having severe consequences for human health in the region (e.g. O'Hara et al., 2000; Whish-Wilson, 2002).

Trace element contamination in the region has received considerably less attention than that of pesticides. Some limited investigations of the trace metal contamination of the Aral Sea have been undertaken (Oreshkin et al., 1993, Juggins, 1997, see section 6.3). However, much work on this subject deals with the effects of metal contamination on the human population in the vicinity of the Aral Sea (e.g. Jensen et al., 1997; Erdinger et al., 2004) rather than attempting to establish a record of anthropogenic trace metal contamination from the lake itself.

6.2 Trace metals and anthropogenic activity

According to Duffus (2002), a trace metal is one found in low concentration (fractions of ppm or less) in a specified source. Aquatic systems and soils are the endpoints for trace metals found in the atmosphere. These include: arsenic (As), cadmium (Cd), copper (Cu), chromium (Cr), mercury (Hg), nickel (Ni), lead (Pb), tin (Sn) and vanadium (V). Prior to the development of the earliest smelting technologies and the extraction of copper (Cu) ca. 7000 yr BP (Settle and Patterson, 1980), a range of natural sources were solely responsible for the presence of trace metals in the atmosphere, i.e. volcanic eruptions, rock and soil weathering, sea-spray, forest fires and marine biogenic particulates and volatiles (Nriagu and Picanya, 1988). Anthropogenic activities have since added to their concentration, particularly since the start of the industrial revolution ca. 1850 AD, and the exponential increase in the use of metals and consequently emissions (Nriagu, 1996).

While there is always a natural contribution to the atmosphere of the metals listed above (Boyle, 2002), natural emissions of Cd, Hg and Pb are considerably less than those caused by human activity (Figure 6.1) and as such these metals are able to provide a reliable indication of anthropogenic pollution on both regional and global scales. By the 1970s, records of atmospheric pollution of Hg had been derived for sites in the vicinity of industrialised areas in Canada (Thomas, 1972) and the United Kingdom (Aston et al., 1973; Lee and Tallis, 1973). A record documenting increased Pb contamination was similarly recorded in the sediments of Lake Washington in Seattle (Crecelius and Piper, 1973). A wide range of studies then followed (e.g. Norton and Hess, 1980; Davis et al., 1983; Nriagu and Wong, 1983; Verta et al., 1989; Engstrom et al., 1994), highlighting increased accumulation of Cd, Cu, Pb, Zn and Hg in sediment profiles over the last ca. 150 years. The analysis of sediments in remote locations, far from centres of industry, has also helped to develop a picture of long-range transport of trace metals, in particular Pb (e.g. Renberg et al., 1994; 2002; Branvaal et al., 1997; 2001) and Hg (Seigneur et al., 2003).

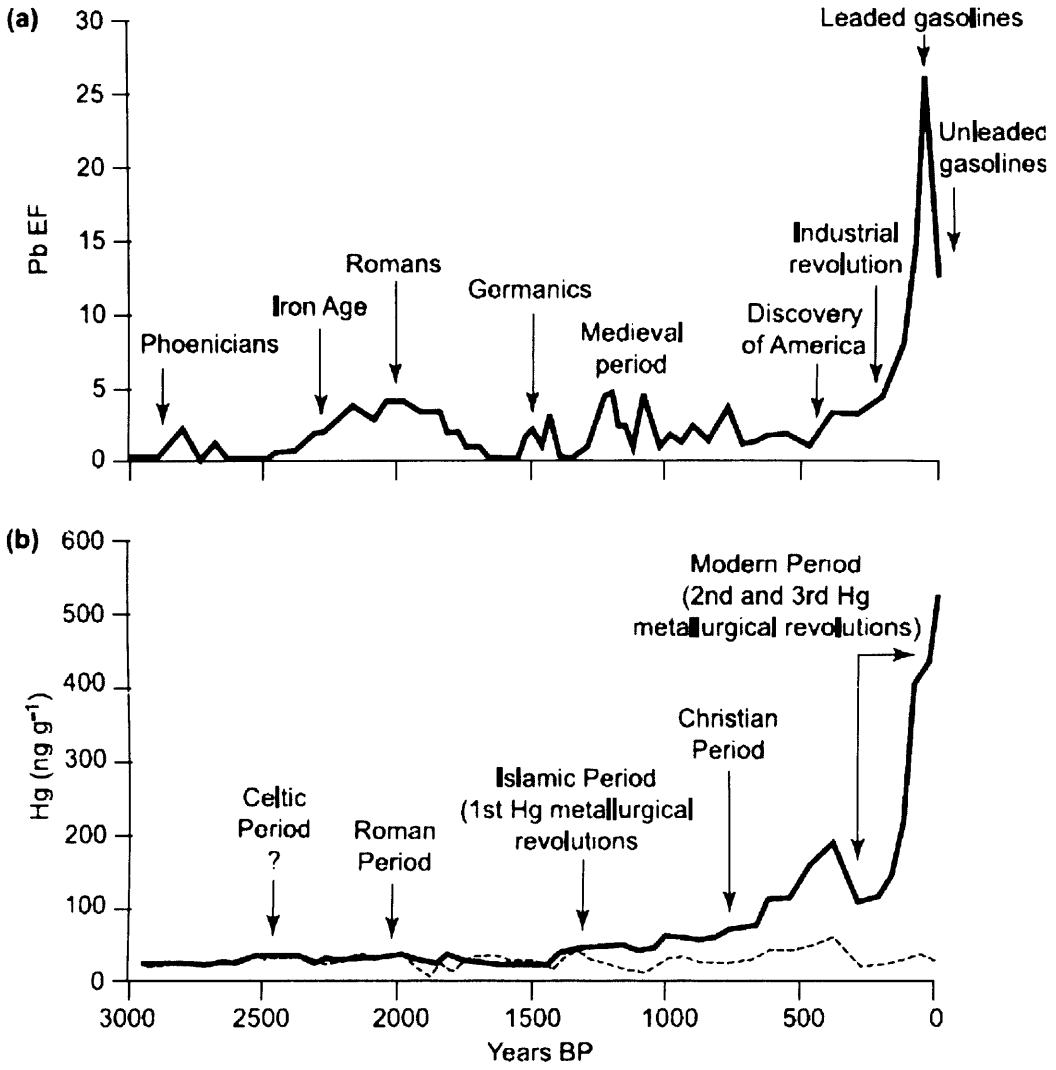

Figure 6.1. Pb enrichment (a) and total mercury concentrations (b) from Penido Vello a peat profile from Northern Spain set against a series of historical events, cultural stages and technological changes from 3000 yr BP. From Dearing et al., (2006).

However, earlier, pre-industrial-revolution atmospheric enrichment of Pb as a result of anthropogenic activity has been detected in Greenland ice cores ca. 2000 yr BP (Hong et al., 1994; 1996) and is contemporaneous with Pb and Hg concentrations above background level recorded in ombotrophic peat bogs in Spain (Martinez-Cortizas et al., 1997; 1999) and Switzerland (Shotyk et al., 1998) and lake sediments in Sweden (Renberg et al., 1994; Brannvaal et al., 2001), Ireland (Schetler and Ramer, 2006) and the United Kingdom (Oldfield et al., 2003). All provide evidence of early atmospheric pollution having occurred as natural resources were exploited and new technologies developed, in particular the cupellation of silver (Ag) at the height of the Roman Empire (Figure 6.1) predominantly from lead sulphide ores, of which Pb is an

almost 400-1 by product (Settle and Patterson, 1980), and the later use of Hg as an amalgamation agent in the refining of silver and gold (Hylander and Meili, 2003).

The fall of the Roman Empire saw a shift in production of Ag away from the Ibero-British mining complexes to Central Asia, where from 480 – 1130 AD and in four distinctive cycles (480 – 650 AD, 730/50 – 850 AD, 850 – 950 AD and 950 – 1140 AD), precious metals (in particular Ag from argentiferous lead ores) dominated the world's coin markets (Blanchard, 2002). Production was based in the foothills of the Tien Shan and Pamir through which the headwaters and tributaries of the Amu Darya and Syr Darya flow.

6.2.1 Lake sediments and trace metals

The presence of trace metals in lake sediments may be influenced by increased soil erosion within the catchment due to climate and subsequent vegetation change or may reflect former land-use histories (e.g. Oldfield et al., 2003; Yang et al., 2003). The presence of allogenic metals within lake sediments may be attributed to four sets of factors:

1. Atmospheric deposition directly on to a lake's surface. This is a result of the dry deposition of micro-sized particles, or wet deposition in which aerosol particles are scavenged from the atmosphere by precipitation.
2. The weathering of rocks and soil within the catchment.
3. Seepage from industrial sources. This may be particularly prominent close to mining and smelting operations.
4. Fluvial transport of trace metals (which may have been acquired by any of the above processes) in conjunction with suspended particulate matter.

Once in the water column, metals are scavenged by particulate matter and deposited within the sediments which will, as a result, have a higher metal concentration than the overlying water (Rognerud and Fjeld, 2001).

6.2.2 Factors effecting interpretation

When interpreting the record of the trace element concentrations within sediment profiles, it is of vital importance to determine whether there has been any enrichment of the sediment surface or if post-burial remobilization of metals has occurred. This process may seriously alter the sediment record, or appear to indicate episodes of contamination where in fact none may have occurred (Lockhart et al., 2000). One of the main processes leading to this contamination is diagenesis. This results in dissolved ions of Fe^{2+} and Mn^{2+} being oxidised to a solid state in response to a gradient in dissolved metals within a sediment profile. Other metals such as Cu, Ni and Zn are commonly removed along with Fe and Mn due to adsorbtion or co-precipitation. The observed metal distribution within a profile is then contaminated and cannot be used as a historical record. (See Boudreau (1999) for a full review of the subject).

Due to their solubility and multiple oxidation states, further metals (i.e. As, Cr, and V) are susceptible to migration within the sediments in response to increased Fe and Mn oxide concentrations. Surface enrichment of Cd is not uncommon due to trace element cycling in lakes, but Boyle (2002) states that these are temporary and consequently unlikely to impact upon the long-term sediment record. Whether Hg is susceptible to surface enrichment has long been the subject of debate. Rasmussen (1994) suggested that increased Hg concentration near the sediment surface reflected diagenesis rather than increased atmospheric flux. However, in an effort to determine whether Hg within lake sediments was providing a true reflection of contamination, the Hg records derived from sediment cores obtained from three Canadian lakes, all with known sources of local Hg pollution (a chlor-alkali plant, gold mine and a mercury mine), were compared with historical records of contamination and found to agree well with the known inputs of Hg, suggesting that peaks are indeed capable of reflecting contamination events (Lockhart et al., 2000).

To conclude, this process is generally thought to have little or no effect on Cd, Pb and Hg (Fitzgerald et al., 1998; Boyle, 2002) and is believed to be limited to sites with very low sediment mass accumulation rates (Gobeil, 1999; Boyle, 2000a) which is not the case with the material retrieved from Chernyshov Bay.

6.3 Previous trace element studies undertaken in the Aral Sea

Oreshkin et al., (1993) detail the Cd concentration of bottom sediments from 128 locations sampled in 1978. This ranged from 0.012 to 0.61 μg/g (mean 0.16 μg/g) and was generally highest near the river mouths and clay sediments in the centre of the eastern basin.

In order to assess the timing of trace metal contamination in the Aral Sea, the concentrations of Cd, Mn, Co, Ni, Pb, Zn and Cu were established from Tastubek Bay in the Small Aral Sea for the period 1960 – 1995. During this period Cd exhibited no trend, while Pb remained stable, increasing in the 1990s only. Cu, Ni and Zn were elevated above background levels, increasing towards the top of the core (Juggins, 1997).There is to date, no published work on Hg concentrations in sediments of the Aral Sea.

6.4 Aims and objectives

In an effort to determine episodes of climatic and landscape change in the Aral Sea Basin, Sorrel et al., (in review2) have recently established records of Ca, Fe, K, Mn, Sr and Ti within the sediments at Chernyshov Bay. However, as has already been established, anthropogenic activity during the last ca. 1600 cal. yr BP has had a particularly large impact on the Aral Sea. None more so than the current regression, which while not (yet) as severe as the previous low lake level stands observed, is set firmly apart due to the intensity of cultivation in the region and the corresponding mass application of pesticides and fertilizers (Boomer et al., 2000). Consequently the primary aim of this chapter is to establish the sediment profiles of Cd, Pb and Hg within the gravity core, Ar-9, retrieved from Chernyshov Bay to estimate the extent of anthropogenic heavy metal contamination of the lake over the last ca. 75 years.

In order to ascertain whether earlier global or regional anthropogenic activity such as those illustrated in figure 6.1, and the increased production of Ag in Central Asia outlined above, resulted in the deposition of trace metals in the Aral Sea region over the last ca. 1600 cal. yr BP the sediment profiles of these metals in CH-1 will also be established.

6.5. Methods

6.5.1 Sample preparation

Samples for the determination of Cd and Pb were taken at 1 cm resolution from 0 – 20 cm (although no material was available for samples at 1 cm, 14 cm and 15 cm) and 2 cm resolution for the remainder of Ar-9. Samples for the determination of Hg in Ar-9 was every 2 cm however no sediment was available from depths of 14 cm and 34 cm. In CH-1, Pb and Cd were sub-sampled at 4 cm intervals and Hg at 16 cm intervals. Due to insufficient sediment no samples were prepared for the interval between 650 – 748 cm (ca. 1280 – 1380 cal. yr BP / ca. 720 – 620 AD) in CH-1. Extraction of metals followed the following procedure:

1. 0.3 g of freeze-dried sediment was placed into acid washed (HCl) Teflon beakers.
2. 10 ml of concentrated HNO_3 was added to the beakers.
3. The beakers were then heated at 100°C on a hot plate for 1 hour.
4. These were then allowed to cool and the sediment to settle. The supernatant was then decanted into a 30 ml sterelin container. The remaining sediment was then washed with 10 ml de-ionised water, allowed to settle and the water then decanted to the sterelin containing the supernatant. This was repeated until each sterelin contained ca. 25 ml of solution. These were then topped up to 30 ml with de-ionised water, shaken vigorously and allowed to settle overnight.
5. A pipette was then used to extract the top 10 ml from each sterelin and added to a centrifuge tube for the analysis of Cd and Pb.
6. The remaining 20 ml in each sterelin was then used for the analysis of Hg.

6.5.2 Cd and Pb analysis using Flame Atomic Absorption Spectrometry (FAAS)

AAS is a single element method based on the absorption of free atoms of light at a specific wavelength. Two types are common, i) electrothermal atomic absorption spectrometry (EAAS) and ii) flame atomic absorption spectrometry (FAAS). Here, the latter method was used, the sample being aspirated into a flame which is placed in the path of a light provided by a hollow cathode lamp specific to the element being

analysed. A slotted silica tube is placed in the flame, increasing measurement sensitivity for both Cd and Pb (x3 and x8 respectively).

Analysis for Cd and Pb was performed by Irene Cooper at the Department of Geography, University of Liverpool. Atomic absorption spectrometry (AAS) was undertaken using a Unicam 939 Atomic Absorption Spectrometer. Quality control was ascertained through the measurement of blank samples and a standard reagent solution of 10 ng/l every 9 samples in Ar-9 and every 20 samples in CH-1.

6.5.3 Hg analysis using cold vapour atomic absorption spectrometry (CV-AAS)

Measurements of Hg were similarly analysed on the Unicam 939 AAS although the method is different, employing a closed system with $SnCl_2$ (tin chloride) used to reduce dissolved Hg to its elemental gaseous state which is then aerated from the solution into a circular system, the vapour then passing through a quartz absorption cell placed in the light path of the spectrometer and its absorption measured. Quality control was ascertained through the measurement of blank samples and a standard reagent solution of 10 ng/l every 9 samples in Ar-9 and every 10 samples in CH-1.

6.6 Ar-9 Results (ca. 1925 – 2002 AD)

The temporal trends of Cd, Hg and Pb over the last ca. 75 years as recorded in the sediments of Chernyshov Bay are seen in figure 6.2, along with TOC and diatom concentration, plotted against depth and age (year AD). The zones shown are those determined by CONISS on the percent diatom abundance (figure 4.2).

The factors leading to the presence of trace metals within lake sediments have been discussed. The low rates of precipitation over the Aral Sea mean that any anthropogenic records of Cd, Pb and Hg within the sediment profiles at Chernyshov Bay are most likely to reflect regional activity and the transport to the lake of metals in conjunction with fluvial sediment rather than provide a record of global atmospheric pollution. Consequently in this study, results are presented as concentration (ng/g and μg/g) as opposed to accumulation rates (e.g. ng/cm^2/year), the reliable record of which may be further hampered by the range of annual

sedimentation rates exhibited in CH-1 which will significantly alter the supply of trace elements to the lake. A reliable estimate of accumulation at this site is further complicated by the difference in sedimentation rates exhibited in Ar-9 to the depth at which the ^{137}Cs peak is observed (0.46 cm/year) and the equivalent depth in CH-1 (1.12 cm/year). By contrast however, concentration will record subtle changes in the supplied sediment, is more precise, less open to interference and easier to interpret. See (Boyle, 2001) for a full review.

Pb concentration fluctuates between 1.43 and 13.5 μg/g (mean = 8.11 μg/g, s.d = 3.26) and despite these variations, values are low. The concentrations of Cd are also low but nevertheless increase throughout the core fluctuating between 0.16 and 0.48 μg/g (mean = 0.28 μg/g, s.d. = 0.08). Similarly, Hg concentration is low, values fluctuating between 6.38 to 73.41 ng/g (mean = 28.97 ng/g, s.d. 21.76).

In **Ar9-z1** initial Pb values of 10 μg/g at ca. 1925 AD decline to 4.82 μg/g at the top of the zone at around 1955 AD. During this period the concentration of Cd increases from 0.16 μg/g to 0.27 μg/g. Hg fluctuates at the base of this zone with initial values of 60.26 μg/g declining to 35.49 from which point there is an increase to 73.69, the highest values within the core, at around 1945 AD. At the top of Ar9-z1 Hg concentration has fallen to 21.94 μg/g. In the overlying zone, **Ar9-z2** Pb concentrations increase from initial values of 4.82 μg/g to 9.15 μg/g by ca. 1960 AD. Values then remain stable until ca. 1980 AD when concentrations decrease to 2.88 μg/g. At the top of this zone values are 5.67 μg/g. Values of Cd fluctuate between 0.21 and 0.35 μg/g with a high value of 0.48 μg/g recorded at ca 1980 AD. Hg concentrations decline steadily throughout this zone falling from 21.94 ng/g to 11.31 ng/g at the top of the zone in ca 1985 AD. In the uppermost zone **Ar9-z3** from ca. 1985 to the present day, values of Pb show an increasing trend, reaching 12.44 μg/g before falling to just 1.33 μg/g in the very next and uppermost sample. Cd exhibits a generally increasing trend throughout this zone with initial values of 0.33 reaching 0.45 at the top of the core. During this time Hg concentrations have continued to decline with values of just 6.58 ng/g recorded for the uppermost sample.

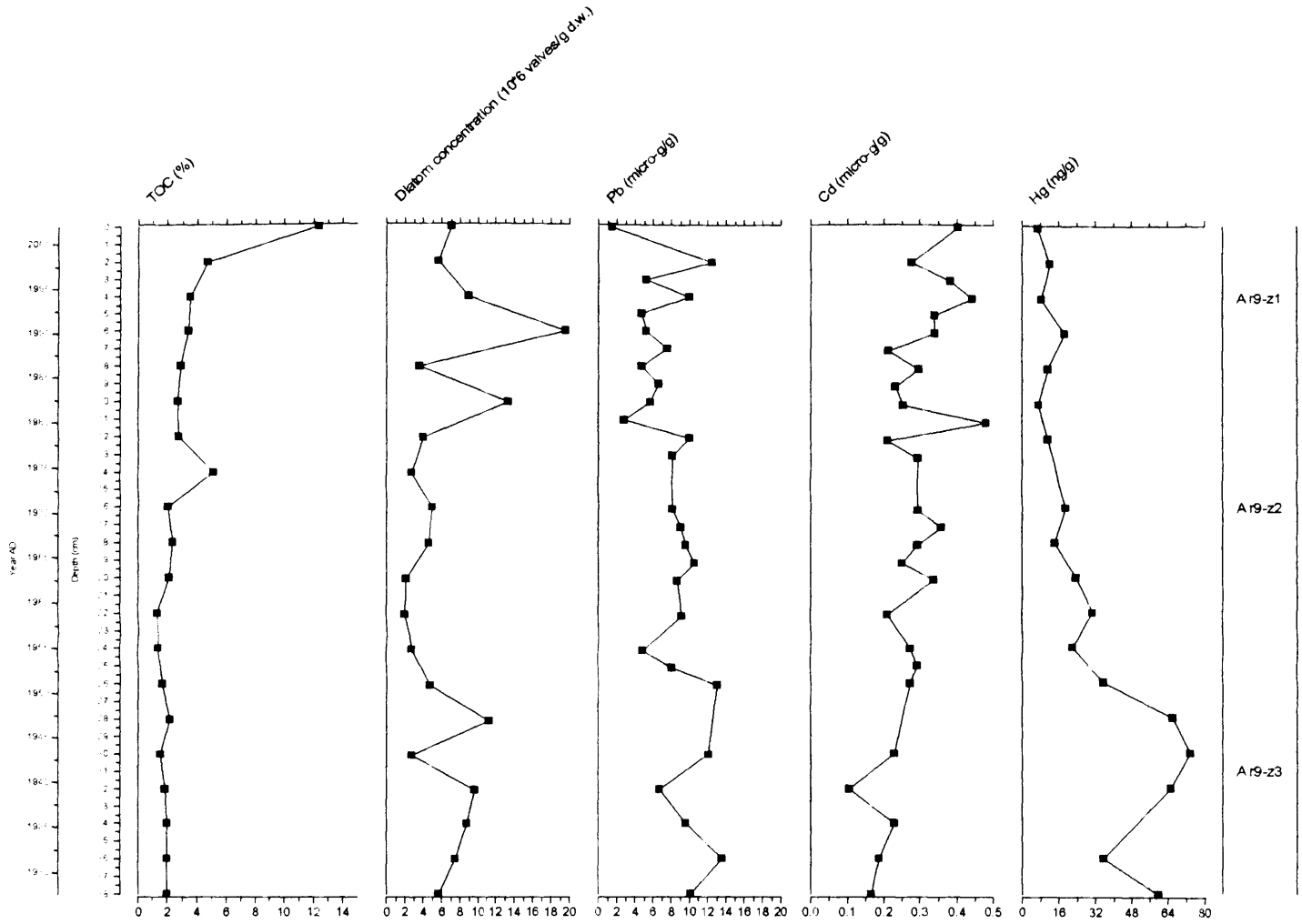

Figure 6.2 Down-core elemental profiles of Cd, Pb and Hg (acid extractable concentrations) plotted against age and depth (^{210}Pb) of the Aral Sea as recorded in the sediments of Chernyshov Bay. Also shown are the crustal averages for each element (red dashed line), the total organic carbon content (TOC) and diatom concentration.

Many studies have highlighted the correlation of Cd, Pb and Hg with organic matter (e.g. Bilali et al., 2002; Outridge et al., 2005). In this study, both Pb and Cd are correlated with TOC (table 6.1) while Hg and TOC exhibit no significant relationship.

Table 6.1 Correlation between trace elements total organic carbon (TOC) and diatom concentration in Ar-9. (* $p \leq 0.05$).

	Cd	Pb	Hg	TOC	concentration
Cd	-	-0.45*	-0.67*	0.52*	0.09
Pb	-	-	0.40	-0.51*	-0.35
Hg	-	-	-	-0.41	-0.08

6.7 Results CH-1 ca 1600 – 0 cal. yr BP

The down core distribution of Pb, Cd and Hg as recorded in the sediments of Chernyshov Bay are seen in Figure 6.3 plotted against both depth and age (year AD). As the diatom assemblages are seen to reflect the series of regressions and transgressions observed over the last ca. 1600 cal. yr BP the results are presented in the context of the diatom assemblage zones determined by CONISS on the percent diatom abundance (figure 4.2). As with Ar-9 metal concentrations throughout the core were low, generally fluctuating around the average abundance of each metal within the earth's crust given by Wedepohl (1995). Mean values were: Pb = 12.36 μg/g, (s.d. = 3.95), Cd = 0.10 μg/g (s.d. = 0.08) and Hg = 10.38 ng/g (s.d. = 8.52)

In the basal unit, **CH1-z1**, Pb and Cd exhibit contrasting trends. Pb rises from ca 7 μg/g in the lowermost sample, and doubles to around 14 μg/g at the top of the zone ca. 440 AD. In contrast, Cd has values that fluctuate between 0.29 and 0.40 μg/g until at 1076 cm (ca. 420 AD) concentration steadily declines, reaching 0.15 μg/g at ca. 440 AD. Hg has values of ca. 35 ng/g at the base of the core, these decline throughout the zone, and Hg concentration is just 7 ng/g by 1032 cm (ca. 440 AD).

The increasing trend of Pb observed in CH1-z1 is seen to continue into the overlying zone, **CH1-z2** where concentration is around 22 μg/g at 1008 cm. Values then decline

to about 3 μg/g and fluctuate between 5 – 12 μg/g for the rest of this zone with one positive excursion to 23 μg/g at 920 cm (ca. 500 AD). Cd shows an initial decline with values then fluctuating between 0.03 and 0.18 μg/g for the duration of the zone. In contrast, Hg increases in concentration from 3 ng/g at the base of CH1-z2 to 32 ng/g by 884 cm (ca. 515 AD), declining to 21 ng/g at the top of the zone.

In **CH1-z3**, Pb fluctuates between 7 – 17 μg/g (mean = 12 μg/g). Values exhibit a small increase from around 9 μg/g at the start of this zone to ca. 14 μg/g at 748 cm (ca. 620 AD) during this period, Cd similarly increases from a low of 0.04 to 0.17 μg/g at which point there is a gap in the record to 650 cm (ca. 715 AD) where values of around 15 μg/g are recorded for Pb, with very little fluctuation observed, whereas Cd exhibits a slight declining trend with values of 0.11 μg/g by the start of the overlying zone. The decreasing trend observed in the Hg record in CH1-z2 continues, with values of around 7 ng/g at 756 cm (ca. 615 AD), values then increase to 28 ng/g by 610 cm (ca. 760 AD) but by the last sample in this zone, they have fallen to just 4 ng/g.

In **CH1-z4**, values of Pb 5 μg/g at 494 cm (ca. 1280 AD) increase to 16 μg/g by 486 cm (ca. 1315 AD), reaching 10 μg/g in the uppermost sample. Cd values of 0.18 μg/g are seen to have fallen to 0.14 μg/g over the same period. This zone contains only two Hg values, of 6 ng/g at 490 cm (ca. 1290 AD) and 474 cm (ca. 1350 AD).

In **CH1-z5**, the values of Pb again remain low, fluctuating very little (6 – 19 μg/g mean = 15 μg/g) with the exception of one measurement of 39 μg/g at 456 cm (ca. 1360 AD). Cd however exhibits a generally decreasing trend which started in the underlying zone, with particularly low values of between 0.01 – 0.03 μg/g between 444 cm and 420 cm (ca. 1365 – 1380 AD). Low values are seen to occur throughout the zone, with the exception of 420 cm (Cd = 0.6). Valued of Hg are seen to increase initially from 7 – 14 ng/g between 452 – 420 cm (ca. 1360 – 1380 AD). This is followed by a drop to around 3 ng/g at 404 cm (ca. 1385 AD) after which point values again have an increasing trend, reaching ca. 27 ng/g in the uppermost sample.

The concentrations of Pb (9 – 18 μg/g) and Cd (0.05 – 0.20 μg/g) again show small fluctuations throughout **CH1-z6**. Hg values of 26 and 7 ng/g were recorded in just two samples, 260 cm (ca. 1465 AD) and 128 cm (ca. 1615 AD) respectively.

In the uppermost sample, **CH1-z7**, Pb fluctuates between 3 – 18 μg/g exhibiting a fluctuating but declining trend from values of 18 μg/g at 40 cm (ca. 1968 AD) to just 3 μg/g in the uppermost sediment. Cd however, fluctuates between 0.04 and 0.19 μg/g throughout the zone with values of ca. 0.12 μg/g characteristic of the uppermost 12 cm of the profile. The sediment concentrations of Hg in CH1-1 show a clear increasing trend from 0.8 ng/g at 64 cm (ca. 1880 AD) to values of around 7 ng/g in the uppermost sample.

Due to the natural source of Cd and Pb within the sediments, concentrations should vary with soil mineral tracers such as Ti, which, being predominantly lithogenic in origin provide a picture of natural erosion processes within the catchment. Ti (cps) concentrations have been determined by Sorrel et al (in review) and are seen to correlate well with the magnetic susceptibility record over the last ca. 1600 cal. yr BP (Sorrel pers. comm.) suggesting that it reflects natural sediment supply from the catchment. Ti abundance (cps) and Pb concentrations are weakly correlated, ($r = 0.23$, $p < 0.05$), while Ti and Cd exhibit a negative correlation ($r = -0.30$, $p < 0.05$). There is no significant correlation between Cd and Pb.

This suggests that while Ti reflects natural input from the catchment and would appear to correspond well with the record of fluvial input, the trace element record of Cd and Pb is more complicated, possibly reflecting a variety of natural sources, including aeolian deposition, fluvial input from the Amu Darya and Syr Darya and erosion of local material due to flash flooding. Although the latter process might be expected to transport terrestrially derived organic material to the lake, the C/N ratio is < 10 throughout the core (section 5.5.2) and reflects the absence of terrestrially derived organic material in the vicinity of the coring site, rather than the potential for transport of clastic material as a result of localised severe precipitation events.

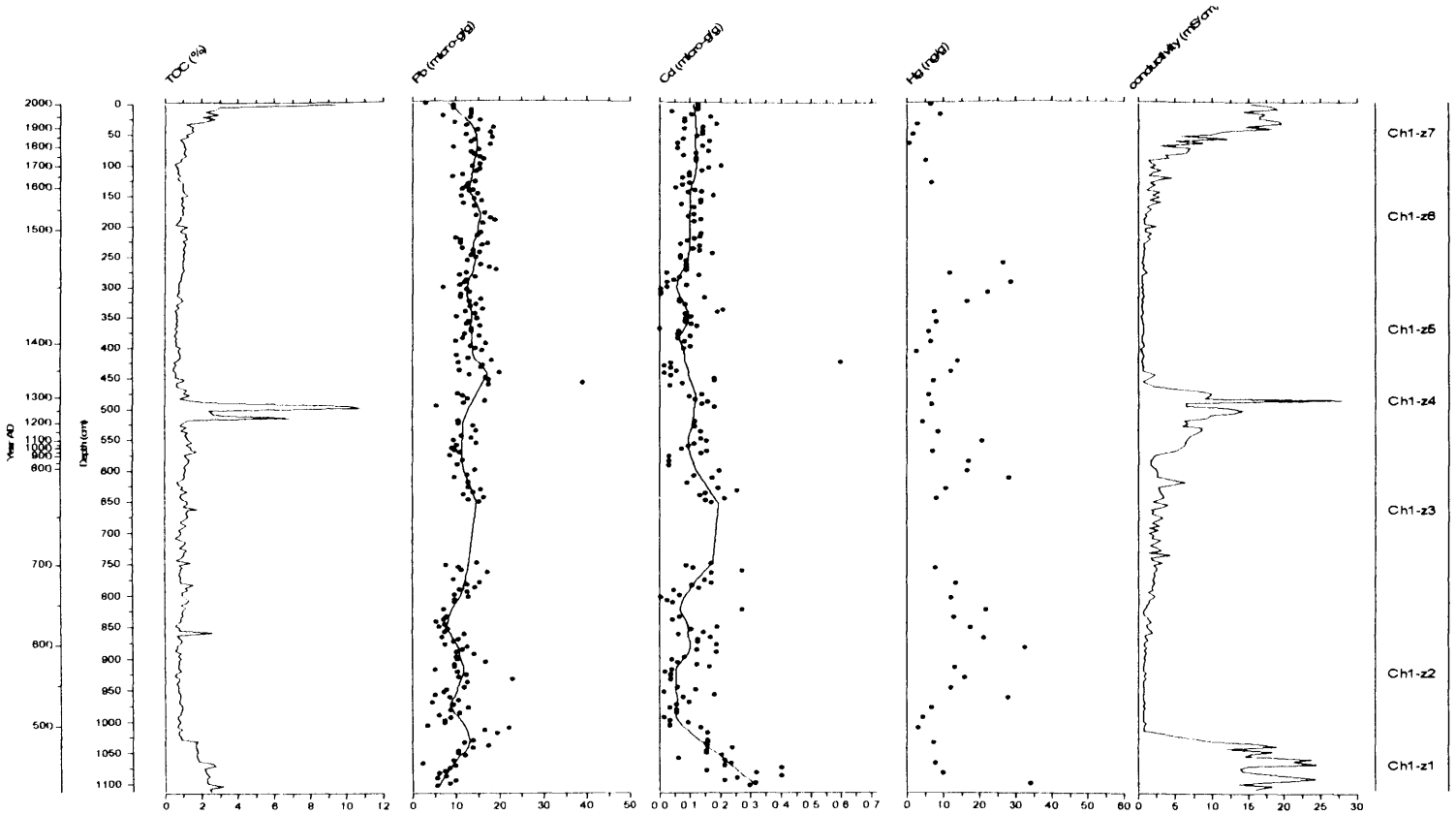

Figure 6.3 Down-core elemental profiles of Pb, Cd and Hg (acid extractable concentrations) fitted with a smooth line (0.1), plotted against age (year AD) and depth of the Aral Sea as recorded in the sediments of Chernyshov Bay. Also shown are the crustal averages of for each element (red dashed line) and the diatom inferred conductivity.

6.8 Discussion

6.8.1 Ar-9 trace element history (ca. 1925 AD – the present day.)

Passell et al., (2003) established that Pb concentrations in the bottom sediments of two sites on the lower reaches of the Amu Darya were 12 μg/g and 9± 4 μg/g while values in nearby soils measured 7 μg/g and 15 μg/g. Similar concentrations were recorded from the Syr Darya (19 – 20 μg/g for both bottom sediments and soils), suggesting little or no influence of anthropogenic Pb emissions in soils and rivers near the Aral Sea. The low records of Pb 1.43 – 13.5 μg/g (mean = 8.11 μg/g) over the last ca. 75 years, from Chernyshov Bay are in agreement with this range. These results are also consistent with the mean value of 14 μg/g found in the earth's continental crust (Wedepohl, 1995) and that of 19 μg/g (range = 0.3 – 170 μg) in sedimentary rocks in Uzbekistan (Inayatov et al., 2004) across which the Amu Darya flows. The values recorded in the Aral Sea compare with pre anthropogenic records of 10.9 μg/g in Lake Baikal (Boyle et al., 1998), 11.7 μg/g in Lake Tahoe, California (Heyvaert et al., 2000), 2 – 15 μg/g in Swedish Lakes (Renberg et al., 1994), 20.2 μg/g from Laguna Lobato in the Bolivian Andes (Abbott and Wolfe, 2003) and ~ 17 μg/g in western Ireland (Schettler and Romer, 2006).

With the exception of the northern part of Lake Baikal (Boyle et al., 1998), the above lakes and numerous others in the United States (Norton et al., 1992) all show an increasing trend in Pb over the last 100 years, being particularly prominent after the 1920s and the concordant growth in the consumption of leaded petrol. A declining trend in Pb is then seen in sediment profiles from lakes in northern Sweden (Brannvall et al., 1999), Lake Geneva, Switzerland, (Monna et al., 1999) and Lake Tahoe, California (Heyvaert et al., 2000) due to regulations reducing the Pb content within petrol implemented in the mid 1970s and the almost halving of global anthropogenic loading of Pb to the atmosphere from 332,350 to 119,250 tonnes during the period 1983 – 1995 (Pacyna and Pacyna, 2001). These trends are not recorded in Ar-9.

Two key factors may contribute to the lack of an anthropogenic record at Chernyshov Bay. Firstly while leaded petrol still accounts for 74% of the global anthropogenic emissions of Pb (Pacyna and Pacyna, 2001), it is estimated that in excess of 50% of

automotive Pb exists as particles > 1μm accumulating within ca. 100 m from roadways (Nriagu, 1979). In Uzbekistan, automotive emissions account for ca. 90% of total Pb emissions, the majority of which is limited to the Tashkent area (http://enrin.grida.no/htmls/uzbek/env2001/content/soe/english/atmosphe.htm). The majority of the population in the immediate vicinity of the Aral Sea is limited to two towns, Aralsk in the north and Muynak to the south thus any potential record of the use of petrol such as those detailed at Lake Tahoe (Heyvaert et al., 2000) around which vehicles may easily drive, is unlikely to be recorded at Chernyshov Bay. It is more likely that contamination will be greatest nearest inhabited areas. This is true for the Caspian Sea, (de Mora et al., 2004) where Pb concentrations from surface sediments are highest around the city of Baku in Azerbiajan, reflecting local pollution. In contrast, the rest of the lake has varying low concentrations due to natural input and its variability. Increased contamination is also likely in regions where stationary fossil fuel combustion and non ferrous metal production is high, however Aralsk and Muynak were dominated by fishing and related industries (i.e. canning) consequently any record of anthropogenic Pb contamination form the Aral Sea is likely to be minor and limited to sediments closest to these urban areas, in common with the Caspian Sea findings de Mora et al., (2004).

Secondly, the deposition of atmospheric Pb transported from outside the region is largely dependent upon precipitation and the scavenging of airborne aerosols. In an investigation of lakes in the Canadian High Arctic, Outridge et al., (2002, 2005) suggest that low rates of precipitation in the region result in negligible input of anthropogenic Pb. The same argument may be used here for the metals record from Chernyshov Bay due to the low rates of precipitation over the lake (mean = 100 to 140 mm/year). Evidence of localised Pb pollution is seen in other urban areas and close to mining operations such as those in Almalyk and Angren in the east of Uzbekistan (Navruz 2003), however these are too far from the Aral Sea to contribute directly to the Pb loading of the lake.

Pb deposited in the Amu Darya and Syr Darya (or its tributaries and headwaters) might be transported to the Aral Sea, however, Trefey et al., (1985) were able to show that concentrations of Pb in sediments 30 – 40 km from the Mississippi delta in the Gulf of Mexico increased 10 fold close to the river mouth. Consequently Chernyshov

Bay, due its distance from both the Amu Darya and Syr Darya, is likely to receive little or no input, with deposition of Pb during high lake level phases most likely to be highest around the river mouths. During low lake level stands, the fluvial transport of Pb (and of course other trace metals) to the lake is obviously diminished on two counts; i) no flow results in no trace element transport by fluvial processes and ii) even if water from the Amu Darya and Syr Darya do reach the lake, due to the inception of such wide scale irrigation it is possible that much of the sediment and associated trace elements from these rivers accumulates in reservoirs and canals within the irrigation system itself (Glazovsky, 1995). This is known to occur in the Volga, where the collection of contaminated sediments within reservoirs along its course results in its deltaic sediments having low concentrations of trace metals (Winkels et al., 1998).

Interestingly fluvial inputs to the lake were almost zero during the 1980s (section 2.6.1) and yet there is no significant change in the Pb profile of Ar-9. Thus it is possible to conclude that over the last 75 years, the Pb concentration of the sediments at Chernyshov Bay is not totally reliant upon the hydrological regime in place at any given time and may be due, in part, to the aeolian influx of terrigenous material from the surrounding area.

The basal concentration of 0.17 μg/g of Cd is close to that given by Wedepohl (1995) of 0.1 μg/g for the earth's continental crust and 1.5 μg/g (range = 0.06 – 2.5 μg) for sedimentary rocks in Uzbekistan (Inyatov et al., (2004). Records of the concentration of Cd within the sediments of the Aral Sea during 1978-1979 were determined by Oreshkin et al., (1993) with values from 128 locations varying between 0.012 – 0.66 μg/g (mean = 0.16 μg/g) with highest concentrations closest to the river mouths, (strengthening the argument for the higher concentration of metals in these areas) and in sediments dominated by clays in the centre of the eastern basin. The two measurements they recorded from Chernyshov Bay of 0.12 μg/g and 0.028 μg/g are both lower than that of 0.21 μg/g recorded for 1980 in Ar-9 illustrating the variation in the spatial distribution within the sediments. Cd is clearly seen to increase over the last ca. 75 years and in particular since ca. 1990, from which time the mean concentration has increased from pre 1990 mean values of 0.25 μg/g to 0.36 μg/g in the uppermost sediments (Fig 6.3).

An estimated 5 – 10% of wintertime Cd emissions by Eurasiatic countries is routinely deposited in Arctic regions (Nordic Council of Ministers, 2003) providing evidence for long range transport for this element. However as already discussed, the low precipitation will result in little or no wet deposition across the lake. This suggests that the Cd record at Chernyshov Bay is controlled by: i) natural variability of Cd concentration within the catchment and/or b) anthropogenic activity, principally in the form of the increased application of phosphorus (P_2O_5) fertilizers. The use of P_2O_5 fertilizers which, if derived from the former Soviet Union have a Cd content of typically 1mg/kg (FAO, 2003), has increased in tandem with the area of land under cultivation and resulted in their leaching to the Amu Darya and Syr Darya (Glazovsky, 1995). However as already outlined, the collection of sediments within the irrigation system will have reduced their input by fluvial transport. Consequently in the initial stages of the present regression, the deposition of Cd as a result of the application of P_2O_5 based fertilizers might well have increased, only to subsequently decline in conjunction with fluvial inputs, leaving more recent Cd deposition to the lake bed largely dependent upon aeolian activity. If this mechanism of transport of anthropogenic Cd is a factor, the northerly surface winds that dominate the region mean that the source area will generally be restricted to the Syr Darya river valley and the former lakebed of the eastern basin (Singer et al., 2003), which may have accumulated Cd in the same fashion as other pesticide residues (O'Hara et al., 2000). Consequently, the deposition of fine grain material is generally highest to the south of the Aral Sea in the Karakum region (Figure 6.4) rather than sites closer to the lake where coarser grained material is generally deposited (O' Hara et al., 2000; Singer et al., 2003).

Determining whether anthropogenic activity has contributed to the observed values at Chernyshov Bay is not possible, but it cannot be ruled out. Increased blood levels of both Cd and Pb in children near the Aral Sea have been reported, however this is due to the irrigation of crops with water that is already heavily contaminated with these metals, leading to their incorporation into the food chain and subsequent uptake (Jensen et al., 1997). Rather than being the result of fluvial transport, Cd deposition during the present regression is most likely a consequence of: the remobilization of fine marginal sediment from the eastern basin, much of which, Oreshkin et al., (1993)

report as having concentrations above the crustal average, and the aeolian input of Cd with terriginous material which may include contaminated material from soils in the Syr Darya region and the former bed of the Aral Sea.

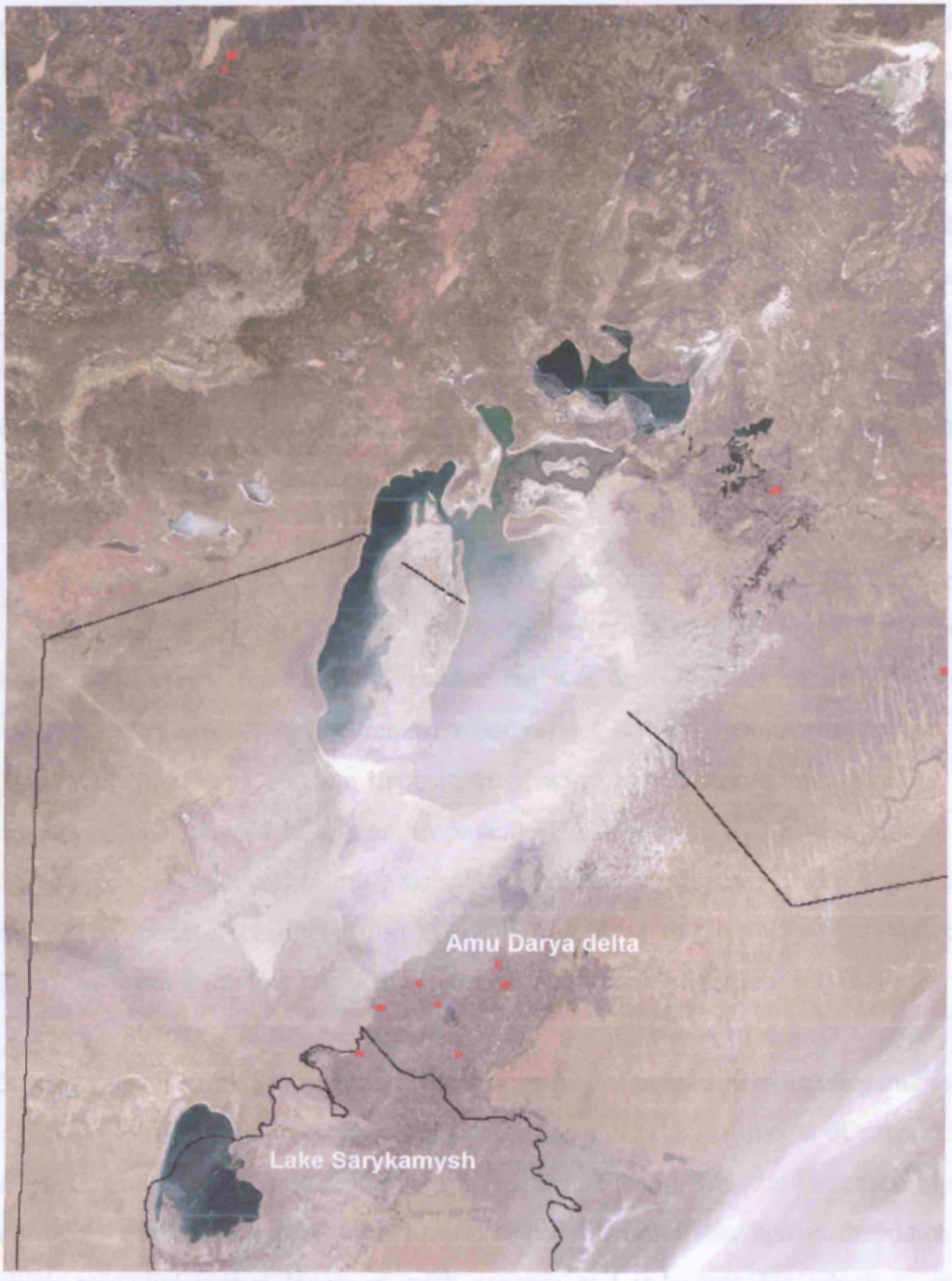

Figure 6.4. Dust storm over the Aral Sea (September 2004), clearly showing a) the major source of aeolian material as the former bed of the eastern basin and b) the south westerly trajectory of material towards the upper reaches of the Amu Darya and Lake Sarykamysh. The filled red circles are heat anomalies (fires) detected by the satellite. (http://visibleearth.nasa.gov/view_rec.php?id=5252)

In contrast to Cd, Hg exhibits a distinctive decreasing trend from values of 60 ng/g in ca. 1925 AD to concentrations of just 6 ng/g by 2002. Concentrations of between 63 – 73 ng/g characterise the profile between 1920 and 1940 AD and are higher than the estimates of mean Hg concentration in the continental crust of 40 ng/g (Wedepohl, 1995) but as with both Pb and Cd, the values are consistent with the value of 70 ng/g (range = 6 – 250 ng/g) from sedimentary rocks in Uzbekistan (Inayatov et al., 2004). The atmospheric residence time of particulate Hg is generally in the region of about 4 days (Saklys and Kvietkus, 2002), with deposition occurring between 100 – 1000 km of the source (UNEP, 2002), however the gaseous nature of the majority of Hg emissions results in an atmospheric residence time for as long as two years (UNEP, 2002). This allows long range transport, with as much as 30 – 70% of continental Hg deposition being derived from external sources (Travnikov and Ryaboshapko 2002). This supports the concept of Hg as a 'global pollutant' with increased Hg concentration recorded in profiles far from emission sites in the Canadian Arctic (Barrie et al., 1992; Landers et al., 1998) and Greenland (Bindler et al., 2001).

The declining values in Chernyshov Bay do not appear to reflect the records of global emissions recorded in the studies mentioned above. As with Pb and Cd the lack of precipitation across the lake will reduce the wet deposition of gaseous Hg in the atmosphere, consequently the record must reflect sediment transport via the Amu Darya and Syr Darya and the deposition of wind blown terriginous material, both almost certainly devoid of any anthropogenic Hg. Health-related investigations have determined that Hg levels in urine samples of children from Aralsk, were significantly lower than those of children from industrialised areas in Germany (Erdinger et al., 2004) confirming the low levels of Hg contamination in the region.

Outridge et. al, (2005) determined that diatom abundance rather than organic carbon explained much of the variance in Hg concentration in the sediments of several lakes in the Canadian High Arctic. The reason, they postulated, was the increased input of meltwater during the spring and the enhanced erosion rates across the catchment which provided higher levels of both organic and inorganic Hg which is readily incorporated by littoral algae during periods of high productivity and their subsequent senessance and deposition through sediment focusing into the deeper parts of the lake. This increase in trace element concentration including that of Hg is seen in the upper

reaches of the Amu Darya and Syr Darya during spring (Passell et al., 2003). If Outridge et al., (2005) are correct in their assertion, episodes of high lake level and the dominance of the sediment profile by benthic species might result in higher Hg concentrations in the Aral Sea. Equally, the observed decline in the Hg concentration at Chernyshov Bay over the last ca. 75 years may reflect; i) the decrease in benthic diatoms and the increased abundance of planktonic species such as *C. choctawhatcheeana* which is restricted to the lake's deeper areas and ii) the reduction in fluvial inputs over the past 40 years, not only resulting in declining abundances of benthic flora which may incorporate Hg but more simply the failure of fluvial mechanisms to transport Hg to the lake. There is however no significant correlation between diatom concentration and that of Hg over the last ca. 75 years at Chernyshov Bay (Table 6.1).

6.8.2 Trace element history from ca. 400 AD to the present day

As with Ar-9, the record of Pb (mean, 12.36 μg/g), Cd (mean, 0.10 μg/g) from Chernyshov Bay indicate little or no evidence of an anthropogenic contribution since ca. 400 AD, suggesting that the variable concentrations observed reflect catchment geology. The only prominent shift in the record of Pb is observed at the base of the core from ca. 400 AD to ca. 440 AD during which time Pb increases in concentration from ca. 5 μg/g to ca. 16 μg/g. This coincides with the return to high lake levels as inferred by the diatom flora (section 4.11). While values still remain below the crustal average, several mechanisms may contribute to this observed increase, all of which are linked to the redirection of the Amu Darya from the Sarykamysh to the Aral Sea.

1. The modern day concentrations of soils in the irrigated areas close to the Aral Sea are ca. 20 μg/g (Passell et al., 2003), close to the crustal average. Alloway (1990) states that top soils will preferentially accumulate trace elements. Thus one might find increased concentration within the Chernyshov Bay sediments as a consequence of the re-routing of the Amu Darya from the Caspian to the Aral Sea and the erosion of soils from formerly cultivated land. Similarly the re-routing of the Amu Darya may have simply resulted in the erosion of sediment with a higher concentration of Pb.

2. It has already been established that the regression at ca. 400 AD was followed by a period of intense fluvial input with rapid sedimentation preventing the dissolution of evaporite deposits (Letolle and Maiugnet, 1997; Letolle et al., 2004). The sediment composition of CH1-z1 is composed primarily of silty clays, compared with a higher sand content in the overlying material (Sorrel et al., 2006) and as such will typically contain a higher concentration of natural Pb due to the strong adsorptive properties of clay minerals. The increased flow might also see the extension of the delta of the Amu Darya towards the coring site (although quickly receding as the lake level increased). Consequently trace elements that, during sustained episodes of high lake levels, are deposited closest to the delta regions far from the coring site (e.g. Trefry et al., 1985) may for a short period have been deposited closer to Chernyshov Bay.

The increased concentration of Pb corresponds to a decline in that of Cd, which is initially present in values more than four times that of the crustal average (Wedepohl, 1995) but well within the range (0.06 – 2.5 μg/g) established for Uzbekistan (Inayatov et al., 2004). Cd concentrations in Greenland and Antarctic ice cores indicate that atmospheric concentrations of Cd remained generally unchanged until the industrial revolution (Boutron, 1995; Candelone, 1995). Even then, these changes were not specifically linked to the increased production of Zn (the ores of which have a significant Cd content) as one would expect but took place in the mid-nineteenth century after the isolation of Cd from Zn ores in the early 1800s and the production of the metal. This is also concordant with an increase in Cd in the sediments of UK lakes (Yang and Rose, 2005). Consequently the Cd values observed at the base of CH-z1 from ca. 400 AD are thought to reflect natural variability within the catchment due to the changing course of the Amu Darya.

From ca. 440 – 2002 AD, Values of Pb and Cd fluctuate around the crustal average. Importantly no significant changes are detected during the low lake level stand observed between ca. 1195 – 1355 AD. This seems to confirm that the input of metals to Chernyshov Bay at least, is reliant upon the aeolian deposition of trace elements as a result of dust storms, the frequency and severity of which is seen to increase during low lake level episodes (Zavialov, 2005).

There is no indication of increased Pb deposition that might be expected to coincide with the four episodes of Ag production in Central Asia from 480 – 1130 AD. As previously discussed (section 6.1), no increasing trend was detected at Chernyshov Bay in Ar-9 over the last ca. 75 years, however while atmospheric deposition of significant anthropogenic Pb can be ruled out, an examination of the sediments near the river mouths may contain a record of Pb contamination due to fluvial transport, reflecting this medieval period of Ag production in Central Asia.

Importantly there is no significant increase in the concentration of Pb at the onset of the Industrial Revolution in ca. 1850, which saw global production of ca. 100,000 tonnes/year (Settle and Patterson, 1980), or Cd, the concentrations of both metals fluctuating around the crustal average. The Cd record in CH-1 remained stable until the present day. Pb however, exhibited a declining trend from ca. 1960. This contrasts with the Pb record form Tastubek Bay (Juggins, 1997) and only serves to highlight the temporal differences that exist in trace element records in a lake of this size.

The lower resolution of Hg compared with that of Cd and Pb makes interpretation of the Hg record over the last ca. 1600 cal. yr BP somewhat more problematic. As with Cd and Pb, the Hg values (mean, 10.38 ng/g) recorded in the sediments at Chernyshov Bay would appear to reflect natural variability rather than increased production. The redirection of the Amu Darya and the capture of natural material with differing Hg concentrations is in all probability the cause of the initial decline in Hg observed at the base of the core. Although concentrations remain below the crustal average for the duration of the record, there do however appear to be several peaks in the record at ca. 600 AD, 800 AD and 1450 AD which are not seen in the down-core profiles of Cd and Pb. This may simply be due to more natural variations of Hg within the catchment geology. The lowest Hg values do however coincide with declining lake levels which suggests that Hg might be more reliant upon fluvial input than the other metals and corresponds with the decline in Hg concentration over the last ca. 75 years as recorded in Ar-9.

6.9. Conclusions

Well dated sediment cores have provided invaluable information with regard to the understanding of anthropogenic impacts in lake ecosystems and the extent of these impacts on local, regional and global scales. No such impact is determined from the sediments at Chernyshov Bay. This is not to say that the region has been unaffected by pollution from trace elements, it almost certainly has, however the location of Chernyshov Bay, far from Aralsk and Muynak and the mouths of the Amu Darya and Syr Darya mean that the sediments here are unlikely to contain a record of trace elements that have been the subject of fluvial transport to the lake. Similarly the low precipitation rates observed across the region mean that any atmospherically derived trace element contamination is likely to be both minor and localised with any potential signal being diluted by periods of high sedimentation rates within the lake.

That the record of all three metals in CH-1 for the past 75 years, contrasts with that obtained from Ar-9 is hardly surprising and would appear to characterise the complexities in the sediments from Chernyshov Bay, which sees not only trace element concentrations differ over the same time period but organic isotopes, diatom inferred conductivity, and ostracod assemblage

Chapter Seven

Summary, conclusions and recommendations for future research.

7.1 Introduction

The main aim of this investigation has been to use diatoms obtained from Chernyshov Bay, in the north of the western basin of the Aral Sea, in both a qualitative and quantitative fashion in order to reconstruct both palaeoconductivity and lake level history of the Aral Sea for the last ca. 1600 cal. yr BP. Secondly, in an effort to determine whether the recorded fluctuations were a consequence of human activity or natural variations in climate over this period, the analysis of the $\delta^{13}C$ organic isotope record has provided important information regarding the origin of organic material found within the sediments. The information derived from these proxies have then been used to link changes recorded in the Chernyshov Bay sediments with recent archaeological investigations in the area and historical records of human activity and records of climatic variability in the region, notably the Eastern Mediterranean which is the prime source of moisture for both the Aral Sea basin and the Tien Shan and Pamir mountains, in which the headwaters of the Amu Darya and the Syr Darya rivers are located. Lastly, in an effort to further investigate anthropogenic impact on the lake, the establishment of trace metal records (Cd, Pb and Hg) was undertaken in order to determine if the Aral Sea has been subjected to contamination by heavy metals to the same degree as other lakes across the globe since the start of the industrial revolution ca. 1850 AD and on a longer time scale with particular reference to Pb and Hg.

What follows in this chapter is a synthesis of the results obtained and recommendations for future research.

7.2 Lake-level change of the Aral Sea since ca. 400 AD.

Both diatom-inferred palaeoconductivity of the Aral Sea and the ratio of planktonic to benthic diatoms have highlighted three periods of high conductivity and low lake levels since ca. 400 AD. Despite poorly reconstructing the extent of conductivity change, the transfer function nevertheless highlighted fluctuations in conductivity, from which the detrermination of lake-level change over this period was made possible.

The earliest regression is represented by the presence of gypsum at the base of the core in CH1-z1, which is seen to correspond with deposition of mirabilite in other areas of the western basin. It has been suggested that the deposition of mirabilite would require lake levels to reach 23 m a.s.l., some 30 m lower than the stable phase of the lake from 1911 – 1960 AD (~53 m) and 8 m lower than was the case during the retrieval of the core material in 2002. At this time the Amu Darya is thought to have been flowing towards Lake Sarykamysh. The preservation of the gypsum at Chernyshov Bay is seen to have been a consequence of the rapid refilling of the lake as the Amu Darya was diverted northwards to the Aral Sea and this would appear to be confirmed not only by the overlying diatom assemblages in CH1-z1 (which are characterised by several species indicative of fluvial conditions) but also the $\delta^{13}C_{org}$ record, in which, according to the age model, values decrease from -22‰ to -26‰ in the space of ~5 years. The C/N ratio (< 10) throughout this period is indicative of algal production thus the decreasing isotopic values represent processes occurring within the lake rather than the in-wash of terrestrial vegetation.

From ca. 440 – 985 AD a period of high lake levels has been recorded. After which time, both the build up of sediment within the bed of the Amu Darya, resulting in its natural diversion away from the Aral Sea towards the Sarykamysh, and a concordant increase in irrigation, initiate a period of declining lake levels and increased conductivity. At ca. 1185 AD in CH1-z4, a second severe regression is initiated due to the total diversion of the Amu Darya away form the Aral Sea. The diatom assemblages indicate an increase in conductivity and low lake levels which is confirmed by the dominance of planktonic and tychoplanktonic species. These provide an indication of the loss of the extensive littoral zone of the eastern basin as

lake levels decline. During this period, the $\delta^{13}C_{org}$ reaches its highest values of -17‰ the low C/N ratios (< 10) indicate that algal productivity is still the dominant control on $\delta^{13}C_{org}$ values. The presence of finely laminated sediments at this time also suggests that the lake was possibly meromictic during this period as a result of high conductivity and a salinity gradient, as was the case at the time of coring in 2002 AD

From ca. 1355 – 1780 AD a further period of high lake level and low conductivity is recorded by the diatoms. This is seen to contradict historical evidence which suggest that flow from the Amu Darya did not return to the Aral Sea until the end of the 1500s. This is supported by recent archaeological investigations. The presence of a settlement at an elevation of 32 m a.s.l. would not have been possible without a freshwater supply thus it might be concluded that as lake levels were low, Chernyshov Bay may have existed in isolation as a small fresh/brackish water lake. At this time increased nutrient availability from the former lake bed resulted in increasing algal productivity and values of $\delta^{13}C_{org}$.

Increased conductivity and low lake levels are seen to occur from 1780 AD. Again this contradicts the historical records which indicate high levels of around 53 m with minor fluctuations (~3 m). These fluctuations however result in the loss of a large portion of available benthic habitat and their cyclicity over the last ca. 200 years suggests that planktonic flora may contribute more to the diatom assemblages than during more stable conditions.

7.3 Natural climatic variability or anthropogenic activity

One of the major goals of this project has been to determine the principal cause of lake level changes over the past ca. 1600 cal. yr BP. The cause of the severe regression that has inflicted the Aral Sea since 1960 AD is a consequence of anthropogenic activity and specifically increased irrigation. What is certain is that all of the low lake level stands during this longer period have also been associated with human activity. The question is, then, whether increased aridity and a decline in the supply of freshwater has forced the local population to turn to the Amu Darya (and to a lesser extent the Syr Darya) to retain a stable water supply. Or whether human activity independent of climate, (i.e. due to increased irrigation or military conflict

and social upheaval) is the principal cause of the severe regressions observed in common with that occurring today. While differentiating between various forcing factors may prove difficult in many environments, the recent archaeological findings and wealth of historical records means that for the Aral Sea this is less of a problem.

The first regression which ended at ca. 400 AD is thought to have followed a period during which the region was in receipt of a substantial water supply due to the easterly migration of depressions formed in the Eastern Mediterranean and irrigation technologies were such that flow from the Amu Darya was maintained towards both the Aral Sea and the Sarykamysh. According to the dating of a settlement in the western basin of the Aral Sea, lake levels were high at ca. 200 AD. The return to high lake levels at ca. 400 AD, as indicated by the age model, means that there is a 200 year window when the initial regression may have occurred. This is also a period when historical records indicate that the Huns destroyed irrigation facilities along the Amu Darya, resulting in its diversion away from the Aral Sea towards the Sarykamysh. Meanwhile the Syr Darya was still discharging into the lake. Consequently it is possible to conclude that human activity, in the form of military conflict, played a major role in the first recorded regression which ended at ca. 400 AD. Whether natural climatic variability in the form of increased aridity played a role is difficult to tell, it may well have been a contributory factor in this regression but it is doubtful that it was responsible for its severity.

The later reduction in water supply in the Prisarykamysh region southwest of the Aral Sea in the 4^{th} – 5^{th} centuries AD occurred not as a result of increased aridity across the region but the diversion of the Amu Darya northwards to the Aral Sea. This was in all probability due to the lack of water management that followed the invasion of the Huns. This combined with increased moisture which is recorded in the Aral Sea basin and the Eastern Mediterranean resulted in the rapid return of the Amu Darya to the Aral Sea.

The second severe regression, between ca. 1185 – 1350 AD, is seen having occurred during a period of maximum moisture availability and a wet MWP in the Eastern Mediterranean. This contrasts with increased aridity in the Pamir and Tien Shan. The $\delta^{13}C_{org}$ values continue to provide a record of within-lake productivity rather than

signify any significant changes in vegetation cover in and around the lake and its subsequent in-wash, both of which might be expected with increased precipitation. It is suggested that the cyclones formed in the Eastern Mediterranean were, at this time unable to penetrate the more continental regions of Central Asia (i.e. the Pamir and Tien Shan). Consequently it is felt that an increase in aridity in the headwaters of the Amu Darya and Syr Darya, contributed to this regression. However as with the initial low lake-level stand, the destruction of irrigation facilities on the Amu Darya by the Mongols in 1221 AD, which led to the diversion of water to the Sarykamysh and on to the Caspian Sea played a major role. Historical records indicate that the Amu Darya did not discharge into the Aral Sea until the late 1500s. This was again due to the natural diversion of the river back to the present day Aral Sea.

7.4 Heavy metal pollution of the Aral Sea.

The record of anthropogenic heavy metal pollution over the last ~75 years indicates that Chernyshov Bay has suffered little to this effect with regard to Pb and Hg, the concentrations of which are below the global crustal average. This contrast with the values of Cd which show an increasing trend over the last century and may possibly be linked to increased fertilizer use across the region and the subsequent deposition of Cd across the lake, or more specifically Chernyshov Bay, a result of the many dust storms that occur every year. It is however difficult to determine just to what extent the lake as a whole has suffered over this period from just one location, especially one that is a far from both the deltas of the Amu Darya and Syr Darya and the two main centres of population, Aralsk and Muynak.

Over a longer time scale, the record of Cd, Hg and Pb stretching back to 400 AD provided no indication of anthropogenic contamination of these metals. Despite Central Asia being the world's foremost centre of silver production during the Medieval period no impact (in the form of Pb, a significant by product in the production of silver from the high lead containing ores found in this region) is detected. It would appear that the variations in these metals over the last ~1600 years is a consequence of natural variations in the catchment geology.

The wet deposition of Hg is as likely to occur at Chernyshov Bay as anywhere else across the lake, thus one might conclude that the overall lack of rainfall has spared the lake the effects of long range contamination of this particularly harmful metal. It is reassuring to know that over the last 1600 years the lake (or at least Chernyshov Bay) has not had to deal with serious heavy metal contamination as well as periodic regressions which will presumably have damaged the lake's ecology in a similar fashion to the present day.

7.5 Suggestions for future work

This project has provided a high-resolution record of lake-level change over the last ca. 1600 cal. yr BP and it is clear that the lake is extremely sensitive to changes in its hydrological inputs. However, this record has been obtained from just a single core from a lake which may, when not undergoing a regressive phase have a surface area of ca. 66,000 km^2. Consequently the investigation of further cores at high resolution over this important time period would help to confirm the changes inferred from the Chernyshov Bay material.

The original aim of the CLIMAN project had been to obtain record for the duration of the Holocene and into the Late-Glacial. Obtaining such a record, although difficult in terms of logistics, would then provide an indication of just how lake levels have fluctuated prior to extensive anthropogenic activity in the region. From this a clear sign of just how, and to what extent the lake is affected by known natural climatic variation in the region, upstream in the Eastern Mediterranean and down stream in the Pamir and Tien Shan may be obtained. The headwaters of the Amu Darya and Syr Darya in the Pamir and Tien Shan respectively mean that their flow will be linked to changes in these mountainous regions. Consequently the examination at high resolution of sediment cores obtained from lakes in the Pamir and Tien Shan would be particularly helpful in providing an indication of climatic fluctuations. This might include the establishment of transfer functions to reconstruct air temperature using chironomids, diatoms and pollen.

What does appear to be unresolved is the extent just to which the region is under the influence of atmospheric teleconnections (i.e. the AO/NAO and ENSO). The present

regression is anthropogenic in nature and has had a direct effect on the climate of the region. Therefore a comparison of precipitation and temperature records from meteorological stations in the region prior to 1960 AD would provide an indication of just how the region has been affected by natural variability. This could also be undertaken by the determination of flow rates of the Amu Darya and Syr Darya and also, if accurate records are available the timing of ice onset across the lake and its duration. Correlation coefficients between these parameters and both Northern and Southern Hemisphere atmospheric circulation patterns may then be derived in order to assess the role of AO/NAO and ENSO on changing conditions in the region.

8. References

Abbott, M.B., Bindford, M.W., Brenner, M. and Kelts, K.R. (1997). A 3500 ^{14}C yr high-resolution record of water-level changes in Lake Titicaca, Bolivia/Peru. *Quarternary Research*, 47, 169-180.

Abbott, M.B. and Wolfe, A.P. (2003). Intensive Pre-Incan metallurgy recorded by lake sediments from the Bolivian Andes. *Science*, 301, 1893-1895.

Adshead, S.A.M. (1993). *Central Asia in World History*. Macmillan, London.

Aizen, E.M., Aizen, V.B. Melack, J.M. Nakamura, T. and Ohta, T. (2001) Precipitation and Atmospheric Circulation Patterns at Mid-Latitudes of Asia. *International Journal of Climatology*, 21, 535-556.

Aleshinskaya, Z.V., Tarasov, P.E. and Harrison, S.P., (1996a). Aral Sea, Kazakhstan-Uzbekistan. Lake Status Records, FSU and Mongolia. Available online at http://www.ncdc.noaa.gov/paleo/lakelevel.html

Aleshinskaya, Z.V., Tarasov, P.E., Harrison, S.P. (1996b). Lake Issyk-kul, Kirghizia. Lake Status Records, FSU and Mongolia. Available online at http://www.ncdc.noaa.gov/paleo/lakelevel.html

Alin, S.R. and Cohen, A.S. (2003). Lake level history of Tanganyika, East Africa for the past 2500 years based on ostracod inferred water depth record. *Palaeogeography Palaeoclimatology Palaeoecology*, 119, 31-49.

Alley, R.B., Mayewski, P.A., Sowers, T., Stuiver, M., Taylor, K.C. and Clark, P.U. (1997). Holocene climatic instability: A prominent, widespread event 8200 yr ago. *Geology*, 25/6, 483-486.

Alloway, BJ, 1990. *Heavy Metals in Soils*. Blackie, Glasgow. p.153-173.

Andrén, E., Shimmield G. and Brand T. (1999). Environmental changes of the last three centuries indicated by siliceous microfossil records from the southwestern Baltic Sea. *The Holocene*, 9/1, 25-38.

Andrianov, B. V. (1995) The history of economic development in the Aral region and its influence on the environment. *GeoJournal*, 35, 11-17.

Arpe, K., Bengtsson, L., Golitsyn, G.S., Mokhov, I.I., Semenov, V.A. and Sporyshev, P.V. (2000). Connection between Caspian Sea level variability and ENSO. *Geophysical Research Letters*, 27/17: doi: 10.1029/1999GL002374.

Aston, S.R., Bruty, D., Chester, R. and Padgham, R.C. (1973). Mercury in lake sediments: a possible indicator of technical growth. *Nature*, 241, 450-451.

Bao, Y., Brauning, A., Yafeng, S. (2003). Late Holocene temperature fluctuations on the Tibetan Plateau. *Quaternary Science Reviews*, 22, 2335-2334.

Bar-Matthews, M., Ayalon, A., Gilmour, M., Matthews, A. and Hawkesworth, C.J. (2003). Sea–land oxygen isotopic relationships from planktonic foraminifera and speleothems in the Eastern Mediterranean region and their implication for paleorainfall during interglacial intervals. *Geochimica et Cosmochimica Acta* 67/17, 3181-3199.

Barber, D.C., Dyke, A., Hillaire-Marcel, C., Jennings, A.E., Andrews, J.T., Kerwin, M.W., Bilodeau, G., McNeely, R., Southon, J., Morehead, M.D. and Gagnon, J-M. (1999). Forcing of the cold event of 8200 years ago by catastrophic drainage of Laurentide lakes. *Nature*, 400, 344-348.

Bard, E., Raisbeck, G., Yiou, F. and Jouzel, J. (2000). Solar irradiance during the last 1200 years based on cosmogenic nuclides. *Tellus*, 52B, 985-992.

Barker, P. (1990). Diatoms as palaeolimnological indicators: a reconstruction of Late Quaternary environments in two East African salt lakes. Unpublished Ph.D. thesis, Loughborough University, U.K. 267 pp.

Barker, P. (1992). Differential diatom dissolution in Late Quaternary sediments from Lake Manyara, Tanzania: an experimental approach. *Journal of Paleolimnology*, 7, 235-251.

Barker, P., J.-C. Fontes, J-C., Gasse, F. and Druart, J-C. (1994). Experimental dissolution of diatom silica in concentrated salt solutions and implications for paleoenvironmental reconstruction, *Limnology and Oceanography*, 39, 99-110.

Barrie L, Gregor D, Hargrave B, Lake R, Muir D. and Shearer R., (1992). Arctic contaminants: sources, occurrence, and pathways. *Science of the Total Environment*, 122, 1-74.

Barrnedos-Vallve, M. and Martin-Vide, J. (1998). Secular climatic oscillations as indicated by catastrophic floods in the Spanish Mediterranean coastal area. *Climatic Change*, 38, 473-491.

Battarbee, R.W. (1986). Diatom Analysis. In: Berglund, B.E. (ed.): *Handbook of Holocene Palaeoecology and Palaeohydrology*. Wiley, Chichester.

Battarbee, R.W. and Kneen, M. (1982). The use of electronically counted microspheres in absolute diatom analysis. *Limnology and Oceanography* 27, 184-188.

Battarbee, R.W., Juggins, S., Gasse, F., Anderson, N.J., Bennion, H. and Cameron, N.G. (2000). European Diatom Database Initiative (EDDI). *An information system for palaeoenvironmental reconstruction. European Climate Science Conference, Vienna City Hall, Vienna, Austria, 19-23 October.* p 1-10.

Battarbee, R.W., Jones, V.J. Flower, R.J. (2001). Diatoms. In: *Smol, J.P. and Birks, H.J.B. (eds.), Tracking Environmental Change Using Lake sediments. Vol. 3. Terrestrial, algal and siliceous indicators*. Kluwer Academic Publishers, Dordrecht, pp. 155-202.

Bauer, E., Claussen, M. and Brovkin, V. (2003). Assessing climate forcings of the earth system for the past millennium. *Geophysical Research Letters*, 30/6, 1276.

Beadle, L. C. (1974). *The inland waters of Tropical Africa: an introduction to tropical limnology*. Longman Group Limited. London.

Beer, J., Siegenthaler, U., Bonani, G., Finkel, R.C., Oeschger, H., Suter, M. and Wolfli, W. (1988). Information on past solar activity and geomagnetism from ^{10}Be in the Camp Century ice core. *Nature*, 331, 675-679.

Beer, J. and 12 others. (1990). Use of ^{10}Be in polar ice to trace the 11-year cycle of solar activity. *Nature*, 347, 164-166.

Beer, J., Mende, W. and Stellmacher, R. (2000). The role of the sun in climate forcing. *Quaternary Science Reviews*, 19, 403-415.

Benson, L.V., Meyers, P.A. and Spencer, R.J. (1991). Change in the size of Walker Lake during the past 5000 years. *Paleogeography, Paleoclimatology, Paleoecology*, 81, 189-214.

Berg, L.S. (1908). *Aral Sea, an attempt of Physical Geographic Description.* Izvestiya Turkestankogo Otdeleniya, Russian Geographic Society, St. Petersburg, 5, 9, 580 pp. [In Russian]

Bertrand C., M.F. Loutre, M.F., Crucifix, M. and Berger, A. (2002) Climate of the Last millennium: a sensitivity study. *Tellus,* 54(A), 221-244.

Bianchi, G.G. and McCave, I.N. (1999). Holocene periodicity in North Atlantic climate and deep ocean flow south. *Nature*, 397, 515-517.

Bigler, C., Lacroque, I., Peglar, S.M., Birks, H.J.B. and Hall, R.I. (2002). Quantitative multiproxy assessment of long term patterns of Holocene environmental change from a small lake near Abisko, northern Sweden. *The Holocene*, 12/4, 481-496.

Bilali, L., Rasmussen, P.E., Hall, G.E.M. and Fortin, D. (2002). Role of sediment composition in trace metal distribution in lake sediments. *Applied Geochemistry*, 7/9, 7-8.

Bindford, M.W., Kolata, A.L., Brenner, M., Janusek, J., Seddon, M.T., Abbott, M.B. and Curtis, J.H. (1997). Climate variation and the rise and fall of an Andean civilization. *Quarternary Research*, 47, 235-248.

Bindler, R., I. Renberg, N.J. Anderson, P.G. Appleby, O. Emteryd and J. Boyle. (2001). Pb isotope ratios of lake sediments in West Greenland: inferences on pollution sources. *Atmospheric Environment*, 35 4675-4685.

Birks, H.J.B. (1994). The importance of pollen and diatom taxonomic precision in quantitative palaeoenvironmental reconstructions. *Review of Palaeobotany and Palynology*, 83, 107-117.

Birks, H.J.B. (1995). Quantitative Palaeoenvironmental Reconstructions. In: Maddy, D. and Brew, J.S. (eds.) *Statistical Modelling of Quaternary Science Data.* Quaternary Research Association, Technical Guide No. 5, Cambridge.

Birks, H.J.B. (1998). Numerical tools in palaeolimnology – progress potentialities and problems. *Journal of Paleolimnology*, 20, 307-332.

Birks, H.J.B. (2003). Quantitative Paleoenvironmental Reconstruction from Holocene Biological Data. In: Mackay, A.W., Battarbee, R.W., Birks, H.J.B. and Oldfield, F. (eds.) *Global change in the Holocene.* p. 107-124.

Blais, J.M and Kalff, J. (1995). The influence of lake morphometry on sediment focusing. *Limnology and Oceanography*, 40, 582-588.

Blanchard, I.M., (2002). *Mining, Metallurgy and Minting in the Middle Ages Vol. 1. Asiatic Supremacy, 425-1125 AD.* Franz Steiner Verlag, Stuttgart.

Bond, G., Showers, W., Cheseby, M., Lotti, R., Almasi, P., deMenocal, P., Priore, P., Cullen, H., Hajdas, I. and Bonani, G. (1997); A pervasive millennial-scale cycle in North Atlantic Holocene and glacial times. *Science*, 278, 1257-1264.

Bookman, R., Enzel, Y., Agnon, A. and Stein, M. (2004). Late Holocene lake-levels of the Dead Sea. *Bulletin of the Geological Society of America*, 116, 555-571.

Boomer, I. (1993). Palaeoenvironmental indicators from Late Holocene and contemporary ostracoda of the Aral Sea. *Palaeogeography Palaeoclimatology Palaeoecology*, 103, 141-153.

Boomer, I., Aladin, N., Plotnikov, I. and Whatley, R. (2000). The palaeolimnology of the Aral Sea. *Quarternary Science Reviews*, 19, 1259-1278.

Boroffka, N.G.O. and 10 others (2004) Human settlements on the northern shores of Lake Aral and water level changes. *Mitigation and Adaptation Strategies for Global Change.* 10, 71-85.

Boroffka, N., Oberhänsli, H., Sorrel, P., Reinhardt, C., Wünnemann, B., Alimov, K., Baratov, S., Rakhimov, K., Saparov, N., Shirinov, T. and Krivonogov, S.K. (In review). Archaeology and Climate: Settlement and lake level changes at the Aral Sea. *Geoarchaeology.*

Bortnik, V.N. and Chistyaeva, S.P. (1990). *Hydrometeorology and Hydrochemistry of the USSR Seas. Vol. VII: The Aral Sea.* Gidrometeoizdat, Leningrad [In Russian].

Boutron, C.F. (1995). Historical reconstruction of the Earth's past atmospheric environment from Greenland and Antarctic snow and ice cores. *Environmental Review*, 3, 1-28.

Boyle, J.F. (2001). Inorganic geochemical methods in palaeolimnology. In: W.M. Last and J. Smol, (eds.) *Tracking environmental change using lake sediments: physical and chemical techniques*. Kluwer Academic, Dordrecht.

Boyle, J.F., Mackay, A.W., Rose, N.L., Flower, R.J. and Appleby, P.G. (1998). Sediment heavy metal record in Lake Baikal: natural and anthropogenic sources. *Journal of Paleolimnology*, 20, 135-150.

Boyle, J.F., Rose, N.L., Appleby, P.G. and Birks, H.J.B. (2004). Recent environmental change and human impact on Svalbard: the lake-sediment geochemical record. *Journal of Paleolimnology*, 31, 515-530.

Bradbury, J.P. (2002). A 1500-year record of climatic and environmental change in Elk Lake Minnesota III, measures of past primary production. *Journal of Paleolimnology*, 10, 213-252.

Bradbury, J.P., Leyden, B. and Salgado-Labouriau (1981). Late-Quarternay history of Lake Valencia. *Science*, 214, 1299-1305.

Bradley, R.S. (2003). Climate Forcing During the Holocene. In: Mackay, A.W., Battarbee, R.W., Birks, H.J.B. and Oldfield, F. (eds.), *Global Change in the Holocene*. Arnold, London.

Bradley, R.S. and Jones, P.D. (1995) *Climate since 1500 AD*. Routledge, London.

Bradley, R.S., Hughes, M.K. and Diaz, H.F. (2003). Climate in Medieval Time. *Science*, 302, 404-405.

Bradley, R.S., Briffa, K.R., Cole, J., Hughes, M.K. and Osborn, T.J. (2003b). The Climate of the Last Millennium. In: Alverson, K.D., Bradley, R.S. and Pedersen, T.F. (eds.) *Palaeoclimate, Global Change and the Future*. Springer, Berlin.

Brännvall, M-L., Bindler, R., Emteryd, O., Nillson, M. and Renberg, I. (1997). Stable isotope concentration of atmospheric lead pollution in peat and lake sediments in Sweden. *Water, Air, Soil Pollution*, 100, 243-252.

Brännvall, M-L., Bindler, R., Emteryd, O., and Renberg, I. (2001). Four thousand years of atmospheric lead pollution in northern Europe: a summary from Swedish lake sediments. *Journal of Paleolimnology*, 25, 421-435.

Briffa, K.R., (2000). Annual variability in the Holocene: interpreting the message of ancient trees. *Quarternary Science Reviews*, 19, 87-105.

Briffa, K.R., Jones, P.D., Schweingruber, F.H. and Osborn, T.J. (1998). Influence of volcanic eruptions on Northern Hemisphere summer temperature over the last 600 years. *Nature*, 393, 450-455.

Briffa, K.R., Osborn, T.J. and Schweinbugrer, F.H. (2001). Low frequency temperature variations from a northern tree-ring density network. *Journal of Geophysical Research*, 106, 2929-2941.

Broecker, W.S. (1994a). An unstoppable superconveyor. *Nature*, 367, 414-415

Broecker, (1994b). Massive iceberg discharges as triggers for global climate change. *Nature*, 372, 421-424.

Broecker, W.S. (2001). Was the Medieval Warm Period global? *Science*, 291, 1497-1499.

Broecker, W.S. and Denton, G.H. (1990). The role of ocean-atmosphere reorganizations in glacial cycles. *Quaternary Science Reviews*, 9, 305-341

Broecker, W.S., Sutherland, S. and Peng, T.-H. (1999). A possible 20th-century slowdown of Southern Ocean deep water formation. *Science* 286, 1132-1135.

Bronk Ramsy, C. (2005). OxCal version 3.10.

Calkin, P.E., Wiles, D.C., and Barclay, D.J. (2001). Holocene coastal glaciation of Alaska. *Quaternary Science Reviews*, 20, 449-461.

Cameron, N.G. and 16 others. (1999). Surface sediment and epilithic diatom pH calibration sets for remote European mountain lakes (AL:PE project) and their comparison with the Surface Waters Acidification Programme (SWAP) calibration set. *Journal of Paleolimnology*, 22, 291-317.

Candelone, J-P., Hong, S., Pellone, C. and Boutron, C.F. (1995). Post-industrial revolution changes in large-scale atmospheric pollution of the northern hemisphere by heavy metals as documented in central Greenland snow and ice. *Journal of Geophysical Research*, 100, 16605-16616.

Carignan, R. and Tessier, A. (1985). Zinc deposition in acid lakes: the role of diffusion. *Science*, 228, 1524-1526.

Carvalho, L., Fritz, S.C., Cox, E.J., Juggins, S., Sims, P.A., Gasse, F. and Battarbee R.W. (1995). Standardising the taxonomy of saline lake Cyclotella species. *Diatom Research*, 10, 229-240.

Chambers, F.M., Ogle, M.I. and Blackford, J.J. (1999). Palaeoenvironmental evidence for solar forcing of Holocene climate: linkages to solar science. *Progress in Physical Geography*, 23, 181-204.

Chu, G. , Liu, J., Sun, Q., Lu, H., Gu, Z., Wang, W. and Liu, T. (2002) The Medieval Warm Period drought recorded in Lake Huguangyan, tropical South China. *The Holocene*, 12/5, 511-516.

Chubb, V.E. (2000). *Climate Change and its Impact on the Natural Resource Potential of Uzbekistan*, SANIGMI, Tashkent, 252 pp [in Russian].

Cloern, J.E., Cole, B.E. and Remland, R.S.O. (1983). Seasonal changes in the chemistry and biology of a meromictic lake (Big Soda Lake, Nevada, U.S.A.). *Hydrobiologia*. 105, 195-206.

Cloern, J.E, Canuel, E.A and Harris, D. (2002) Stable carbon and nitrogen isotope composition of aquatic and terrestrial plants of the San Francisco Bay estuarine system. *Limnolog and Oceanography*, 47, 713–729.

Cobb, K.M., Charles, C.D., Cheng, H. and Edwards, R.L. (2003). El Niño Southern Oscillation and tropical Pacific climate during the last millennium. *Nature*, 424, 271-276.

Cole, J.E., Dunbar, R.B., McClanhan, T.R. and Muthiga, N.A. (2000). Tropical Pacific forcing of decadal SST variability in the western Indian Ocean over the past two centuries. *Science*, 262, 1790-1793.

Cook, E.R., Meko, D.M., Stahle, D.W. and Cleaveland, M.K. (1999). Drought reconstructions for the continental United States. *Journal of Climate*, 12, 1145-1162.

Cook, E. R., D'Arrigo, R. and Buckley, B. (2000). Warm season temperatures since 1600 B.C. reconstructed from Tasmanian tree rings and their relation to large-scale SST anomalies. *Climate Dynamics* 16: 79-91.

Cook, E.R., D'Arrigo, R.D. and Mann, M.E. (2002). A well-verified, multiproxy reconstruction of the Winter North Atlantic Oscillation Index since A.D. 1400. *Journal of Climate* 15: 1754-1764.

Cook, E.R., Woodhouse, C.A., Eakin, C.M., Meko, D.M. and Stahle, D.W. (2004). Long-term Aridity Changes in the Western United States. *Science*, 306, 1015-1019.

Cooke, R., Warren, A. and Goudie, A. (1993). *Desert Geomorphology*. UCL Press.

Cooper, S.R. (1995). Diatoms in sediment cores from the mesosaline Chesapeake Bay. *Diatom Research*, 10/1, 39-89.

Craig, H. (1953). The geochemistry of stable carbon isotopes. *Geochimica Cosmochimica Acta* 3, 53-92.

Craig, H. (1954). Carbon 13 in Plants and the Relationship between Carbon 13 and Carbon 14 variations in Nature. *Journal of Geology*, 62, 115-49.

Crecelius, E.A. and Piper, D.Z. (1973). Particulate lead contamination recorded in sedimentary cores from Lake Washington, Seattle. *Environment Science and Technology*, 7, 1053-1055.

Cremer, H., Wagner, B., Melles, M. and Hibberten, H-W. (2001). The postglacial environment development of Raffles Sø, East Greenland: inferences from a 10,000 year diatom record. *Journal of Paleolimnology*, 26, 67-87.

Crowley, T.J. (2000). Causes of climate change over the past 100 years. *Science*, 289, 270-277.

Crowley, T.J. and Lowery, T.S. (2000). How warm was the Medieval Warm Period? *Ambio*, 29, 51-54.

Cullen, H.M. and deMenocal, P.B. (2000). North Atlantic influence on Tigris-Euphraties streamflow. *Intrenational Journal of Climatology*, 20, 853-863.

Curtis, J.H.. Hodell, D.A., and Brenner, M. (1996). Climate variability on the Yucatan Peninsula (Mexico) during the past 3500 years and implications for Maya cultural evolution. *Quarternary Research*, 47, 37-47.

Curtis, J.H., Brenner, M. and Hoddell, D.A. (1999). Climatic change in the Lake Valencia Basin, Venezuela, ~12 600 yr BP to present. *The Holocene*, 9/5, 609-620.

Dansgaard, W., Johnsen, S.J. and Clausen, H.B. (1993). Evidence of great instability of past climate from a 250-kyr ice-core record. *Nature*, 364, 218-220.

D'Arrigo, R. D., E. R. Cook, J. Salinger, J. Palmer, B. M. Buckley, P. J. Krusic and R. Villalba. (1998). Temperature-sensitive tree-ring records from New Zealand: long-term context for recent warming trend. *Climate Dynamics*, 14,191-199.

D'Arrigo, R., Jacoby, G., Pederson, N., Frank, D., Buckley, B., Baatarbileg, N., Mijiddorj, R., Dugarjav, C. (2000). Mongolian tree rings, temperature sensitivity and reconstructions of Northern Hemisphere temperature. *The Holocene*, 10, 669-672.

Davies, S. J., S. E. Metcalfe, M. Caballero-Miranda and S. Juggins (2002). Developing diatom-based transfer functions for central Mexican lakes. *Hydrobiologia* 467, 199-213.

Davis, R.B., Norton, S.A., Hess, C.T., Braake, D.F. (1983). Paleolimnological reconstruction of the effects of atmospheric deposition of acids and heavy metals on the chemistry and biology of lakes in New England and Norway. *Hydrobiologia*, 103, 113-123.

Dearing, J.A., Battarbee, R.W., Dikau, R., Larocque, I. and Oldfield, F. (2006) Human-environment interactions: learning from the past. *Regional Environemntal Change*, 6, 1-16.

deMartonne (1928). Regions of interior basin drainage. *Geographical Review*, 17, 397-414.

deMenocal, P. (2001). Cultural responses to climate change in the Holocene. *Science*, 292, 667-673.

Denton, G.H. and Karlen, W., (1973), Holocene climatic variations - Their pattern and possible cause, *Quaternary Research*, 3, 155-205.

Desprat, S, Fernanda-Sanchez-Goni, M., Loutre, M.F. (2003)Revealing climatic variability of the last three millennia in northwestern Iberia using pollen influx data. *Earth and Planetary Science Letters*, 213, 63-78.

Dixit, S.S., Smol, J.P., Kingston, J.C. and Charles, D.F. (1992). Diatoms: Powerful indicators of environmental change. *Environmental Science and Technology*, 26, 22-33.

Douglas, M.S.V., Smol, J.P., and Blake Jr., W. (1994) Marked post-18th century environmental change in high-Arctic ecosystems. *Science*, 266, 416-418.

Douglas, M.S.V. and Smol, J.P., (1999). Freshwater diatoms as indicators of environmental change in the High Arctic. In Stoermer, E.F. and Smol, J.P. (eds.) The *Diatoms: Applications for the Environmental and Earth Sciences.* Cambridge University Press 469 pp.

D' Arrigo, R., Jacoby, G., Pederson, N., Frank, D., Buckley, B., Nachin, B., Mijddorj, R. and Dugarjev, C. (2000). Mongolian tree-rings, temperature sensitivity and reconstructions of Northern Hemisphere temperature. *The Holocene*, 10/6, 669-673.

Dansgaard, W., Johnsen, S.J., Reeh, N., Gunderstrup, N., Clausen, H.B. and Hammer, C.U. Climatic changes, Norsemen and modern man. *Nature*, 255, 24-28.

Eddy, J.A. (1976). The Maunder Minimum. *Science*, 192, 1189-1202.

Engstrom, D.R., Swain, E.B., Henning, T.A., Brigham, M.E. and Brezonik, P.L. (1994). Atmospheric mercury deposition to lakes and watersheds – a quantitative reconstruction from multiple sediment cores. *Advances in Chemistry Series*, 237, 33-66.

Enzel,. Y., Kadan, G. and Eyal, Y. (2000). Holocene earthquakes inferred from a fan-delta sequence in the Dead Sea graben. *Quatrenary Research* 53, 34-48.

Enzel, Y., Bookman, R., Sharon, D., Gvittzman, H., Dayan, U., Ziv, B. and Stein, M (2003). Late Holocene climates of the Near East deduced from Dead Sea level variations and modern regional winter rainfall. *Quaternary Research*, 60, 263-273.

Erdinger, L., O. Eckl, F. Ingel, Sh. Khussainova, E. Genova, M. Mann and Th. Gabrio. (2004). The Aral Sea Desaster - Human Biomonitoring of Hg, As, HCB, DDE, and PCBs from Children living in Aralsk and Akchi, Kazakstan. *International Journal of Hygiene and Environmental Health*, 207, 541-547.

Esper, J., Treydte, K., Gartner, H. and Neuwirth, B. (2001). A tree ring reconstruction of climatic extreme years since 1427 AD for Western Central Asia. *Palaeobotanist*, 50, 141-152

Esper, J., Cook, E.R. and Schweingruber, F.H. (2002a). Low frequency signals in long tree-ring chronologies for reconstructing past temperature variability. *Science*, 295, 2250-2253.

Esper, J., Schweingruber, F.H. and Winiger, M. (2002b). 1300 years of climatic history for Western Central Asia inferred from tree-rings. *The Holocene*, 12/3, 267-277.

Esper, J., Shiyatov, S.G., Mazepa, V.S., Wilson, R.J.S., Graybill, D.A. and Funkhouser, G. (2003). Temperature-sensitive Tien Shan tree ring chronologies show multi-centennial growth trends. *Climate Dynamics*, 21, 699-706.

Etheridge, D.M., Steele, L.P., Langenfelds, R.L., Francey, R.J., Barnola, J-M., and Morgan, V.I. (1998a). Natural and anthropogenic changes in atmospheric CO_2 over the last 1000 years from air in Antarctic ice and firn. *Journal of Geophysical Research*, 101, 4115-4128.

Etheridge, D.M., Steele, L.P., Francey, R.J., and Langenfelds, R.L. (1998b). Atmospheric methane between 1000 A.D. and present: evidence of anthropogenic emissions and climatic variability. *Journal of Geophysical Research*, 103(D13):15979-15993.

Eugster, H.P. and Hardie, L.A. (1979). Saline Lakes. In: Lerman, A. (1979). *Lakes: Chemistry, Geology, Physics*. Springer-Verlag, New York..

FAO (2003). Fertilizer use by crop in Uzbekistan. Food and Agriculture Organization of the United Nations. Available online: ftp://ftp.fao.org/docrep/fao/005/y4711e/y4711e00.pdf

Feng, Z., Thompson, L.G., Mosley-Thompson, E. and Yao, T. (1993). Temporal and spatial variations of climate in China during the last 10 000 years. *The Holocene*, 3/2, 174-180.

Fitzgerald, W.F., Engstrom, D.R., Mason, R.P. and Nater, E.A. (1998). The case for atmospheric mercury contamination in remote areas. *Environment Science and Technology*, 32, 1-7.

Fleitmann, D., Burns, S.J., Mudelsee, M., Neff, U., Krammers, J., Mangini, A. and Matter, A. 2003. Holocene forcing of the Indian monsoon recorded in a stalagmite from southern Oman. *Science*, 300, 1737-1739.

Flower, R.J. (1993). Diatom preservation: experiments and observations on dissolution and breakage in modern and fossil material. *Hydrobiologia*, 269/270, 473-484.

Flower, R.J., Stickley, C., Rose, N.L., Peglar, S. Fathi, F.F. and Appleby, P.G. (2006). Environmental changes at the desert margin: an assessment of recent paleolimnological records in Lake Qarun, Middle Egypt. *Journal of Paleolimnology* 35, 1-24.

Folland, C.K. and nine others (2001). Observed climate variability and change. In: Houghten, J.T. (ed.) *Climate Change 2001, the Scientific Basis*. Cambridge University Press, New York.

Friedrich, J. and Oberhaensi, H. (2004). Hydrochemical properties of the Aral Sea water in summer, 2002. *Journal of Marine Systems*, 47, 77-88.

Friss-Christensen, E. and Lassen, K. (1991). Length of the solar cycle: an indicator of solar activity closely linked with climate. *Science*, 254, 698-700.

Fritz, S.C. (1996). Paleolimnological records of climate change in North America. *Limnology and Oceanography*, 41, 882-829.

Fritz, S.C., Juggins, S., Battarbee, R.W. and Engstrom, D.R. (1991). Reconstruction in past changes in salinity and climate using a diatom based transfer function. *Nature*, 352, 706-708.

Fritz, S.C., Engstrom, D.R. and Haskell, B.J. (1993). Little Ice Age aridity in the North American Great Plains: a high resolution reconstruction of salinity fluctuations from Devils Lake, North Dakota, USA. *The Holocene*, 4/1, 69-73.

Fritz, S.C., Cumming, B.F., Gasse, F. and Laird, K.R. (1999) Diatoms as indicators of hydrologic and climatic change in saline lakes. In; Stoermer, E.F. and Smol, J.P. (1999) The *Diatoms: Applications for the Environmental and Earth Sciences*. Cambridge.

Froebrich, J and Kayumov, O. (2004): Water management aspects of Amu Darya In: Nihoul, P., Zavialov, P.O. and Micklin, P.P. (eds.) *Dying and Dead Seas - Climatic Versus Anthropic Causes*. Kluwer Academic Publishers, Dordrecht

Frolich, C and Lean, J. (1998). The sun's total irradiance: cycles and trends in the past two decades and associates climate change uncertainties. *Geophysical Research Letters*, 25, 4377-4380.

Frumkin, A., Magaritz, M., Carmi, I. and Zak, I., 1991. The Holocene climatic record of the salt caves of Mount Sedom, Israel. *The Holocene* 1/3, 191-200.

Gasse, F. (1986). *East African diatoms*. J. Cramer, Berlin.

Gasse, F., Fontes, J.C., Plaziat, J.C., Carbonel, P., Kaczmarska, I., DeDecker, P., Soulie-Marsche, I., Callot, Y., and Dupeuble, P.A. (1987). Biological remains, geochemistry and stable isotopes for the reconstruction of environmental and hydrological changes in the in the Holocene lakes from North Sahara. *Palaeogeography, Palaeoclimatology, Palaeoecology*, 60, 1-46.

Gasse, F., Juggins, S and Ben Khelifa, L. (1995). Diatom-based transfer functions for inferring hydrochemical characteristics of African palaeolakes. *Palaeogeography, Palaeoclimatology, Palaeoecology* 117, 31-54.

Gasse, F., Barker, P., Gell, P., Fritz, S.C., and Chalie, F. (1997). Diatom-inferred salinity in paleolakes: an indirect tracer of climate change. *Quaternary Science Reviews*, 16, 547-563.

Gauch, H.G. (1982). *Multivariate analysis in community ecology*. Cambridge University Press, London. 574 pp.

Gerber, S., F. Joos, P. Brügger, T. F. Stocker, M. E. Mann, S. Sitch, and M. Scholze, (2003). Constraining temperature variations over the last millennium by comparing simulated and observed atmospheric CO_2. *Climate Dynamics* 20, 281-299, 2003.

Germain, H. (1981). *Flore Des Diatomees, eaux douces et saumatres*. Societe Nouvelle Des Editions Boubee. Paris. 444 pp.

Ginzburg, A.I., Kostianoy, A.G. and Sheremet, N.A. (2004). Thermal regime of the Aral Sea in the modern period (1982-2000) as revealed by satellite data. *Journal of Marine Systems*, 43, 19-30.

Giralt, S., Julia, R., Leroy, S. and Gasse, F. (2003). Cyclic water level oscillations of the KaraBogazGol-Caspian Sea system. *Earth and Planetary Science Letters*, 212, 225-239.

Giralt, S. and 13 others (2004). 1,000-years of environmental history of lake Issyk-kul. In: Niouhl, J., Zavialov, P.O. and Micklin, P.P. (eds.) *Dying and Dead Seas – Climatic versus Anthropic Causes*. Kluwer Academic Publishers, Dordrecht. pp. 253-285.

Glasser, N.F., Harrison, S., Winchester, V. and Amiya, M. (2004). Late Pleistocene and Holocene palaeoclimate and glacier fluctuations in Patagonia. *Global and Planetary Change*, 43: 79-101.

Glazovsky, N.F. (1995). Aral Sea. In: Mandaych, A.F. (ed.) *Enclosed Seas and Large Lakes of Eastern Europe and Middle Asia*. SPB Academic Publishing bv., Amsterdam, pp. 119-155.

Gleser, S.I., Jouse, A.P., Makarova, I.V. Proshkina-Lavrenko, A.I. and Sheshukova-Poretzkaya, V.S. (1974). *The Diatoms of the USSR*. Leningrad.

Gleser, S. I., Makarova, I. V., Moisseeva, A. I. and Nikolae, V. A., (1988). *The diatoms of the USSR: Fossil and Recent, v. I.* St Petersburgh. [In Russian].

Gleser, S. I., Makarova, I. V., Moisseeva, A. I. and Nikolae, V. A., (1992). *The diatoms of the USSR: Fossil and Recent, v. II.* St Petersburgh. [In Russian].

Gobeil, C., Halliday, J.R. and Smith, J.N. (1999). Mercury profiles in sediments of the Arctic Ocean basins. *Environmental Science and Technology*, 33, 4194-4198.

Gorbunov, A.P. (1996). Monitoring the evolution of permafrost in the Tien Shan. Permafrost and Periglacial Processes, 7/3, 297-298.

Grimm, E.C. (1987). CONISS: a FORTRAN 77 program for stratigraphically constrained cluster analysis by the method of incremental sum of squares. Comp. Geosci 13, 13-55.

Grove, J.M. (1988). *The Little Ice Age*. Methuen, London.

Grove, J.M. (2001). The Initiation of the "Little Ice Age" in regions around the North Atlantic. *Climatic Change*, 48/1, 53-82.

Guilizzoni, P., Lami, A., Marchetto, A., Jones, V.J., Manca, M. and Bettinetti, A. (2002). Palaeoproductivity and environmental changes in the Holocene in central Italy as recorded in two crater lakes (Albano and Nemin). *Quaternary International*, 88, 57-68.

Haberzettl, T., Fey, M., Lücke, A., Maidana, N., Mayr, C., Ohlendorf, C., Schäbitz, F., Schleser, G. H., Wille, M. and Zolitschka, B. (2005). Climatically induced lake level changes during the last two millennia as reflected in sediments of Laguna Potrok Aike, southern Patagonia. *Journal of Paleolimnology*, 33, 283-302.

Hakansson, H., Hadju, S., Snoejis, P. and Loginova, L. (1993). *Cyclotella hakanssoniae* Wendker and its relationship to *C. caspia* Grunow and other small brackish water *Cyclotella* species. *Diatom Research* 8, 333-347.

Hardie, L.A. and Eugster, H.P. (1970). The evolution of closed-basin brines. *Mineralogical Society of America* special publication, 3, 273-290.

Hasle, G.R. (1978). Some freshwater and brackish water species of the diatom genus *Thalassiosira* Cleve. *Phycologia* 17/3, 263-292.

Hassan, K.M., Swinehart, J.B., Spalding, R.F. (1997). Evidence for Holocene environmental change from C/N ratios and $\delta^{13}C$ and $\delta^{13}N$ values in Swan Lake sediments, western Sand Hills, Nebraska, *Journal of Paleolimnology*, 18, 121-130.

Hatch, M.D. and Slack, C.R. (1968). A new enzyme for the interconversion of pyruvate and phosphopyruvate and its role in the C_4 dicarboxylic acid pathway of photosynthesis. *Biochemical Journal*, 106, 141-146.

Haug, G.H., Gunther, D., Peterson, L.C., Sigman, D.M., Hughen, K.A. and Aeschlimann, B. 2003. Climate and the collapse of Maya civilization. *Science*, 299, 1731-1735.

Hays, J.D., Imbrie, J. and Shackleton, N.J., (1976).Variations in the earth's orbit: pacemaker of the Ice Ages. *Science*, 194, 1121-1132.

Heyvaert, A.C., Reuter, J.E., Slotton, D.G., and Goldman, C.R. (2000). Paleolimnolohical reconstruction of historical atmospheric lead and mercury deposition at Lake Tahoe, California-Nevada. *Environmental Science and Technology*, 34, 3588.

Hill, M.O. and Gauch, H.G. (1980). Detrended correspondence analysis: an improved ordination technique. *Vegetatio* 42, 47-58.

Hinman, N.W. (1990). Chemical factors influencing the rates and sequences of silica phase transition; effects of organic constituents. *Geochimica et Cosmochimica Acta*, 54, 1563-1574.

Hilton, J.A. (1985). A conceptual framework for predicting the occurrence of sediment focusing and sediment redistribution in small lakes. *Limnology and Oceanography*, 30, 1131-1143.

Hirschfeld, Y., (2004). A climatic change in the Early Byzantine Period: some archaeological evidence. *Palestine Exploration Quarterly*, 136/2, 133-149.

Hodell, D.A., Curtis, J.H. and Brenner, M. (1995). Possible role of climate in the collapse of Classic Maya civilization. *Nature*, 375, 391-394.

Hodell, D.A. and Schelske, C.L. (1998). Production, sedimentation and isotopic composition of organic matter in Lake Ontario. *Limnology and Oceanography*, 43/2, 200-214.

Hodell, D.A., Brener, M., Curtis, J.H. and Guilderson, T. (2001). Solar Forcing of Drought Frequency in the Maya Lowlands. *Science*, 292, 1367-1370.

Hodell, D.A., M. Brenner, J.H. Curtis, R. Medina-Gonzalez, M.F. Rosenmeier, T.P. Guilderson, E.I. Chan-Can, and A. Albornaz-Pat. (2005). Climate change on the Yucatan Peninsula during the Little Ice Age. *Quaternary Research*, 63:109-121.

Hoffman, D.J., and Solomon, S. (1989). Ozone destruction through heterogeneous chemistry following the eruption of El Chichon. *Journal of Geophysical Research*, 94, 5029-5041.

Holzhauser, H., Magny, M and Zumbuhl, H-J. (2005). Glacier and lake-level variations in west central Europe over the last 3500 years. *The Holocene*, 6, 789-801.

Hong, S., Candelone, J-P., Patterson, C., and Boutron, C.F. (1994). Greenland ice evidence of hemispheric lead pollution two millennia ago by Greek and Roman civilizations. *Science*, 265, 1841-1843.

Hong, S., Candelone, J-P., Patterson, C., and Boutron, C.F. (1996). History of ancient copper smelting pollution during Roman and Medieval times recorded in Greenland ice. *Science*, 272, 246-248.

Hong, Y.T. and nine others (2000). Response of climate to solar forcing recorded in a 6000 year $\delta^{18}O$ time-series of Chinese peat cellulose. *The Holocene*, 10, 1-7.

Houghten, J.T., Ding, Y. Griggs, D.J., Noguer, M., van der Linden, P.J., Xiaosu, D. (eds) (2001). *Climate change: the scientific basis. Contribution of Working Group 1 to the Third Assessment Report of the Intergovernmental Panel on Climate Change (IPCC)*. Cambridge University Press, Cambridge.

Huang, S., Pollack, H.N., Shen, C.Y. (1997a). Late Quaternary temperature changes seen in the worldwide continental heat flow measurements. *Geophysical Research Letters*, 23, 1947-1950.

Huang, S., Pollack, H.N., Shen, C.Y. (1997b). Temperature trends over the past five centuries rreconstructed from borehole temperatures. *Nature*, 403, 756-758.

Huang, S., Pollack, H.N. and Shen, P.-Y. (2000). Temperature trends over the past five centuries reconstructed from borehole temperatures. *Nature* 403, 756-758.

Hughes, M.K. and Diaz, H.F. (1994). Was there a 'Medieval Warm Period', and if so, where and when? *Climatic Change*, 26/2-3, 109-142.

Hurrell, J.W. (1995). Decadal trends in the North Atlantic Oscillation: regional temperatures and precipitation. *Science*, 269, 676-679.

Hurrell, J.W. (1996). Influence of variations in climate associated with the North Atlantic Oscillation. *Geophysical Research Letters*, 23, 665-668.

Hurrell, J.W. (2000). Climate: North Atlantic and Arctic Oscillation (NAO/AO). In: J. Holton, J. Pyle, and J. Curry (eds.) *Encyclopedia of Atmospheric Sciences*. Academic Press

Hurrell, J.W. and van Loon, H. (1997). Decadal variations in climate associated with the North Atlantic Oscillation. *Climatic Change*, 36:301-326.

Hustedt, F. (1953). Die Systematik der Diatomeen in ihren Beziehungen zur Geologie und Ökologie nebst einer Revision des Halobien-Systems. *Sv. Bot. Tidskr.* 47, 509-519.

Hustedt, F. (1957). Die Diatomeenflora des Fluss-Systems der Weser im Gebiet der Hansestadt Bremen. *Abh. Naturw. Ver. Bremen*, 34, 181 440.

Hutchinson, G.E. (1957). *A Treatise on Limnology. Volume I, Geography, Physics and Chemistry*. Chapman and Hall, London.

Hylander, L.D. and Meili, M. (2003). 500 years of mercury production: global annual inventory by region until 2000 and associated emissions. *Science of the Total Environment*, 304, 13-27.

Imbrie, J. and 17 others (1992). On the structure and origin of major glaciation cycles, 1. Linear responses to Milankovitch forcing. *Paleoceanography*, 7, 710-738.

Imbrie, J., Berger, A. and Shackleton, N.J. (1993). Role of orbital forcing: a two-million-year perspective. In, Eddy, J.A. and Oeschger, H. (eds.) *Global Changes in the Perspective of the Past*, 263-277. John Wiley, Chichester

Inayatov, A. Kh, Kosolapov, A.D., Muminov, I.T., Rashidova, D. Sh, Kholbaev, I. and Khudaiberdiev, A.T. (2004). Elemental composition and radioactivity of certain sedimentary rocks, soils and plants in Uzbekistan. *Atomic Energy*, 96, 294-299.

Issar, A.S. (1998). Climate change and history during the Holocene in the eastern Mediterranean region. In: Issar, A.S. and Brown, N. (eds.), *Water, Environment, Society in Times of Climate Change*. Kluwer Academic Publishers.

Jaboyedoff, M, Derron, J.H. and Manly, G. (2005). Note on seismic hazard assessment using gradient uplift velocities in the Turan Block (Central Asia). *Natural Hazards and Earth Systems Sciences*, 5, 43-47.

Jacoby, G., D'Arrigo, R. and Davaajamts (1996). Mongolian tree rings and 20th century warming. *Science*, 273, 771-773.

Jarso, J. and Destouni, G. (2004). Groundwater discharge into the Aral Sea after 1960. *Journal of Marine Systems*, 47, 109-120.

Jellison, R., Anderson, R.F., Melack, J.M. and Heil, D. (1996). Organic matter accumulation in sediments of hypersaline Mono Lake during a period of changing salinity. *Limnology and Oceanography*, 41/7, 1539-1544.

Jensen, K.G., Kuijpers, A., Koc, N. and Heinemeier, J. (2004). Diatom evidence of hydrographic changes and ice conditions in Igaliku Fjord, South Greenland, during the past 1500 years. *The Holocene* 14, 152-164.

Jensen, S., Mazhitova, Z. and Zetterstrom, R. (1997). Environmental pollution and child health in the Aral Sea region in Kazakhstan. *Science of the Total Environment*, 206, 187-193.

Ji, J., Shen, J., Balsam, W., Chen, J., Lianwen, L. and Liu, X. (2005). Asian monsoon oscillations in the northeastern Qinghai-Tibet Plateau since the late glacial as interpreted from visible reflectance of Qinghai Lake sediments. *Earth and Planetary Science Letters*, 233, 61-70.

Johnson, T. C., Barry, S. L., Chan, Y., and Wilkinson, P., (2001). Decadal record of climate variability spanning the last 700 years in the Southern Tropics of East Africa. *Geology*, 29/1, 83-86.

Jones, P.D., Bradley, R.S. and Jouzel, J. (1996). *Climate Variations and Forcing Mechanisms of the Last 2000 Years*. Springer, Berlin.

Jones, P.D., Osborn, T.J. and Briffa, K.R. (2001). The evolution of climate over the last millennium. *Science*, 292, 662-667.

Jones, P.D. and Thompson, R. (2003). Instrumental Records. In: Mackay, A.W., Battarbee, R.W., Birks, H.J.B. and Oldfield, F. (eds.) *Global Change in the Holocene*. Arnold, London. P. 140-158.

Jones, P.D. and Mann, M.E. (2004). Climate over past millennia. Reviews of Geophysics, 42.

Joynt, E.H. III., and Wolfe, W.P. (2001). Palaeoenvironmental inference models from sediment diatom assemblages in Baffin Island lakes (Nunavut, Canada) and reconstruction of summer water temperature. *Canadian Journal of Fisheries and Aquatic Sciences*, 58, 1222-1243.

Juggins, S. J. (1992). Diatoms in the Thames estuary, England: ecology, paleoecology, and salinity transfer function. *Bibliotecha. Diatomologica*, 25. 216 pp.

Juggins, S.J.. (1997). Climate change and lake sediments in South East Russia and Southern Kazakhstan. INTAS Project No:b INTAS-93-1491.

Juggins, S.J. (2002). WinTran version 1.5., unpublished computer software.

Juggins, S.J. (2004). C2 version 1.4., unpublished computer software.

Kaushal, S. and Binford, M.W. (1999). Relationship between C/N ratios of lake sediment, organic matter sources, and historical deforestation in Lake Pleasant, Massachussetts, USA. *Journal of Paleolimnology*, 22, 439-442.

Kawabata, Y., Nakhara, H. and Katayama (1996). Diatoms of the Aral Sea Sediments. In: Mayama, S., Idei, M. and Koizumi (1999). *Proceedings of the fourteenth international diatom symposium*. Koeltz, Koenigstein.

Keeley, J. E., Sandquist, D.R. (1992). Carbon: freshwater plants. *Plant, Cell and Environment*, 15, 1021-1035.

Keigwin, L.D. (1996). The Little Ice Age and the Medieval Warm Period in the Sargasso Sea. *Science*, 274, 1504-1508.

Keigwin, L.D. and Pickert, R.S. (1999). Slope water current over the Laurentian Fan on interannual to millennial time scales. Science, 286, 520-523.

Kelly, P.M., (1979) Solar influence on North Atlantic MSL pressure. In: McCormac, B.M. and Seliga, T.A (eds.) *Solar-Terrestrial Influences on Weather and Climate*. Reidel, Dordrecht. pp. 297-298.

Kent, M. and P. Coker. (1996). *Vegetation Description and Analysis. A Practical Approach*. John Wiley and Sons, New York, USA. 363 pp.

Kes, A.S. (1995). Chronology of the Aral Sea and the Sub-Aral Region. *GeoJournal*, 35, 7-10.

Kiss, K. T., Coste, M., LeCohu, R. and Nausch, M. (1988). Cyclotella caspia (Bacillariophyceae) in some rivers and lakes in Europe: morphological observations. *Cryptogamie, Algologie*, 9, 27-42.

Kiss, K.T. and Genkal, S.I. (1993). Winter blooms of centric diatoms in the River Danube and in its side arms near Budapest. In. H. van Dam, (ed) *Twelfth International Diatom Symposium*. Kluwer Academic publishers. Hydrobiologia 269/270:317-326.

Klige, R.K., Hong, L., and Selivanov, A.O. (1996). Regime of the Aral Sea during historical time. *Water Resources*, 23/4, 375-380.

Klinger, Y., Avouac, J.P., Bourles, D. and Tisnerat, N. (2003). Alluvial deposition and lake level fluctuations forced by late Quaternary climatic change: the Dead Sea case example. *Sedimentary Geology* 162, 119-139.

Koinig, K.A., Schmidt, R., Sommeragu-Wograth, S., Tessadri, R. and Psenner, R. (1998). Climate change as the primary cause for pH shifts in a high alpine lake. *Water, Air and Soil Pollution*, 104, 167-180.

Kolbe, R.W. (1927), Zur okologie, morphologie, und systematic der brackwasser-diatomeen. *Pflanzenforschung*, 7, 1-146.

Korhola, A., Weckstrom, J., Holmstrom, L. and Erasto, P. (2000). A Quantitative Holocene Climatic Record from Diatoms in Northern Fennoscandia. *Quaternary Research*, 54/2, 284-294.

Koronkevick, N. (2002) Rivers, Lakes, Inland Seas and Wetlands. In: Shahgedanova, M. (ed.) *The Physical Geography of Northern Eurasia*. Oxford University Press.

Kouraev, A.V., Papa, F., Buharizin, P.I., Cazenave, A., Cretaux, J-F., Dozortseva, J. and Remy, F. (2003). Ice cover variability in the Caspian and Aral seas from active and passive microwave satellite data. *Polar Research*, 22/1, 43-50.

Kouraev, A.V., Papa, F., Mognard, N.M., Buharizin, P.I., Cazenave, A., Cretaux, J-F., Dozortseva, J. and Remy, F. (2004). Sea ice cover in the Caspian and Aral Seas from historical and satellite data. *Journal of Marine Systems*, 47, 89-106.

Kovach, W.L. (1995). Multivariate data analysis. In: Maddy, D. and Brew, J.S. (eds.) *Statistical Modelling of Quaternary Science Data*. Quaternary Research Association, Technical Guide No. 5, Cambridge. 1-36.

Krammer, K. and Lange-Bertalot, H., (1986-1991). Süßwasserflora von Mitteleuropa, vols. 2/1-2/4. Gustav Fischer Verlag, Stuttgart.

Kravtsova, V.I. (2001). Analysis of Changes in the Aral Sea Coastal Zone in 1975-1999. *Water Resources*, 28/6, 569-603.

Kreutz, K.J., Wake, C.P., Aizen, V.B., DeWayne, C.L. and Synal, H.A. (2003). Seasonal deuterium excess in a Tien Shan ice core: Influence of moisture transport and recycling in Central Asia. *Geophysical Research Letters*, 30/18, doi: 10.10/29/2003GL017896.

Krishnamurthy, R.V., Syrup, K.A., Baskaran, M., and Long, A., (1995). Late glacial climate record of midwestern United States from the hydrogen isotope ratio of lake organic matter. *Science*, 269, 1565–1567.

Labeyrie, L., Cole, J., Alverson, K. and Stocker, T. (2003). The History of Climate Dynamics in the Late Quaternary. In: Alverson, K.D., Bradley, R.S. and Pedersen, T.F. (eds.) *Palaeoclimate, Global Change and the Future*. Springer, Berlin.

Labitzke, K. and van Loon, H. (1988). Associations between the 11 year solar cycle and the atmosphere: I, the troposphere and the atmosphere in the northern winter. *Journal of Atmospheric and Terrestrial Sciences*, 50, 197-206.

Laird, K.R., Fritz, S.C. and Cumming, B.F. (1998). A diatom based reconstruction of drought intensity, duration and frequency from Moon Lake, North Dakota: a sub-decadal record of the last 2300 years. *Journal of Palaeolimnology*, 19, 161-179.

Lamb, A.L., Leng, M.J., Mohammed, M.U., Lamb, H.F. (2004). Holocene climate and vegetation change in the Main Ethopian Rift Valley, inferred from the composition (C/N and $\delta^{13}C$) of lacustrine organic matter. *Quaternary Science Reviews*, 23, 881-891.

Lamb, A.L., Wilson, G.P. and Leng, M.J. (2006). A review of coastal palaeoclimate and relative sea-level reconstructions using $\delta^{13}C$ and C/N ratios in organic material. *Earth Science Reviews*, 74, 29-57.

Lamb, H.H. (1965). The early medieval warm epoch and its sequel. *Palaeogeography, Palaeoclimatology and Palaeoecology*, 1, 13-37.

Lamb, H.H. (1970). Volcanic dust in the atmosphere: *Philosophical Transactions of the Royal Society of London*, series A, 266, no. 1178, 425-533.

Lamb, H.H. (1977). *Climate: Past, Present and Future. Volume 2, Climatic History and Future*. Methuen, London.

Landers, D.J., Gubala, C., Verta, M., Lucotte, M., Johannsson, K., Vlasova, T. and Lockhart, W.T. (1998). Using lake sediment mercury flux ratios to evaluate the regional and continental dimensions of mercury deposition in Arctic and boreal ecosystems. *Atmospheric Environment*, 32/5, 919-928.

Landsell, H. (1885). *Russian Central Asia*. Low, Marston, Searle and Rivington. London.

Lange, C.B. and Tiffany, M.A. (2002). The diatom flora of the Salton Sea, California. *Hydrobiologia* 473, 179-201.

Lara, A. and Villalba, R. (1993). A 3620 year temperature reconstruction from *Fitzroya cupressoides* tree rings in southern South America. *Science*, 260, 1104-1106.

Lean, J.L., Skumanich, A. and White, 0.R. (1992). Estimating the sun's radiative output during the Maunder Minimum. *Geophysical Research Letters*, 19, 1591-1594.

Lean, J.L. (2000). Evolution of the Sun's Spectral Irradiance Since the Maunder Minimum. *Geophysical Research Letters*, 27/16, 2425-2428.

Lean, J.L., Beer, J. and Bradley, R.S. (1995). Reconstruction of solar irradiance since AD 1600 and implications for climate change. *Geophysical Research Letters*, 22, 3195-3198.

Le Blanc, M., Gajewski, K. and Hamilton, P.B. (2004). A diatom-based Holocene palaeoenvironmental record from a mid-arctic lake on Boothia Peninsula, Nunavut, Canada. *The Holocene*, 14/4, 417-425.

Le Callonnec, L., Person, A., Renard, M., Letolle, R., Nebout, N., Ben Khelifa, L. and Rubanov, I. (2005). Preliminary data on chemical changes in the Aral Sea during low-level periods from the last 9000 years. *Comptes Rendus Geoscience*, 337, 1035-1044.

Lee, J. and Tallis, J. (1973). Regional and historical aspects of lead pollution in Britain. *Nature*, 245, 216-220.

Lemcke, G., Sturm, M., (1996). ^{18}O and trace element measurements as proxy for the reconstruction of climate changes at Lake Van (Turkey). In: Dalfes, H.N., Kukla, G., Weiss, H. (Eds.), *Third Millenium BC; Climate Change and Old World Collapse*. NATO ASI Series I, vol. 49. Springer Verlag, pp. 653-678.

Leng, M.J. (2003). Stable isotopes in lakes and lake sediment archives. In: Mackay, A.W., Battarbee, R.W., Birks, H.J.B. and Oldfield, F. (eds.) (2003). *Global Change in the Holocene*. Arnold, London 124-139.

Leng, M.J. and Marshall, J. (2004). Palaeoclimate interpretation of stable isotope data from lake sediment archives. *Quaternary Science Reviews*, 23, 811-831.

Leng, M.J., Metcalfe, S.E. and Davies, S.J. (2005). Investigating Late Holocene climate variability in central Mexico using carbon isotope ratios in organic materials and oxygen isotope ratios from diatom silica within lacustrine sediments. *Journal of Paleolimnology*, 34, 413-431.

Lepš, J. and Šmilauer, P. (2003). *Multivariate analysis of ecological data using CANOCO*. Cambridge University Press. Cambridge.

Lerman, A. (1979). *Lakes: Chemistry, Geology, Physics*. Springer-Verlag, New York.

Leroy, S.A.G., Marret, F., Giralt, S. and Bulatov, S.A. (2006). Natural and anthropogenic rapid changes in the Kara-Bogaz-Gol over the last two centuries reconstructed from palynological analyses and a comparison to instrumental records. *Quaternary International*, in press.

Letolle, R. (2000) Histoire de l' Ouzboi, cours fossil de l' Amou Darya: synthese et elements nouveaux. *Studia Irinaca*, 29/2, 195-240.

Letolle, R. and Mainguet, M. (1993). *Aral*. Springer –Verlag, Paris.

Letolle, R. and Mainguet, M. (1997). Histoire de la mer d'Aral (Asie centrale) depuis le dernier maximum glaciaire. *Bulletin Societe Geologique de France*, 168/3, 387-398.

Letolle R. and Chesterikoff, A. (2000). Salinity of surface waters in the Aral Sea region. *International Journal of Salt Lake Research*, 8, 293-306.

Letolle, R., Aladin, N., Filipov, I. and Boroffka, N.G.O. (2004). The future chemical evolution of the Aral Sea from 2000 to the years 2050. *Mitigation and Adaptation Strategies for Global Change*, 47/1-4, 81-92.

Létolle, R., Micklin. P., Aladin, N. and Plotnikov, I. (In review). Uzboy and the Aral regressions: a hydrological approach. *Geoarchaeology*.

Li, H-C. and Ku, T-L. (1997) $\delta^{13}C$ - $\delta^{18}O$ covariance as a paleohydrological indicator for closed-basin lakes. *Paleogeography, Paleoclimatology, Paleoecology*, 133, 69-80.

Linsley, B.K., Wellington, G.M and Schrag, D.P. (2000). Decadal sea surface temperature variability in the subtropical south pacific from 1726 to 1997 AD. *Science*, 290, 1145-1148.

Lioubimtseva, E. (2004). Arid Environments. In: Shahgedanova, M. (ed.) *The Physical Geography of Northern Eurasia*. Oxford University Press.

Lioubimtseva, E., Cole, R., Adams, J.M. and Kapustin, G., (2005). Impacts of climate and land-cover changes in arid lands of Central Asia. *Journal of Arid Environments*, 62, 285-308.

Liu, K-b., Yao, Z. and Thompson, L.G. (1998) A pollen record of Holocene climatic changes from the Dunde ice cap, Qinghai-Tibetan Plateau. *Geology*, 26/2, 135-138.

Lockhart, W. L., Macdonald, R. W., Outridge, P. M., Wilkinson, P., DeLaronde, J. B., and Rudd, J. W. M. (2000). Tests of the fidelity of lake sediment core records of mercury deposition to known histories of mercury contamination. *Science of the Total Environment*, 260, 171–180.

Luckman, B.H. and Villalba, R. (2001). Assessing the Synchroneity of Glacier Fluctuations in the Western Cordillera of the Americas During the Last Millenium. In: Markgraf., V. (ed.). *Interhemispheric Climate Linkages*. Academic Press, San Diego.

Lucke, A., Schleser, G.H., Zolitschka, B. and Negendank, J.F.W. (2003) A Lateglacial and Holocene organic carbon isotope record of lacustrine palaeoproductivity and climatic change derived from varved lake sediments of Lake Holzmaar, Germany. *Quaternary Science Reviews*, 22, 569-580.

Luterbacher, J. (2002). Extending North Atlantic Oscillation reconstructions back to 1500. *Atmospheric Science Letters*, 2, 114-124.

Luterbacher, J., Dietrich, D., Xoplaki, E., Grosjean, M. and Wanner, H. (2004). European Seasonal and Annual Temperature Variability, Trends and Extremes Since 1500. *Science*, 303, 1499-1503.

Lydolph, P.E. (1977). *Climates of the Soviet Union*. Elsevier Scientific Publishing. New York.

McDermott, F., Mattey, D.P. and Hawkesworth, C.J. (2001). Centennial-scale Holocene climate variability revealed by high-resolution speleothem $\delta^{18}O$ record from SW Ireland. *Science*, 294, 1328-1331.

Mackay, A.W., Battarbee, R.W., Birks, H.J.B. and Oldfield, F. (2003). *Global Change in the Holocene*. Arnold, London.

Mackay, A.W., Ryves, D.B., Battarbee, R.W. Flower, R.J., Jewson, D., Rioual, P. and Sturm, M. (2005) 1000 years of climate variability in Central Asia: assessing the evidence using Lake Baikal (Russia) diatom assemblages and the application of a diatom-inferred model of snow cover on the lake. *Global and Planetary Change*, 46, 281-297.

Maeda, H., Nakahara, H., Katayama, Y., Nishimura, K., Kawabata, Y. and Kakeda, T. (1996). Limnological features of lakes in Central Asia: Aral Sea and Lake Balkash. In: *Symposium of the Aral Sea and the Surrounding Region: Irrigated Agriculture and the Environment.* United Nations Environmental Programme (UNEP). Available online at: http://www.unep.or.jp/ietc/Publications/techpublications/TechPub-4/limno2-6.as

Maev, E. G., Karpychev, Yu, A., (1999). Radiocarbon dating of bottom sediments in the Aral Sea: Age deposits and sea level fluctuations. *Water Resources*, 26/2, 187-194.

Mainguet, M., Letolle, R. and Dumay, F. (2002). Le systeme regional d'action eolienne (SRAE) du basin de l'Aral (Kazakhstan, Ouzbekistan et Turkmenistan). *C.R. Geoscience*, 334, 475-480.

Mann, M.E., Bradley, R.S. and Hughes, M.K. (1998). Global scale temperature patterns and climate forcing over the past six centuries. *Nature*, 392, 779-787.

Mann, M. E., Bradley, R.S. and Hughes, M.K. (1999). Temperatures during the last millennium: Inferences, Uncertainties and Limitations. *Geophysical Research Letters*, 26, 759-762

Mann, M.E. and Jones, P.D. (2003). Global surface temperatures over the past two millennia. *Geophysical Research Letters*, 30/15.

Manrique, E. and Fernandez-Cancio, A. (2000). Extreme climatic events in dendroclimatic reconstructions from Spain. *Climatic Change*, 44, 123-138.

Martinez-Cortizas, A., X. Pontevedra-Pombal, J.C. Novoa-Munoz, and E. Garcia-Rodeja, (1997). Four thousand years of atmospheric Pb, Cd and Zn deposition recorded by the ombotrophic peat bog of Penido Vello (northwestern Spain). *Water Air Soil Pollution*, 100, 387-403.

Martinez-Cortizas, A., X. Pontevedra-Pombal, E. Garcia-Rodeja, J.C. Novoa-Munoz, and W. Shotyk, (1999). Mercury in a Spanish peat bog: archive of climate change and atmospheric metal deposition. *Science*, 284, 939-942.

Maslin, M.A., Pike, J., Stickley, C. and Ettwein, V. (2003). Evidence of Holocene Climate Variability in Marine Sediments. In: Mackay, A.W., Battarbee, R.W., Birks, H.J.B. and Oldfield, F. (eds.), *Global Change in the Holocene*. Arnold, London

Mauquoy D, van Geel, B., Blaauw, M. and van der Plicht, J. (2002). Evidence from northwest European bogs shows 'Little Ice Age' climatic changes driven by variations in solar activity. *The Holocene*, 12/1, 1-6.

Mayewski, P.A. and 16 others (2004). Holocene climate variability. *Quarternary Research*, 62, 243-255.

McKenzie, J.A., (1985). Carbon isotopes and productivity in the lacustrine and marine environment. In: Stumm, W., (ed.) *Chemical Processes in Lakes*. Wiley, New York.

Metzeltin, D. and Witkowski, A. (1996) *Diatomeen der Baren-Insel.* Koeltz, Konigstein.

Meyers, P.A., and Ishiwatari, R., (1993). Lacustrine organic geochemistry—An overview of indicators of organic matter sources and diagenesis in lake sediments. *Organic Geochemistry*, 20, 867–900.

Meyers, P.A., Lebo, M.E. and Reuter, J.E. (1998). Sedimentary record of sources and accumulation of organic matter in Pyramid Lake, Nevada over the past 1,000 years. *Limnology and Oceanography*, 43/1, 160-169.

Meyers, P.A. and Lallier-Verges, E. (1999). Lacustrine sedimentary organic matter records of Late Quaternary paleoclimates. *Journal of Paleolimnology*, 241, 345-372.

Meyers, P.A and Teranes, J.L. (2001). Sediment organic matter. In: Last, W.M. and Smol, J.P. (eds.) *Tracking Environmental Change Using Lake Sediments. Volume 2, Physical and Geochemical Methods.* Kluwer, Dortrecht. 239-269.

Mirabdullayev, I.M., Joldasova, I.M., Mustafaeva, Z.A., Kazakhbaev, S., Lyubimova, S.A. and Tashmukhamedov, B.A. (2004). Succession of the ecosystems of the Aral Sea during its transition from oligohaline to polyhaline waterbody. *Journal of Marine Systems*, 47, 101-107.

Mokhov, I.I. and Khon, V. Ch. (2004). Atmospheric centres of action: changes from observations and simulations. *Geophysical Research Abstracts*, Vol 6, 05942.

Monna, F., Dominik, J., Loizeau, J.-L., Pardos M and Arpagaus P. (1999) Origin and evolution of Pb in sediments of lake Geneva (Switzerland-France) – Stable Pb record. *Environment Science and Technology*, 33, 2850–7.

Mook, W.G., Bommerson, J.C., Staverman, W.H. (1974). Carbon isotope fractionation between dissolved bicarbonate and gaseous carbon dioxide. *Earth and Planetary Science Letters*, 22, 169-176.

Moore, J.J., Hughen, K.A., Miller, G.H. and Overpeck, J.T. (2001). Little Ice Age recorded in summer temperature reconstruction from varved sediments of Donard Lake, Baffin Island, Canada. *Journal of Paleolimnology*, 25, 503-517.

Muller, A. and Mathesius, U. (1999). The palaeoenvironments of coastal lagoons in the southern Baltic Sea, 1. The application of sedimentary C_{org}/N ratios as source indicators of organic matter. *Paleogeography, Paleoclimatology, Paleoecology*, 145, 1-16.

Nalivkin, D. V. (1973). *Geology of the U.S.S.R.* Oliver & Boyd, Edinburgh, 877 pp.

Narama, C. (2002). Late Holocene variation of the Riagorodskogo Glacier and climate change in the Pamir-Alai, Central Asia. *Catena*, 48, 21-37.

Nesje, A. and Dahl, S.O. (2003). The 'Little Ice Age' – only temperature? *The Holocene*, 13/1, 139-145.

Nezlin, N.P., Kostianoy, A.G. and Lebedev, S.A. (2004). Interannual variations of the discharge of the Amu Darya and Syr Darya estimated from global atmospheric precipitation. *Journal of Marine Systems*, 47, 57-65.

Ni, A., Nurtaev, B., Petrov, M., Tikhanovskaya, A. and Tomashevskaya, I. (2004). The share of a glacial feeding in water balance of the Aral Sea and Karakul Lake. *Journal of Marine Systems*, 47, 143-146.

Ninglian, W., Thompsom, L.G., Davis, M.E., Mosley-Thompson, E., Tandong, Y. and Jianshen, P. (2003). Influence of variations in NAO and SO on air temperatures over the north Tibetan Plateau as measured by $\delta^{18}O$ in the Malan Ice Cap. Geophysical Research Letters, 30/22, doi:10.1029/2003GL018188.

Norton, S.A., Biernet, R.W., Bindford, M.W. and Kahl, J.S. (1992). Stratigraphy of total metals in PIRLA sediment cores. *Journal of Paleolimnology*, 7, 191-314.

Nourgaliev, D.K., Heller, F., Borisov, A.S., Hajdas, I., Bonani, G., Iassonov, P.G., Oberhänsli, H., (2003). Very high resolution paleosecular variation record for the last 1200 years from the Aral Sea. *Geophysical Research Letters* 30/17, 41-44.

Nordic Council of Ministers. (2003). Cadmium Review. Available online at: www.norden.org/miljoe/uk/NMR_cadmium.pdf

Nriagu, J.O. (1979). Global inventory of natural and anthropogenic emissions of trace metals to the atmosphere. *Nature*, 279, 409-411.

Nriagu, J.O. (1996). A history of global metal pollution. *Science*, 272, 223-224.

Nriagu, J. O., Wong, H. K. T. and Coker, R.D. (1982). Deposition and chemistry of particulate metals in lakes around the smelters at Sudbury, Ontario. *Environment Science and Technology*, 16, 551-560

Nriagu, J.O. and Pacyna, J.M. (1988). Quantitative assessment of worldwide contamination of air, water and soils by trace metals. *Nature*, 333, 134-139.

Nurtaev, B. (2004). Aral Sea basin evolution: geodynamic aspect. In: Nihoul, J.C.J., Zavialov, P.O. and Micklin, P.P (eds.). *Dying and dead seas: climatic versus anthropic causes: proceedings of the NATO Advanced Research Workshop, Liège, Belgium, 7-10 May, 2003. Nato Science Series: 4. Earth and Environmental Sciences,* 36: pp. 91-97

O'Brien, S.R., Mayewski, P.A., Meeker, L.D., Meese, D.A., Twickler, M.S. and Whitlow, S.I. (1995) Complexity of Holocene climate as reconstructed from a Greenland ice core. *Science*, 270, 1962-1964.

O'Hara, S.L., Wiggs, G.F.S., Mamedov, B., Davidson, G. and Hubbard, R.B. (2000). Exposure to airborne dust contaminated with pesticide in the Aral Sea region. *The Lancet*, 355, 627-628.

O'Leary, M.H. (1981). Carbon fractionation in plants. *Phytochemistry*, 20, 553-567.

O'Sullivan, P.E., Moyeed, R., Cooper, M.C. and Nicholson, M.J. (2002). Comparison between instrumental, observational and high resolution proxy sedimentary records of Late Holocene climatic change – a discussion of possibilities. *Quaternary International*, 88, 27-44.

Ogilvie, A.E.J. and Jonsson, T. (2001a) "Little Ice Age" Research: A Perspective from Iceland. *Climatic Change*, 48/1, 9-52.

Ogilvie, A.E.J. and Jonsson, T. (2001b). The Iceberg in the Mist: Northern Research in Pursuit of a "Little Ice Age". *Climatic Change*, 48/1, 1-272.

Oldfield, F., Wake, R., Boyle, J., Jones, R., Nolan, S., Gibbs, Z., Appleby, P., Fisher, E. and Wolff, G. (2003). The late Holocene history of Gormire Lake (NE England) and its catchment: a multiproxy reconstruction of human impact. *The Holocene*, 13/5, 677-690.

Oreshkin, V.N. Khaitov, I.G. and Rubanov, I.V. (1993). Cadmium in the bottom sediments of the Aral Sea. *Water Resources*, 20/3, 376-379.

Orlova, M.I. and Rusakova, O.M. (1999). Characteristics of coastal phytoplankton near Cape Tastubec (northern Aral Sea), September 1993. *International Journal of Salt Lake Research*, 8, 7-18.

Osborn, T.J. and Briffa, K.R. (2006) The spatial extent of 20th century warmth in the context of the past 1200 years. *Science*, 311, 841-844.

Outridge, P.M., Hermanson, M.H. and Lockhart, W.L. (2002). Regional variations in atmospheric deposition and sources of anthropogenic lead in lake sediments across the Canadian Arctic. *Geochimica et Cosmochimica Acta*, 66, 3521-3531.

Outridge, P.M., Stern, G.A., Hamilton, P.B., Percival, J.B., McNeely, R. and Lockhart, W.L. (2005). Trace metal profiles in the varved sediment of an Arctic lake. *Geochimica et Cosmochimica Acta*, 69, 4881-4894.

Overpeck, J. and 16 others (1997). Arctic Environmental Change of the Last Four Centuries. *Science*, 278, 1251-1256.

Pacyna, J.M. and Pacyna, E.G. (2001) An assessment of global and regional emissions of trace metals to the atmosphere from anthropogenic sources worldwide. *Environmental Review*, 9, 269-298.

Passell, H. and 16 others (2003). The Navruz project: Transboundary Monitoring for Radionuclides and Metals in Central Asian Rivers. Data Report available online at: http://ironside.sandia.gov/Central/reports/SAND2003-1149.pdf

Paulsen D.E., Li, H-c and Ku, T-l (2003). Climate variability in central China over the last 1270 years revealed by high-resolution stalagmite records. *Quarternary Science Reviews*, 22, 691-702.

Peneva, E.L., Stanev, E.V., Stanychni, S.V., Salokhiddinov, A. and Stulina, G. (2004). The recent evolution of the Aral Sea level and water properties: analysis of satellite, gague and hydrometeorological data. *Journal of Marine Systems*, 47, 11-24.

Pfister, C. (1995). Monthly temperature and precipitation in central Europe from 1525-1979: quantifying documentary evidence on weather and its effects. In: Bradley, R.S. and Jones, P.D. (1995) *Climate since 1500 AD*. Routledge, London.

Pienitz, R., Smol, J.P. and Birks, H.J.B. (1995). Assessment of freshwater diatoms as quantitative indicators of past climatic change in the Yukon and Northwest Territories. *Journal of Paleolimnology*, 13, 21-49.

Pisas, N., Dauphin, J.P. and Sancetta, R. (1973). Spectral analysis of late Pleistocene-Holocene sediments. *Quarternary Research*, 3, 3-9.

Porter, S.C. (1986). Pattern and forcing of the Northern Hemisphere glacier variations during the last millennium. *Quaternary Research*, 26, 27-48.

Prasad, A.K.. and Nienow, J.A., (2006). The centric diatom genus *Cyclotella* (Stephanodiscaceae: Bacillariaophyta) from Florida Bay, USA, with special reference to *Cyclotella choctawhatcheeana* and *Cyclotella desikacharyi* a new marine species related to the *Cyclotella striata* complex. *Phycologia*, 45(2), 127-140.

Prasad, A.K., Nienow, J.A. and Livingston, J.R. (1990). The genus *Cyclotella* (Bacillariophyta) in Choctawhatchee Bay, Florida, with special reference to *C. striata* and *C. choctawhatcheeana* sp. nov. *Phycologia* 29, 418-436.

Psenner, R and Schmidt, R. (1992). Climate driven pH control of remote alpine lakes and effects of acid deposition. *Nature*, 356, 781-783.

Procter, C.J., Baker, A., Barnes, W.L. and Gilmour, M.A. (2000). A thousand year speleothem proxy record of North Atlantic climate from Scotland. *Climate Dynamics*, 16, 815-820.

Quinn, T.M., Crowley, T.J., Taylor, F.W., Henin, C., Joannot, P. and Yoin, Y. (1998). A multicentury stable isotope record from a New Caledonia coral: interannual and decadal sea surface temperature variability in the southwest Pacific since 1657 AD. *Paleoceanography*, 13, 412-426.

Racca, J.M.J. and Prairie, Y.T. (2004). Apparent and real bias in numerical transfer functions in palaeolimnology. *Journal of Paleolimnology* 31, 117-124.

Rasmussen, P.E., (1994). Current methods of estimating atmospheric mercury fluxes in remote areas. *Environment Science and Technology*, 28/18, 2233-2241.

Raynaud, D., Chappellaz, J., Ritz, C. and Martinerie, P. 1997. Air content along the Greenland ice core. A record of surface climatic parameters and elevation in central Greenland. *Journal of Geophysical Research*, 102, 26607-26614.

Reed, J. M., (1995). *The potential of diatoms and other palaeolimnological indicators for Holocene palaeoclimate reconstruction from Spanish salt lakes, with special reference to the Laguna de Medina (Cádiz, southwest Spain).* PhD thesis, University College London.

Reed, J.M. (1998). A diatom conductivity-transfer function for Spanish salt lakes. *Journal of Paleolimnology*, 19, 339-416.

Reid, G.C., (1987). Influence of solar variability on global sea surface temperatures. *Nature*, 329, 142-143.

Reid, G.C. (1997a). The sun-climate connection: a challenge to conventional wisdom? *Climatic Change*, 37, 387-390.

Reid, G.C. (1997b). Solar forcing of global climatic change since the mid-17th century. *Climatic Change*, 37, 391-405.

Reid, G.C. (2000). Solar variability and the earth's climate: introduction and overview. *Space Science Reviews*, 94, 1-11.

Renberg, I., Persson, M.W. and Emteryd, O. (1994). Pre Industrial atmospheric lead contamination detected in Swedish lake sediments. *Nature* 368, 323-326.

Renberg, I., Brännvall, M.-L., Bindler, R., Emteryd, O. (2002). Stable lead isotope analyses and lake sediments - a useful combination for the study of atmospheric lead pollution history. *Science of the Total Environment*, 292, 45-54.

R. D. Ricketts, T. C. Johnson, E. T. Brown, K. A. Rasmussen, and V. V. Romanovsky, (2001). Trace element and stable isotope study of the Holocene paleoclimate of Lake Issyk-Kul. *Palaeogeography, Palaeoclimatology, Palaeoecology*, 176, 207-227.

Ridame C. and Guieu C. (2002). Saharan input of phosphorus to the oligotrophic water of the open western Mediterranean, *Limnology and Oceanography*, 47/3, 856-869.

Rind, D. (2002). The sun's role in climate variations. *Science*, 296, 673-677.

Roberts, D and McMinn, A, (1998). A weighted-averaging regression and calibration model for inferring lakewater salinity from fossil diatom assemblages in saline lakes of the Vestfold Hills: a new tool for interpreting Holocene lake histories in Antarctica. *Journal of Paleolimnology*, 19/1, 99-113.

Robock, A. (2000). Volcanic eruptions and climate. *Reviews of Geophysics*, 38, 191-219.

Robock, A and Mao, J. (1992). Winter warming from large volcanic eruptions. *Geophysical Research Letters*, 19, 2405-2408.

Romashkin, V.S. and Samoilenko, V.S. (1953). Hydrometeorological characteristics of the Aral Sea. *Trudy GOIN*, 12, 98-129.

Rognerud, S. and Fjeld, E. (2001). Trace Element Contamination of Norwegian Lake Sediments. *Ambio*, 30: 11-19.

Rosen, P., Hall., R., Korsman, T. and Renberg, I. (2000). Diatom transfer-functions for quantifying past air temperature, pH and total organic carbon concentrations from lakes in Northern Sweden. *Journal of Paleolimnology*, 24, 109-123.

Ruddiman, W.F. (2003). The anthropogenic greenhouse era began thousands of years ago. *Climatic Change*, 61, 261-293.

Ruddiman, W.F., Vavrus, S.J. and Kutzbach, J.E. (2005). A test of the overdue-glaciation hypothesis. *Quaternary Science Reviews*, 24, 1-10.

Rusakova, O.M. (1995). Brief characteristics of the qualitative content of phytoplankton of the Aral Sea during Spring and Autumn 1992. *Proceedings of the Zoological Institute, Russian Academy of Science*, 262 (1), 195-207 [in Russian]

Ryves, D.B. (1994). *Diatom dissolution in saline lake sediments; an experimental study in the Great Plains of North America*. PhD thesis, University of London.

Ryves, D.B., Juggins, S., Fritz, S.C. & Battarbee, R.W. (2001). Experimental diatom dissolution and the quantification of microfossil preservation in sediments, *Palaeogeography, Palaeoclimatology, Palaeoecology*, 172, 99-113.

Ryves, D.B., McGowan, S. and Anderson, N.J. (2002) Development and evaluation of a diatom-conductivity model from lakes in West Greenland. *Freshwater Biology*, 47, 995-1014.

Safunda, J., Cermak, V. and Bordi, L. (1997). Climate history inferred from borehole temperatures, data from the Czech Republic. *Surveys in Geophysics*, 18, 192-212.

Saiko, T.A. and Zonn, I.S. (2000). Irrigation expansion and dynamics of desertification in the Circum-Aral region of Central Asia. *Applied Geography*, 20, 349-367.

Sakalys J and Kvietkus K. (2002). Lifetime of gaseous and particulate mercury in the atmosphere. *Environmental Chemistry and Physics*, 24, 191-195.

Salokhiddinnov, A.T. and Khakimov, Z.M. (2004). Ways the Aral Sea behaves. *Journal of Marine Systems*, 47, 127-136.

Sampei, Y., and Matsumoto, E. (2001). C/N ratios in a sediment core from Nakaumi Lagoon, Southwest Japan—Usefulness as an organic source indicator. *Geochemical Journal*, 35, 189–205.

Savoskul, O.S. (1997). Modern and Little Ice Age glaciers in 'humid' and 'arid' areas of the Tien Shan, Central Asia: two different patterns of fluctuation. *Annals of Glaciology*, 24, 142-148.

Savoskul, O.S. and Solomina, O.N. (1996) Late Holocene glacier variations in the frontal and inner ranges of the Tien Shan, Central Asia. *The Holocene*, 6/1, 25-35.

Schettler, G. and Romer, R.L. (2006). Atmospheric Pb pollution by pre-medieval mining detected in the sediments of the brackish karst lake An Loch Mor, western Ireland. *Applied Geochemistry*, 21, 58-82.

Schilman, B., Bar-Matthews, M., Almogi-Laban, A. and Luz, B. (2001). Global climate instability reflected by Eastern Mediterranean marine records during the late Holocene. *Palaeogeography, Palaeoclimatology, Palaeoecology*, 176, 157-176.

Schilman, B., Ayalon, A., Bar-Matthews, M., Kagan, E.J., Almogi-Labin, A., (2002). Sea–land palaeoclimate correlation in the Eastern Mediterranean region during the Late Holocene. *Israel Journal of Earth Sciences*, 51, 181-190.

Schmidt, G.A., Shindell, D.T., Miller, R.L., Mann, M.E. and Rind, D. (2004). General circulation modelling of Holocene climate variability. *Quarternary Science Reviews*, 23, 2167-2181.

Seigneur, C., Lohman, K., Vijayaraghavan, K. and Shia, R-L. (2003). Contributions of global and regional sources to mercury deposition in New York State. *Environmental Pollution*, 123, 365-373.

Serebryanny, L.R. and Solomina, O.N. (1996). Glaciers and climates of the mountains of the former USSR during the Neoglacial. *Mountain Research and Development*, 16/2, 157-166.

Servant-Vildary, S. and Roux, M. (1990). Multivariate analysis of diatoms and water chemistry in Bolivian saline lakes. *Hydrobiologia* 197, 267-290.

Settle, D.M. and Patterson, C.C. (1980). Lead in Albacore: Guide to lead pollution in Ameriacns. *Science*, 207, 1167-1176.

Shermatov, E., Nurtayev, B., Muhamedgalieva, U. and Shermatov, U. (2004). Analysis of water resources variability of the Caspian and Aral sea basins on the basis of solar activity. *Journal of Marine Systems*, 47, 137-142.

Shindell, D.T., Schmidt, G.A., Mann, M.E., Rind, D. and Waple, A. (2001). Solar forcing of regional climate during the Maunder Minimum. *Science*, 294, 2149-2152.

Shotyk, W., Weiss, D., Appleby, P.G., Cheburkin, A.K., Frei, R., Gloor, M., Krammers J.D., Reese S and van der Knaap W.O. (1998) History of atmospheric lead deposition since 12,370 ^{14}C yr BP from a peat bog, Jura Mountains, Switzerland. *Science*, 281,1635–1640.

Simonsen, R. (1962). Untersuchungen zur Systematik und Ökologie der Bodendiatomeen der westlichen Ostsee. *Int. Rev. Gesamten Hydrobiol., Syst. Beih.* 1, 1-144.

Singer, A., Zobeck, T., Poberezsky, L. and Argaman, E. (2003). The PM_{10} and $PM_{2.5}$ dust generation potential of soils/sediments in the Southern Aral Sea Basin, Uzbekistan. *Journal of Arid Environments*, 54, 705-728.

Sirjacobs, D., Gregoire, M., Delhez, E. and Nihoul, J.C.J. (2004). Influence of the Aral Sea negative water balance on its seasonal circulation patterns: use of a 3D hydrodynamic model. *Journal of Marine Systems*, 47, 51-66.

Small, E.E., Giorgi, F., Sloan, L.C. and Hostetler, S. (2001a). The effects of desiccation and climatic change on the hydrology of the Aral Sea. *Journal of Climate*, 14, 300-323.

Small, E.E., Sloan, L.C. and Nychka, D. (2001b). Changes in surface temperature caused by desiccation of the Aral Sea. *Journal of Climate*, 14, 285-300.

Smith, B.N. and S. Epstein. (1971). Two categories of $^{13}C/^{12}C$ ratios for higher plants. *Plant Physiology*, 47: 380-384.

Smith, I.R. (2002). Diatom based Holocene palaeoenvoronmental records from continental sites on northeastern Ellesmere Island, high Arctic, Canada. *Journal of Palaeolimnology*, 27, 9-28.

Smol, J.P. (1988). Paleoclimate proxy data from freshwater arctic diatoms. *Verh. Internat. Verein. Limnol.* 23, 837-844.

Snoeijs, P. (ed.) (1996). *Intercalibration and distribution of diatom species in the Baltic Sea.* Opulus, Upsala

Solomina, O.N., Savoskul, O.S. and Cherkinsky, A.E. (1994). Glacier variations, mudflow activity and landscape development in the Aksay Valley (Tien Shan) during the late Holocene. *The Holocene*, 4/1, 25-31.

Solomina, O.S. and Alverson, K. (2004). High latitude Eurasian paleoenvironments: introduction and synthesis. *Palaeogeagraphy, Palaeoclimatology, Palaeoecology*, 209, 1-18.

Sommergau-Wograth, S. Koinig, K.A., Schmidt, R. Sommergau, R., Tessadri, R. and Psenner, R. (1997). Temperature effects on the acidity of remote alpine lakes. *Nature*, 387, 64-67.

Soon, W. and Baliunas, S. (2003) Proxy environmental climatic changes of the past 1000 years. *Climate Research*, 23, 89-110.

Sorrel, P., Popescu, S.-M., Head, M.J., Suc, J.P., Klotz, S., Oberhänsli, H. (2006). Hydrographic development of the Aral Sea during the last 2000 years based on a quantitative analysis of dinoflagellate cysts. *Palaeogeography, Palaeoclimatology and Palaeoecology*, **234**, 304 – 327.

Sorrel, P., Popescu, S.P., Klotz, S., Suc, J-P. and Oberhänsli, H. (In review). Climate variability in the Aral Sea Basin (Central Asia) during the late Holocene based on vegetation changes.

Sorrel, P., Oberhänsli, H., Boroffka, N., Nourgaliev, D., Dulski, P. and Rohl, U. (In review). Control of wind dynamics in the Aral Sea Basin during the late Holocene

Stager, J.C., Cumming, B. and Meeker, L. (1997). A high-resolution 11,400-Yr diatom record from Lake Victoria, East Africa. *Quaternary Research*, 47, 81-89.

Stahle, D.W., Cleaveland, M.K., Banton, D.B., Therrell, M.D. and Gay, D.A. (1998). The lost colony and the Jamestown droughts. *Science*, 280,564-567.

Steig E. J, E. J. Brook, J. W. C. White (1998). Synchronous climate changes in Antarctica and the North Atlantic. *Science* 282, 92-95.

Stevens, L.R., Stone, J.R., Campbell, J. and Fritz, S.C. (2006). A 2200-yr record of hydrologic variability from Lake Foy, Montana, USA, inferred from diatom and geochemical data. *Quaternary Research*, 65, 264-274.

Stine, S. (1994). Extreme and persistent drought in California and Patagonia during medieval time. *Nature*, 369, 546-549.

Stoermer, E.F. and Smol, J.P. (1999) *The Diatoms: Applications for the Environmental and Earth Sciences*. Cambridge.

Stone, J.R. and Fritz, S.C., (2004). Three-dimensional modelling of lacustrine diatom habitat areas: improving paleolimnological interpretation of planktic:benthic ratios. *Limnology and Oceanography*, 49/5, 1540-1548.

Stott, P.A., Tett, S.F.B., Jones, G.S.M Allen, M.R., Ingram, W.J. and Mitchell, J.F.B. (2001). Attribution of twentieth century climate change to natural and anthropogenic causes. *Climate Dynamics*, 17, 1-21.

Street-Perrott, F.A., Holmes, J.A., Waller, M.P., Allen, M.J., Barber, N.G.H., Fothergill, P.A., Harkness, D.D., Ivanovich, M., Kroon, D. and Perrott, R.A. (2000). Drought and dust deposition in the West African Sahel: a 5500-year record from Kajemarum Oasis, northeastern Nigeria. *The Holocene*, 10/3, 293-302.

Stuiver, M. (1965). Carbon-14 content of 18^{th} and 19^{th} century wood: Variations correlated with sun spot activity. *Science*, 149, 533-534.

Stuiver, M. and Quay, P.D. (1980). Changes in atmospheric carbon-14 attributed to a variable sun. *Science*, 207, 11-19.

Stuiver, M. and Braziunas, T.F. (1993). Sun, ocean and climatic $^{14}CO_2$: an evaluation of causal and spectral relationships. *The Holocene*, 3, 289-305.

Stuiver, M., Grootes, P.M., Braziunas, T.F. (1995) The GISP2 δ18O record of the past 16,5000 years and the role of the sun, ocean and volcanoes. *Quaternary Research*, 44, 341-354.

Tapia, P.M., Fritz, S.C., Baker, P.A., Seltzer, G.O. and Dunbar, R.B., (2003). A late Quaternary diatom record of tropical climatic history from Lake Titicaca (Peru and Bolivia). *Palaeogeography, Palaeoclimatology, Palaeoecology*, 194, 139-164.

Telford, R.J., Heegard, E and Birks, H.J.B. (2004). All age-depth models are wrong, but how badly? *Quaternary Science Reviews*, 23, 1-5.

Ter Braak, C.J.F. (1995). Ordination. In: Jonghman, R.G.H. Ter Braak, C.J.F. and van Tongeren, O.F.R (eds.). *Data Analysis in Landscape and Community Ecology*. Cambridge University Press. Cambridge. 91-174.

Ter Braak, C.J.F. and Juggins, S. (1993). Weighted averaging partial least squares regression (WA-PLS): an improved method for reconstructing environmental variables from species assemblages. *Hydrobiologia*, 269/270, 485-502.

Ter Braak, C.J.F. and Smilauer, P. (2002). CANOCO for Windows 4.5. Biometrics, The Netherlands.

Ter Braak, C.J.F. and Smilauer, P. (2002). CANOCO reference manual and user's guide to Canoco for Windows: software for Canonical Community Ordination version 4.5. Microcomputer Power, Ithica, NY.

Ter Braak, C.J.F. and Looman, C.W.N. (1999). Regression. In: JongHman, R.H.G., Ter Braak, C.J.F. and van Tongeren, O.F.R. *Data Analysis in Community and Landscape Ecology*. Cambridge University Press.

Thomas, R.L., (1972). The distribution of mercury in the sediments of Lake Ontario. *Canadian Journal of Earth Sciences*, 9, 636-651.

Thompson, D.W.J., and Wallace, J.M. (1998). The Arctic Oscillation signature in the wintertime geopotential height and temperature fields. *Geophysical Research Letters* 25, 1297-1300.

Thompson, D.W.J., Baldwin, M.P. and Wallace, J.M. (2002). Stratospheric connection to Northern Hemisphere wintertime weather: implications for prediction. *Journal of Climate*, 15, 1421-1442.

Thompson, L.G., Mosley-Thompson, E., Bolzan, J.F. and Koci, B.R. (1985). A 1500-Year Record of Tropical Precipitation in Ice Cores from the Quelccaya Ice Cap, Peru. *Science*, 229, 971-973.

Thompson, L.G., Mosley-Thompson, Dansgaard, W. and Grootes, P.M. (1986). The Little Ice Age as Recorded in the Stratigraphy of the Tropical Quelccaya Ice Cap. *Science*, 234, 361-364.

Thompson, L.G., Davis, M.E., Mosley-Thompson, E. and Liu, K-b (1988). Pre-Incan agricultural activity recorded in dust layers in two tropical ice cores. *Nature*, 336, 763-765.

Thompson, L.G., Mosley-Thompson, E., Davis, M.E., Lin, P.N., Dai, J. and Bolzan, J.F. (1995). A 1000 year climate ice-core record from the Guliya ice cap, China: its relationship to global climate variability. *Annals of Glaciology*, 21, 175-181.

Thompson, L.G. and 10 others (2002) Kilimanjaro Ice Core Rescords: Evidence of Holocene Climate Change in the Tropics. *Science*, 298, 589-593.

Tillo, A.A. (1877). *Description of Aral-Caspian Levelling Performed in 1874 at Request of the Russian Geographic Society and its Orenberg Division*. Russian Geographic Society, St Petersburgh.

Todd, M.C. and Mackay, A.W. (2003). Large-scale climatic controls on Lake Baikal ice cover. *Journal of Climate*, 16, 3186-3199.

Travnikov, O. and Ryaboshapko, A. (2002). Modelling of Mercury Hemispheric Transport and Depositions. MSC-E Technical Report 6/2002. Available online at: http://www.msceast.org/publications.html#2002

Tsvetsinskaya, E.A., Vainberg, B.I. and Glushko, E.V. (2002).An intergrated assessment of landscape evolution, long-term climate variability, and land use in the Amu Darya Prisarykamysh delta. *Journal of Arid Environments*, 51, 363-381.

Trefry, K.H., Metz, S., Trocine, R.P. and Nelsen, T.A. (1985). A decline in lead transport by the Mississippi River. *Science*, 230, 439-441.

Treydte, K.S., Schleser, G.H., Helle, G., Frank, D.C., Winiger, M., Haug, G.H. and Esper, J. (2006). The twentieth century was the wettest period on northern Pakistan over the past millennium. *Nature*, 220, 1179-1182.

Tyson, P.D. and Lindesay, J.A. (1992). The climate of the last 2000 years in southern Africa. *The Holocene*, 2, 271-278.

Tyson, R. V. (1995). *Sedimentary organic matter*. Chapman and Hall, London.

UNEP (2002). Global Mercury Assessment. Available online at: www.unep.org/gc/gc22/Document/UNEP-GC22-INF3.pdf

Urban, F.E., Cole, J.E., and Overpeck, J.T. (2000). Influence of mean climate change on climate variability from a 155-year tropical Pacific coral record. *Nature*, 407, 986-993.

Valero-Garces, B.L., Delgado-Huertas, A., Ratto, N., Navas, A. and Edwards, L. (2000). Paleohydrology of Andean saline lakes from sedimentological and isotopic records, Northwestern Argentina. *Journal of Paleolimnology*, 24, 343-359.

Verschuren, D., Laird, K.R. and Cumming, B.F. (2000) Rainfall and drought in equatorial east Africa during the past 1,100 years. *Nature*, 403, 408-413.

Verta, M., Tolonen, K. and Simola, H. (1989). History of heavy metal pollution in Finland as recorded by lake sediments. *Science of the Total Environment*, 87/88, 1-18.

Villalba, R. (1994). Tree ring and glacial evidence for the medieval warm epoch and the Little Ice Age in southern South America. *Climatic Change*, 26, 183-197.

Villalba, R., Boninsenga, J.A., Lara, A., Velben, T.T., Roig, F.A., Arvena, J-C. and Ripalta, A. (1996). Interdecadal climatic variations in millennial temperature reconstructions from southern South America. In: Jones, P.D., Bradley, R.S. and Jouzel, J. (eds.), *Climate Variations and Forcing Mechanisms of the Last 2000 Years*. Springer, Berlin, pp 161-189.

Visbeck, M.H., Hurrell, J.W., Polvnavl, L. and Cullen, H.M. (2001). The North Atlantic Oscillation: Past, present and future. *Proceedings of the National Academy of Sciences*, 98, 12876-12877.

Vos, P.C. and de Wolf, H. (1993). Diatoms as a tool for reconstructing sedimentary environments in coastal wetlands; methodological aspects. *Hydrobiologia*, 269-270/1, 285-286.

Walter, H. and Box, O.E. (1983). Middle Asia Deserts. In: West, N. (ed.), *Temperate deserts and semi-deserts, Ecosystems of the World, Vol. 5*. Elsevier Scientific Publishers, Amsterdam.

Wang, Y., Cheng, H., Edwards, R.L., He, Y., Kong, X., An, Z., Wu, J., Kelly, M.J., Dykoski, C.A. and Li, X. (2005). The Holocene Asian monsoon: Links to solar changes and North Atlantic climate. *Science* 308: 854-857.

Weckstrom, J., Korhola, A., Erasto, P. and Holmstrom (2006). Temperature patterns over the past eight centuries in Northern Fennoscandia inferred from sedimentary diatoms. *Quaternary Research*, in press.

Wedepohl, K.H. (1995) The composition of the continental crust. *Geochimica et Cosmochimica Acta*, 59, 1217-1232.

Wetzel, R.G. (2001) *Limnology: Lake and River Ecosystems*. Academic press, San Diego.

Wickman, F.E., (1952), Variation in the relative abundance of carbon isotopes in plants, *Geochimica et Cosmochimica Acta*, 2, 243–254.

Widmann, M., and Tett, S.F.B. (2003). Simulating the climate of the last millennium. *Pages Newsletter*, 11, 2/3, 21-23.

Wilderman, C.C. (1987). Patterns of distribution of diatom assemblages along environmental gradients in the Severn River Estuary, Chesapeake Bay, Maryland. *Journal of Phycology* 23, 209-217.

Wiles, G.C. and Calkin, P.E. (1994). Late Holocene, high resolution glacial chronologies and climate, Kenai Mountains, Alaska. *Geological Society of America Bulletin*, 106, 281-303,

Wiles, G.C., Post, A., Muller, E.H. and Molina, B.F. (1999). Dendrochronology and late Holocene history of Bering Piedmont Glacier, Alaska. *Quarternary Research*, 52, 185-195.

Williams, P.W., Marshall, A., Ford, D.C. and Jenkinson, A.V. (1999). Palaeoclimatic interpretation of stable isotope data from Holocene speleothems of the Waitomo district, North Island, New Zealand. *The Holocene*, 9/6, 649-657.

Williams, W.D. (1981). Inland salt lakes: An introduction. *Hydrobiologia*, 81, 1-14.

Williams, W.D. and Sherwood, J.E. (1994). Definition and measurement of salinity in salt lakes. *International Journal of Salt Lake Research*. 3, 53-63.

Willson, R.C. (1997). Total solar irradiance trend over cycles 21 and 22. *Science*, 277, 1963-1965.

Willson, R.C. and Hudson, H.S. (1991). The sun's luminosity over a complete solar cycle. *Nature*, 351, 42-44.

Wilson, A.T., Hendy, C.H. and Reynolds, C.P. (1979). Short term climate change and New Zealand temperatures during the last millennium. *Nature*, 279, 315-317.

Wilson, S.E., .Cumming, B.F., and Smol, J.P. (1996). Assessing the reliability of salinity inference models from diatom assemblages: An examination of a 219 lake data set from Western North America. *Canadian Journal of Fisheries and Aquatic Sciences* 53, 1580-1594.

Winkels, H.J., Kroonenberg, S.B., Lychagin, M.Y., Marin, G., Rusakov, G.V. and Kasimov, N.S. (1998). Geochronology of priority pollutants in sedimentation zones of the Volga and Danube delta in comparison with the Rhine delta. *Applied Geochemistry*, 13/5, 581-591.

Winkler, S. (2000). The 'Little Ice Age' maximum in the Southern Alps, New Zealand: preliminary results at Mueller Glacier. *Holocene*, 10/5, 643-647.

Witkowski, A. (1994*). Recent and fossil diatom flora of the Gulf of Gdansk, Southern Baltic Sea.* J. Cramer, Berlin.

Witkowski, A., Lange-Bertalot, H. and Metzelin, D. (2000). *Diatom Flora of Marine Coasts, I.* Koeltz, Koenigstein. 925 pp.

Wolfe, B. B., T. W. D. Edwards, T.W.D. and Aravena, R. (1999). Changes in carbon and nitrogen cycling regimes during tree-line retreat recorded in the isotopic content of lacustrine organic matter, western Taimyr Peninsula, Russia. *The Holocene* 9, 215–222.

Wood, H. (1876). *The Shores of Lake Aral*. Smith-Elder, London

Wolin, J.A. and Duthie H.C. (1999). Diatoms as indicators of water level change in freshwater lakes. In Stoermer, E.F. and Smol, J.P. (eds.) *The Diatoms: Applications for the Environmental and Earth Sciences*. Cambridge. .pp. 183-204.

Yafeng, S. and Jiawen, R. (1990) Glacier recession and lake shrinkage indicating a climatic warming and drying trend in Central Asia. *Annals of Glaciology*, 14, 261-265.

Yagodin, V.N. The Medieval Aral Sea Crisis. *Eurasia Antiqua* (accepted).

Yakir, Y, Issar, A., Gat, J., Adar, E., Trimborn, P. and Lipp. J. ^{13}C and ^{18}O of wood from the Roman siege rampart in Masada, Israel (AD 70-73): evidence for a less arid climate in the region. Geochimica et Cosmochimica Acta 58 (16), 3535-3539.

Yang, H., Rose, N.L. and Battarbee, R.W. (2002). Distribution of some trace metals in Loch Nagar, a Scottish mountain lake ecosystem and its catchment. *Science of the Total Environment*, 285, 197-208.

Yang, H. and Rose, N.L (2005). Trace element pollution records in some UK lake sediments, their history, influence factors and regional differences. *Environment International*, 31, 63-75.

Yang, X., Kamenik, C., Schmidt, R. and Wang, S. (2003). Diatom-based conductivity and water level inference models from Eastern Tibetan (Qinghai-Xizang) Plateau lakes. *Journal of Paleolimnology* 31, 1-19.

Yang, Z.R., Graham, E.Y. and Lyons, W.B. (2003). Geochemistry of Pyramid Lake sediments: influence of anthropogenic activities and climatic variations within the basin. *Environmental Geology*, 43, 688-697

Yechieli, Y., Magaritz, M., Levy, Y., Weber, U., Kafri, U., Woelfli, U. and Bonani, G. (1993). Late Quaternary geological history of the Dead Sea area, Israel. *Quaternary Research*, 39, 59-67.

Yao, T and Thompson, L.G. (1992). Trends and features of climatic changes in the past 5000 years recorded in the Dunde ice core. *Annals of Glaciology*, 16, 21-24.

Yong, Y.T., Jiang, H.B., Liu, T.S., Zhou, L.P., Beer, J., Li, H.D., Leng, X.T., Hong, B. and Qin, X.G. (2000) Response of climate to solar forcing recorded in a 6000 year $\delta^{18}O$ time-series of Chinese peat cellulose. *The Holocene*, 10/1, 1-8.

Yoysef, S.M. (2006). 80-120 yr Long-term solar induced effects on the earth, past and predictions. *Physics and Chemistry of the Earth*, in press.

Zavialov, P. (2005). *Physical Oceanography of the Dying Aral Sea*. Springer, Chichester, UK 146 pp.

Zhamoida, V.A., Butylin, V.P., Popova, E.A. and Aladin, N.V. (1997) sedimentation processes in the Northern Aral Sea. *International Journal of Research*, 6, 67-81.

Zhang, Y., Wallace, J.M. and Battisti, A.J. (1997). ENSO-like interdecadal 1900-93. Journal of Climate, 10, 1004-1020.

Zielinski, G.A., Mayewski, P.A. and Meeker, L.D. (1994). Record of volcanism since 7000 B.C. from the GISP2 Greenland ice core and implic the volcano climate system. *Science*, 264, 948-952.

Zielinski, G.A., Mayewski, P.A. and Meeker, L.D. (1997). Volcanic aeros and tephrochronology of the Summit, Greenalnd ice cores. *Special Issue of J Geophysical Research Letters*, 102, 26625-26640.